Sede Amministrativa: Università degli Studi di Padova
Dipartimento di Biologia

SCUOLA DI DOTTORATO DI RICERCA IN BIOSCIENZE E BIOTECNOLOGIE
INDIRIZZO: BIOTECNOLOGIE
CICLO XVII

Plant-inspired solutions for modern food technology: Ice Structuring Proteins from winter wheat

Direttore della Scuola: Ch.mo Prof. Giuseppe Zanotti
Coordinatore d'indirizzo: Ch.mo Prof. Fiorella Lo Schiavo
Supervisore: Ch.mo Prof. Luigi Bubacco

Dottorando: **Federico Lanciai**

ABSTRACT

In a quest to find novel methods to improve food preservation, food companies product pipelines are largely driven by the growing customers' request for natural solutions.

To date, freezing is still the most efficient method to preserve perishable foods, without altering substantially its taste and texture and avoid the use of preservatives.

The uncontrolled growth of ice crystals, pose however a serious risk for the stability of many frozen goods, threatening their integrity and sensorial features. A paradigm is represented by ice cream, whose ice crystals microstructure is fundamental to impart its characteristic mouthfeel, and as such, need to be preserved. A step forward toward the improvement of techniques to prevent extensive ice crystals growth, was represent by the introduction, a few years ago, of *AntiFreeze* proteins also known as *Ice Structuring Proteins* (ISP).

By directly interacting with the water molecules that make up the crystalline structure of ice, ISP disrupt the regularity of those planes and inhibit, to a certain extent, further addition of water molecules and consequent ice crystal growth.

To date, the only case of application of ISP in commercial products, is that of a fish ISP produced by recombinant *S. cerevisiae*. Besides the technological advantages in ice cream manufacturing enabled by the use of this protein, being a GMO derived product hampered its diffusion in GMO-skeptical communities, like in Europe and other western countries. In this scenario, the aim of this doctoral project, in collaboration with the University of Padova with the support of Food Research & Innovation srl, was focused on finding novel ISP alternatives for preservation of frozen foods. The discovery of novel sources and methods to obtain ISP, were driven by two requirement that needed to be satisfied: 1) the ISP source had be perceived as "safe" from potential consumers, 2) the bioprocess to obtain those ISP compatible with industrial uses. On the basis of requirement n.1, we chose wheat as our preferred source of ISP and, after a thorough

literature search about wheat ISP, we decided to start our investigation from a *Triticum aestivum* Thaumatin-Like Protein (TaTLP), for which the gene sequence was publicly available. The choice fell on TaTLP as this protein was previously recovered from wheat extracts, with the ability to inhibit ice recrystallization in ice cream.

In contrast with data reported in literature for TaTLP isolated from the plant, the recombinant product didn't show any ability to prevent ice crystals grow. After a thorough biochemical investigation, we concluded that the lack of activity wasn't ascribable to incorrect processing or maturation of TaTLP, whose structural features resembled much that of other proteins belonging to the same family. Our hypothesis, is that TaTLP doesn't exhibit any activity toward ice *per se* and that previous studies suggesting the opposite, may have derived from isolations of homologues TLP, that evolved ice binding domains. From our investigations on a wheat apoplastic extract containing ISPs, we found that the activity of those ISPs could be enhanced upon addition to the extract of exogenous proteins, not necessarily ISPs. At the moment, we don't have strong experimental evidences to elucidate the mechanism at the molecular level, but we believe that some wheat ISPs, may have evolved a strategy to enhance their single contribution to the total ice growth inhibition activity of the plant. This enhancement may rely upon the interaction of wheat ISPs with other proteins, similarly to what was observed for AFP from the overwintering insect *D. canadensis*.

In the search of a method to efficiently extract ISP from wheat that could be used as stabilizers of the ice phase in ice cream, we set up a one-step extraction process that involved high temperature treatment of the plant. This method represent a significant step forward in terms of simplicity and yield of ISPs, compared to previous extraction methods. Plus, the ISPs obtained thereof are heat resistant, an essential feature for proteins which are to be used in industrial foods. Wheat ISPs were then used to formulate ice cream in pilot pre-industrial plant; these ice cream were subjected to thermal shock to exacerbate temperature fluctuations experienced by ice cream in its path from the factory to the household freezers. The result is a stabilized ice cream, in which ice crystals growth was inhibited by the addition of a wheat extract containing ISPs. This extract could be

considered as a natural ingredient, lacking the need to be declared as an additive and therefore not falling under the E-number labeling regulation for food ingredients. In parallel to the tests performed on ice cream, isolation and partial characterization of ISP active species from wheat extract were attempted. At the end of the purification process, comprising 3 consecutive chromatographic separations, 5 proteins were eluted in a single fraction showing activity towards ice crystals growth. Being that these proteins have very similar isoelectric points and electrophoretic mobility, we believe that they might be isoforms of the same species.

To conclude, we designed a feasible process to obtain ISP from a vegetal source that successfully stabilized ice cream, this method having all the features required to be implemented on a larger scale for industrial production purposes. From the collateral results obtained from our investigations on wheat extracts, interesting clues about the nature of wheat ISP has emerged, as well and their possible roles in preventing ice growth in a physiological context. Those findings, contribute to broaden the knowledge of a category of ISP that is still poorly characterized and pose the basis for new research lines.

RIASSUNTO

Nell'ambito della conservazione di prodotti alimentari, uno dei trend di mercato in continua espansione e che fonda le proprie basi sul costante incremento della domanda di mercato, riguarda lo sviluppo di soluzioni cosiddette "naturali". Il congelamento è ad oggi l'unica tecnica di conservazione che consente di allungare la vita di cibi deperibili, senza alternarne sostanzialmente sapore e struttura e soprattutto senza ricorrere all'impiego di conservanti.

La crescita incontrollata dei cristalli di ghiaccio pone un problema di stabilità del prodotto, che si ripercuote negativamente sulle proprietà qualitative dello stesso. Un caso emblematico è quello del gelato, in cui è indispensabile che la microstruttura di cristalli di ghiaccio venga mantenuta tale per garantirne la tipiche caratteristiche di palatabilità. Un contributo sostanziale alla tecnologia del controllo dei cristalli di ghiaccio avvenuto negli ultimi anni, è rappresentato dall' introduzione delle cosiddette Proteine *AntiFreeze*, anche note come proteine *Ice Structuring* (ISP). Interagendo specificamente con le molecole d'acqua che costituiscono la struttura cristallina del ghiaccio, le ISP sono in grado di perturbarne la regolarità ed impedire, entro certi limiti, l'accrescimento incontrollato di cristalli di ghiaccio.

L'unico esempio di ISP attualmente impiegata in ambito alimentare riguarda una proteina di pesce artico prodotta mediante tecnologia del DNA ricombinante con l'impiego di *S. cerevisiae*. Nonostante gli indubbi vantaggi e le possibilità che l'impiego di tale proteina ha consentito ai produttori di gelato, il suo successo in Europa e alcuni paesi occidentali è stato rallentato dalla diffidenza nei confronti dei prodotti a base di OGM. In questo scenario, alla base di questo progetto di ricerca, svolto nel contesto della scuola di dottorato presso l'Università degli Studi di Padova e grazie al contributo dell'azienda Food Research & Innovation srl, vi era la necessità di ricercare soluzioni alternative alle ISP già in commercio. Tali soluzioni dovevano necessariamente rispondere a due requisiti: 1) che le ISP venissero ricavate da fonti ritenute "affidabili" dal potenziale consumatore e 2) che

il procedimento produttivo per l'ottenimento di tali ISP fosse compatibile con requisiti di applicabilità industriale.

Sulla base del primo requisito, abbiamo scelto di utilizzare germogli di grano (*T. aestivum*) come fonte di ISP. Come prima cosa, a seguito di un'estensiva ricerca in letteratura delle ISP di grano, abbiamo scelto di partire con una Thaumatin-Like protein di *Triticum aestivum* (TaTLP), della quale era disponibile la sequenza genica. La nostra scelta è ricaduta su TaTLP, poiché tale proteina è stata ritrovata in estratti di grano con la capacità di inibire il processo di ricristallizzazione dei ghiaccio in campioni di gelato. Contrariamente a quanto riportato in letteratura sulla proteina isolata dalla pianta, la proteina ricombinante da noi ottenuta non ha alcun effetto sulla crescita dei cristalli di ghiaccio. A seguito di un' approfondita caratterizzazione biochimica, abbiamo potuto stabilire che la mancata di attività non è da attribuire all'incorretta maturazione della proteina, che risulta strutturalmente e funzionalmente simile ad altre proteine appartenenti alla stessa classe. La nostra ipotesi è che la proteina in questione non abbia alcuna attività nei confronti dei cristalli di ghiaccio, e che gli studi precedenti si siano basati su proteine omologhe in cui tale attività è mediata da domini proteici specifici. A seguito di un indagine sperimentale su un estratto di ISP apoplastiche di grano, abbiamo scoperto che l'attività di tale proteine può essere incrementata, mediante l'aggiunta di proteine esogene all'estratto, non necessariamente ISP. Al momento, non siamo in possesso di solide evidenze sperimentali che ci consentano di validare un modello a livello molecolare. Tuttavia, riteniamo che alcune ISP di grano, possano aver evoluto un sistema per incrementare il proprio contributo, all'attività di prevenzione dalla crescita dei cristalli di ghiaccio a livello di organismo. L'incremento dell'attività delle ISP di grano potrebbe essere mediato dall'interazione diretta con altre proteine, in maniera simile a quanto riscontrato nel caso delle ISP ritrovate nelle larve dell' insetto *D. canadensis*.

Con lo scopo di identificare un processo per isolare le ISP dal grano da impiegare nella stabilizzazione del gelato, abbiamo messo a punto un procedimento di estrazione che consiste in una singola fase di estrazione a caldo dal materiale fogliare. Tale procedimento rappresenta un significativo miglioramento di processi estrattivi attualmente in uso, in

ottica di semplicità del metodo e resa di ISP. Un ulteriore vantaggio è costituito dal fatto che al termine del processo, si ottengono ISP resistenti al calore, una caratteristica indispensabile per la loro applicabilità a cibi prodotti a livello industriale.

Con le ISP ottenute in questo modo, sono stati preparati dei gelati in impianti pilota pre-industriali, i quali sono stati poi sottoposti a shock termico, per esasperare le fluttuazioni di temperatura che avvengono durante il ciclo di vita di un gelato, dal produttore al freezer del consumatore. Il risultato è un gelato stabilizzato in cui la crescita dei cristalli di ghiaccio dovuta allo stress termico è inibita mediante l'aggiunta di un estratto di grano come fonte di ISP. Tale estratto si configura come un ingrediente naturale, per il quale non è previsto un numero E con il quale vengono normalmente catalogati gli additivi alimentari. Parallelamente ai test sul gelato, abbiamo condotto una procedura di isolamento e caratterizzazione delle componenti ISP contenute dell'estratto. Al termine di un processo di purificazione che comprende 3 passaggi cromatografici, abbiamo ottenuto 5 specie proteiche che eluiscono in una singola frazione cromatografica ad alta attività. Date le simili proprietà di carica e peso molecolare verificate in gel bidimensionali, ipotizziamo che tali proteine siano isoforme di un' unica specie.

In conclusione, abbiamo definito un processo per l'ottenimento di ISP da fonte vegetale, compatibile con requisiti di produzione industriale ed efficacie nello stabilizzare il gelato. Dai risultati collaterali di questa ricerca sono emersi importanti informazioni in merito alla natura delle ISP di grano, così come spunti interessanti sul comportamento di queste proteine in un contesto fisiologico. Queste scoperte contribuiscono ad ampliare la conoscenza di una categoria di ISP sino ad oggi poco caratterizzata e pongono le basi per nuovi filoni di ricerca.

NOMENCLATURE

Disclaimer:

The name AntiFreeze Protein (AFP) derives from the very first findings of proteins that enabled polar fish to avoid freezing. Other features were later discovered to be peculiar to AFPs, such as the ability to inhibit ice recrystallization and modify the growth habit of ice crystals. Some authors started referring to AFPs also as either Thermal Hysteresis Proteins (THP) or Ice Recrystallization Inhibition proteins (IRIP). On the basis of the consideration that AFPs share the features of interacting with ice and influencing its growth, the comprehensive name of Ice Structuring Proteins (ISP) was proposed. Throughout this thesis, the ISP nomenclature will be used to refer to this class of proteins, except in cases where the term AFP was kept to maintain coherence with literature data.

List of abbreviations:

AWWE: cold Acclimated Winter Wheat Extracts

AE: Apoplastic Extract

Ae: Apoplstic protein extraction

AF: AntiFreeze

AFP: AntiFreeze Protein

C.Tryp: Bovine α-Chymotrypsinogen

CA: Cold Acclimated

CA_AE: Cold Acclimated Apoplastic Extract

CA_AE II: CA_AE 2nd production batch

CD: Circular Dichroism

CLP: Chitinase-Like Protein

Co-TT: Co-Translational Translocation

DAFP: *Dendroides canadensis* AFP

DAFP-1,4: *Dendroides Canadensis* hemolymph AFP number 1 and 4

DcTLP: *Dendroides canadiensis* Thaumatin-Like Protein

DcAFP: *Daucus carota* AFP

ER: Endoplasmatic Reticulum

fl TaTLP: full length TaTLP

FP: Freezing Point

FT: Freezing and Thawing

FW: Fresh Weight

GF: Gel Filtration

GLP: Glucanase-Like Protein

INP: Ice nucleating Protein

IBS: Ice Binding Site

IRI: Ice Recrystallization Inhibition

IRIP: Ice Recrystallization Inhibition protein

LDE: Leaves Decoction Extracts

LDe: Leaves Decoction protein extraction

LpAFP: *Lolium perenne* AFP

MpAFP: Marinomonas prmoryensis AFP

msGFP: monomeric superfolder GFP

MW: Molecular Weight

NA: Non Acclimated

NA_AE (Non Acclimated Apoplastic Extract)

NA_LDE: Leaves Decoction Extract from Non Acclimated plants

NP: Native Proteins

OD_{600nm}: Optical Density recorded at 600nm

Ost1: Post-translational signal sequence

PGIP: Polygalacturonase Inhibitor Protein

pI: Isoelectric point

Po-TT: Post-Translational Translocation

PR5: Pathogenesis Related protein 5 family

pre: pre region of S. cerevisiae α-mating factor

pro: pro region of S. cerevisiae α-mating factor

SASA: Solvent Accessible Surface Area

SS: Signal sequence

Ta: *Triticum aestivum*

TaIRI-1 and TaIRI-1: *T. aestivum* Ice Recrystallization Inhibition transcript 1 and 2

TaISP: *Triticum aestivum* Ice Structuring Protein

TaTLP: Triticum aestivum Thaumatin-Like Protein

Th: Thaumatin

TH: Thermal Hysteresis

ThyroGl: Thyroglobulin

THP: Thermal hysteresis Protein

TLP: Thaumatin-Like Protein

TL: Thaumatin-Like

TPE: Total Protein Extract

TPe: Total Protein extraction

Trp: Tryptophan

TS: Thermal Shock

TABLE OF CONTENT

GENERAL INTRODUCTION

1.2. CONTROLLING THE ICE PHASE: LESSONS FROM NATURE

1.2.1. Freezing stress in biological systems

Organisms encounter two different stress conditions as they approach freezing temperatures, depending on whether they are in a *chilled* or *frozen* state. *Chill* is defined as the condition at which the temperature is low enough to stress the organisms, but not to cause it to freeze (Hayward, Manso et al. 2014). Slower metabolic rates and impairment of membrane functionality are the first consequences of the chilled state. In case of freezing, ice starts forming in the extracellular space, increasing the concentrations of solutes in the remaining unfrozen water. This phenomenon leads to water diffusing out of the cell to compensate for the increased chemical potential of the extracellular fluid. As a result of water flowing out, the cell might experience dehydration stress and hyperosmotic conditions that impair the biochemistry of several physiological processes.

The effect of cell shrinkage and increased viscosity of the lipid double-layer induced by low temperature, can solicit the membrane bilayer stability and provoke its cracking (Bligh 1990).

At the macroscopic level, uncontrolled ice formation and propagation outside the cell can lead to the rupture of vessels and capillaries (Sinensky 1974, Mazur 1984).

Organisms that lack the ability to regulate their internal temperature (*i.e.* Ectotherm), have evolved two different strategies to survive at moderately (-2°C) to extremely low temperatures (< -20°C): Freeze avoidance and Freeze tolerance.

Accumulation of low molecular weight solutes is one common mechanisms adopted by cold adapted organisms to lower their freezing point (FP) and avoid freezing. The contribution of each Osmole of solute to the FP depression of water is 1.86 °C, according to the Raoult equation: $\Delta T = Kf\ C_{[sol]}$, where ΔT indicates FP depression, Kf is the FP constant (-1.86 in the case of water) and $C_{[sol]}$ the osmolar concentration of the solute

(Raoult 1884). Small sugars and organic acids are the most common cryoprotectants present in biological systems, however, their maximum concentration achievable in body fluids is limited to avoid the negative consequences of osmotic imbalance. A paradigm is the cold adapted polar fish, which are able to survive without freezing at seawater temperatures around -1.9°C. The evidence for a non-colligative FP depression came from the finding that those fishes are hyposmotic to seawater, meaning that the concentrations of solutes within their body fluids is lower that of surrounding water, the latter being around 1000 mOsm. 400-600 mOsm are average osmolarity values reported for body fluids of cold-adapted fish species, thus meaning that they would freeze at -0.75 °C to -1.3 °C (Cheng 2003). In 1970 it was found that the temperature gap coverage that allowed those fish to avoid freezing was mediated by a novel category of proteins, named AntiFreeze Proteins (AFP) (DeVries 1971). The extent of non-colligative freezing point depression mediated by AFP is indicated as Thermal Hysteresis (TH), and is a hallmark of all AFPs.

AFPs were later found also in freeze tolerant organisms such as plants (Urrutia, Duman et al. 1992). Another peculiar feature of AFPs, which allow the survival of freeze tolerant organisms in a semi frozen state, is their ability to inhibit recrystallization of ice crystals. This activity is also referred to as Ice Recrystallization Inhibition (IRI) (see Paragraph 1.1.2.3).

Both TH and IRI are direct effect of AFP bound to the surface of ice nuclei, therefore when referring to TH and IRI proteins the general nomenclature of Ice Binding Proteins is often adopted.

1.2.2. Ice Stuctuting Proteins (ISPs)

1.2.2.1. Physiological roles

Several Ice Binding proteins have been discovered so far in different taxa, from unicellular eukaryotes to plants, bacteria, fungi, fish, crustaceans and insects (Sorhannus 2011) . The

name AntiFreeze Protein, relates to their ability to confer freeze avoidance to organisms living at subzero temperatures. The TH effect provided by fish AFPs is necessary to push the freezing point of their body fluids below seawater temperature (**Figure 1.1.1)**. While the highest TH activity measured for purified fish AFPs is 2 °C (Marshall, Fletcher et al. 2004), some insects AFPs were named "hyperactive" after the finding that their maximal TH activity could account for more than 5°C of total TH measured for their hemolymph (Graham, Liou et al. 1997); furthermore their specific TH activity is 10-100 fold higher than that of "moderate" AFPs on a molar basis (Scotter, Marshall et al. 2006). It was later found that TH activity of insect AFPs could be significantly enhanced by synergistic interactions between AFPs as well as other endogenous elicitors (see Chapter III). The resulting TH activity of overwintering insects hemolymph lies within the range of 5-10°C (Duman 2001), a necessary condition to avoid freezing at temperatures that are much lower than those faced by polar fishes.

Besides TH, AFPs are also known for their ability to slow down or inhibit ice recrystallization (**Figure 1.1.2**). This property was found to be particularly accentuated in organisms that can tolerate freezing. Winter resistant plants represent the classical example of freezing tolerant organisms whose AFP evolved to maximize IRI activity.

Depending on whether ISPs are found in freeze avoiding or freeze tolerant organisms, they are also referred to as Thermal Hysteresis Proteins (THP) or Ice Recrystallization Inhibition Proteins (IRIP) respectively. Being that both THP and IRIP can impart characteristic shapes to the ice crystal when the temperature is changed within the TH gap (see next Paragraph), a novel nomenclature was proposed for this category: Ice Structuring Proteins (ISPs) (Clarke, Buckley et al. 2002) .

The discovery that some sea ice microalgae secrete their ISPs in the surrounding medium, or bacteria colonizing Arctic lakes project the ice binding domains of transmembrane proteins outside of the cell (Raymond 2011, Guo, Garnham et al. 2012), posed interesting new perspectives on the physiological roles of this category of ISPs. In the case of MpAFP, a Calcium dependent protein from the arctic bacteria *M. primoryensis*, the hypothesis is that its binding site (IBS), found at the end of long extracellular rod-like domain, could play

a strategic role in making the bacteria adhere to the ice in the higher reaches of lake water (**Figure 1.1.3 A**) ((Guo, Garnham et al. 2012). In this way, *M. primoryensis* would be able to colonize a niche with high availability of nutrients and oxygen.

Other hints that ISPs enable microorganism to thrive in temperature challenging environments, aside from preventing them to freeze, came from the observations that ISPs from ice sea algae can affect the microstructure of frozen seawater to which they are attached. It was proposed that once those ISPs are secreted in proximity of the microalgae, they could prevent its enclosure and entrapping into the surrounding ice (**Figure 1.1.3 B**).

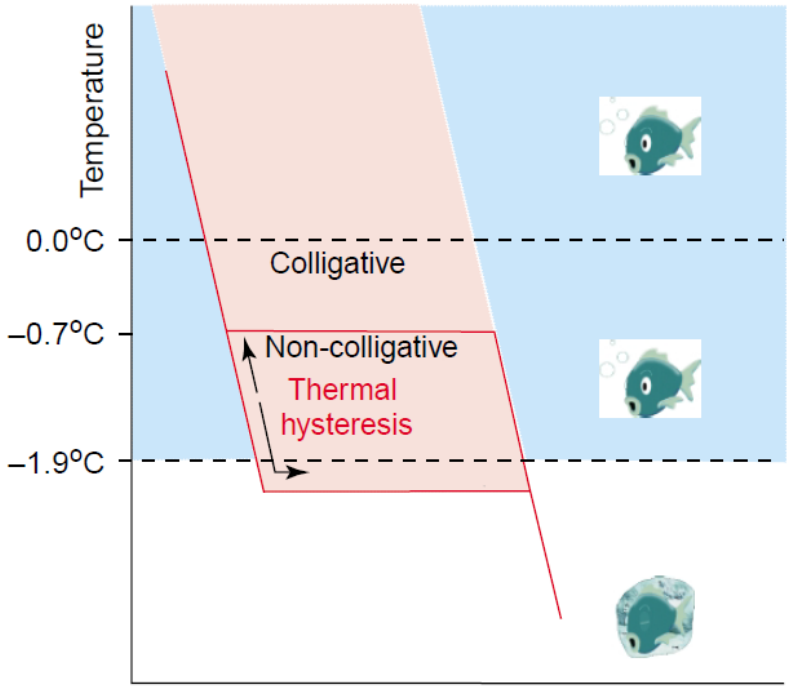

Figure 1.1.1: Thermal hystereses enable polar fish blood to "supercool" below seawater temperature without freezing. Adapted from (Jia, Davies 2002)

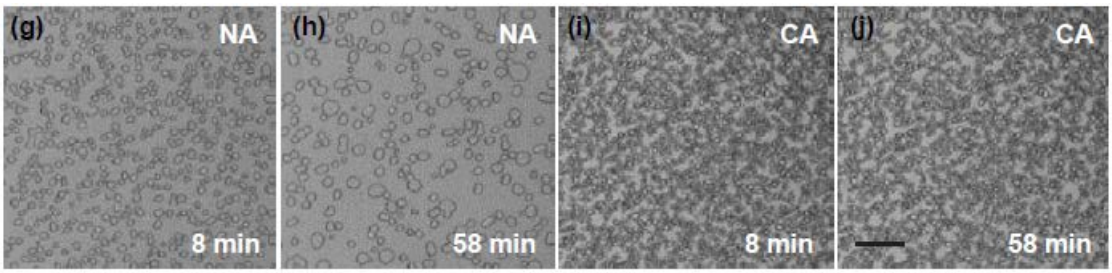

Figure 1.1.2: Effects of plant ISPs on ice recrystallization rates. Total soluble extracts from nonacclimated (NA) and cold acclimated (CA) winter rye leaves were added to a 26% sucrose-water solution, flash-frozen at -50 °C and held isothermally at -8 °C to allow ice recrystallization for 8 (g, i) and 58 min (h, j). NA extracts didn't inhibited ice recrystallization as fewer and larger ice were observed after 58 min (h). On the contrary, ISPs within CA extracts effectively inhibited ice crystals growth, leaving their size and total number almost unaltered (i-j). Adapted from (Griffith, Yaish 2004)

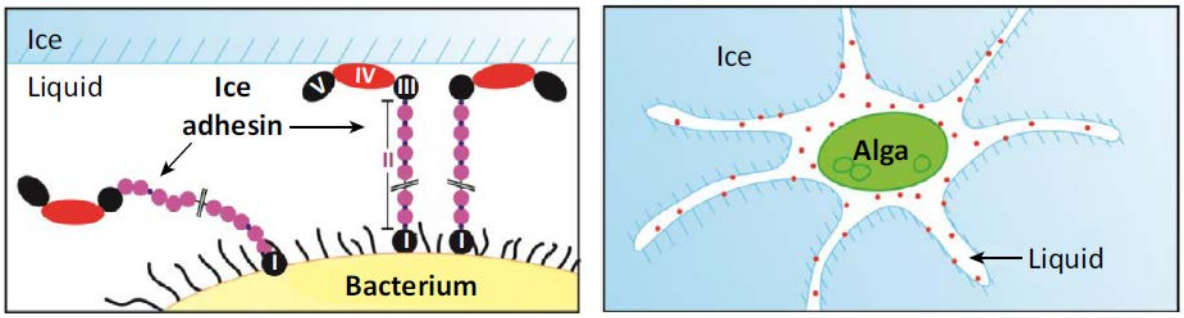

A **B**

Figure 1.1.3: Proposed extracellular role of ISPs from A) *M. primorymonas* and B) sea ice microalgae. A) MpAFP is composed of 4 domains (RI, RII, RIII, RIV), of whom only RIV has ice binding ability. The rigid conformation of RII domain is stabilized by Calcium ions. B) ISPs are depicted by red dots along ice water channels. Images are adapted from (Davies 2014)

1.2.2.2. Ice binding mechanism

A striking feature of ISPs, is the significant structural heterogeneity that marks this protein family with a common function: ice binding. It is nearly impossible to predict novel ISPs or Ice Binding Domains just on the basis of sequence similarity. Ice Binding sites variability among species is thought to be the result of ISPs co-evolution (Cheng 1998) and the structurally heterologous nature of their ligand, ice.

At atmospheric pressure and temperatures, water molecules freeze yielding an hexagonal structure known as Ice Ih (Hobbs 2010). Four different planes can be identified on this

hexagonal ice crystalline unit, each showing different patterns of water molecules arrays (**Figure 1.1.4**).

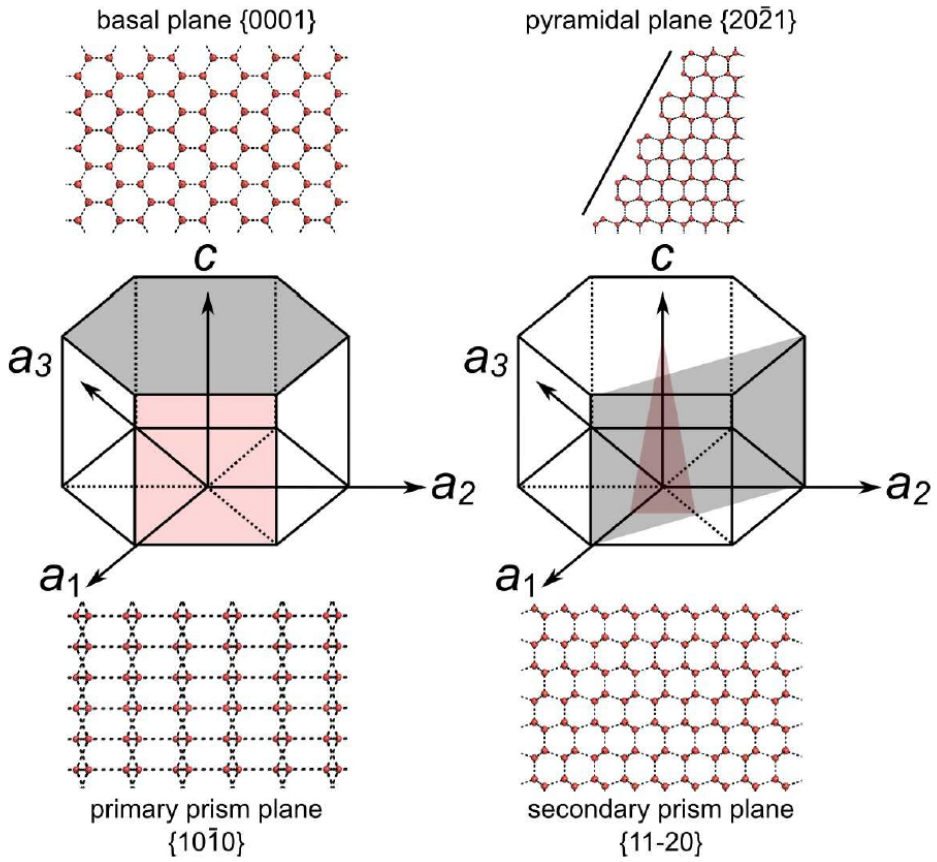

Figure 1.1.4: Structural features of ice Ih crystalline unit. *Left column*: basal plane (grey) and primary prism plane (pink). *Right column*: secondary prism plane (grey), pyramidal plane (pink). The Miller index is indicated below each plane. Oxygen atoms are depicted in red, hydrogen bonds as dotted lines. Adapted from {{243 Garnham, C.P. 2011}}

The first evidences of the role of ice binding sites in ISPs, came from mutagenesis studies that identified those amino acid residues critical for TH activity. Observation that those amino acid moieties within the IBS matched almost perfectly the regularity of oxygen and hydrogen atoms along the surface of the ice planes, was a further confirmation of the correct identification of the IBS. For some ISPs, this surface-to-surface similarity could be extended to more than one ice plane and thought to be at the basis of the hyperactive activity of insect ISPs (**Figure 1.1.5**) (Hughes, Schart et al. 2013).

From the comparison of ice binding domains of different ISPs structures, the first speculative hypothesis regarding the mechanisms of ice binding, assumed that van der Vaals contacts between protein and ice are the key interactions that drive ISPs absorbance on the ice plane, with only limited contribution by hydrogen bonding (Davies, Baardsnes et al. 2002). This model was refined after the discovery of ice-like ordered water molecules along the IBS of crystallographic structures of MpAFP (Garnham, Campbell et al. 2011) (**Figure 1.1.6 A**). This finding offered the experimental confirmation to previous speculations and Molecular Dynamics simulations (Nutt, Smith 2008), suggesting that ISPs can arrange water molecules in the proximity of IBS in a way that closely resemble the orientation of the quasi-ice water layers surrounding the ice surface.

Garnham and colleagues (Garnham, Campbell et al. 2011) elucidated this mechanism at a molecular scale; according to the model proposed, the "anchored clathrate model", the relative hydrophobicity of IBS causes the surrounding water molecules to arrange in an ice-like-lattice. Those ordered waters are anchored to the IBS via hydrogen bonds (**Figure 1.1.6 B**).

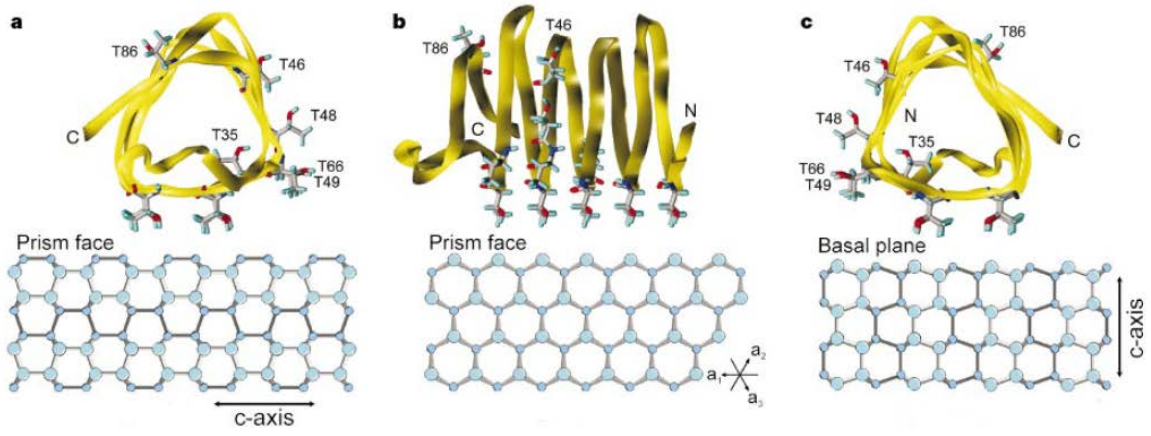

Figure 1.1.5: Structure alignment of IBS of Spruce budworm AFP (SbwAFP) over two different ice planes (prims and basal). Cyan circles represent oxygen molecules in the ice lattice. Threonine lateral chains protruding toward the lattice are depicted as sticks. Each lattice surface is visualized as indicated by the orientation of c and a axes. As shown in (a) and (c), some oxygen couples in the lattice have the same inter-atomic distance in the basal and prism planes. In (b), SbwAFP loops matching with ice water oxygen atoms of the prism face. Adapted from (Hughes, Schart et al. 2013)

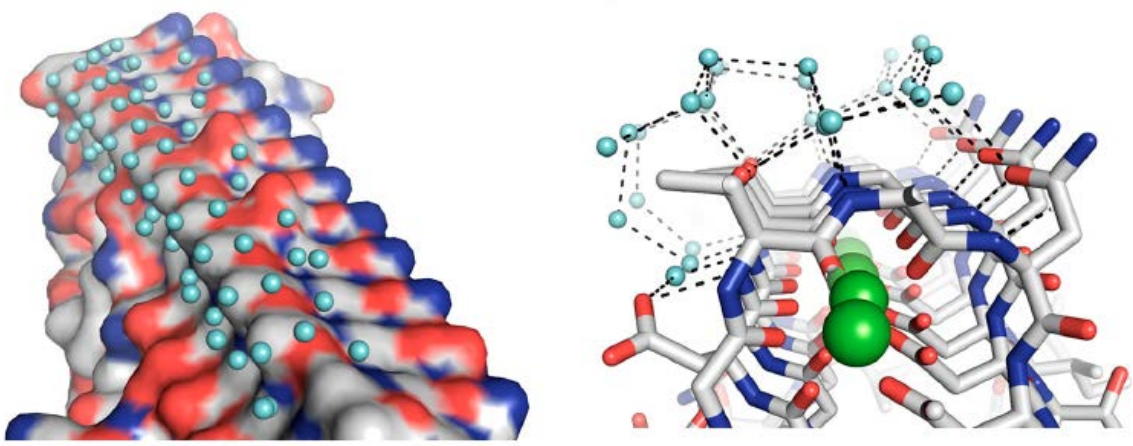

A B

Figure 1.1.6: Crystal structure of MpAFP_RIV. A: ordered water molecules (cyan spheres) along the IBS surface of MpAFP-RIV B: Ice-like water molecules enclose the γ-methyl of Thr in the xGTGND repeat. This cage is anchored to the IBS by hydrogen bonds to the main-chain nitrogen and side chain oxygen of each Asn (xGTGND). Adapted from (Garnham, Campbell et al. 2011)

1.2.2.3. Ice binding phenotypes

The most accredited mechanism to explain how ISPs can affect ice crystals growth and produce Thermal Hysteresis and Recrystallization Inhibition is called the Absorption-Inhibition model, proposed by Raymond and DeVries in 1977 (DeVries 1971) . According to this model, absorption of water molecules at the site of ISPs binding is inhibited; the remaining ISPs-free ice surface is thus forced to grow assuming a curvature radius that increase the surface to volume ratio, resulting in local freezing point depression (**Figure 1.1.7**) (Barrett 2001). At this stage, ice propagation is stopped until temperature is decreased to a point at which ISPs can't no longer inhibit ice growth, and the crystals "burst" (**Figure 1.1.8**). The temperature gap between the ice crystals melting and bursting is referred to as Thermal Hysteresis gap. The concept of THhys was recently extended by the observation that some ISPs can also stabilize ice crystals in a superheated state, i.e. above melting point (Celik, Graham et al. 2010) .

In the absence of ISPs, single crystals don't grow evenly when temperature is slowly lowered below their freezing point. Being that the fastest growth occurs at the prism plane toward the a-axis (**Figure 1.1.4**), the crystals will tend to grow forming disc-like sheets (**Figure 1.1.8**, w/o ISPs).

In the presence of ISPs, temperatures changes will cause the crystal to assume a bi-pyramidal shape (**Figure 1.1.8**, + ISPs), due to the preferential binding of ISPs to the prism planes and consequent inhibition of ice growth normal to this plane. It has been shown that in the case of ISPs with hyperactive activity, ice crystals melting within the TH gap resulted in peculiar ice crystal shapes other than bi-pyramidal (Bar-Dolev, Celik et al. 2012). Another feature that mark the difference between ISPs with moderate and hyperactive TH is their freezing behavior below the TH gap. Ice crystal burst parallel or normal to the c-axis in the presence of respectively moderate and hyperactive THP (**Figure 1.1.8**). Besides Thermal Hysteresis, another peculiar feature of ISPs is their ability to inhibit ice crystals growth due to recrystallization processes. Ice Recrystallization is the result of structural rearrangement of ice crystals that tend to minimize their free energy by reducing their surface to volume ratio. One of the consequences on ice crystals population, is the disappear of small crystals, that for the abovementioned reasons are more"unstable", at the expenses of larger ones (Brown, Seymour et al. 2014) (For a more comprehensive description of Ice Recrystallization, see Paragraph 1.2)

Almost all known ISPs show both TH and IRI; the predominant activity depending on the survival strategy adopted by the organisms.

It is not yet clear what structural differences determine predominant IRI or TH activity, partly because of the poor availability of crystals structures for IRIP.

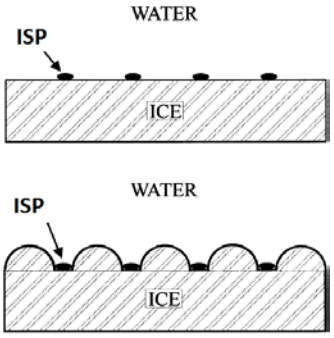

Figure 1.1.7: The ice absorption inhibition model explained by the "mattress button" effect. Ice surface lying within consecutives ice bound ISPs is forced to grow by increasing its curvature. As a result, local freezing point depression occurs and temperature need to be decreased to induce further ice growth. Adapted from (Barrett 2001)

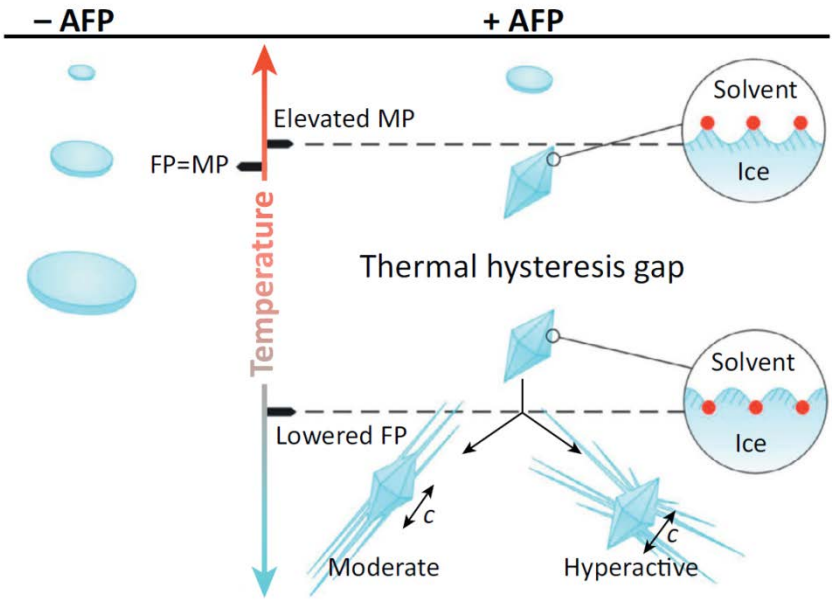

Figure 1.1.8: Effect of ISPs on single ice crystal growth. On the left, in absence of ISPs the ice crystal shrink and grow maintaining a disc shape as the temperature rises or decreases. On the right, once the ice crystals has bound ISPs, the further decrease of temperature within the TH gap causes it to grow with a bi-pyramidal shape (e.g. fish ISPs). At temperature below the TH gap, ice burst occurs.
Depending on whether the ISPs has moderate of hyperactive TH activity, the ice will burst parallel or perpendicular to the c-axis. On circles, the ISPs bound to the ice are represented as red spheres. Within the TH gap, ISPs bound to the ice surface inhibit the growth of supercooled crystals, or shrinkage in superheated conditions. MP: Melting Point, FP: Freezing Point. Adapted from (Davies 2014)

1.2.2.4. Methods to detect and measure ISPs activity

To ascertain whether ISPs are present in a biological sample, one of the following condition must be verified:

- Thermal Hysteresis
- Ice shaping ability
- Ice Recrystallization Inhibition

The simultaneous presence of all these activities is the strongest evidence for the presence of ISPs. Alternatively, to confirm that one of the features mentioned above is mediated by proteins, a loss of activity should be observed upon proteolytic digestion of the sample.

1.2.2.4.1. Thermal Hysteresis and Ice shaping ability

The standard method to detect TH activity relies on visual observation of ice crystal freezing behavior using a nanoliter osmometer and an optical microscope (Bayer-Giraldi, Jin et al. 2014) (**Figure 1.1.9**). Briefly, a few nanoliters of aqueous solution containing ISPs (or THP) are resuspended in mineral oil and loaded on micro wells on a copper plate. The plate is then placed on a temperature-controlled stage and the sample is rapidly frozen. By gradually heating the sample, ice crystals will progressively melts until only one crystals is obtained. This temperature is indicated conventionally as the melting point. At this stage, the temperature is slowly decreased until ice bursts is observed; this temperature is defined as the freezing temperature and the gap between melting and freezing points is the Thermal Hysteresis gap. Within the TH gap, peculiar ice crystals growth morphology are observed upon ISPs binding to ice.

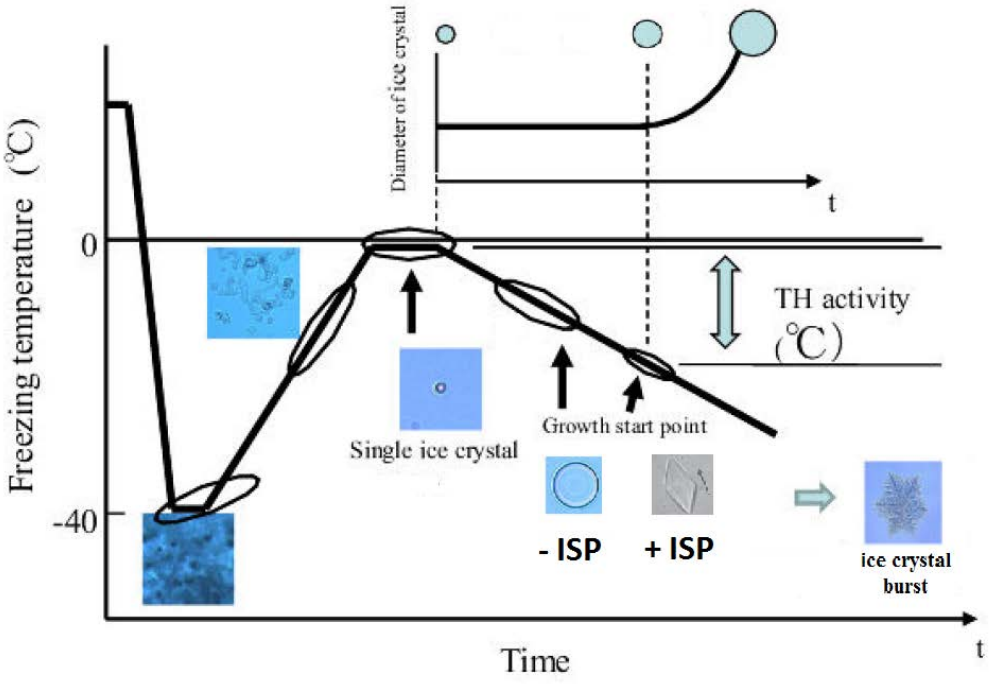

Figure 1.1.9: TH measurement using nanoliter osmometer. Sample is rapidly frozen to -40°C, then the temperature is brought up until a single crystal is obtained (melting temperature). Within the TH gap, ice growth in the presence of ISPs result in by-pyramiadal ice shaped crystals. TH is measured as the interval between the melting and freezing (the point at which ice burst) tempertures. Adapted from (Hidehisa)

Differential Scanning Calorimetry has also been used to measure precisely freezing and melting temperatures of a sample and calculate TH of ISPs (Hansen, Baust 1988) (Lu, Wang et al. 2002b). This method has the advantage of providing accurate and reproducible data being that it does not rely on visual evaluation. Conversely, no information on the ice crystals dimensions and shapes can be obtained with this method.

1.2.2.4.2. Ice Recrystallization Inhibition activity

Ice Recrystallization Inhibition assay measure the progressive increase of ice crystals in a solution at constant or fluctuating temperatures. Several methods have been developed so far, both for qualitative and quantitative determination of IRI activity.

In the early "splat assay" developed in 1988 by Knight (Knight, Hallett et al. 1988) , a thin layer of ice was obtained by expelling a drop of ISPs solution from a height of 3 m onto a microscope slide laid on a liquid nitrogen cooled metal plate. The slide was then placed on over a temperature controlled plate and analyzed by optical microscopy. A simplified version of the splat assay was proposed by Smallwood in 1999 with the introduction of the sucrose-sandwich-splat assay. Thin layers of liquid between two microscope slides were snap frozen in liquid nitrogen (Smallwood, Worrall et al. 1999a) . 30% sucrose solution was added to the samples to minimize the effect of small solutes on IR rates (Knight, Hallett et al. 1988) .

Both of these method suffers from poor reproducibility and are merely quantitative. The output of IRI splat assays is often expressed at RI endpoint, i.e. the lower ISPs concentration at which RI is still observed. IRI assays became more accurate with the introduction of computer controlled temperature controlled stages. The most recent IRI assay proposed by Reagand & Goff in 2005 (Regand, Goff 2005), adopts a rapid freezing step, followed by temperature cycling between -10°C and – 4°C to obtain a population of ice crystals with homogenous size. The temperature is then kept below 0°C for prolonged periods; ice recrystallization is measured by calculating the increase in the average size of ice crystals at different time points. In **Figure 1.1.10**, the temperature cycle applied to

assess IRI in our lab is reported in **Figure 1.1.10**. A more detailed description of the IRI assay is available in the Material and Methods section of Chapter II.

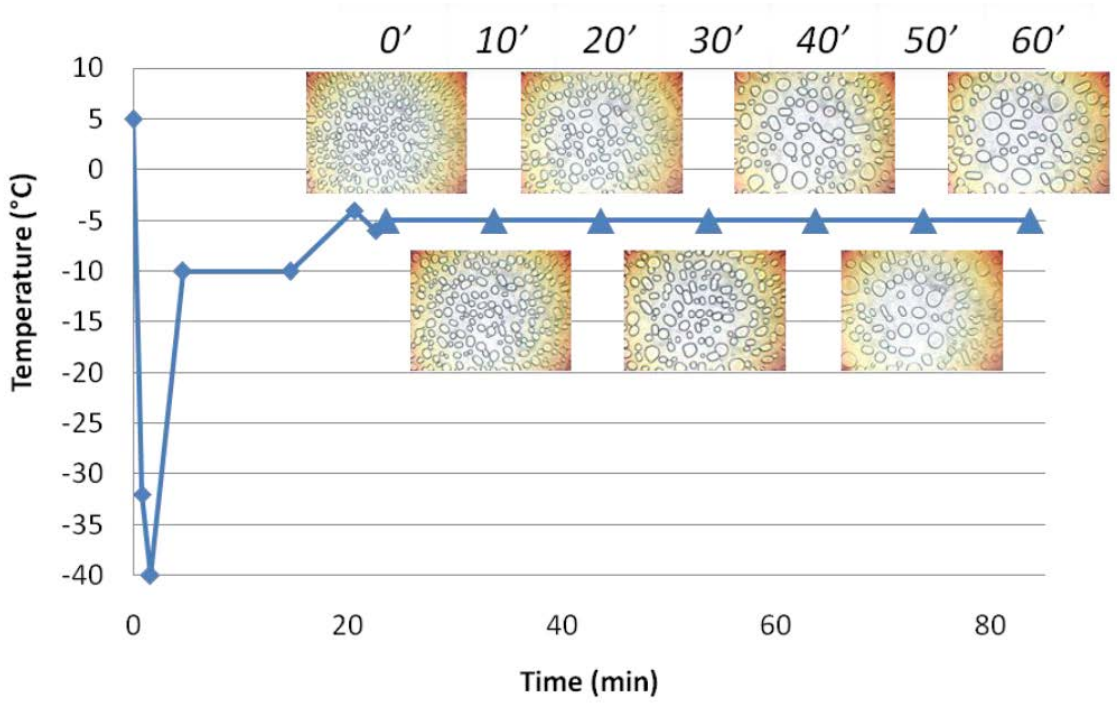

Figure 1.1.10: Temperature cycle applied for IRI measurement in our lab. Photos were taken at constant -5°C temperature every 10 minutes.

1.1. CONTROLLING THE ICE PHASE IN FROZEN FOODS: THE ICE CREAM CASE

ISPs hold great potential for biotechnological applications related to the conservation of frozen biological material. Being the scope of this thesis limited to ISPs applications in food products, other proposed uses for ISPs such as cryopreservation or crops improvement won't be object of this dissertation.

One of the most critical aspect associated with freezing preservation, is the uncontrolled growth of ice crystals. Large ice crystals represent a problem for different category of products. In vegetables and meat, intracellular freezing lead to the rupture of cell structures and consequent destruction of cell compartmentalization. To date, limited success was obtained for these products with the use of ISPs, the greatest limitation being the delivery of ISPs inside the cells.

In the case of bread dough, frozen storage would allow manufacturers to extend the short shelf life of this product, but ice crystals can disrupt the gluten network as well as damage the yeasts and impair efficient leavening. The resulting bread has reduced volume, decrease in the proportion of gas content, weakened structure and a poor texture (Hassas-Roudsari, Goff 2012). Two different studies demonstrated that addition of winter wheat ISPs and Type I AFP to bread dough, are effective in preventing structural deterioration and loss in leavening capacity after freezing (Ribotta, Leon et al. 2001, Panadero, Randez-Gil et al. 2005, Zhang, Zhang et al. 2007) .

Besides their potential applicability to a vast range of frozen food products, to date, the only food formulated with ISPs available on the market is ice cream.

1.1.1. Ice cream structure

1.1.1.1. Colloidal properties of ice cream

From a physical point of view, ice cream is one of the most complex foods. Three different phases co-exist in ice cream in a delicate unstable equilibrium that requires strict control of temperature throughout its manufacturing, storage and delivery process. A typical ice cream consists of about 20-30 % ice, 50 % air and 5 % fat, each in the form of a colloidal dispersion of micrometric particles over the unfrozen matrix **Figure 1.2.1** and **Table 1.2.1** (Crilly, Russell et al. 2008). Ice cream is an example of unstable colloidal suspension, where each of the three components (air, fat and ice) tend to minimize its surface free energy by forming a continuous phase. The effect of particles merging together must be finely regulated throughout ice cream manufacturing process. Partial coalescence of fat particles is desired to impart to ice cream resistance to melting as well as stabilization of the air phase (Goff 1997) . Conversely, ice crystals merging together is to be avoided, being that larger crystals impart a grainy texture to the food. Given the highly interconnected structural network that exists between ice crystals, air bubbles and fat particles, small changes in each component can impact the integrity of the whole system.

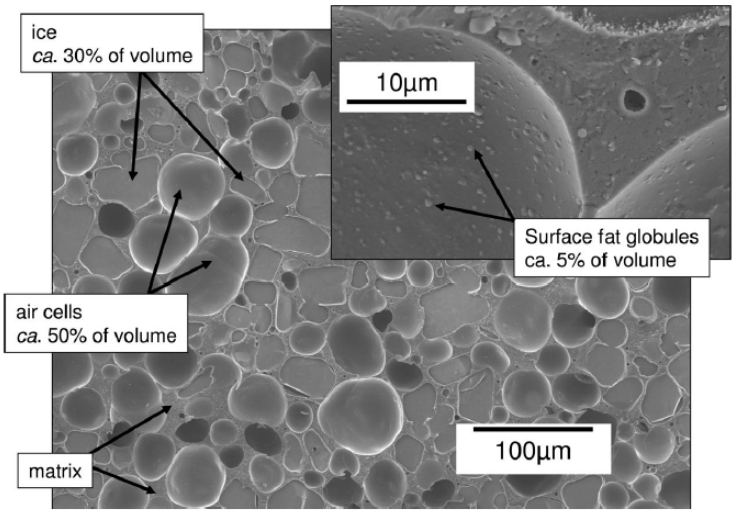

Figure 1.2.1: Scanning electron microscopy of ice cream microstructure. In the insert, large air bubbles stabilized by a coating of fat droplets and the viscous matrix. Adapted from (Crilly, Russell et al. 2008)

Component	*Volume fraction (%)*	*Size (µm)*	*Number/Liter*	*Surface are (m^2/Lt.)*
Ice	30	50	5×10^9	40
Air	50	60	4×10^9	50
Fat	5	1	1×10^{14}	300
Matrix	15			

Table 1.2.1: Average parameters of principal components of ice cream. Adapted from (Clarke 2012)

1.1.1.2. Ice crystals formation and recrystallization process

In the process of ice formation and propagation, the high dynamicity of the ice phase can be described by three categories of events: nucleation, growth and recrystallization. Nucleation occurs at supercooled conditions and depends on the casual aggregation of water molecules to give stable ice nuclei. Ice growth is mediated by further addition of water molecules to pre-formed nuclei at temperatures below freezing point. During recrystallization, ice crystals are re-shaped to minimize their surface-to volume ratio, without changes in the fractions of frozen and liquid water () . Two different recrystallization behaviors are described in the literature on ice cream (**Figure 1.2.2**): accretive recrystallization and migratory recrystallization, the latter also known as Ostwald ripening when it occurs at constant temperature (Hassas-Roudsari, Goff 2012). Accretion

of ice crystals takes place when two or more crystals make contact; the negative curvature of the contact area results in the formation of a neck. (**Figure 1.2.2** red arrow) (Crilly, Russell et al. 2008) . Migratory recrystallization involves the transfer of water molecules in between crystals and it is driven by the tendency of each crystal to minimize its surface free energy . This condition tends to favor the crystals with a larger radius of curvature causing the smaller ones to vanish. This phenomenon occurs slowly at isothermal conditions, but is greatly increased by temperature fluctuations.

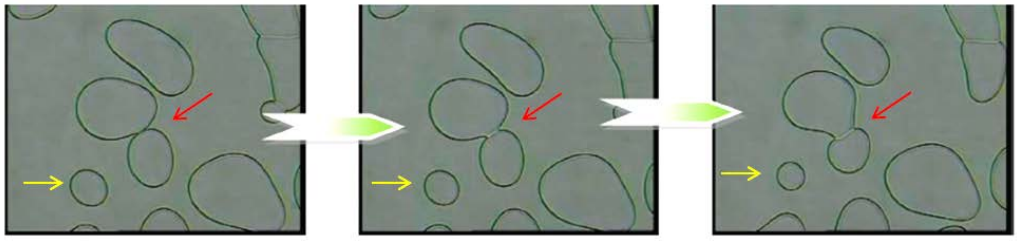

Figure 1.2.2: Ice recrystallization at constant temperature. Accretive recrystallization is indicated by a red arrow and occurs via the formation of a neck between two crystals. Migratory recrystallization involves the transfer of water molecules from smaller crystals to bigger ones, with consequent shrinkage of small ice crystals (yellow arrow). Adapted from (Crilly, Russell et al. 2008)

1.1.1.3. Effect of ice crystals size on mouthfeel

When referring to the perceived texture of a food, several physical features of the product, such as stiffness, coarseness and viscosity are considered. An exhaustive review of the current opinion on the physiology of texture perception can be found in a paper by Engelen and Van der Bilt (ENGELEN, VAN DER BILT 2008).

Mechanoreceptors involved in the perception of tactile stimuli are thought to be responsible for sensing the textural properties of a food. The oral cavity, especially the tongue, owes its extraordinary tactile resolution ability to the high density of tactile receptors that innervates its tissues. Size, shape and concentration of particles in a food contribute significantly to the texture perceived in the mouth. Both the tongue and the palate seem to be able to discriminate particle of different sizes. In a test where the participants rubbed a sample of particles dispersed in a semi-solid between the tongue and the palate, particles size in the range of 2-200 µm were successfully discriminated.

Being those particles too small to activate distinct pressure receptors, it was proposed that perception of coarseness could be mediated by friction and vibrational stimuli. A series of experiments seems to validate this hypothesis. The observation that irregular shaped particles were perceived as larger in comparison to rounder equivalent particles was explained by their increased friction coefficient that was contextually measured with *in vitro* methods. Moreover, the addition of substances that decrease the extent of particles friction in the mouth, such as fats, lead to underestimation of particle size.

Different grades of coarseness could be discriminated by a panel tasting SiO_2 particles in the range 2-200 µm, with the strongest sensation of roughness perceived with 80-140 µm particles.

In the case of ice cream, a correlation between the dimensions of ice crystals and the perceived coarseness/creaminess of its texture is established (**Figure 1.2.3**) (Russell, Cheney et al. 1999) .

The general consensus is that the lower ice crystals size that can impart a grainy mouthfeel is approximately 50 µm (diameter) (Cook, Hartel 2010b).

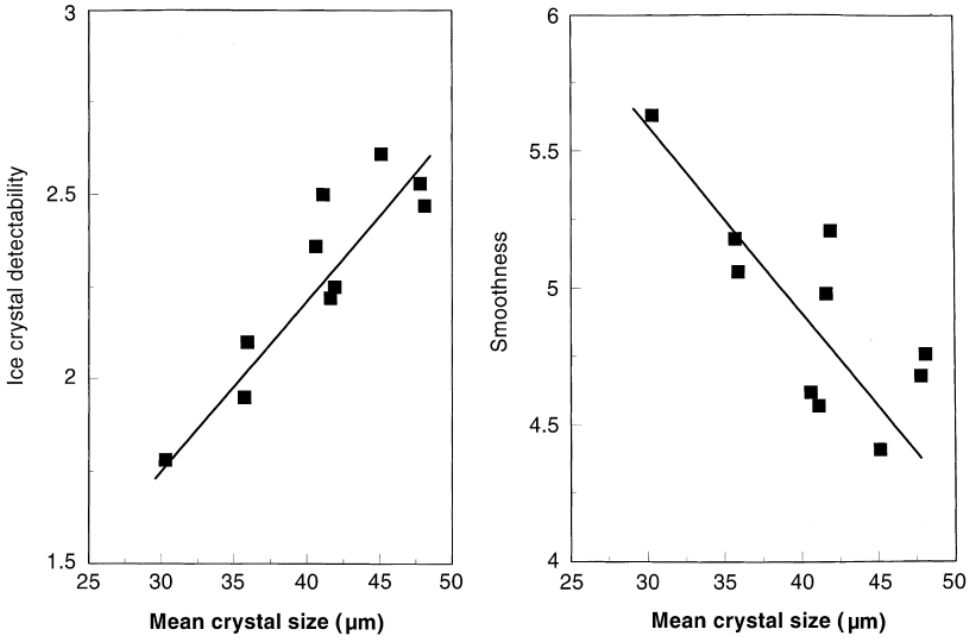

Figure 1.2.3: Scores from a trained sensory panel for ice crystal detectability and smoothness versus mean of ice crystal size. Adapted from (Russell, Cheney et al. 1999)

1.1.2. Means to control the ice phase in ice cream:

The typical temperature at which ice cream is drawn from the factory freezer is – 5°C (Clarke 2012). The higher the ice cream temperature, the more water mobility will contribute to ice recrystallization. For this reason, a "hardening" step that consists in temperature abatement down to -20/-40 °C step is required after ice cream exits the freezer. Although this step is meant to slow down the progressive increase of ice crystals size by decreasing the entropy of the system, those temperatures are not sufficient to completely halt ice crystals growth. **Figure 1.2.4** depicts the evolution of the ice crystals population of ice cream freshly-drawn, hardened and stored at constant temperature; in **Figure 1.2.5** the effect of subzero fluctuating temperatures is reported. While ice crystals growth occurring upon hardening is due to the increased frozen water content (**Figure 1.2.4**, open squares), in all other cases ice recrystallization mediates only rearrangements of the ice crystal population, favoring the survival of larger crystals at the expenses of smaller ones. This effect is particularly exacerbated when multiple freezing and thawing events occur (**Figure 1.2.5**).

Controlling the inevitable increase of ice crystals size throughout the ice cream manufacturing process it is mandatory to avoid deterioration of product quality. To this end, two strategies can be adopted: minimize the initial dimensions of ice crystals and/or slow down the recrystallization process.

Conventional methods to achieve these results involve the tuning of processing parameters as well as the use of additives that increase matrix viscosity, therefore limiting water diffusion in between crystals. Ice Structuring Proteins were only recently introduced in ice cream manufacturing for their ability to inhibit ice recrystallization (Crilly, Russell et al. 2008), offering significant advances over previous existing methods.

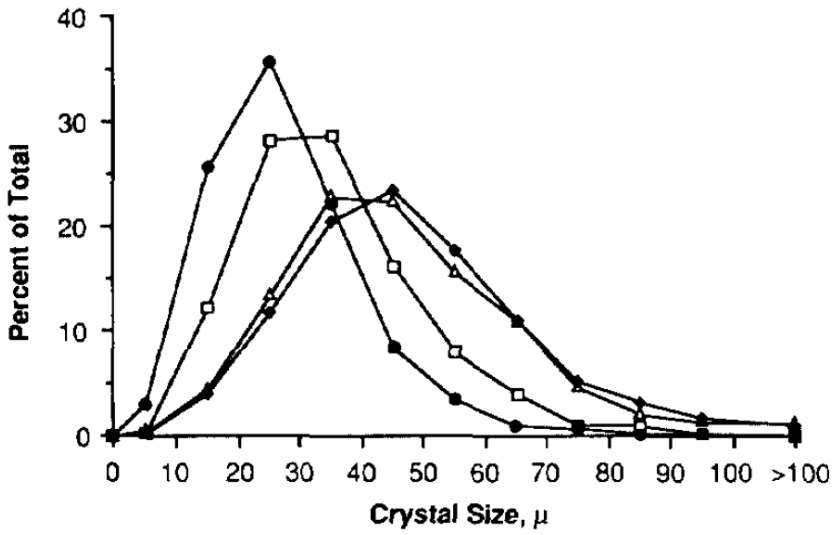

Figure 1.2.4: Ice crystal size distribution of ice cream after drawing (●), hardening (□), 7 (♦) and 14 weeks of storage (△). Adapted from (Donhowe, Hartel et al. 1991)

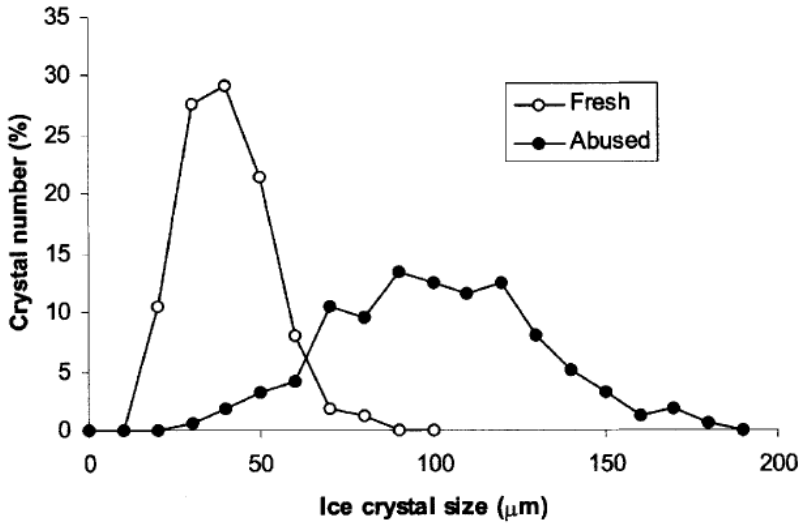

Figure 1.2.5: Ice crystal size distribution in a sample of hardened ice before (○) and after (●) thermal abuse. The abuse treatment consisted in temperature cyclying between -20 °C and -10 °C every twelve hours for 3 weeks. Adapted from (Clarke 2012)

1.1.3. Conventional methods

Among the components of a mix that directly impact on the ice phase of ice cream, sugars, total solids and polymers are the most relevant. While the percentage of total solids determines the amount of freezable water, sugars are added at high concentrations to decrease the freezing point of the mix, determining the ice phase content of ice cream

at a given temperature (Clarke 2012). The role of hydrocolloids is to increase ice cream viscosity and reduce diffusion of water molecules that result in ice crystals growth mediated by recrystallization (Clarke 2012). A hydrocolloid is defined as a suspension of particles in water, where the particles are molecules that bind to water and to one another. Those particles act on the ice cream by reducing its fluidity, solidifying into a gel.

Most common polymers used in ice cream formulations are polysaccharides, such as xanthan and locust bean gum, Carrageenan, etc. Although many of them are extracted from plants, current EU regulation requires them to be declared as additives and declared with E-number.

Polymers increase the solution viscosity at a relatively low concentration (0.2%). Above a certain threshold, reached upon freezing concentration, the increases of viscosity generated by polymers is more pronounced. It was proposed that at low concentrations, each polymer chain acquires the form of a separate coil. While above a threshold concentration (known as the entanglement concentration) the polymers chains begin to overlap and become entangled, resulting in significantly increased viscosity(Clarke 2012).

By controlling a few operational parameters, the production process to obtain ice cream can be designed in order to minimize ice crystals dimensions at the drawing stage. Modern industrial ice cream is produced on scraped surface heat exchangers. Those freezers consist of a barrel with refrigerated walls and a steel dasher that simultaneously agitates the mix and scrape off the layer of ice crystals that forms on the barrel wall. As new mix is pumped in the barrel, at the opposite end the ice cream is drawn at the desired temperture (draw temperature).

Researchers at Unilever found that ice crystallization within the freezer barrel is dominated by recrystallization processes such as accretion and migration (Russell, Cheney et al. 1999). These mechanisms appear to have larger contribution than nucleation events in determining the final average dimensions of ice crystals. It was proposed that coarsening and melt/regrow of larger ice crystals within the barrel can be controlled by 1) reducing the residence time of the mix in the freezer and 2) controlling the release of hea,t resulting from dissipation of frictional energy caused by high dasher speed.

A relatively modern technology to obtain ice cream with smoother texture is called low-temperature extrusion and involve a single screw extruder that replace conventional hardening. This technology consists in the coupling of a traditional scraped surface freezer with an extruder that allow lower draw temperatures (-10 °C). This is made possible because of the lower mechanical energy dissipation experienced by the ice cream within the extruder. Low temperature extrusion leads to a much finer microstructure of air and ice crystals particle. However, it has to be remembered that no protection from ice recrystallization is offered by methods that rely only on improvements of the productive process.

1.1.4. Unconventional methods: Ice Structuring Proteins

The use of ISPs offers several advantages over the conventional methods to control ice recrystallization in ice cream. The most prominent feature of this protein family is their selectivity for the ice phase, which enables their use at extremely low concentrations (parts per millions). Low concentrations mean that ISPs can effectively prevent ice recrystallization without: 1) significantly increase the calorie count, 2) impart unwanted tastes, 3) alter the rheological and textural properties of the system.
From the point of view of marketing, ISPs hold great potential being that they can be extracted from natural sources. This aspect is undoubtedly important for producers of food commodities, when considering that consumer awareness towards natural products is an established trend.

1.1.4.1. ISPs from fish

To date only one ISPs is implemented in commercial ice cream products, the type III AFP from the Ocean pout *M. americanus* (Graether, DeLuca et al. 1999). Since 2003, this proteins was implemented in more than 40 ice cream products, some specifically designed for their use, others representing improved version of existing products (Crilly, Russell et

al. 2008). However, given that this technology was largely implemented in research project controlled by private companies, very scanty information is available on formulations and effects on the final products. Few details about applications of ISPs type III in ice cream are reported in a paper reviewing research conducted at Unilever laboratories (Crilly, Russell et al. 2008).

We know that beyond its ability to control ice recrystallization, AFP type III possess also peculiar ice crystals shaping ability, yielding ice crystals with spicular shapes that result in a highly interconnected network of ice. This network can form microcavities that efficiently encapsulate the matrix phase containing colors and aromas. The result is a frozen product with improved ability to retain color and flavor upon its consuming and melting.

Another great technological advantage offered by ISPs is the improvement of the textural and sensorial qualities of low fat ice creams. Removing substantial quantities of fat comes with increased water content and therefore increased ice phase.

One way to compensate for increased ice phase content would be to decrease the freezing point temperature or increase total solids in the recipe. Those alternatives require the use of sugars or other ingredients that would significantly increase the total calorie count. Being calories reduction the goal of fat removal from food, the abovementioned methods do not represent feasible solutions.

Increased ice content means increased frequency of contacts among ice crystals and therefore higher susceptibility to accretion. ISPs are able to stabilize the conspicuous population of ice crystals in low fat ice cream, that would otherwise coalesce into larger clusters imparting a grainy and unpleasant texture. Extremely low amounts of ISPs are required for this task, with no contribution on the total calories count.

So far, the commercial exploitation of ISPs have been limited by the high costs associated with their production and extraction from natural sources (Venketesh, Dayananda 2008b). Unilever itself, the manufacturer of ISPs type III, patented a method to produce recombinant ISPs from genetically modified yeasts. The GMO status of ISPs has limited so

far its use in Europe and other western countries, where this category of foods has never met general public acceptance.

1.1.4.2. ISPs from plants

Plants hold great promises as viable sources of ISPs; the potential high costs associated with their sourcing might be mitigated by two aspects: 1) plant ISPs are several fold more active in preventing ice recrystallization than all other ISPs, therefore reduced quantities of those proteins will be required to formulate ice cream; 2) they represent a natural source of ingredients that could potentially replace artificial stabilizers and additives. The "natural" status, increases the perceived value of the product for which consumers could be willing to accept higher prices.

ISPs from cold Acclimated Winter Wheat Extracts (AWWE) have been partially characterized by Regand and Goff for their ability to inhibit ice recrystallization in both sucrose solutions and ice cream (Regand, Goff 2005, Regand, Goff 2006b). The addition of 0.25 % total protein from AWWE to a sucrose solution and ice cream mix, resulted in both case in significant inhibition of ice recrystallization, as shown by limited increase of ice crystals size throughout a 5.5 hours period at a constant temperature of – 5°C (**Figure 1.2.6**).

Addition of 0.00375 % of TPE from AWWE inhibited ice crystals growth by 46 % in ice cream samples that underwent thermal shock (temperature fluctuations). This result was confirmed by sensory evaluations of samples; addition of ISPs resulted in thermal shocked ice cream with improved textural properties over control ice cream. Pasteurization didn't affect significantly the recrystallization inhibition activity of AWWE, indicating that the active ISPs are thermo-tolerant. This latter feature is of great advantage for industrial purposes.

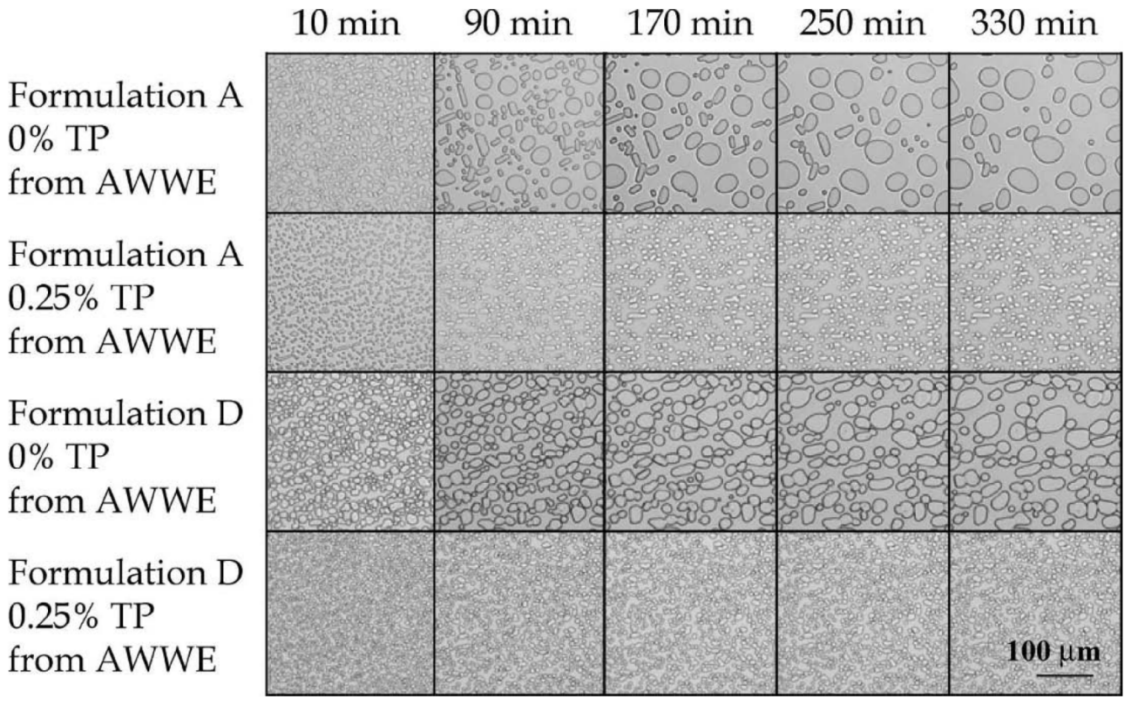

Figure 1.2.6: Brighfield images acquired every 80 minutes at -5°C from sucrose (Formulation A) and ice cream mix (Formulation D), ,formulate with 0 and 0.25% total proteins from AWWE (Acclimated Winter Wheat Extracts). Adapted from (Regand, Goff 2006b)

2. HETEROLOGOUS EXPRESSION OF A RECOMBINANT ICE STRUCTURING PROTEIN FROM WINTER WHEAT

2.1. ABSTRACT

The ability of ISPs to efficiently control ice crystals growth has attracted the interest of frozen food manufacturers since the first AFPs were discovered. To date, the only case of ISP applied to food products is that of Type III AFP from the ocean pout *M. americanus*. Being that extraction of the protein from its natural source poses some challenges at an industrial levels, recombinant Type III AFPs is obtained from yeast fermentation and used to formulate ice creams with improved stability performances.

In an attempt to evaluate alternative ISPs to be used in manufacturing of ice cream, we focused our attention on plants derived proteins, being that the latter were reported to be more effective at preventing ice recrystallization than fish ones. Given the prospective to use the protein in food products, we chose a plant source with a long history of human consumption. The choice fell on a Thaumatin-Like Protein from *T. aestivum* (TaTLP) that was previously reported to efficiently inhibit Ice crystals growth when ice cream was formulated with it (Kontogiorgos, Regand et al. 2007). Its amino acid sequence was retrieved from databases, and the gene cloned in *P. pastoris* for heterologous expression. Structural and functional characterization revealed that the protein was correctly processed and in a folded state. Features typical of other proteins belonging to the Thaumatin-Like (TL) family were observed, such as tertiary structure and enzymatic activity. However, when the protein was tested for its ability to limit ice crystals growth in IRI assay, no significant activity on ice crystals could be detected.

2.2. INTRODUCTION

2.2.1. Thaumatin-Like proteins with ice structuring properties in winter wheat

First reports of ISPs in higher plants came from earlier studies on the freezing survival ability of cold acclimated winter rye (Griffith, Ala et al. 1992). Proteins with ice crystals shaping ability were found to accumulate in the cells apoplast during cold acclimation. Most of the same proteins were also expressed as a result of plant attack by fungal pathogens (Hiilovaara-Teijo, Hannukkala et al. 1999) and treatment with Abscisic Acid (Yu, Griffith 2001) ,but it these last cases lacked Antifreeze activity. Moreover, proteins identical to some ISPs were also detected at lower concentration in apoplastic extracts of non-acclimated plants, which totally lacked Antifreeze activity (Yu, Griffith 1999).

Winter rye ISPs were found to belong to the family of Pathogenesis-Related Proteins and named after their homology with some subclasses of protein: Thaumatin-like, Glucanases and Chitinases (Hon, Griffith et al. 1995). The same ISPs were also found to be expressed upon cold acclimation by other cereals, among which the wheat *T. aestivum* (*Ta*) (Antikainen, Griffith 1997).

Wheat was the first source of plant ISPs to be evaluated for its ability to prevent recrystallization of ice crystals in frozen food products. A commercial source of apoplastic extracts from cold acclimated winter wheat seedlings (Ice Biotech, Flamborough, Canada) was found to be effective in reducing ice recrystallization rate in ice cream by 40%, when used at a final concentration of 0.0025% of total protein (Regand, Goff 2006a). Further investigations on the nature of the Antifreeze active component of the extract, confirmed that the IRI activity was protein mediated as treatment with protease completely extinguished ice crystals growth inhibition (Kontogiorgos, Regand et al. 2007). Size Exclusion Chromatography allowed ultimately the separation of an IRI active protein (21 kDa) from inactive (12.9 kDa) that co-eluted from the initial purification steps (**Figure 2.2.1 A**). The 21 kDa protein significantly inhibited ice crystals growth in IRI assays , while the 12.9 kDa didn't significantly differed from the control buffer (**Figure 2.2.1 B**).

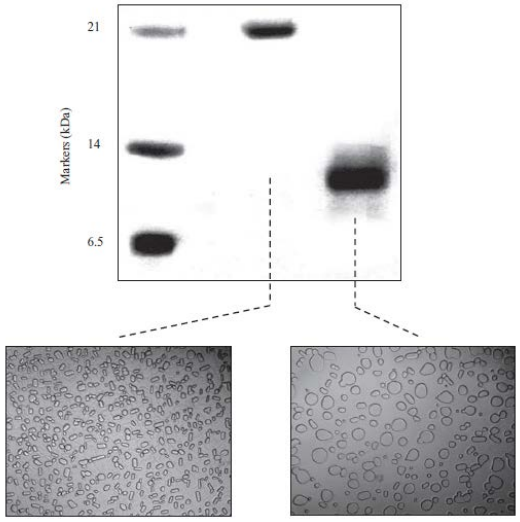

A

Sample	Final crystal size (µm)*
Elution buffer	22.2[a]
Raw extract	16.5[b]
12.9 kDa protein	25.7[a]
21 kDa protein	18.8[b]

*Values with the same letter are not significantly different (P>0.05)

B

Figure 2.2.1: A: Electrophoretic profile and IRI activity of chromatographically isolated proteins from winter wheat extracts; SDS PAGE: left lane, molecular weights; middle and right lane; 10 µg of purified total protein. B: Results of IRI assay performed on 23% sucrose solutions. Values are expressed as ice crystals mean equivalent radius. Purified proteins were tested at a final concentration of 1.25 g/L. Adapted from (Kontogiorgos, Regand et al. 2007).

Mass fingerprinting and sequencing results performed on the 21 kDa protein indicated homology with Thaumatin-Like protein from *Hordenum vulgare* (TLP-6 and 7), *Orzya sativa* (TLP-7) and the strongest homology with *Ta* Q8S4P7 (Uniprot Identifier). Total coverage of *T. aestivum* TLP sequence by peptide fragments was 47% as shown in **Figure 2.2.2**. Q8S4P was previously found to be expressed in winter wheat extracts that were cold acclimated or either treated with Abscisic Acid (Kuwabara, Arakawa et al. 1999). N-terminal sequencing of a winter rye TLP with Antifreeze activity also revealed a 29 amino acid sequence that matched exactly the first 29 amino acid of Q8S4P7.

Interestingly, when recombinant Q8S4P7 was produced in wheat cell cultures, it had antifungal ability but lacked Antifreeze activity (Kuwabara, Arakawa et al. 1999).

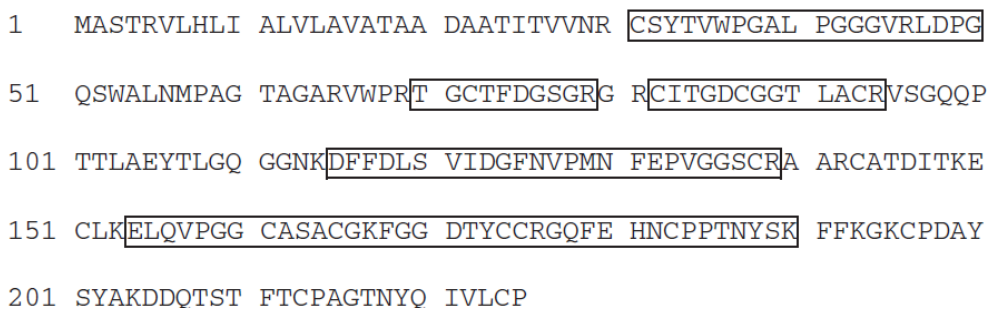

Figure 2.2.2: Results of MS/MS sequencing on 21 kDa IRI active protein. Tryptic peptides that matched Q8S4P7 are boxed. Adapted from (Kontogiorgos, Regand et al. 2007).

Determination of the molecular weight of the IRI active TLP using mass spectrometry revealed that the protein was 21.3 kDa in size, confirming data from SDS-PAGE and MS/MS prediction. The authors reported that protein was not glycosylated. Starting from the observation that IRI activity persisted after the first purification step involving high temperature treatment (75°C for 15'), protein folding was investigated by means of Circular Dichroism (CD) at three temperatures: 5°C, 25°C and 75°C (**Figure 2.2.3**). . On the basis of the observation that the CD spectrum evidenced a negative peak at 222 nm and a positive peak at 195 nm, a hallmark of proteins characterized by high β structures content, the authors concluded that the CD profile could be assigned to a protein rich in β secondary structure.

(**Figure 2.2.3 A**). 4 different secondary structures prediction software predicted that β and random coil structures composed 80-90% of the protein, while α-helical portion accounted for 10% of the signal (**Figure 2.2.3 B**). According to the authors, the structure was generally unaltered at 75°C, the shift of the negative 220 nm peak indicating however that changes may start taking places at this temperature. Being that other ISPs were previously found to contain high amount of β secondary structures, structural analogies were made by the authors with ISP from *Lolium perenne* (Pudney, Buckley et al. 2003) and *A. mongolicus* (Lu, Wang et al. 2002a) as well as beetle AFPs. The analogy with these proteins also extends to the thermostability feature, that allows those proteins to refold and regain their activity after heat denaturation.

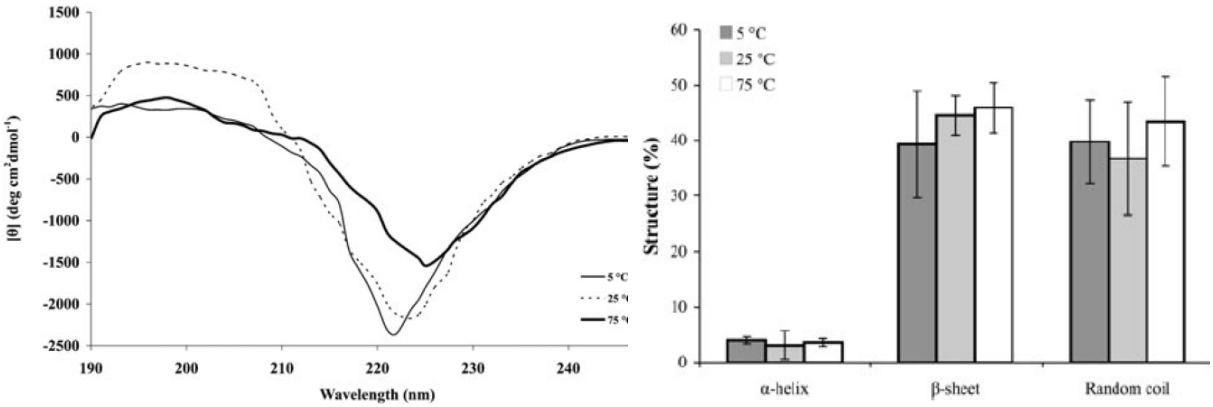

Figure 2.2.3: A: CD spectra of 21 kDa T. aestivum TLP in the far UV at 5°C (ahded), 25°C (dotted), 75°C (bold). Protein concentration was 0.4 g/L. B: Secondary structures estimation from CD data. Mean values from 4 prediction softwares are reported. Adapted from (Kontogiorgos, Regand et al. 2007).

2.2.2. Thaumatin-Like proteins

TLPs are expressed by a large gene family, which is involved in stress response to biotic and abiotic *stimuli*. Traces of TLPs or TLP transcripts were found so far in fungi, plants, insects and animals (Liu, Sturrock et al. 2010). TLPs are polypeptides ranging from 140 to 230 amino acid residues, named after the sweet protein Thaumatin with whom they share peculiar sequence and structural homologies (**Figure 2.2.4**). Most of TLPs shares the family signature PS00316: G-x-[GF]-x-X-x-T-[GA]-D-C-x(1,2)-[GQ]-x(2,3)-C (Liu, Sturrock et al. 2010)(Liu, Sturrock et al. 2010)(Liu, Sturrock et al. 2010)(Liu, Sturrock et al. 2010) and have molecular weights ranging from 21 to 26 kDa (Liu, Sturrock et al. 2010). Those larger TaTLPs contain 16 conserved cysteines, forming 8 disulfide bridges as found in Thaumatin (Kaneko, Kitabatake 1999) (**Figure 2.2.5 A**). Smaller TLPs from conifer and cereals have sizes around 16 kDa and only 10 cysteins due to an internal deletion of approximately 58 amino acids. The network of disulfide bridges is believed to confer to this family of protein high thermal and pH stability as well as resistance to proteolysis (Roberts, Selitrennikoff 1990). Both animal and plant TLPs share a signal sequence at the N-terminal, that targets the mature protein into the secretory pathway

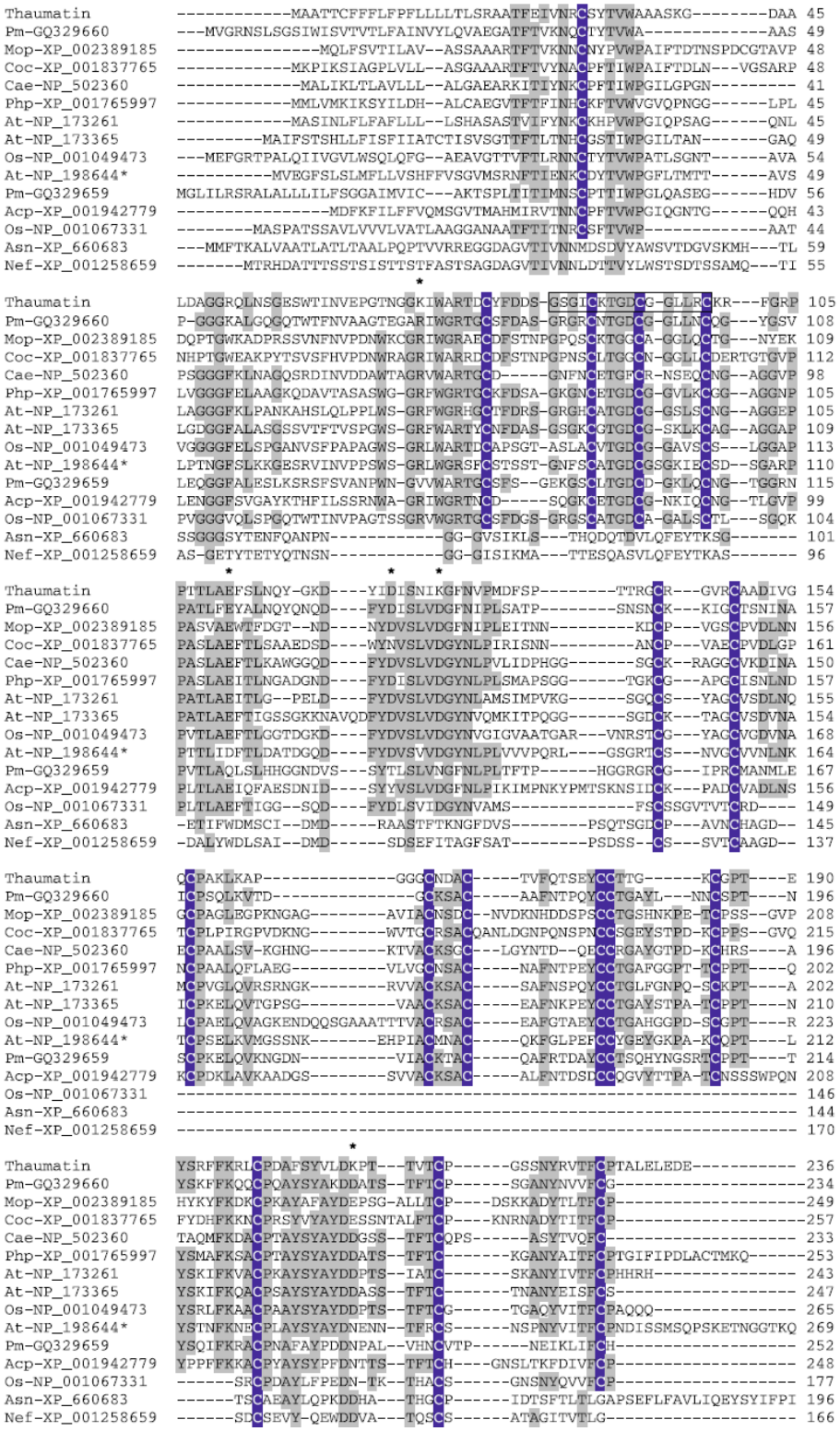

Figure 2.2.4: Sequence alignement of 15 TLPs from different taxa. Thaumatococcus daniellii (thaumatin, AB265690), moss Physcomitrella patens subsp. (XP_001765997), conifer Pinus monticola (GQ329659 and GQ329660), Arabidopsis (NP_173261 and NP_173365 for TLPs, and NP_198644 for PR5K), rice

(NP_001049473 and NP_001067331), nematode (Caenorhabditis elegans, NP_502360), pea aphid (Acyrthosiphon pisum, XP_001942779), basidiomycete fungi Coprinopsis cinerea (XP_001837765) and Moniliophthora perniciosa (XP_002389185), and ascomycete fungi Aspergillus nidulans (XP_660683) and Neosartorya fischeri (XP_001258659). TLP family signature in thaumatin, G-x-[GF]-x-X-x-T-[GA]-D-C-x(1,2)-[GQ]-x(2,3)-C is boxed. Conserved cysteines are indicated by a blue background and other conserved residues by a gray shadow. Conserved positions of 5 residues responsible for topology and surface electrostatic potential around TLP cleft are marked by an asterisk. Adapted from {{142 Liu,J.J. 2010}}

So far, 13 crystallographic structures o TLPs have been deposited in the Protein Data Bank, all of them deriving from plant proteins. The topological structure of those TLPs show a three domain arrangement (**Figure 2.2.5 A**): domain I is a lectin-like β-barrel that constitutes the compact core of the protein, flanked at both sides by Domain I and Domain II made of up respectively of one and several loops. Each domain is stabilized by at least one disulfide bond. Very similar topological model can be derived by homology modelling of other plant TLPs (**Figure 2.2.6 B**)

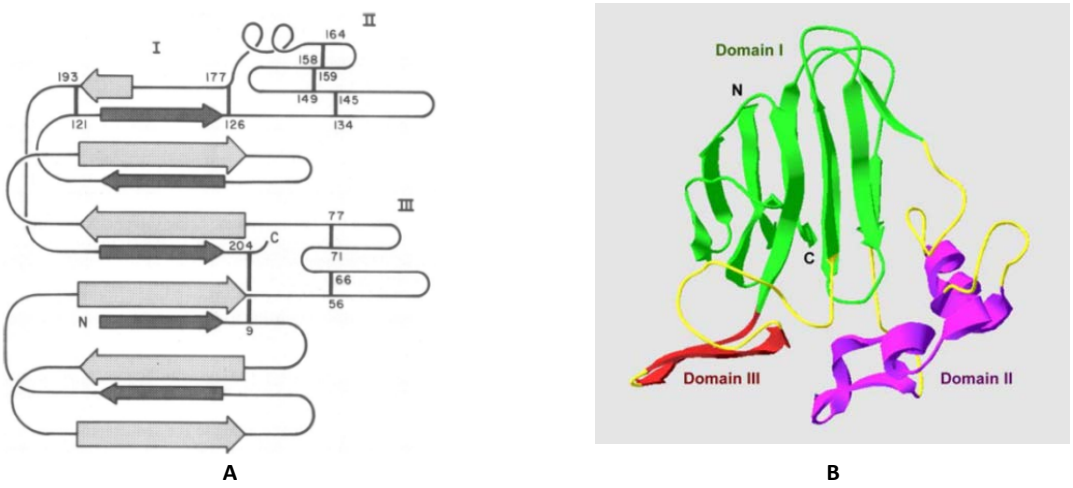

A B

Figure 2.2.5: A: Topological representation of Thaumatin 3D structure derived from crystallographic data: top β-strands are indicated by wide arrows, those on the bottom sheet by a narrow one. The three domain are reported as I (compact core), II and III (loop regions). Disulfide bonds are shown with vertical lines. Adapted from (de Vos, Hatada et al. 1985). B: 3D structure of *Pinus monticola* TLP (PmTLP-L1: GQ329659) predicted by SWISS-MODEL software. Three structural domains are indicated with different colors. Adapted from (Liu, Sturrock et al. 2010)

It is believed that TLPs specificity to their target receptors or ligands is highly dependent on the electrostatic nature of cleft between Domain I and II, which greatly contributes to the observed heterogeneity of function among TLPs (Min, Ha et al. 2004).

In this region, Thaumatin show a unique sequence very similar to some peptide sweeteners (Min, Ha et al. 2004) and predominant basic surface (**Figure 2.2.6 D**). On the contrary, the cleft surface of all plant PR-5 (Pathogenesis-Related) with known antifungal activity is acidic because of 5 amino acids in highly conserved positions (**Figure 2.2.6 A,B,C**). The acidic nature of the cleft was therefore believed to be a determinant for TLP antifungal activity, until it was discovered that other TLP with acidic cleft displayed very low/no antifungal activity (Menu-Bouaouiche, Vriet et al. 2003)

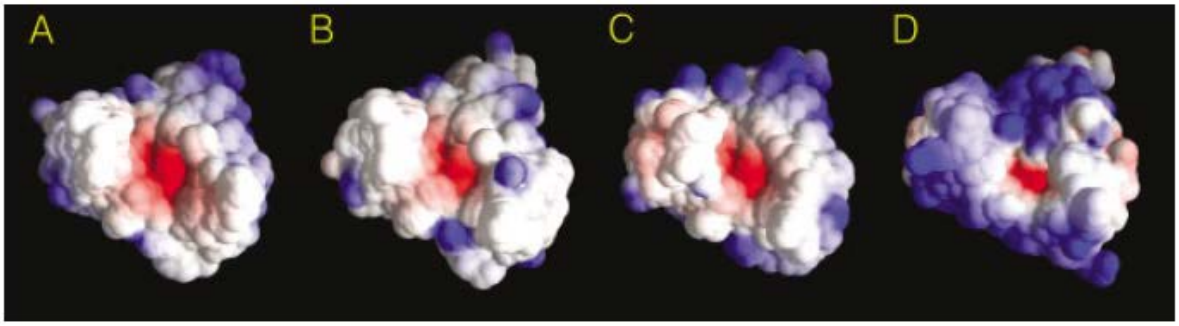

Figure 2.2.6: Surface electrostatic potential of the clefts of osmotin (A), PR-5d (B), Zeamatin (C) and Thaumatin (D). Blue and red represents respectively positive and negative potential. Adapted from (Min, Ha et al. 2004)

It has been reported that several plant TLPs share the ability to bind electively some 1,3-β-glucans (Trudel, Grenier et al. 1998). The binding site is believed to be located within the acidic cleft as suggested by molecular docking of (1,3)-β-D-glucans to TLPs models from tomato and barley (**Figure 2.2.7**) (Ghosh, Chakrabarti 2008, Osmond, Hrmova et al. 2001). When the electrostatic nature of the cleft is predominantly basic, as in the case of Thaumatin, the protein loses the ability to bind glucans (Ghosh, Chakrabarti 2008). There are however evidences that this interaction might be regulated at a more subtle molecular level, being that no significant differences could be found between the residues within the acidic clefts of two *Hordedum vulgare* TLP isoforms HcPR5c and HcPR5b, which respectively bind and do not bind to (1,3)-β-D-glucans (Osmond, Hrmova et al. 2001).

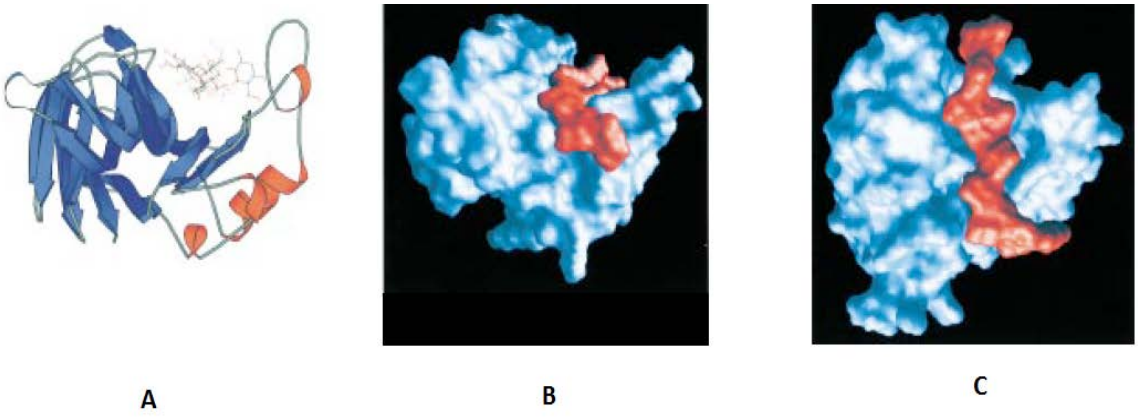

Figure 2.2.7: Location of a (1,3)-β-d-glucan binding site on the surface of HvPR5c. A: Schematic topology diagram of HvPR5c, showing the location of the docked (1,3)-b-d-glucan nonasaccharide in the cleft of HvPR5c. B and C: Models of HvPR5c and the docked (1,3)-b-d-glucan oligosaccharide showing the molecular surfaces in blue and red, respectively. The models are viewed from a side-on aspect (B), and from above the cleft of HvPR5c (C). Adapted from (Osmond, Hrmova et al. 2001)

Furthermore, some of these TLPs were shown to exhibit 1,3-β-Glucanse activity on soluble and insoluble β-glucans (Grenier, Potvin et al. 1999a); it is believed that Glu and Asp residues within the acidic cleft are critical for the cleavage of the glycosidic bond (Ghosh, Chakrabarti 2008). The ability to bind and further process β-glucans by some TLPs was correlated in some cases to their Antifungal activity (Grenier, Potvin et al. 1999b). It was suggested that TLPs reactivity towards β-glucans may exert a toxic effect against fungal species either by degrading their cell wall structure or by sticking to it and blocking hyphal growth. It has to be noted however that β-glucanase activity *per se* doesn't necessarily confer antifugal ability to TLP (Liu, Sturrock et al. 2010).

Another mechanisms by which plant TLP belonging to the PR-5 family are thought to exert their antifungal properties, is the generation of transmembrane pore on the membrane of the microbial host, as in the case of Zeamatin (Roberts, Selitrennikoff 1990). This subject is still a matter of debate and earlier hypothesis on this mechanism envisaged again the involvement of the acidic cleft of antifungal TLP.

Plant TLPs were found to be expressed in response to the attack of pathogens and environmental stress; while in the first case the reason seems obvious given their antimicrobial properties, the latter need more in-depth considerations. Are TLPs required to prevent pathogen attack when the plant is exposed to stress conditions or do TLPs

themselves counteract the physiological stress due to environmental factors? The answer appears to be “both”.

beiTLPs from cold acclimated winter rye and wheat can bind to ice crystals and inhibit and prevent their uncrontrolled growth, which would be otherwise detrimental for the plant at freezing temperatures. Similarly, in the overwintering larvae of *Dendroides Canadensis*, a TLP was found to enhance the Thermal Hysteresis of endogenous AFPs (see next chapter). In addition to enhancing cold tolerance, overexpression of TLPs in transgenic plants improved their ability to cope with salinity and drought stress (Barthakur, Babu et al.). It is believed that new functions were acquired by original PR proteins by gene duplications events followed by mutations (Yeh, Moffatt et al. 2000). This must be the case of winter rye Antifreeze proteins, where TLPs expressed by stimuli other than cold didn’t showed any ice binding activity.

Besides their involvement in plant response to external stimuli, in the case of some fruits the expression of some TLPs was found to be organ specific as well as regulated at the developmental stage level (Van Damme, Charels et al.).

2.3. MATERIAL & METHODS

2.3.1. Cloning in *P. pastoris*

P. pastoris strains, vectors and transformations protocols are the same as described by previous literature from our lab (Reghelin 2011).

Briefly, pGAP was obtained from a pPICαA vector (Invitrogen^{TM}), by replacing the promotor sequence of AOX1 with the *P. pastoris* genomic PCR-amplified sequence of the constitutive promoter PGAP (5’-CACTTGACAGGATCCTTTTTTGTAG-3’ and 3’-CATCGTTTCGAAATAGTTGTTCAATTG-5’ primers were used). The resulting vector pGAPZαA for constitutive expression of protein is reported in **Figure 2.3.1**.

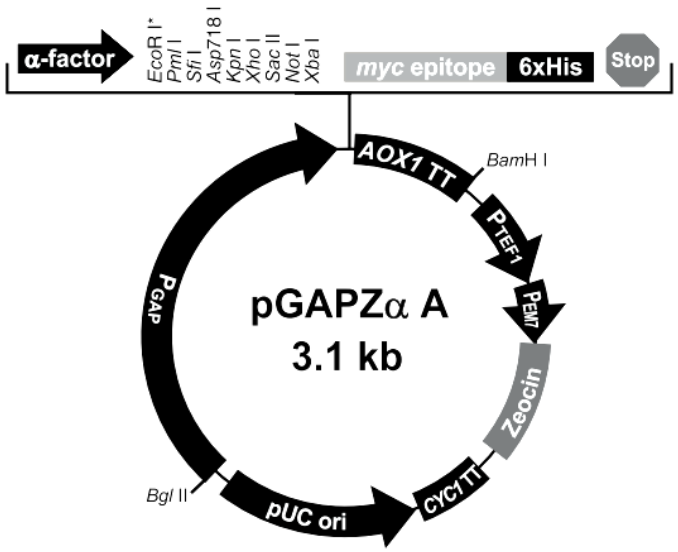

Figure 2.3.1: pGAP vector for constitutive expression obtained from pPICzαA. Pgap: promoter; α-facor: Secretion signal; myc epitope (optional): C-terminal myc tag; 6xHis (optional): His tag; AOX1 TT: AOX terminator; PEM7: promotor; Zeocin:Sh ble gene conferring resistance to Zeocin; cyc1TTT: terminator; pUC ori: replication origin for *E. coli*

The full length TaTLP (fl TaTLP) cDNA was obtained from the amino acid sequence of Q8S4P7 (Uniprot Database) by chemical synthesis (GeneART) with optimization of codon usage for the expression in *E. coli* and *P. pastoris* and flanking restriction sites for XhoI and NotI. fl-TaTLP was inserted in the multiple cloning site after digestion with XhoI and NotI.
The deletion of the 22 aa native signal sequence from fl-TaTLP was obtained by mutagenic PCR directly on pGAPZαA fl-TaTLP. Primers sequences were specifically designed to anneal with vector DNA sequences flanking the deleted portion of fl-TaTLP:

1. <u>*Forward Primer*</u>: GAG AAG AGA GCT ACT ATC ACT GTT GTT AAC AGA TGT TCC TAC AC
2. <u>*Reverse Primer*</u>: GAT AGT AGC TCT CTT CTC GAG AGA TAC CCC TTC TTC TTT AGC AG

Mutagenic PCR was performed on 5-50 µg of plasmidic DNA, in a final reaction mix with 0.2 mM DNTPs, 0.25 µM primers and 1.5 Units of Pfu DNA Polymerase (Promega). The PCR reaction cycle was set as follow: 1’ 90°C, 30’’ 95°C, 1’ 55°C, 6’ 72°C, 5’ 72°C for a total of 15 cycles.
Unmodified plasmid DNA is digested with DpnI for 2h at 37°C.

2.3.2. Protein Expression and Purification

Protein expression in flasks and rich YPD medium was performed as described by the commercial supplier of yeasts and plasmid (Invitrogen Corp 2010). Briefly, transformed *P. pastoris* cells were pre-inoculated from streaks on YPD Agar plates in liquid YPD medium over night at 30°C in agitation, then inoculated at a final optical density of 1 in 10-400 ml of YPD. For TaTLP expression, flasks were kept at 18°C for 3 days at constant agitation in a rotary shaker. After 3 days, yeasts are separated from supernatant by centrifugation at 5000g for 10 minutes at 18°C. To remove residual yeast cells that can clog ultrafiltration membranes, supernatant can be centrifuged at 10000 g for 20 minutes and then passed through a 0.45 µm filter.

When processing large volumes (400 ml or more), a concentration step before Ammonium Sulphate precipitation is preferable. In this case, 400ml Amicon Ultrafiltration stirring device equipped with 10 kDa PLGC membranes (Millipore) is used to concentrate the supernatant to a final volume of 50 ml.

Ammonium Sulphate is added to the supernatant to a final saturation concentration of 60% under stirring and kept on ice for 30 minutes, precipitated proteins are pelleted by centrifugation at 16.000 g for 30' at 0 °C afterwards.

Pellet is resuspended in Sodium Acetate 50 mM pH 5, dialyzed against 100 volumes of the same buffer overnight at 4°C and loaded on a Resource S 6 ml column mounted on an AKTA FPLC system (GE heathcare). A linear gradient from 0 to 50% 1M NaCl in 50 mM Sodium Acetate pH 5 is applied to the column and the protein recovered in total 4.5 ml volume.

This sample is concentrated to a final volume of 0.5 ml and injected in Gel Filtration Superdex g75 10/300 column (GE Healthcare) at a flux of 0.5 ml /minute in 50 mM Sodium Acetate buffer. Protein is eluted in 2 ml and quantified by measuring the Absorbance at 280 nm (ε= 1.305 M-1 cm-1). Protein is brought to the desired concentration with 5 kDa Vivaspin concentrators (GE Healthcare).

Supernatants and samples from each step of the purification are checked for protein quantity and purity by electrophoresis in Tris Tricine gel (13%), SDS-PAGE 12%.

Lysis of *P. pastoris* cells was performed as previously described (Ide, Masuda et al. 2007a). Briefly, the equivalent pellet obtained from 500 µL of a culture at OD_{600} 25, is resuspended in lysis buffer (50 mM Sodium Phosphate pH 7, 1mM EDTA, 1mM PMSF, 5% Glycerol), vortexed with 0.9 g of acid washed 0.5 mm glass beads (Sigma Aldrich) for 30 s and incubated in ice for 1 minute for 10 consecutive times. Supernatant collected after centrifugation at 15000 g for 10 minutes at 4°C contains the cytosolic protein fraction of the cells. Membrane fraction is recovered in the supernatant after resuspending the pellet with 2% SDS and pelleting the insoluble material at 2500 g for 5 minutes at 4°C. TaTLP expression trials in Bioreactor were run fun in a 3L Bioflow 110 (New Brunswick Scientific). Fermentation was conducted as indicated in the guidelines supplied by *P. pastoris* strains and vectors manufacturer (Invitrogen Corp), in 1.5 L of Basal Salt Medium at 18°C. After initial 24h batch phase with glycerol as a carbon source, the culture was switched to Glucose in fed batch mode at a feed rate of 3.6 ml/hour per liter of initial volume and maintained until the end of fermentation

(feeding solution: 550 g/l glucose, 12 ml/l PTM_1). Dissolved oxygen concentration was kept above 20% of total saturation level and pH close to 5, by addition of a solution of Ammonium Hydroxide.

2.3.3. Biochemical characterization

2.3.3.1. Protein Identification by MS spectroscopy

After the last purification step (Gel Filtration), TaTLP was loaded on a C4 column (Phenomenex) and eluted with a linear gradient of 95% Acetonitrile. A 0.7 ml fraction containing TaTLP was collected and either 1) dried on a SpeedVac and loaded on a Tris Tricine 4-20% gradient precast gel (Biorad). After overnight staining with Colloidal Coomassie (0.1% BBG-250, 25% Methanol, 5% Acetic acid), the gel was de-stained with a few washes of MilliQ water to allow protein visualization. The band relative to TaTLP was

cut and sent to Prof. O. Marinat the CRIBI biotechnology center (university of Padova), where it was further digested with Trypsin and analyzed by MS/MS spectrometry.Giorgia De Franceschi (P. Polverino's lab, CRIBI) performed mass spectroscopy measurements (ESI-MS) and data analysis on purified TaTLP.

2.3.3.2. Gel filtration

Gel filtration (GF) experiments for TaTLP size estimation were run AKTA FPLC system (GE Healthcare). TaTLP and standards were diluted in Sodium Acetate 50 mM pH 5 and injected in a Superdex G-75 column at a constant flux of 0.5 ml/min in the same buffer. The following volumes and concentration were used: 100 uL BSA (Bovine Serum Albumin) 1 mg/ml; 100 uL CEA (Chicken Egg Albumin) 1 mg/ml; 100 uL CA (Carbonic Anhydrase) 0.375 mg/ml; 100 uL TaTLP 0.2 mg/ml; 200 uL RA (Ribonuclease A) 1 mg/ml; 200 uL B (Brazzein) 0.34 mg/ml.
All proteins standards were purchased from Sigma Aldrich, except for Brazzein that was previously expressed and purified in recombinant form in our laboratory.

2.3.3.3. Homology modeling and structural prediction software tools

The amino acid sequence of TaTLP retrieved from Uniprot Database (Q8S4P7_WHEAT) without the N-terminal 22 aa secretion signal was loaded as a FASTA file on the web interface form of SWISS-MODEL (swissmodel.expasy.org/interactive). The automatic "build model" tool was launched and a 3D model was chosen among the three whose templates scored the highest sequence homology with TaTLP. The quality of the 3D generated structure was assessed by SWISS-MODEL defined descriptors (such as QMEAN) and by calculating RMSD value obtained by alignment of the PDB of 3D model with template using PyMOL software (Schrödinger).
Electrostatic calculation on the protein surface of the model was performed loading the SWISS-MODEL generated pdb of the model on the pdb2pqr server (nbcr-

222.ucsd.edu/pdb2pqr_1.8/) (Dolinsky, Nielsen et al. 2004), setting all the parameters as default. Results were visualized via the Jmol applet provided by pdb2pqrserver; negative potential was colored red and displayed at -5 *kT* level while positive potential was colored in blue and displayed at +5 *kt* level. Neutral surfaces were indicated in white.

K2D3 software (k2d3.ogic.ca/) was used to predict TaTLP secondary structures content from CD generated data. 41 data points expressing mean residue ellipticity values in the range from 200 to 240 nm obtained from CD spectrum of TaTLP were used to generate the prediction.

The online Structools program (http://helixweb.nih.gov/structbio/basic.html), provided by the Helix System Group at NIH was used as a complementary tool to evaluate secondary structural content from the 3D model of TaTLP. The PDB was loaded via the online data submission interface and calculated secondary structures were output in graphical format.

GetArea software provided by The University of Texas Medical Branch was our preferred choice to obtain calculation of the solvent accessible surface area of TaTLP Tryptophan residues. The PDB of TaTLP model was uploaded via the web interface (curie.utmb.edu/getarea.html) and all parameters for calculation set as default.

PyMOL visualization software was used to generate TaTLP 3D images displaying Solvent Accessible Surface Area (SASA) of the whole protein and for each Tryptophan residue. SASA is usually defined as the surface traced out by the center of a water sphere, having a radius of about 1.4 angstroms, rolled over the protein atoms. To visualize SASA using spheres under the surface visualization tool in PyMOL, the software was instructed with the command:

"alter all,vdw=vdw+1.4

show spheres"

Spheres were colored in dark gray tint and transparency value set to 0.3, while the main amino acid chain was visualized as white lines below the surface. Carbons of Tryptophan were visualized as green sticks and their relative surface accessible area highlighted in green.

2.3.3.4. Circular Dichroism

CD measurements were performed on a JASCO J-715 spectropolarimeter (JASCO inc.) kindly provided by Dr. P.P. de Laureto (University of Padova) equipped with J-700 software for data analysis. Spectra of purified TaTLP at a final concentration of 0.2 mg/ml were obtained in Sodium Acetate Buffer 50 mM pH 5 in 1 mm optical path length quartz cuvette at room temperature. Measurements were performed in the range from 200-260 nm, setting a bandwidth of 2 nm, 4 s time constant and 50 nm/min scansion speed. Signal to noise ratio was minimized by accumulating 4 consecutive scans for each sample. Final spectrum was subtracted of the blank (Buffer alone).

2.3.3.5. Tryptophan fluorescence

Fluorescence measurements were performed on a Cary Eclipse Spectrophotometer (Agilent Technologies) kindly provided by Prof. E. Reddi (University of Padova). Emission spectra of purified TaTLP at a final concentration of 0.125 mg/ml were obtained in MOPS buffer 50 mM, pH 7 at room temp, in 1 cm optical path length quartz cuvette. Excitation wavelength was set at 280nm (slit 10nm) and emission recorded from 300 to 400 nm (slits 5 nm) at a scan rate of 120 nm/minute. The results from 3 consecutive spectra were averaged and corrected for the blank (buffer solution).

2.3.3.6. Elmann's reagent thiol quantification

The protocol was adapted from (Ellman 1959) with minor modifications. Briefly, a 10 mM DTNB solution (Sigma Aldrich) with 0,1M Tris, 1mM EDTA at pH 8.3, is diluted with 50mM Tris, 150 mM NaCl pH 7 to a final concentration of 0.14 mM. One volume of the resulting solution is added to 0.2 volumes of the sample to be quantified or to water/buffer for blank. After 30 minutes of incubation, samples are transferred to a quartz cuvette and Absorbance measured at 412 nm using a diode-array Agilent 8453 UV-visible

spectrophotometer. Free cysteine concentration is calculated as the amount of DTNB that reacted with thiols, assuming a molar extinction coefficient at 412 nm of 13.6 mM^{-1} cm^{-1}.

2.3.4. Functional Characterization

2.3.4.1. Glucan binding assay

5 mg of insoluble β-glucans were weighted on 1.5 ml eppendorf tubes, washed with 200 uL of binding buffer (25 mM Sodium Acetate pH 5) and incubated with 200 µL of 0.2 mg/ml TaTLP, Thaumatin or BSA at room temperature under constant agitation for 1 h in binding buffer. Glucans were then pelleted at 15000 g for 5 minutes and the supernatant collected to estimate the unbound protein fraction. Pellet was washed with 1 ml of binding buffer and then resuspended in 200 uL of electrophoresis denaturing Sample Buffer 1x. After 10 minutes of incubation under vortex agitation, samples were pelleted and supernatant collected to estimate the fraction of protein bound to the resin. Supernatants were boiled for 10 minutes and 20 uL loaded on 13% SDS PAGE. Paramylon, Zymosan , Thaumatin and BSA were purchased from Sigma Aldrich.

2.3.4.2. 1,3-β-glucanase Activity

Glucanase activity on 1,3-β-glucans was detected by quantification of the released reducing sugars using the colorimetric assay DNS for glucose (Miller 1959). Paramylon, Zymosan or Laminarin were added at a final concentration of 1% to 27 uL of 50 mM Sodium Acetate pH 5. 3 uL of 1 mg/ml TaTLP or 1 mg/ml *Helix pomatia* 1,3-β-glucanase were added to the solution and incubated at 37°C under agitation in a rotary microplate shaker (Talboys Microplate Minishaker). 3 µL of Sodium Acetate buffer were added as negative control.

After 24 hours, 30 µl of DNS solution (1% DNS, 0.2% Phenol, 0.05% Sodium disulfite, 1% Sodium Hydroxide) was added 1:1 to the samples and boiled for 5 minutes. The colour

was stabilized by addition of 10 µl of a 40% Potassium tartrate solution to the warm reaction mix and Absorbance measured at 570 nm. A calibration curve was obtained with Glucose Standard solution (0, 0.25, 0.5, 1, 2 g/L). Each measure was blanked against the solution containing the respective β-glucan substrate.

B-glucans, *Hp* glucanase and DNS were purchased from Sigma Aldrich.

2.3.4.3. Ice Recrystallization Inhibition Assay – The Cold Stage

IRI was measured as the ability of a molecule to inhibit progressive growth of ice crystals due to recrystallization processes. The assay was adapted from previous literature reports on the study of IR activity of winter wheat ISPs (Regand, Goff 2005).

Samples are added in a 1:1 volume ratio to a 46% Sucrose solution, then 5 µL are deposited on a cover slip which is gently deposited and pressed on a microscope slide (75 x 25 mm, 1 mm thick) to allow complete dispersion of the sample within the glasses and to avoid air entrapment.

The slide is then laid over the platinum *peltier* of LTS 120 cold stage mounted on a bright filed microscope, previously set at 24°C. The system is closed and purged with Nitrogen or degassed air for 2-3 minutes to remove aqueous vapor. To induce the formation of a homogenous ice crystals population, the sample is quickly frozen at -40°C at a 30 °C/min rate and brought to -5°C stepwise. Samples are kept at -5°C and images are collected after 60 minutes (optionally also at 0 minutes to evaluate the growth rate of ice crystals) by a camera mounted on a microscope with 10x magnification (for temperature cycling details see **Figure 2.3.1**).

For each sample at least 4 photographs representing each a different field of the slide are taken and further evaluated by Image J software (NIH), yielding an average of total 10000 crystals. Ice crystals are automatically detected and measured by the Analyze particle tool (minimum area size threshold: 10 pixel^2, aspect ratio: 0.1-1) (**Figure 2.3.2 A**). Pixels are converted to micrometers by applying a correction factor obtained from calibration measures on a micrometric slide.

Frequency count is performed on the logarithms of the area of ice crystals and the resulting population distribution fitted to a normal distribution (Figure 2.3.2 B). The median value of the distribution is calculated using software Origin Pro 8 Non Linear fitting Tool. One way ANOVA was performed to compare the median area values of ice crystals populations produced by different treatments ($P<0.05$). Cold Stage LTS 120 equipped with Linksys 32 Temperature controlled software, PE-95 system controller and Linkam Imaging station Bright field optical microscope are Linkam Scientific Instruments™ products. The camera used for taking pictures of microscope images is a QiCam Color by Qimaging. All data analysis and visualization were performed using Origin Pro 8 platform (OriginLab). TaTLP was tested at a final concentration of 1.25 mg/ml after addition of sucrose, in Sodium Acetate buffer pH 5 mM and MOPS 20 mM pH 8. FIsh AFPs (type A) (a kind gift of Nichirei Food Company), was dissolved in Sodium Acetate and tested at final concentration of 0.03 g/L

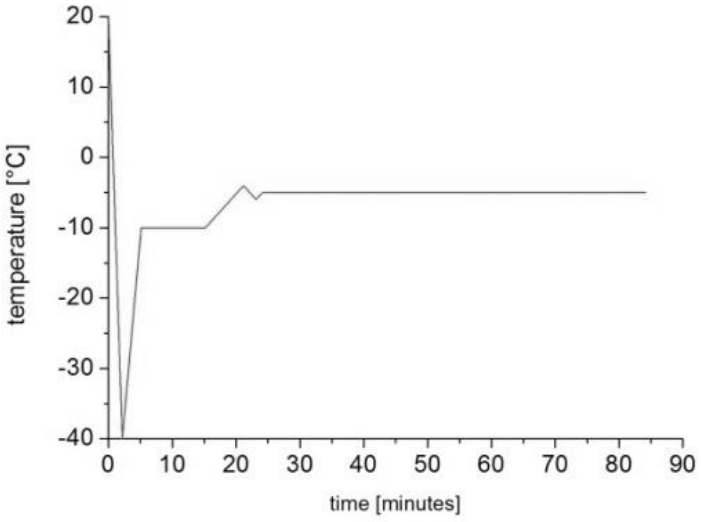

temp [°C]	rate [°C/min]	Time
-40	30	0
-10	10	10
-4	1	0
-6	1	0
-5	1	60

Figure 2.3.1: Temperature cycle applied to sample in IRI assay

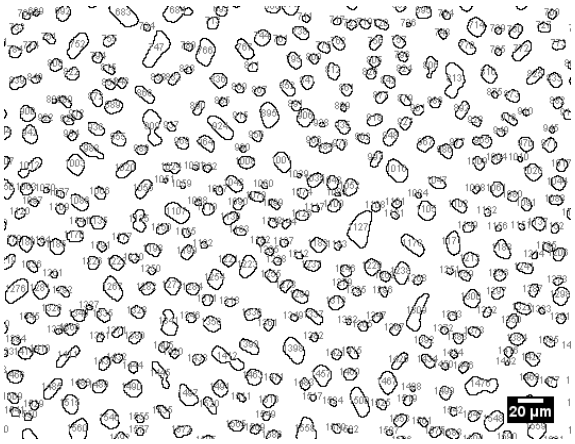

A

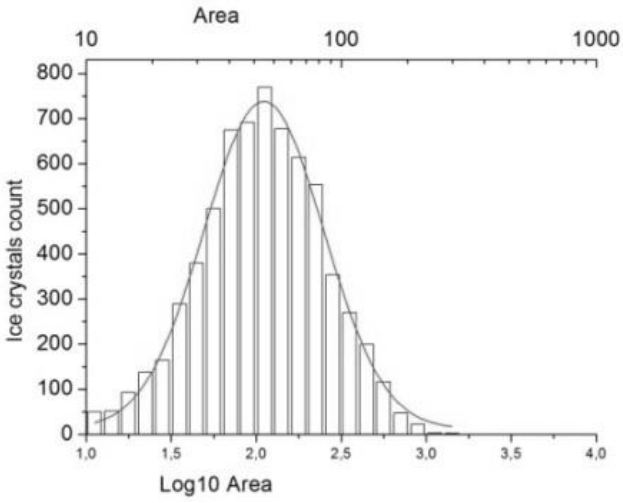

B

Figure 2.3.2: IRI assay Image processing: A: Ice crystals recognition by Image J Analyze particle tool (zoomed area, scale bar 20 µm); B: Frequency count of ice crystals area population (lower scale bar: logarithmic area value; upper scale bar: Area value, Bin size on lower scale: 0.1)

2.4. RESULTS

Previous attempts to express TaTLP in heterologous expression systems gave poor results in terms of protein solubility and expression levels both in bacteria and yeasts (Reghelin 2011). We couldn't obtain soluble TaTLP from *E. coli*, possibly because of its unsuitableness to perform most of the eukaryotic post translational modifications required for proper protein folding such as disulfide bonds. The most critical step in TaTLP protein expression and folding is arguably the formation of the disulfide bonds network found in TLPs (8 cysteine forming non-consecutive S-S bridges, **Figure 2.2.5 A**). A soluble

protein couldn't be recovered even when commercial strain of *E.coli* (Origami) with enhanced disulfide bridges forming capacity were used to express TaTLP.

Switching to a yeast expression system would have allowed us to both 1) overcome the bottlenecks in proteins expression encountered with *E. coli* and 2) obtain the protein from a food grade (Generally Recognizes as Safe, GRAS) source, as this was one of desired outcome of the project. Yeast would also have enabled the possibility to obtain the protein secreted in the culturing media, significantly simplifying downstream processing and protein recovery. *P. pastoris* was chosen over *S. cerevisiae* considering its ability to produce higher protein titers at high density cell cultures (Darby, Cartwright et al. 2012), looking at future perspectives for the scaling up of the process. Constitutive expression was preferred to inducible expression as the latter relies on Methanol, whose implementation in large fermenters and food manufacturing plants can pose serious harm related to its high explosive potential and toxicity.

The amino acid sequence of TaTLP was retrieved from GenBank (AAM15877.1) and cloned into pGAP *P. pastoris* vector in frame with the α-factor pre-pro sequence for extracellular secretion (**Figure 2.4.1**).

Topology prediction software tools predicted a N-terminal 22 amino acid signal sequence (SS) that target the protein into the secretory pathway and it is eventually removed from the mature protein (Perin 2012). This finding is consistent with apoplastic localization of plant TLPs (Griffith, Ala et al. 1992, Hon, Griffith et al. 1995, Hassas-Roudsari 2011). Since it was reported that protein own native signal sequences are in some cases sufficient to ameliorate protein secretion in *P pastoris* (Vadhana, Samuel et al. 2013, Cereghino, Cregg 2000b), α-factor secretion signal was removed from TaTLP gene construct, assuming that secretion was the critical step to obtain the protein.

As showed in **Figure 2.4.2 A**, no differences in protein expression profile at 72h were noticed in culture supernatant when pGAP-α factor TaTLP *P. pastoris* was compared to a clone harbouring an empty vector. In a 7-day monitoring experiment, a protein migrating at approx. 23 kDa was noticed in the supernatant of 5 days cultures (red arrow, **Figure**

2.4.2 B). This protein was later identified as TaTLP (uniprot ID: Q8S4P7_WHEAT) by MS/MS analysis (see Results **Paragraph 2.4.2.1**)

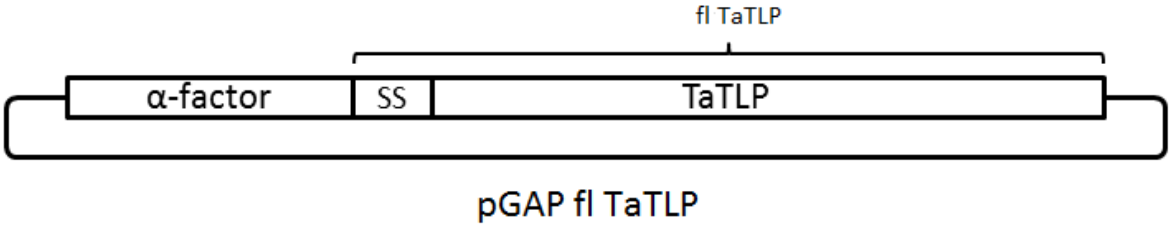

Figure 2.4.1: Schematic representation of fl TaTLP cloned within PGAP vector. *α-factor*: 86 aa; SS (native TaTLP Secretion Signal Sequence): 22 aa; *TaTLP* (mature protein): 204 aa; *fl TaTLP* (full length TaTLP, as predicted by RNA transcript): 226 aa

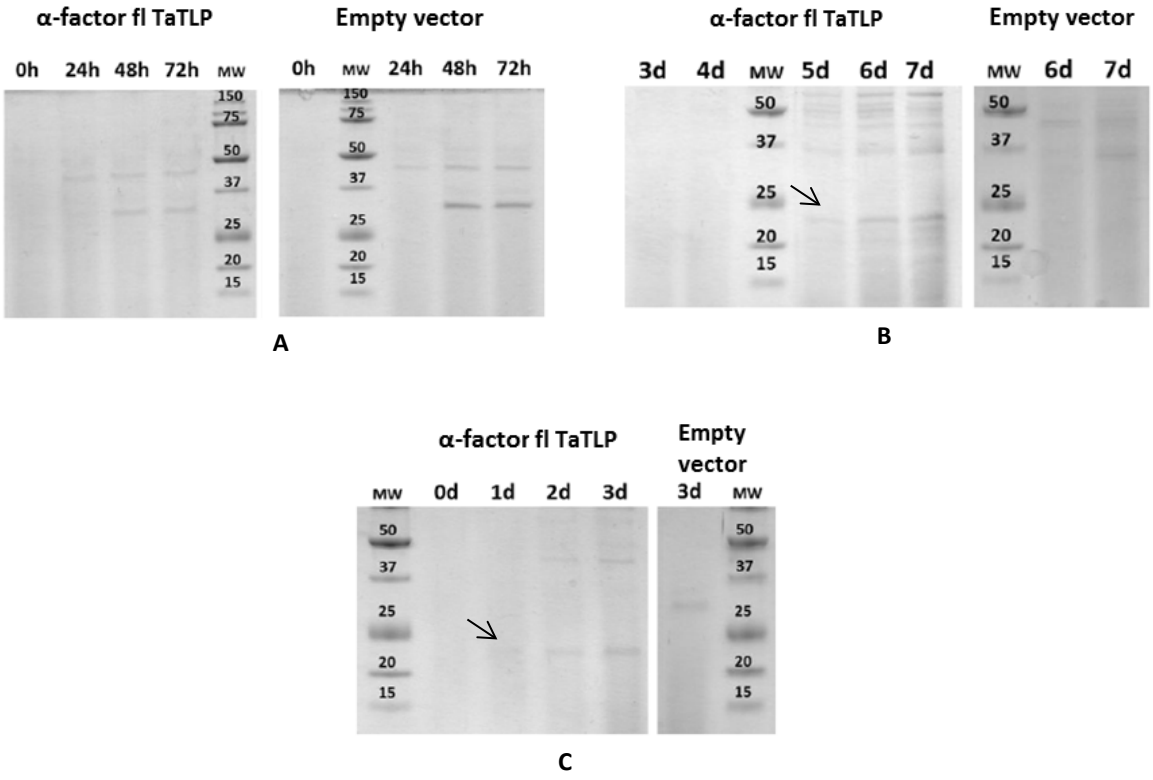

Figure 2.4.2: Time points of P. pastoris cultures supernatant loaded on Tris-Tricine 16% gel (21 ul each sample). A: 30°C, 72h expression, B: 30°C, 7 d. expression, C: 18°C, 3 d. expression. Adapted from (Reghelin 2011)

Even though after 5 days other proteins appeared as well, TaTLP seemed to be expressed at higher level (day 5 and 6), moreover the protein wasn't found in the supernatant of the empty vector control. Since the expression level and activity of a fish AFP was found to be

greatly influence by temperature in *P. pastoris* (Li, Xiong et al. 2001), we evaluated the effect of decreasing cultivation temperature to 18°C on protein secretion levels (**Figure 2.4.2 C**). As a result of temperature decrease, the 23 kDa protein was detectable by Coomassie staining of gel in the supernatant right after 1 day of culturing, as opposites to the 5 days required for its appearance in cultures at 30°C. In the empty vector there was no trace of such protein.

Interestingly, no protein was detected when TaTLP was expressed without the *P. pastoris* α-factor secretion signal; addition of a Histidine Tag at protein C-terminal also resulted detrimental for protein expression since none of the abovementioned constructs yielded positive hits for the 23 kDa protein at 30°C and 18°C.

Given this premises, the objectives of further experimental work were: 1) identify critical steps in protein expression to increase TaTLP productivity, 2) confirm whether recombinant TaTLP purified from culture supernatants had Ice Recrystallization Inhibition activity as reported in literature (Kontogiorgos, Regand et al. 2007).

2.4.1. Expression trials of TaTLP in *P. pastoris*

The observation that TaTLP secretion signal alone was detrimental for protein secretion when α-factor was removed, suggested that the choice of the signal sequence was critical parameter for the optimization of TaTLP expression and secretion by *P. pastoris*.

Moreover, when TaTLP purified protein was characterized by mass spectroscopy, species at higher molecular weights were found, corresponding to isoforms bearing residual amino acids of the signal sequence at the N-terminal (see Paragraph 2.4.2.1). This data were indicative of incorrect processing of protein N-terminal throughout the secretion process.

Thus, we decided to test if the removal of TaTLP native secretion signal would have any positive effect of protein secretion, testing a construct where α-factor was cloned in frame with the mature sequence of the protein (**Figure 2.4.3**).

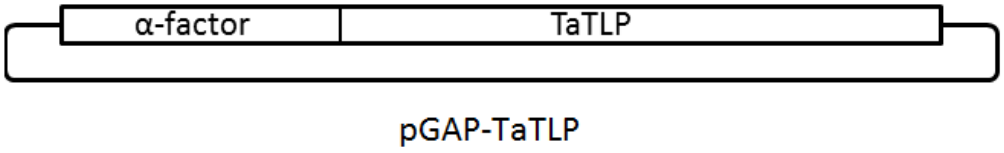

Figure 2.4.3: Schematic representation of TaTLP cloned within PGAP vector. *α-factor*: 86 aa; *TaTLP* (mature protein): 204 aa;

We also evaluated if variables such as proteolytic degradation and medium pH could influence the stability of the TaTLP within the supernatant.

2.4.1.1. Protein expression optimization

The first striking evidence noticed after SS removal from *fl TaTLP*, was the dramatic decrease of yeast cells viability. **In Figure 2.4.3**, the OD_{600nm} of *P. pastoris* cultures transformed with either pGAP fl TaTLP or PGAP TaTLP, cultivated at 30°C and 18°C are shown.

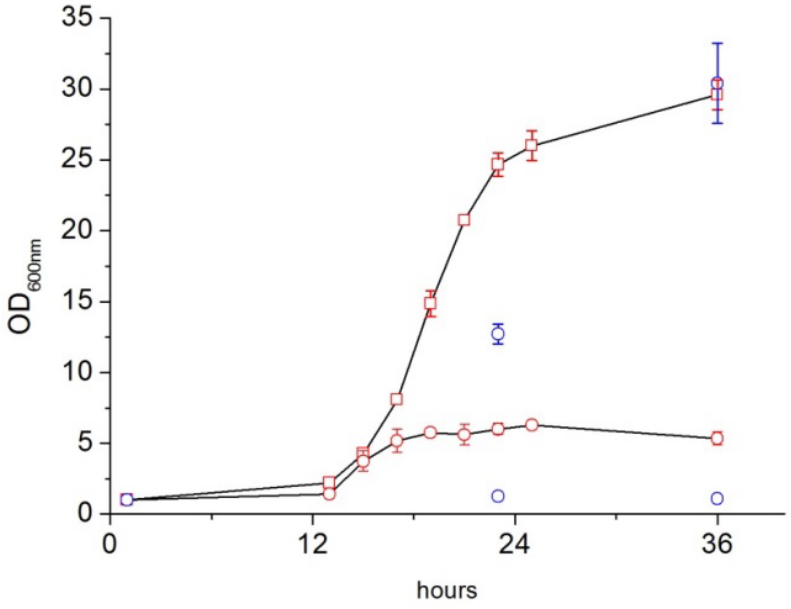

Figure 2.4.3: Growth curves of *P. pastoris* cultures in flask in YPD medium, at 18°C (blue) and 30°C (red). □: *pGAP-fl TaTLP*; ○: *pGAP TaTLP*. Optical density measured at 600nm is plotter against time points. Time point sampling was limited at three event in the case of 18 °C cultures, to compensate for the effect of growth perturbation at each sampling. Data are means of duplicate measurements on two different clones.

SS deletion results in cells reaching a maximum density at 30°C, which is only 21% of the maximum value obtained with fl TaTLP. At 18°C, yeast growth in TaTLP transformed yeasts is practically halted , while lower temperature only caused slower growth kinetics on *P. pastoris* cells transformed with the fl TaTLP gene. As predictable, inhibited growth of *P. pastoris* cells at 18°C transformed with pGAP fl TaTLP resulted in no detectable TaTLP protein in supernatant of 3 days cultures (Lane 2, **Figure 2.4.4**)

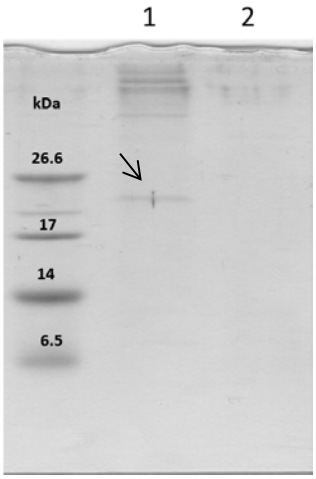

Figure 2.4.4: Supernatant of 18°C 72h *P. pastoris* cells transformed with 1) pGAP fl-TaTLP, 2) pGAP TaTLP. 21 uL samples loaded on 16% Tris Tricine gel. Arrow highlights the protein migrating at 23 kDa expressed by pGAP fl-TaTLP clone.

The hypothesis that *P. pastoris* growth inhibition was caused by an incorrect integration event of pGAP vector within *P. pastoris* genome, was excluded by screening multiple clones and by repeating the transformations a second time. Speculating about the possibility that the removal of the secretion signal from full length TaTLP could result in a low efficiency protein secretion and retention by *P. pastoris*, we investigated TaTLP presence in cytosolic and membrane fractions of lysed yeast cells.

No protein appeared to be significantly expressed and retained in the cytosolic/membrane fraction, as no significant band were detected in the gel at the expected molecular weight (**Figure 2.4.5**); for comparison, purified TaTLP was loaded in the gel (ctr).

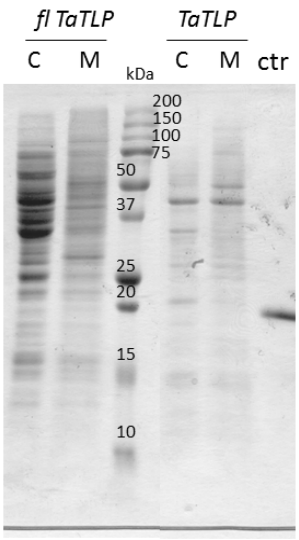

Figure 2.4.5: *P. pastoris* cells harboring the fl TaTLP or TaTLP gene construct were cultivated for 3 days at 18°C and lysed. *C*: cytosolic fraction; *M*: membrane fraction; *ctr*: recombinant TaTLP purified from the supertant of fl TaTLP cultures. See materials and methods (Paragraph 2.3.2) for details of samples processing. 10ul samples were loaded on 13% Tris Tricine gel. The slight increase of electrophoretic mobility of TaTLP (ctr), in this case migrating at approx. 20 kDa, could be due to the intrinsic variability between acrylamide gels (16% Tris tricine PAGE vs 12% SDS PAGE)

Up to this point, of all the experiments that were run on the effect of α-factor and SS on protein levels in the supernatant of *P. pastoris* cultures, the only genetic construct that yielded recombinant TaTLP was the pGAP fl-TaTLP, i.e. the full length TaTLP amino acidic sequence cloned in frame with *S. cerevisiae* α-factor. The protein levels though were significantly lower than what we have previously experienced with other proteins (Reghelin 2011). We've already ascertained that low TaTLP titer in the supernatant wasn't caused by faulty secretion responsible for protein retention inside cells, as no significant protein band appeared in cytosolic and membrane fractions of *P. pastoris* lysates (**Figure 2.4.5**, fl-TaTLP). So far, TaTLP secretion in the supernatant was achieved only at two conditions: 1) at 30°C after 5 days of cultivation, 2) at 18 °C right after 24 hours. Those evidences suggested that besides low temperature, also acidic pH cloud have a substantial contribution to protein accumulation in the extracellular compartment. 5 days cultures of *P. pastoris* at 30°C were in fact found to acidify the medium to pH 3. Low pH values and temperatures are known to be suboptimal conditions for microbial protease activity (Salamin, Sriranganadane et al. 2010); furthermore the release of endogenous proteins by

P. pastoris cells was reported to be one common cause of low secreted proteins levels. Even though this phenomenon is more pronounced at high cells density (e.g. fermentation in Bioreactors) (Sinha, Plantz et al. 2005), we decided to investigate if TaTLP stability in *P. pastoris* supernatants could account for its low titer, by evaluating the potential contribution of *P. pastoris* endogenous proteases at different pH. Purified TaTLP was incubated with the supernatant of 48h cultures of *P. pastoris* transformed with pGAP fl-TaTLP, buffered at pH values from 4 to 7. To denature and exclude protein degradation by potential endogenous *P. pastoris* proteases released in the medium, supernatants were boiled for 10 minutes. Samples were incubated over night at 18°C to simulate the culture conditions and residual TaTLP levels evaluated by visual examination of SDS PAGE gels (**Figure 2.4.6**). The pH interval was chosen within the maximum pH activity range reported for *P. pastoris* (Sinha, Plantz et al. 2005). Levels of purified TaTLP weren't significantly influenced after overnight incubation in boiled (100°C) supernatants. No proteolytic product appeared at lower molecular weights when TaTLP was incubated with unboiled supernatants and protein levels didn't seemed to be affected consequently (**Figure 2.4.6**). Moreover, proteins yield after 3 days of cultivation at 18°C did not increase even when alternative substrates for proteases were supplied in the growing medium (Casamino acid, 1%) (data not showed) (Werten, van den Bosch et al. 1999). We could ultimately conclude that proteases secreted in the supernatant weren't likely to be the cause of the observed low levels of recombinant TaTLP.

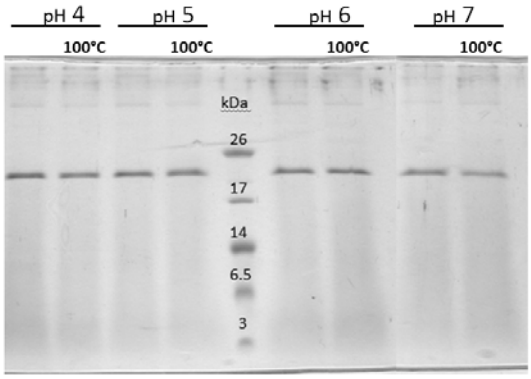

Figure 2.4.6.: Analysis of protein stability in 48h *P. pastoris* supernatant. Purified TaTLP was added at a final concentration of 25 µg/ml. 20 ul of total samples were loaded in 16% Tris Tricine gels. pH values of supernatant were obtained as described in materials and methods. 100°C indicate supernatants that were boiled before incubation with TaTLP.

In our previous experience, fermentation in a bioreactor enabled *P. pastoris* to reach higher cell densities that it turn resulted in significantly increased levels of recombinant protein in the medium (Reghelin 2011).

Cultivation of a *P. pastoris* pGAP fl-TaTLP transformed strain was performed in a 3L bioreactor in 1.5 L of Basal Medium Salts, with a constant feeding rate of Glucose as the carbon source, at constant pH (5) and temperature (18°C).

Supernatants were collected at intervals of 24h and loaded in acrylamide gel to check for TaTLP production (**Figure 2.4.7**). A 72 hours supernatant from 400ml cultures in flasks with YPD medium was also loaded to compare final levels of TaTLP. Optical density of *P. pastoris* cells obtained with the two cultivation methods are shown in **Figure 2.4.7**.

The use of a Bioreactor did not increase significantly the levels of TaTLP in the supernatant in comparison to the standard flask cultivation method, even though cells density was increased by almost 4-fold. Along with poor TaTLP productivity, the Bioreactor cultivation system appeared also to be associated with more protein species in the supernatant, resulting in lower purity of TaTLP. This could be due to the lysis of a small fraction of cells associated with *P. pastoris* high growth rate at high cell density, resulting in the release of endogenous proteins.

Considering the complexity associated with the adoption of a Bioreactor-based workflow and the poor productivity experienced with TaTLP, we opted for the ease of use of the flask cultivation system for the further experimental phases.

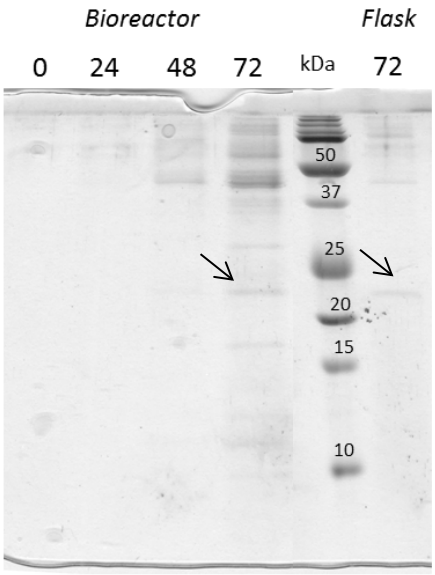

Figure 2.4.6.: Supernatants of *P. pastoris* cultures expressing fl-TaTLP obtained in bioreactors (0-72h) and flasks (72h). The arrow highlights TaTLP.

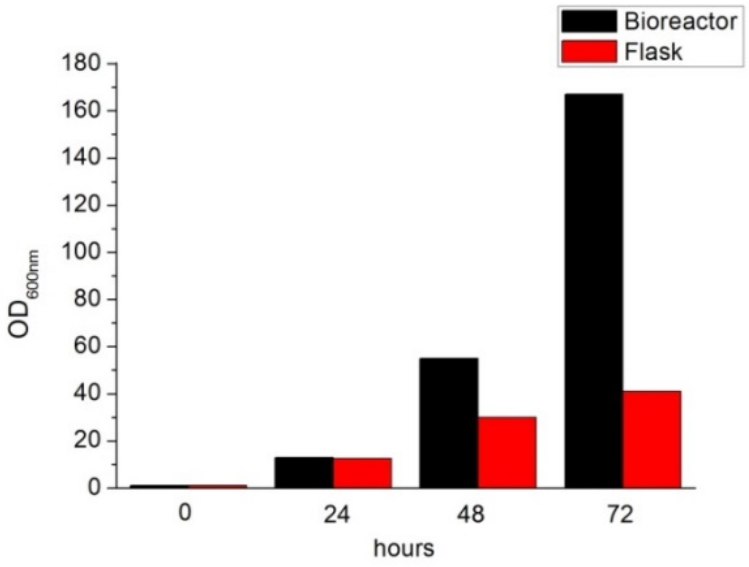

Figure 2.4.7: Cell cultures Optical density measured at 2h intervals.

2.4.1.2. Protein purification

The pGAP fl-TaTLP was the only gene construct that in our hands secreted soluble TaTLP once cloned in *P. pastoris*. A 400 ml culture of this strain in YPD medium was used as the source of TaTLP for the following purification steps (see this chapter material and methods paragraph for details).

The setting up of a viable purification process for TaTLP was complicated by absence of any molecular tag, since addition of a His tag at the C-terminal have been shown to be detrimental for protein expression (Reghelin 2011).

Figure 2.4.8.A depicts a flow chart of TaTLP purification, starting from *P. pastoris* culture supernatant. TaTLP enrichment was checked at each step in Tris Tricine gels (**Figure 2.4.8.B**).

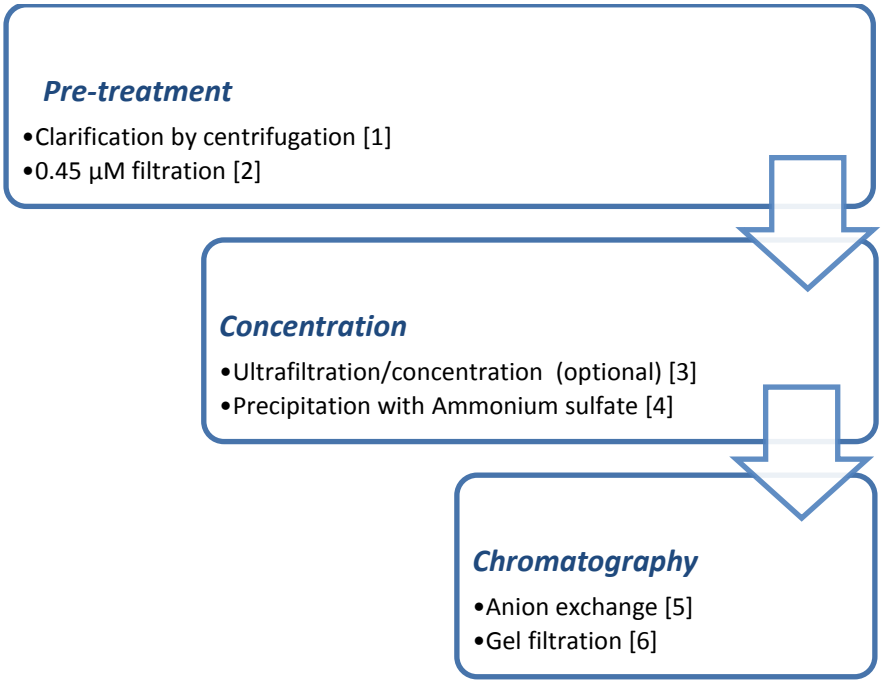

Figure 2.4.8.A: TaTLP purification workflow from *P. pastoris* cultures supernatant

After the last purification step [6] 0.8 mg of TaTLP were obtained from initial 400 ml cultures. TaTLP purity at this step was approx. 98% as estimated by RP-HPLC chromatography (**Figure 2.4.9**).

The yield of the whole process was thus calculated to be 2 mg per liter of initial culture. TaTLP solution at a final concentration of 1.5 g/L was snap frozen in liquid Nitrogen and stored at -80 °C until use.

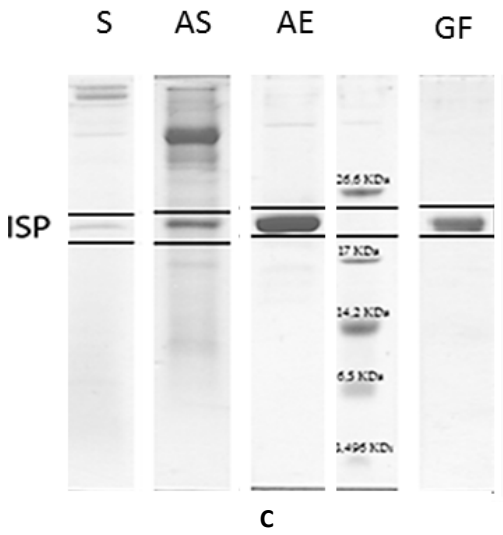

Figure 2.4.8.B : *S*: 72h supernatant; *AS*: 60% Ammonium sulfate pellet; *AE*: TaTLP enriched fraction from Anion exchange chromatography; GF: TaTLP enriched fraction from GF chromatography.

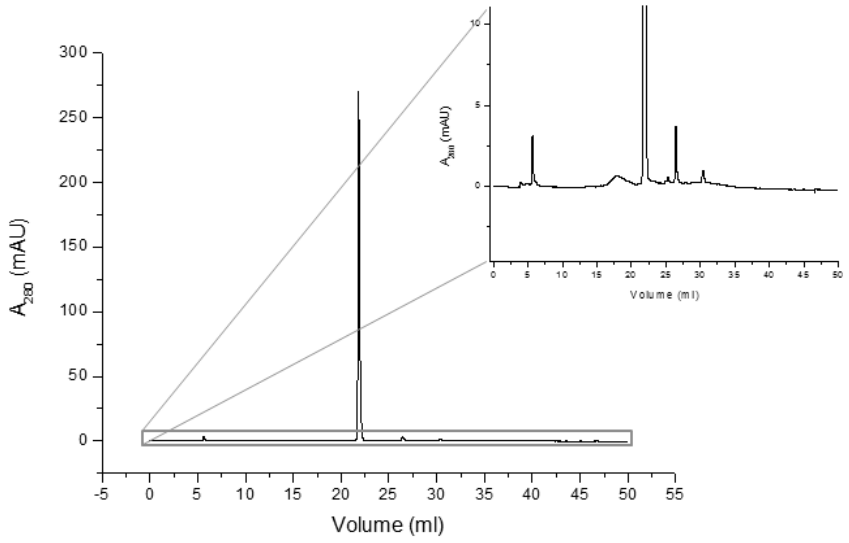

Figure 2.4.9: RP-HPLC of purified TaTLP after purification step [6].

2.4.2. Biochemical characterization

2.4.2.1. Protein Identification by MS/MS and MS

Purified recombinant TaTLP was obtained by cutting the relative band from Tris Tricine gel after gel filtration (**Figure 2.4.8**, Lane GF) and further digested with Trypsin for MS/MS analysis. The results of tryptic fragment analysis were launched against the Uniprot comprehensive and non-redundant database.

12 peptides were found to match the amino acid sequence of the wheat Thaumatin-Like Protein Q8S4P7, covering 81% of the total length of translated transcript (**Figure 2.4.10).**

{MASTRVLHLIALVLAVATAADA}ATITVVNRCSYTVWPGALPGGGVRLDPGQSWALN
MPAGTAGARVWPRTGCTFDGSGRGRCITGDCGGTLACRVSGQQPTTLAEYTLGQGGN
KDFFDLSVIDGFNVPMNFEPVGGSCRAARCATDITKECLKELQVPGGCASACGKFGGDT
YCCRGQFEHNCPPTN*YSKFFKGKCPDAYSYAKDDQTSTFTCPAGTNYQIVLCP

Figure 2.4.10: Amino acid sequence of *Triticum aestivum* TaTLP as predicted from cDNA (Uniprot Q8S4P7_WHE). In red is highlighted the part of the sequence covered by MS/MS analysis of recombinant TaTLP. The 22 aa secretion signal sequence is enclosed within brackets. Asparagine 187 within the predicted glycosylation motif (underline) is indicated by an asterisk.

Mass Spectroscopy performed on the purified intact protein eluted from RP-HPLC after GF (**Figure 2.4.9**) confirmed that the most abundant species in the sample has a MW of 21393 Da, consistent with the MW calculated from the cDNA predicted transcript of TaTLP without the 22 aa secretion signal sequence and all the 16 cysteines forming disulfide bridges (21392 Da). Other species with higher molecular weight were found (**Table 2.4.1**); we interpreted this data as the result of oxidation events and incorrect or inefficient TaTLP own signal sequence processing by *P. pastoris*.

Species	**MW** *(MS data) [Dalton]*	**Predicted modification**	**Predicted MW** [Dalton]
1	21393,3 ± 0.6	TaTLP w/o 22a signal sequence and all cysteines forming disulfide bridges	21392
2	21409.2 ± 0.3	Species 1 + 1 oxidation [+ 16 Da]	21409
3	21424 ± 0.5	Species 1 + 2 oxidations [+32 Da]	21424
4	21734.3 ± 1.5	Species 2 + AADA peptide left at N-term [+340 Da]	21737
5	22093 ± 1.6	Species 2 + AVATAADA peptide left at N-term [+688 Da	22094

Table 2.4.1: Mass spectroscopy data of purified TaTLP

Variability of N-terminal amino acid composition is not uncommon with *P. pastoris* when the α-factor mediated secretion system is adopted (Cereghino, Cregg 2000a) especially when conflict between different signalling sequences could arise. In this case the presence of both yeast and plant endogenous secretion signal sequences couldn't be avoided, being that the combination of α-factor + TaTLP secretion signal (**Figure2.4.1**) was the only condition that enabled successful TaTLP expression with *P. pastoris*.

Oxidations events are likely to account for MW increases of 16 and 32 Da, possibly due to spontaneous oxidation of methionine residues occurred during protein handling and storage before MS analysis.

When a NetNGlyc 1.0 and NetOGlyc 4.0 online software (*cbs.dtu.dk/services/NetNGlyc*) were launched against TaTLP mature sequence, a potential N-glycosilation site was predicted at Asp187 (see **Figure 2.4.9**). MS analysis however did not revealed species with molecular weight increases compatible with the addition of glycan structures (8-10 mannose residues, 1440-1800 kDa) as typically observed for fungal glycosylated proteins (Cremata, Montesino et al. 1998).

2.4.2.2. Size estimation by Gel Filtration

The possibility that TaTLP could acquire multimeric conformations in solution was inquired by means of GF chromatography. Low to medium molecular weight protein standards were run to obtain indications of TaTLP size in solution. Results are reported in **Figure 2.4.11**.

TaTLP elutes between Carbonic Anhydrase (29 kDa) and Ribonuclease A (13.7 kDa); this data are consistent with TaTLP being in the monomeric state at the tested conditions.

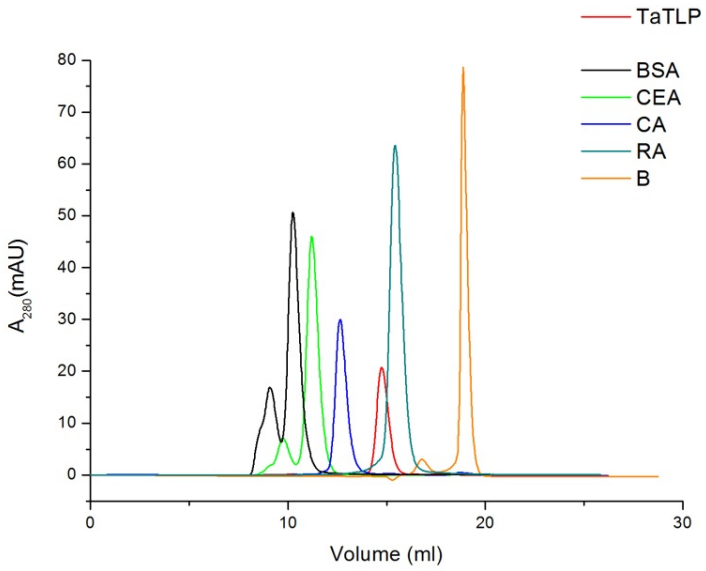

	MW expected [kDa]	Elution vol. [ml]
BSA	66	10,24
CEA	44,2	11,2
CA	29	12,64
TaTLP	21,3	14,73
RA	13,7	15,4
B	6,5	18,8

Figure 2.4.11: GF elution profiles of TaTLP and standards (Superdex G-75 column)

2.4.2.3. Circular Dichroism, homology modelling and secondary structure prediction

CD spectrum of TaTLP in the near-UV was obtained to gain insights about the folding of the protein (**Figure 2.4.12**). Two common features with other CD spectra form TL proteins were observed: negative predominant peak at around 210 nm and a cross over at 202 nm (Fuchs, Bohle et al. 2006)(Perri, Romitelli et al. 2008)(Perri, Romitelli et al. 2008)(Perri, Romitelli et al. 2008)(Perri, Romitelli et al. 2008). The weak positive band usually found in zeamatin and thaumatin is absent in this case, being replaced instead by slight negative signal at 237 nm and resembling better the spectrum of a beta strand rich protein (Perri, Romitelli et al. 2008).

K2D3 was used to estimate the relative contribution of α and β secondary structures to the experimental CD data (Louis-Jeune, Andrade-Navarro et al. 2012). K2D3 predictions rely on the assumption that the CD spectra of two proteins that have similar secondary

structures content will be also very similar, so given the CD spectrum of a protein for which the crystallographic structures is known, proteins with similar CD spectra are likely to share common structural features. To overcome the limitation of the low number of available verified CD spectra in databases, K2D3 takes advantage of the improved accuracy of modern predictive software such as DichroCalc (Bulheller, Hirst 2009), that can calculate CD spectra from protein crystallographic data publicly available in Protein Data Bank.

Given the experimental CD spectrum of a protein, K2D3 software can compare it to all the theoretical CD spectra available in databases and estimate the query protein's proportion of secondary structures from those of the most similar spectra (Louis-Jeune, Andrade-Navarro et al. 2012). **Figure 2.4.13** shows the output of K2D3 analysis: the green dataset represent the input CD spectrum normalized for protein length (202 aa) while in red the closest CD spectrum as predicted by DichroCalc calculations is reported. The predicted contribution of α and β structures to TaTLP CD spectrum (Figure 2.4.11), were estimated by K2D3 software to be respectively 13 and 30 %.

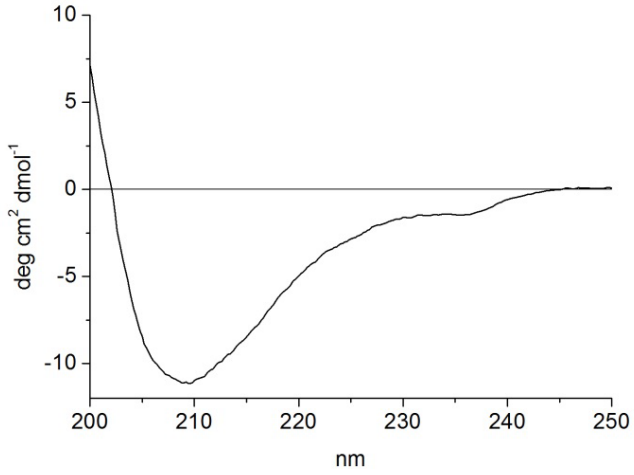

Figure 2.4.12: Far UV CD spectrum of 0.2 mg/ml TaTLP in Sodium Acetate Buffer 50 mM, pH 5. Spectrum was obtained on a Jasco J-715 as a mean of 4 consecutive measurements.

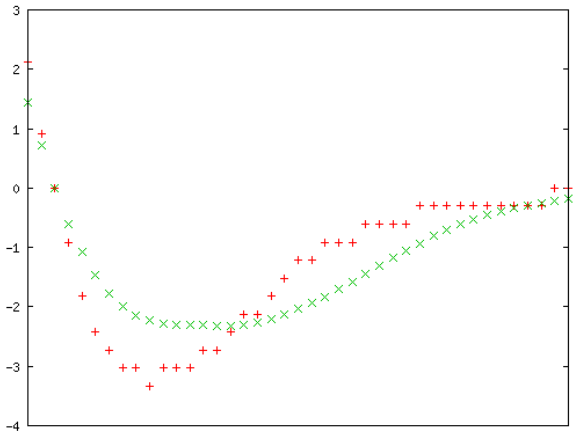

Figure 2.4.13: Visual output of K2D3. *Red*: Experimental CD spectrum of Figure 2.4.11 A (normalized); *Green*: template CD spectrum retrieved by the software.

A 3D model for TaTLP was generated from SWISS-MODEL to validate the secondary structures prediction obtained from CD data (**Figure 2.4.14 A.I**). Among the homologous protein for which structural data were available, two TLP sequences scored the highest identity (62%) with TaTLP amino acid sequence: a banana Antifungal TLP (PDB 1z3Q) and a Kiwi allergen TLP (PDB 4bct.1). The first was chosen as the template to build the 3D model as also structural-functional correlation data were available for this protein (Leone, Menu-Bouaouiche et al. 2006). The structural alignment of the generated model (green) with the template (magenta) yielded a global RMSD of 0.214 Å (**Figure 2.4.14 A.II**). Total quality of the overall model (Z-score: -2.04) as well as that relative to local regions was evaluated as a function of QMEAN4 values and represented on the model in a two color code:red and blue respectively indicating poor and well modelled region in comparison to the template . Visualization of the electrostatic potential on the protein surface revealed the presence of a localized pronounced electronegative region within the cleft of between Domain I and II (**Figure 2.4.14 B.I**)

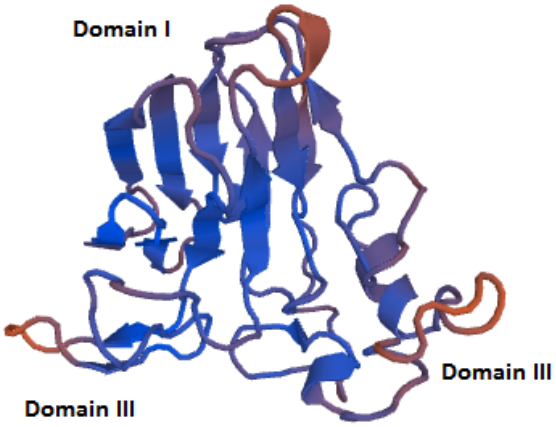

I

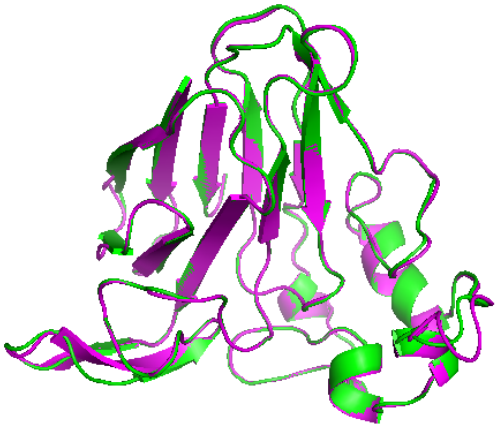

II

```
Model_03 ATITVVNRCSYTVWPGALPGGGVRLDPGQSWALNMPAGTAGARVWPRTGCTFDGSGRGRCITGDCGGTLACRVSGQQPTTLAEYT
1z3q.1.A ATFEIVNRCSYTVWAAAVPGGGRQLNQGQSWTINVNAGTTGGRIWGRTGCSFDGSGRGRCQTGDCGGVLSCTAYGNPPNTLAEFA

Model_03 NKDFFDLSVIDGFNVPMNFEPVGGSCRAARCATDITKECLKELQVPGGCASACGKFGGDTYCCRGQFEHNCPPTNYSKFFKGKCP
1z3q.1.A NLDFFDISLVDGFNVPMDFSPTSGGCRGIRCAADINGQCPGALKAPGGCNNPCTVFKTDQYCCN---SGACSPTDYSQFFKRNCP

Model_03 AKDDQTSTFTCPAGTNYQIVLCP
1z3q.1.A PKDDQTTTFTCPGGTNYRVVFCP
```

III

Figure 2.4.14 A: I: SWISS-MODEL derived 3D homology model of TaTLP, the three main domain common to TLP family are shown II: Structural alignment of template 1z3Q (green) and TaTLP model (magenta). RMSD: 0.214; III: Alignment of TaTLP (model_03) with template "ripening associated protein" (Uniprot:022322, PDB:1z3Q). Mismatching residues are faded and gaps are indicated with dashes. Amino acids forming secondary structures in the template are enclosed within arrows (beta structures) and rounded rectangles (helical structures). In A and B, red and blue indicate respectively poorly and well modelled regions

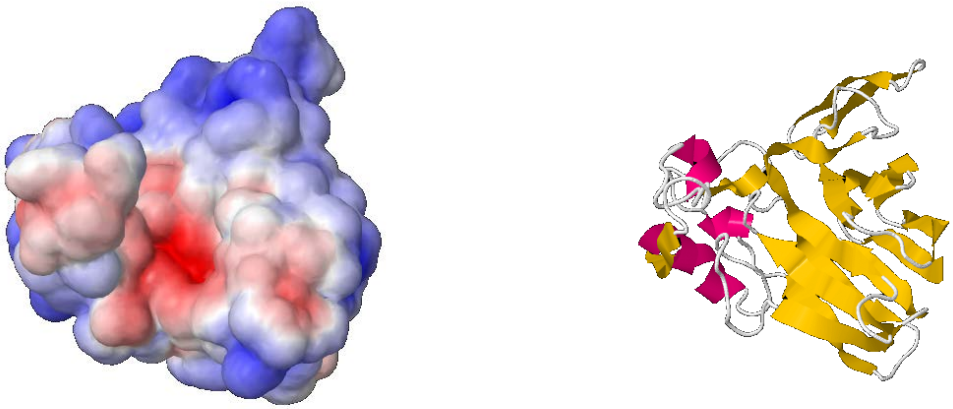

I II

Figure 2.4.14 B. I: Electrostatic Surface Potential of TaTLP model. Blue: negative potential residue, Red: Positive potential residue. White; neutral potential; II: Cartoon view of structure of I, same orientation.

From the structural data obtained from the model we managed to estimate the relative amount of secondary structures by using the online *StrucTools* software provided by the Helix Systems platform of NIH. The software is available as a web based interface that implements the STRIDE algorithm (Frishman, Argos 1995) to estimate secondary structural elements from the 3D coordinated of the protein. The algorithm requires parameters such as hydrogen bond energy and main chain dihedral angles that are automatically obtained by the software from the uploaded PDB file. In **Figure 2.4.15** the results of secondary structures prediction on TaTLP model by StrucTools are reported in a graphical output.

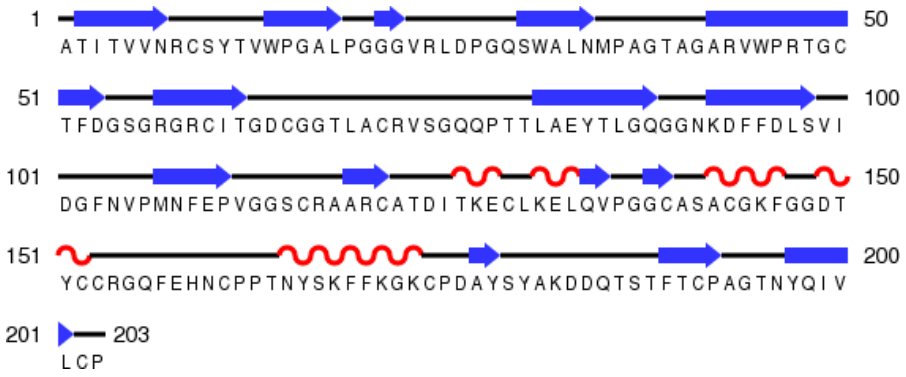

Figure 2.4.15: Secondary structural elements on SWISS-MODEL generated TaTLP model as predicted by StrucTools; *Blue arrows* (beta structures), *Red curves*: helical structures

The percentages of α-helical and β-strands predicted by this method on the 3D model of TaTLP are respectively 12% and 36%, in good accordance with the values estimated with secondary structures prediction based on CD data (respectively 11% and 33%).

2.4.2.4. Tryptophan fluorescence

In addition to Circular Dichroism, fluorescence emission spectrum in the far UV was investigated to obtain indications on the folding state of TaTLP. These data were also used to further validate the TaTLP 3D model obtained with SWISS-MODEL.

Tryptophan fluorescence properties are strongly dependent on the polarity of the solvent surrounding the aromatic moiety; decreasing the polarity of the solvent causes the absorption maximum to shift to shorter wavelengths and increase fluorescence intensity (Gryczynski, Wiczk et al. 1988). According to the hydrophobic effect model proposed for protein folding, the extent of Tryptophan exposure to an apolar environment could ultimately be ascribed to the protein folding state (Krimm 1980). Aromatic residues buried within the hydrophobic core of a protein are generally a good indication of folded state.

Typical spectral emission maxima of Tryptophan residues in folded polypeptide chains show emission maxima at around 330 nm, shifting towards 350 nm upon complete protein denaturation and consequent Tryptophan exposure to aqueous solvent (Lakowicz 1999).

In **Figure 2.4.16** the near UV emission spectrum of TaTLP in solution at 20°C is showed. Fluorescence maximum absorbance is centred at around 330 nm, suggesting that all the three Trp residues in TaTLP are buried within the protein core. This result is compatible with reported fluorescence maxima of other TLPs (Perri, Romitelli et al. 2008)

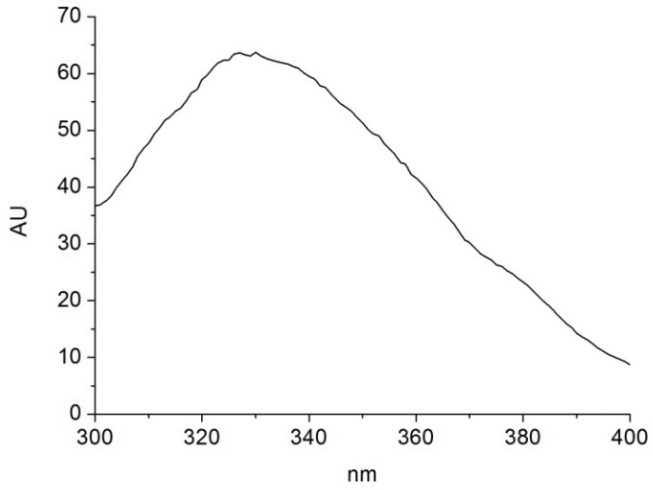

Figure 2.4.16: Emission spectrum of 0.125 mg/ml TaTLP solution in MOPS 50 mM pH 7. Excitation wavelength: 280 nm.

To confirm whether TaTLP 3D model obtained from SWISS-MODEL is in good accordance with data from fluorescence spectroscopy, we measured and visualized Solvent Accessible Surface Area (SASA) for the three Trp residues (W14,W21 and W45).

SASA was automatically calculated by GetArea software algorithm (Fraczkiewicz, Braun 1998) for each amino acid lateral chain from the PDB of the 3D model. SASA values for TaTLP Tryptophans are reported in **Table 2.4.2**. The SASA of a residue X in random coil state is calculated as the average SASA of X in the tripetide Gly-X-Gly in an ensemble of 30 random conformations. The ratio between side chain SASA and the random coil SASA for the X residue is an index that define the extent of amino acid burial within protein core. Residues are considered to be solvent exposed if the ratio value exceeds 50% and to be buried if the ratio is less than 20% (Fraczkiewicz, Braun 1998).

Residue	Position	Random coil SASA	Side chain calculated SASA	SASA Ratio (column 4/column 3) [%]
Trp	14	224.6	23.9	10.7
Trp	31	224.6	52.60	23.4
Trp	45	224.6	0.01	0

Table 2.4.2: SASA values calculated for the Tryptophan residues from the tridimensional atomic coordinates of TaTLP 3D model. Ratio < 20: buried, >50: solvent exposed.

As indicated by low SASA ratio values (**Table 2.4.2**, last column), all three Trp residues in TaTLP 3D model were predicted to be located in low solvent accessible region, thus confirming the experimental data obtained from fluorescence spectroscopy (**Figure 2.4.16**). Trp45 in position 45 is the least solvent accessible Trp amongst the three, while SASA ratio for Trp in position 31 is slightly above the ratio 20% threshold to be properly considered as buried within the protein structure.

Total protein Solvent Accessible Surface Area was visualized directly on TaTLP 3D model as a gray transparent surface over the main polypeptide chain (white sticks) using PyMOL visualization software. Each Trp residue as well as its relative SASA is highlighted in green (**Figure 2.4.17**).

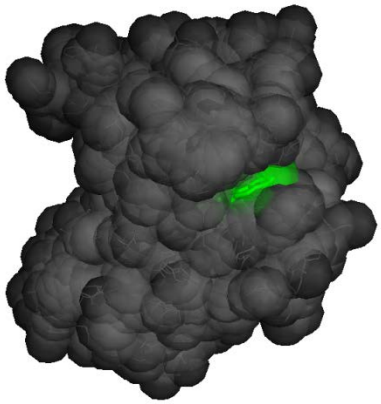

Trp14

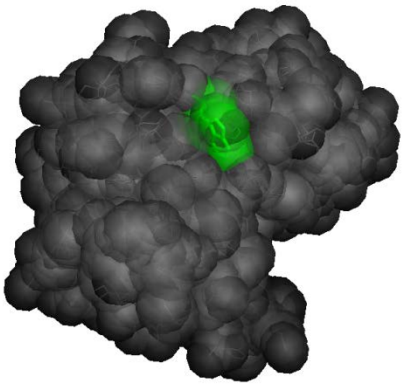

Trp31

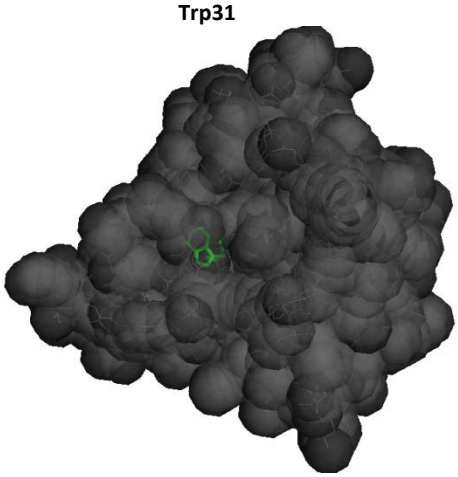

Trp45

Figure 2.4.17: Solvent Accessible Surface Area of TaTLP. *Dark gray spheres*: total protein SASA; *White sticks*: main chain carbon atoms; *Green spheres*: relative Trp SASA; Green sticks: Trp carbon atom. Images were generated with PyMOL software as described in the materials and methods section.

2.4.2.5. Elmann's reagent thiol quantification

All the 16 cysteine of TaTLP sequence were predicted to form disulfide bonds in the 3D homology model generated by SWISS-MODEL. Consecutive and non-consecutive cysteine residues form 8 total disulfide bonds as depicted in **Table 2.4.3**. This network of disulfide bonds is a feature common to other TLP (**Figure 2.2.5**), and believed to be determinant to the heat stability of Thaumatin (Szwacka, Burza et al. 2012).

S-S bond	**Cysteine residues**
1	9-202
2	50-60
3	65-71
4	116-191
5	121-174
6	129-139
7	143-152
8	153-161

Table 2.4.3: S-S network as predicted by TaTLP 3D model

Elmann's reagent (DTNB) was used to verify whether all the cysteine in recombinant TaTLP are effectively involved in the formation of disulfide bonds (Ellman 1959).

In Figure **2.4.18**, the reaction of a thiol (1) with DTNB (2) to yield TNB (3) is showed. Thiols and DTNB react stoichiometrically, with one mole of thiol releasing one mole of TNB. In alkaline/neutral solutions TNB (3) ionizes yielding TNB2- (4), whose concentration can be evaluated by measuring the absorbance at 412 nm, using an extinction coefficient 13.6 mM^{-1} cm^{-1} (Riener, Kada et al. 2002).

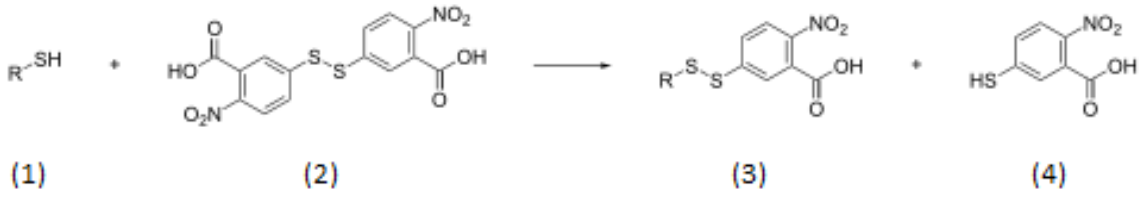

Figure 2.4.18: Reaction of DTNB (2) with thiol (1).

Thiol quantification using Elmann's reagent was performed on a solution of 10 µM recombinant TaTLP. To assess whether TNB^{2-} absorbance was linear within the experimental range of thiol concentrations, we performed a control test on Cysteine standards. Cysteine has only one thiol group, so its molar concentration can be evaluated by measuring thiol concentration with Ellman's reagent. Thiol concentrations calculated from absorbance readings at 412 nm, perfectly matched with cysteine standard concentrations (**Figure 2.4.19** and **Table 2.4.4**).

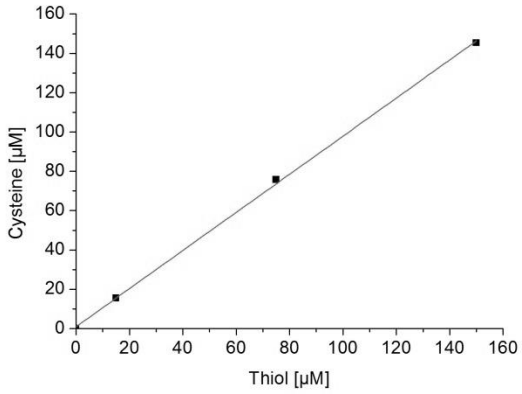

Cysteine Standard [µM]	Abs_{412}	Thiol [µM]
0	0.00	0.00
15	0.21	15.37
75	1.03	75.74
150	1.98	145.29

Table 2.4.4: Estimation of thiol concentration of cysteine standards

TaTLP [µM]	Abs_{412}	Thiol
11	0.017	N.A.

Table 2.4.5: Estimation of thiol concentration of protein samples

Figure 2.4.19: Cysteine concentration of known standard solutions were estimated with Elmann's reagent and calculated by reading the absorbance of TNB^{2-} at 412 nm (ε=13.6 mM^{-1} $cm^{-1)}$; Y-axis: known cysteine standard concentration), X-axis: calculated thiol concentration.

When Elmann's reagent was used to test the concentration of free thiolic groups in a 11 µm solution of TaTLP, the measured absorbance at 412 nm was below the sensitivity of the test (**Table 2.4.5**) . We therefore concluded that all the cysteine thiolic groups in TaTLP are oxidized to yield disulfide bonds.

To test this hypothesis, we tried to reduce all the cysteine by treating the protein at 50°C with the reducing agent TCEP and then quantify again the free thiols. To remove TCEP that would have otherwise interfered with thiol extimation, the solution was dialyzed over

night against reaction buffer. During this step, almost all the protein precipitatedindicating that a proper disulphide bond network is fundamental for TaTLP stability.

2.4.3. Functional Characterization

2.4.3.1. Glucan binding ability

TaTLP was tested for its ability to bind two insoluble 1,3-β-glucans that were previously shown to interact with other TLPs (Trudel, Grenier et al. 1998), namely paramylon and Zymosan. As controls, Thaumatin and BSA were used to assess the specificity of TaTLP binding to the glucans. **Figure 2.4.20** show the bound and unbound fractions of TaTLP, Thaumatin and BSA to Paramylon and Zymosan;.. TaTLP showed specific affinity for β glucans contained in Paramylon while Thaumatin and BSA didn't. On the contrary, Zymosan' lack of specificity for the three proteins tested caused the results showed in **Figure 2.4.20**. For a more detailed discussion of the data, refer to the Discussion paragraph of this chapter.

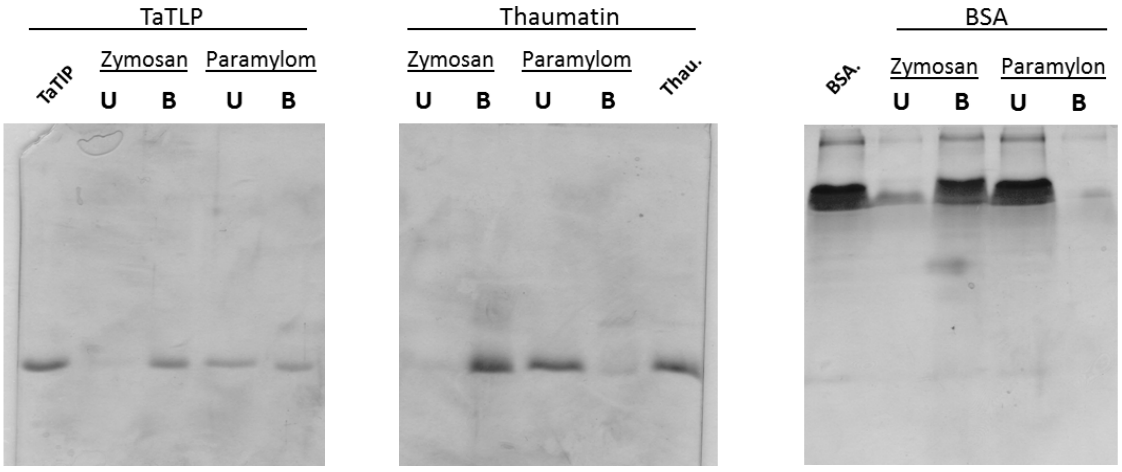

Figure 2.4.20: Results of incubation of 0.2 mg/ml TaTLP, Thaumatin and BSA with Zymosan and Paramylon (5mg). U: Unbound fraction (supernatant after incubation), B: Fraction bound to insoluble glucan (eluted with sample buffer).Samples of TaTLP, Thaumatin and BSA were loaded on a lateral lane before incubation with glucan.

	Zymosan	Paramylon
TaTLP	++	+
Thaumatin	++	-
BSA	++	-

Table 2.4.6: Binding interactions between Glucans and proteins. ++, all protein bound to the glucan, +, half protein bound to the resin, -, no protein bound to glucan

2.4.3.2. 1,3-β-glucans Activity

TaTLP was assayed for 1,3-β-glucanase activity by measuring the release of reducing sugars assay when the protein was incubated with a solution of 1,3-β-glucans. Both soluble (Laminarin) and insoluble glucans (Paramylon and Zymosan) were tested as substrates. 1,3-β-glucanase from *Helix pomatia* was used as a positive control for glucanase activity. The release of reducing sugars was quantified by measuring the increase of Absorbance at 570 nm upon addition of DNS solution to samples (Miller 1959); absolute values are expressed as glucose equivalents (**Table 2.4.7**) obtained by comparison to a glucose standard calibration curve (**Figure 2.4.21**).

After a 24h incubation period with 1 mg of Laminarin, TaTLP yielded 0.08 mg of glucose while *Hp* Glucanase released 5 times more glucose. No significant absorbance increase was detected for control Laminarin samples without w/o enzymes, as a proof that glucose release is the result of enzymatic activity of the two proteins.

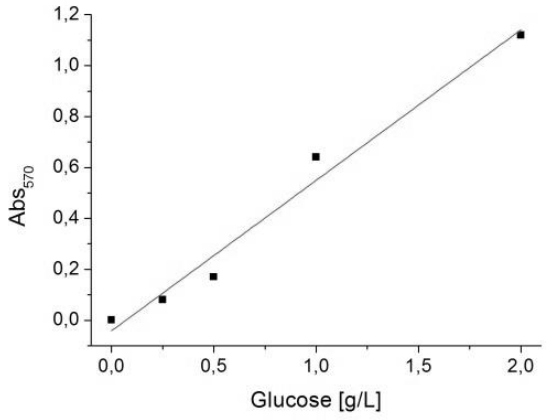

Figure 2.4.21: Glucose standard calibration curve

Enzyme	**Substrate***	**Abs_{570}**	**Gluc. released [g/L]**
TaTLP	Laminarin	0.45 ± 0.07	0.8 ± 0.1
***Hp* Glucanase**	Laminarin	2.3 ± 0.5 **	4 ± 0.8

Table 2.4.7: Glucose released after 24h incubation of 10 g/L Laminarin with 100 µg/ml TaTLP or *Hp* Glucanase. * No significant increase in A_{570} was observed when Paramylon and Zymosan were used as substrates; **A_{570} was measured at 1:10 sample dilution and corrected to initial concentration.

2.4.3.3. Ice Recrystallization Inhibition activity

Once biochemical characterization provided enough data to reasonably assume that recombinant TaTLP was correctly folded, the protein was assayed for its Ice Recrystallization Inhibition activity. By measuring IRI of Thermal Hysteresis, we could: 1) make direct comparison with data reported in literature for TaTLP (Kontogiorgos, Regand et al. 2007) and 2) take advantage of the high sensibility of the method .

By definition, IRI activity is measured by monitoring the evolution of the size of ice crystals at constant subzero temperatures, but most of the literature reports IRI activity by comparing the dimensions of ice crystals of two samples at the end of the freezing/recrystallization cycle in IRI assay.

The second option is a more feasible way to measure IRI, especially in those cases in which more samples are to be analyzed and when the ice crystals at T=0 are too small and packed to be resolved. It is reasonable to assume that ISPs have negligible effect on ice nucleation and growth when the temperature is quickly dropped below the TH range, as is the case of the initial freezing step implemented in our IRI assay (see material and methods).

On the basis of these considerations, we decided to estimate IRI activity by evaluating the final dimensions of ice crystals at the end of the IRI assay (60 minutes). Purified TaTLP was assayed for maximum IRI activity at a final concentration of 1.25 mg/ml as previous reports showed that its IRI activity reaches *plateaux* above 1 mg/ml (Kontogiorgos, Regand et al. 2007). The addition of TaTLP to a 23% sucrose solution didn't inhibited ice

crystals growth mediated by recrystallization process; the median area value of the ice crystals population obtained from the control sample was not significantly different from that of the solution with TaTLP (P=0.05) (**Figure 2.4.22**). As a positive control, fish AFPs from a commercial source were also tested at a final concentration of 0.035 mg/ml.

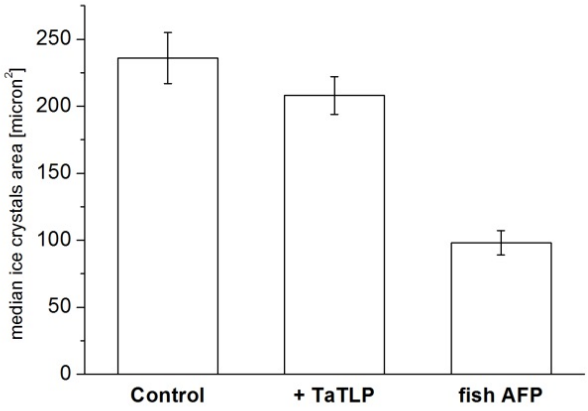

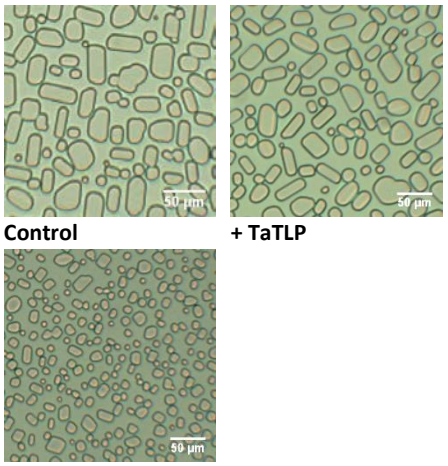

	Area [micron^2]
Control	236 ± 19^a
TaTLP	208 ± 14^a
Fish AFP	98 ± 9^b

Figure 2.4.22: Results of IRI assay. Proteins concentration (before Sucrose addition): Control: 0 mg/L, TaTLP: 1.25 mg/L, Fish AFPs: 0.035 mg/ml. Means with different letters are significantly different at the 0.05 level (ANOVA), n=3.

A more thorough investigation of the effect of TaTLP on the ice phase was performed by extending the analysis to all the size subclasses of the ice crystals population.

One possibility is that TaTLP could still impart changes to the population of ice crystals area,. but those changes are symmetric in respect to the median value of the distribution, leaving this value inalterated. This scenario is depicted in **Figure 2.4.23**; in the representation we simulated that the addition of TaTLP (B) to a solution with no ISP (A), resulted in a sharper distribution of ice crystals without affecting its median value. Assuming that the area threshold value above which ice crystals are perceived in the mouth is located as in **Figure 2.4.23** (dotted line), it's clear that the effect of TaTLP would be fundamental to avoid the icy and grainy texture imparted by the crystals of B. The

curves describing the populations of ice crystals area of Control (CTR) and Control + TaTLP (TaTLP) are represented in **Figure 2.4.24**. A graph showing the changes in relative amounts of ice crytals for each size subclass after addition of TaTLP (TaTLP-CTR), was obtained by subtracting TaTLP data to CTR.

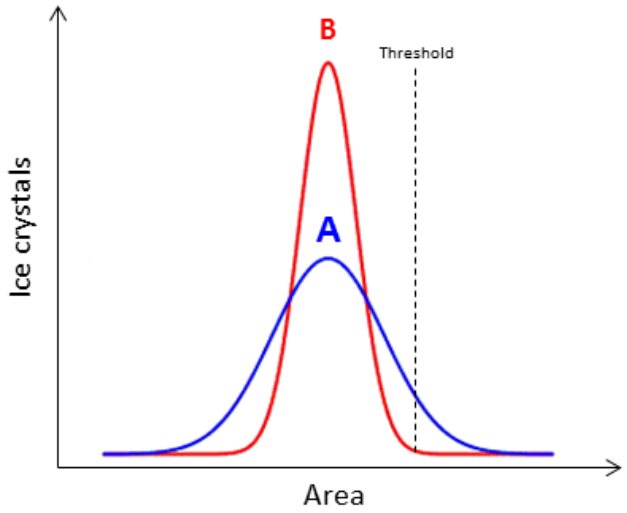

Figure 2.4.23: Simulation of the redistribution of ice crystals population A upon addition of ISP (B)

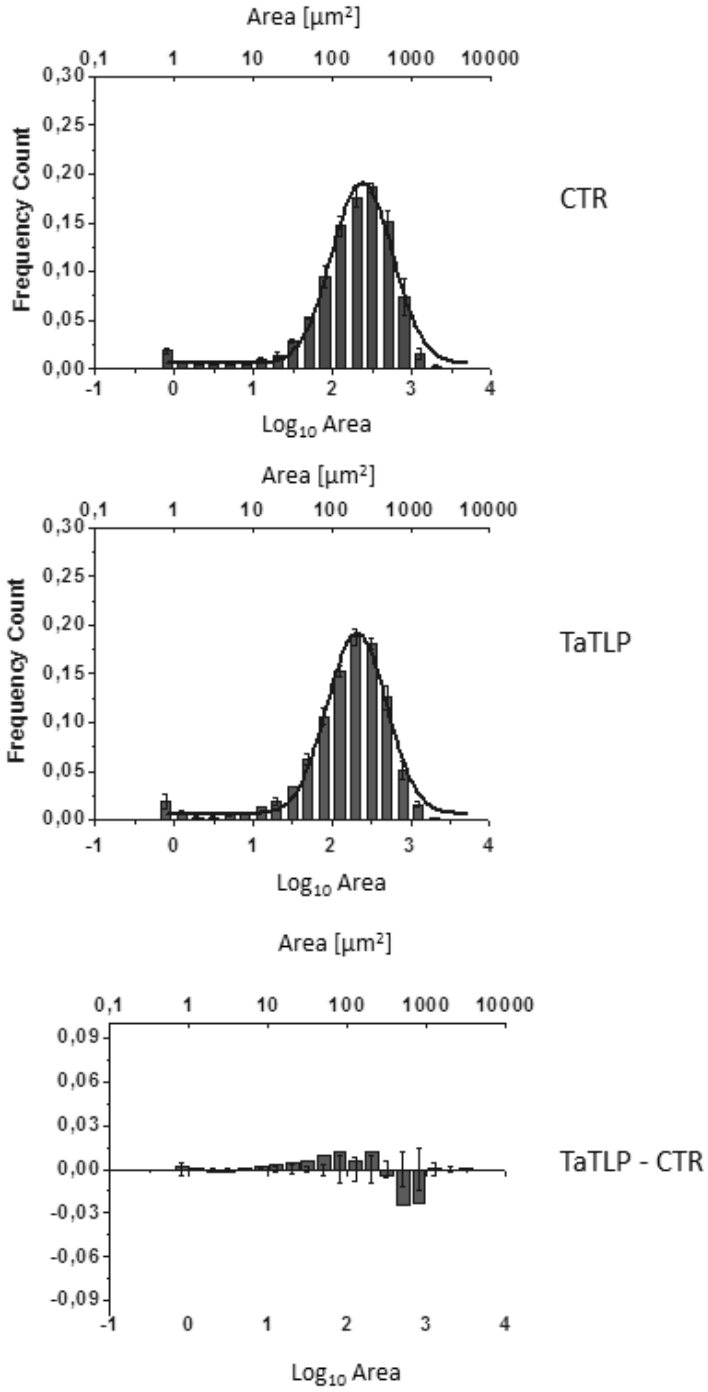

Figure 2.4.24: Changes in relative abundance of each ice crystal size subclass upon addition of TaTLP to control. Data are derived from three replicates.

A small decrease in the relative abundance of some ice crystals at higher area values is observed as well little increase of some crystals populations at smaller sizes; however, the entity of these changes is too little to conclude that recombinant TaTLP possess AF

activity. This consideration is based on the data obtained from our experiments on positive control (Fish AFPs, **Figure 2.4.22**) and native TaTLP by Kontogiorgios (Kontogiorgos, Regand et al. 2007), that reported a decrease of almost 30% of the ice crystals radius in the IRI assay upon addition of TaTLP to the control.

IRI activity couldn't be detected even TaTLP was tested at other pH as well as lower concentrations (data not shown).

To exclude that the purification process could have had a detrimental effect on IRI activity of recombinant TaTLP, we run IRI assays also on fresh supernantants from *P. pastoris* cultures expressing TaTLP (**Figure 2.4.26**). No significant effect on ice crystals dimensions was observed when those supernatants (A) were compared to supernatants from *P. pastoris* carrying empty vectors (B).

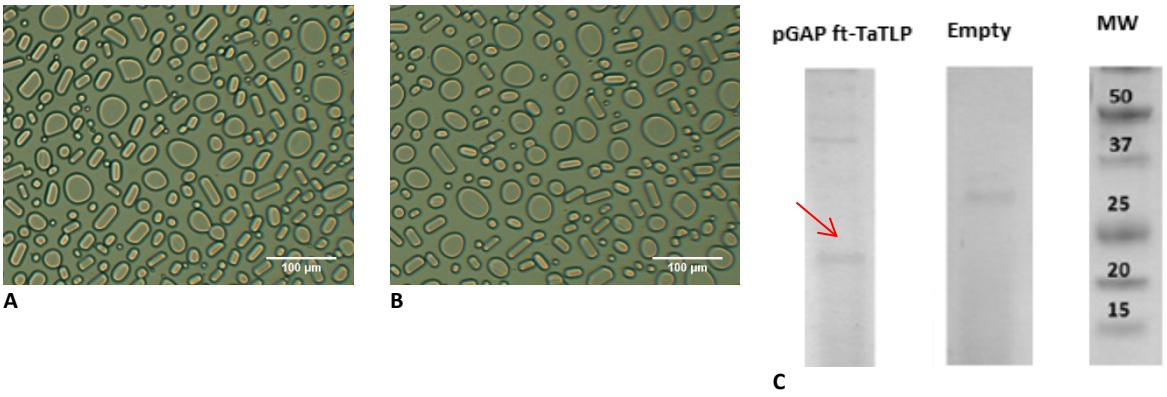

A B C

Figure 2.4.25:Ice crystals obtained from IRI assays on A: supernatants from P. pastoris expressing fl-TaTLP, B: Supertantants from P. pastoris transformed with empty vectors. C: Tris Tricine gel electrophoresis of supernatants. A red arrow highlights TaTLP.

2.5. DISCUSSION

2.5.1. TaTLP expression trials in *P. pastoris*

The results on the expression trials of TaTLP in *P. pastoris*, obtained in this work and previous experiments in our lab (Reghelin 2011), are summarized in **Table 2.5.1**. TaTLP was detected in the supernatant of *P. pastoris* cultures only when the yeast was transformed with a vector harboring construct N. 1, at 18°C or after 5 days at 30°C.

Expressions trials at the same conditions in bioreactors did not significantly increased protein levels in the supernatant. In the case of Construct n. 3, cells viability was drastically reduced.

	Signal sequence			
Construct	**α-factor**	**Native signal**	**Expression level**	**Notes**
1	✓	✓	Low (18°C)	Low TaTLP detected in cultures at 30°C after 5 days
2		✓	N.A.	
3	✓		N.A.	Decreased cells viability

Table 2.5.1: Results of TaTLP expression trials in *P. pastoris*

On the basis of the data presented here and previous literature reports, our hypothesis is that translocation of the protein to and out of the Endoplasmic Reticulum represents the bottleneck for successful TaTLP secretion.

Translocation trough the ER is a necessary step in the sorting of proteins to sub-cellular and extracellular compartments (**Figure 2.5.1**), involving recognition of signal peptides in the cytoplasm that target the protein to its final destination.

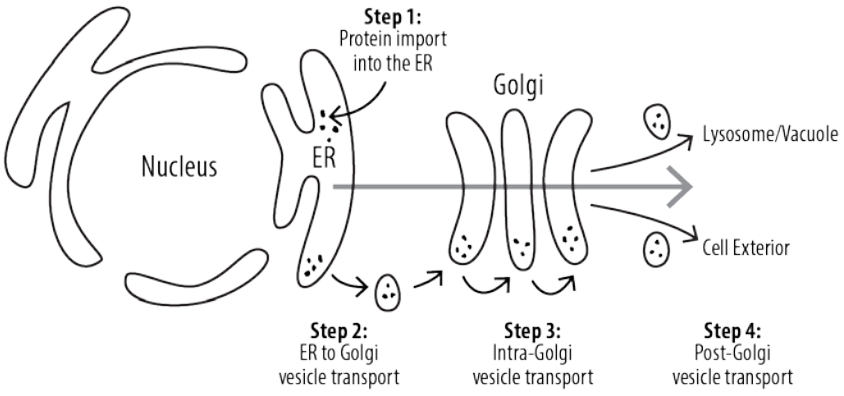

Figure 2.5.1: General scheme of protein sorting pathway to subcellular or extracellular compartment. Adapted from openwetware.org

Protein translocation to the ER is known to occur either post or co-trasnlationally.. Each mechanisms adopts its own set of translocon apparatus and protein sorting signals.

In the case of Post-Translational Translocation (Po-TT), the protein is translocated within the ER after its complete translation in the cytoplasm occurred; for a successful post-translocation it is necessary that the protein remains in an unfolded state as folded domains are probably too bulky to pass through the translocon (Schatz, Dobberstein 1996). The α-mating factor from *S. cerevisiae* is an example of a secreted protein whose translocations to the ER occur post-translationally (Rothblatt, Webb et al. 1987). This 13 aa peptide is synthetized as a larger precursor (165aa), with a typical signal sequence at the N-terminal (the "pre" region) followed by the "pro" region which is further processed by specific peptidases in the late Golgi (Waters, Evans et al. 1988). It is believed that α-factor sorting to the extracellular environment involves receptor mediated translocation to the Golgi (Otte, Barlowe 2004).

To date, the α-factor pre-pro signal sequence is routinely adopted to mediate recombinant protein secretion in *P. pastoris* (Damasceno, Huang et al. 2012).

Co-Translational Translocation (Co-TT) is mediated by the recognition of characteristic amino-acid sequence (signal) by SRPs (Signal Recognition Particles), that blocks the further elongation of the nascent poly-peptide in the cytoplasm and target the protein to the translocon, where translocation and translation could occur simultaneously (Johnson, Powis et al. 2013).

A few evidences suggest that Thaumatin could enter the ER via the Co-TT mechanism: 1) the presence of a cleavable hydrophobic signal sequence typically associated with co-translational translocated proteins (Hegde, Bernstein 2006) and 2) substitution of Thaumatin native signal sequence with *S. cerevisiae* α-factor, resulted in almost undetectable level of secreted protein and imperfect signal sequence processing (Ide, Masuda et al. 2007b). On the contrary, Thaumatin own signal sequence was *per se* sufficient to mediate correct processing and secretion by *P. pastoris* transformed cells.

The observation that in our hands TaTLP was poorly expressed and secreted by *P. pastoris* (**Table 2.5.1**), lead us to consider the impact that different signal sequences would have on protein secretion levels.

The main analogy that can be drawn from our experiments and those previously reported on Thaumatin (Ide, Masuda et al. 2007a), is that the secretion of both proteins was inhibited when the respective native signal sequence were removed from the final constructs. Moreover, the addition of α-factor as an alternative signal sequence couldn't compensate the loss.

It is possible that in the case of Po-TT to the ER (as is the case in which α-factor is adopted as the signal for secretion) globular proteins like TLPs could acquire a partially folded structure upon protrusion of the polypeptide chain out the ribosome. In this scenario, folded protein domains are too bulky to fit in the translocon and protein translocation to ER and its further processing is prevented or become inefficient. Incomplete protein maturation would then result in its targeting to the proteosome mediated degradation pathway (Park, Bolender et al. 2007).

TaTLP native signal alone couldn't mediate efficient secretion of the protein as it was found for Thaumatin, but required the simultaneous presence of α-factor. A recently reported study on secretion of monomeric superfolder GFP (msGFP) in budding yeasts could be used to draw analogies to our case (Fitzgerald, Glick 2014). For msGFP, Po-TT was found to be inefficient when the α-factor pre signal sequence alone was used (pre-αf-msGFP), but stimulated by the pro region (pre-pro-αf-msGFP) as indicated by the increase of msGFP in the supernatant of P. pastoris cultures (**Figure 2.5.2**). Increase in secretion efficiency was also noticed when Ost1 (a signal sequence for Co-TT) was adopted in conjunction with pre-αF (pre-Ost1). The combination of OSt1 and the pre-pro sequence of α-factor resulted in the highest secretion efficiently (pre-Ost1-pro-αf-msGFP).

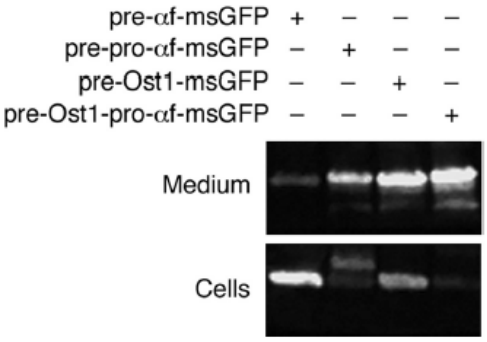

Figure 2.5.2: Effects of the different signal sequences on secretion of msGFP alone in P. pastoris. Medium: fraction of proteins released in the supernatant; Cells: proteins retained in the cytosol.

To explain these results, the authors supported the data by generating msGFP mutants with ER retention signals. They found that the addition of α-pro region increased msGFP secretion by increasing protein traslocation Po-TT to the ER. Conversely, Ost1 signal sequence enabled Co-TT of msGFP that drives protein secretion in a more efficient way. The synergistic combination of the two on secreted protein levels, is the result of 1) increased Po-TT efficiency and 2) activation of the Co-TT pathway.

Besides being involved in the enhancement of post translational translocation, the pro region of α-factor was also suggested to increase the levels of secreted proteins by improving the efficiency of protein secretion out of the ER.

To put the data reported in **Table 2.5.1** into the larger context of the literature mentioned above, possible explanations for the effect of signal sequences on TaTLP expression levels are:

- *Pre α-factor sequence*: enable Po-TT of secreted proteins. However, TaTLP couldn't efficiently translocate across the ER after being synthetized, thus remaining outside the ER and targeted for proteasome mediated degradation or trapped within the translocon (Construct 3). This hypothesis would also offer a possible explanation of why *P. pastoris* harbouring Construct 3 yielded a phenotype with decreased viability. It was reported that microorganisms that grow

at high rates, rely mainly on Po-TT. In this way, protein synthesis which is more time consuming can be uncoupled from translocation, allowing maximal use of a limited number of translocon complexes (Hegde, Bernstein 2006). TaTLP blocking those translocon would then saturate the cell transport machinery and induce stress at high growth rates. Interestingly, the same phenotype on cells viability wasn't noticed when Thaumatin and msGFP were secreted via Po-TT . A possible explanation relies on the consideration that in both cases, inducible expression was adopted, so heterologous protein expression was started when almost all cells reached stationary growth phase

- *Pro α-factor sequence*: increase protein secretion mainly by enhancing exporting out of ER. Its presence is mandatory for secretion of TaTLP in the case of Co-TT (Construct 1).

- *TaTLP signal sequence*: mediates protein secretion via co-TT through the ER. Its presence alone (without α-pro) is not sufficient to efficiently secrete significant amount of TaTLP in the supernatant (Construct 2). α-pro region is required to enhance TaTLP translocation rate in and out of the ER. This finding is in contrast with what previously reported for Thaumatin and msGRP, whose respective native signal sequences alone enabled significant efficiency of protein secretion over the α-pre signal. At the moment, we don't have a satisfactory explanation for that; a possibility is that TaTLP native signal is not as efficiently recognized by SRPs as those of Thaumatin and msGFP.

The positive effect of temperature on TaTLP expression levels, might be regarded as a more general effect on the metabolic load of the cell. Lower temperatures have been shown to improve expression of recombinant proteins that require proper disulfide bonds network formation for their stability, as in the case of TLPs. Cells growth at lower temperatures is significantly reduced, and so is the rate of protein synthesis, allowing

more time for the nascent protein to fold properly (Li, Xiong et al. 2001). The same conditions could be theoretically obtained at higher temperatures when cells have reached a stationary phase. This would explain why TaTLP was found in the supernatant of P. pastoris cultures at 30°C, only after longer period of cultivations.

2.5.2. Structural and functional features of recombinant TaTLP

Once soluble TaTLP was obtained from *P. pastoris*, the first tests were aimed at demonstrating whether the recombinant protein was comparable to the one found in plant, to exclude bias introduced by heterologous expression.

Given the scarce information available for TaTLP (Q8S4P7_ WHEAT), data from other TLPs were used to draw conclusion on the shape and functionality of the recombinant product.

Protein identity was confirmed by MS/MS analysis and MALDI TOF on the purified protein revealed the presence of some isoforms bearing additional amino acid residues at N-terminal. This event is rather frequent when α-factor is used as a signal sequence for proteins secretion, but quite unlikely to have an impact on the ability of the protein to bind to ice.

CD spectroscopy in the far UV generated results similar to previously reported spectra of other TLPs (**Figure 2.5.3**), indicating that random coil and β-structures were the prevalent secondary structures present in the protein.

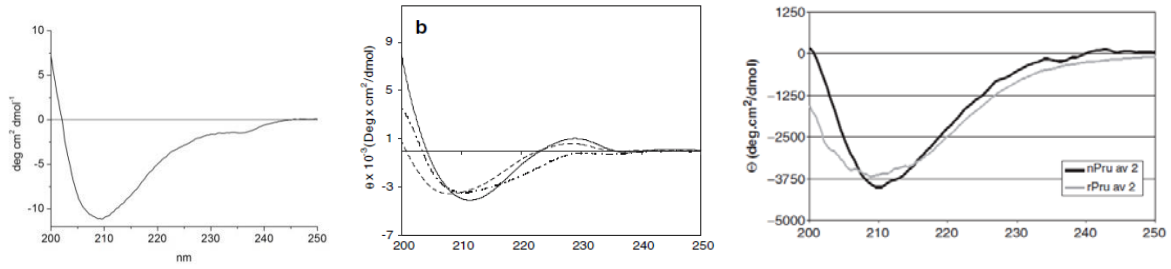

A **B** **C**

Figure 2.5.3: Far UV CD spectra of A: TaTLP, B: — Zeamatin, --- Thaumatin, – .–: CdTLP (Perri, Romitelli et al. 2008)**; C: nPru av** (Fuchs, Bohle et al. 2006)

Fluorescence of Tryptophan residues was measured by excitation at 280 nm; the spectra showed a maximum at around 330 nm, suggesting that the three Tryptophans of TaTLP should be relatively buried within the 3D structure of the protein, a further indication that recombinant TaTLP acquired a folded state.

A 3D homology model for TaTLP was obtained using the crystallographic structure of BanTLP as a template, an Antifungal TLP from banana sharing 62% identity with TaTLP.

The model was used to confirm the structural data obtained from CD and Fluorescence spectra and conversely, experimental data were used to evaluate the accuracy of the model.

The percentage of secondary structural elements in the model, convincingly matched the data predicted from CD spectra. The relative buried position of the three Tryptophans in TaTLP was confirmed by calculating their relative Solvent Accessible Surface Area and visualizing it on the 3D model.

With regard to the functional characterization of the protein, we decided to test whether TaTLP possess any 1,3-β-Glucan processing ability (Trudel, Grenier et al. 1998), as it was found for other TaTLP having marked electronegative potential within their central cleft. 1,3-β-Glucan binding activity was tested by incubating TaTLP and two controls with two insoluble glucans that were previously found to specifically interact with TaTLPs .

While Zymosan was found to strongly interact with all the three proteins tested (no or low protein in the unbound fraction) TaTLP was the only protein that could bind Paramylon. It is possible that the lack of binding specificity observed with Zymosan could be the result of broad electrostatic interactions between the proteins (TaTLP, Thaumatin and BSA) and the mixture of glucan and proteins of which it is made. On the contrary, Paramylon was shown to be selective only for TaTLP, suggesting that this interaction might be driven by specific structural/electrostatic features of the surface of TaTLP . It is unlikely that insoluble β-glucans could bind TLP via the acidic cleft, as they are arranged in a bulky tri-helical chain that could not be fitted whithin the acidic cleft of TaTLP (Osmond, Hrmova et al. 2001).

Insoluble glucans were neither the target of TaTLP 1,3-β-glucanse activity, that compared to enzyme isolated from *Helix pomatia* showed moderate reactivity against the soluble 1,3-β-glucan Laminarin. The physiological relevance of the low glucanase activity and ability to bind glucans by TLPs it is still not understood.

The most astonishing results came when TaTLP was testes for IRI activity; no significant reduction of ice crystals griwth was detected when the protein was tested at concentration (1.25 g/L) at which IRI activity was reported to reach plateau (Kontogiorgos,

Regand et al. 2007). A sample formulated with a source of fish AntiFreeze proteins was tested as a positive control and produced a decrease of the median area of ice crystals population of almost 60%. Considering that 1) IRI assay was shown to have a sensitivity in the nanomolar range (Hughes, Schart et al. 2013) and 2) plants ISPs are reported to be more effective Ice Recrystallization inhibitors than fish AFPs (Sidebottom, Buckley et al. 2000a), we are confident to state that recombinant TaTLP has no IRI activity whatsoever.

We accumulated a reasonable amount of data to support the thesis that recombinant TaTLP secreted by *P. pastoris* acquired the proper conformation to exhibit activity. The possibility that TaTLP could acquire only a "partial" functional folding, that resulted in features typical of TLPs (e.g. glucanse activity) but not of AntiFreeze protein (e.g. IRI activity), is remote.

The more intuitive deduction is that TaTLP (Q8S4P7_WHEAT) has no IRI activity at all. This may not sound surprising as early studies on winter rye ISPs showed that putative ISPs were expressed in both cold acclimated and non-acclimated, in the latter case lacking totally ice binding activity (Yu, Griffith 1999). It is plausible that the TLP with IRI property identified by Kontogiorgos (Kontogiorgos, Regand et al. 2007) could be a Q8S4P7 homologue, but sufficiently different to enable its reactivity toward ice. This hypothesis is confirmed by a study in which Q8S4P7 expressed in recombinant wheat cells didn't exhibit any antifreeze activity (Hiilovaara-Teijo, Hannukkala et al. 1999). The perfect example for this argument is provided by a study on the prediction of Ice Binding Surface on ISPs (Doxey, Yaish et al.). A Lipid Trasnfer Protein from *T. salsuginea* had a predicted Ice Binding Surface described by an ordered array of non-aliphatic carbon atoms on a planar surface of the protein (**Figure 2.5.4 b** LTP1). When the protein was tested for its ability to binding ice and modify its growth, it showed ice crystals shapes typical of AF proteins (**Figure2.5.4 c** LTP1). On the contrary, LTP1 isoform that shared 70% identity with LPT1 (**Figure 2.5.4 a**) didn't showed any ice shaping ability (**Figure 2.5.4 c** LTP2) because of amino acid substitutions that altered the surface of the ice binding.

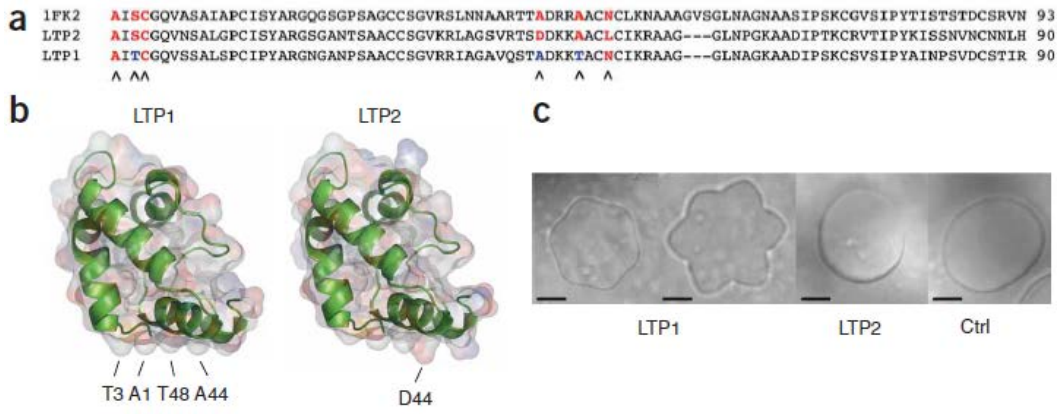

Figure 2.5.4. (a) Sequence alignment of LTP1, LTP2 and template used for homology modeling. Marked residues correspond to predicted ice-binding sites in LTP1. Key substitutions are colored in blue. (b) Structural models of LTP1 and LTP2; The putative ice-binding surface of LTP1 is perpendicular to the plane of this figure; residues in LTP1 are labeled as the corresponding residue and the key substitution A44D is labeled on LTP2. (c) Antifreeze activity of recombinant LTPs by ice-crystal morphology assay. Scale bars:10 mm.

Another possibility is that TLP do not possess any AF activity, but might has been purified together with other ISPs, being active at extremely low concentration but undetectable in PAGE gels.

The recent finding that a dehydrin from peach, previously known to express AF activity, was inactive when produced via heterologous expression, support the thesis of ISP contamination throughout the purification process (Hughes, Schart et al. 2013).

TLPs ability to bind to the ice is far to be elucidated; to date only a few reports on winter rye reports that TLPs induce by cold acclimation have ice shaping properties. TLPs domains lack the typical features that commonly define the Ice Binding site of a protein, namely extension, flatness, hydrophobicity (largely devoid of charged amino-acids) and repeated motifs (Davies 2014).

The expression of other TL proteins isolated from cold adapted organisms is required to further establish their role in freezing tolerance.

3. ENHANCING ICE RECRYSTALLIZATION INHIBITION ACTIVITY OF WINTER WHEAT ICE STRUCTURING PROTEINS

3.1. ABSTRACT

TaTLP was cloned and expressed in *P. pastoris*, the recombinant protein didn't exhibited any significant IRI (Chapter 2) even though we found structural evidences that suggests that the protein has secondary structures, as well as the post translational modifications required for proper folding. We investigated the possibility that the protein IRI activity may depend upon binding of ligands or cofactors, by incubating the recombinant TaTLP with IRI active extracts from cold acclimated *Ta* seedlings. The observation that upon addition of TaTLP the overall IRI activity of the extract was increased, seemed to indicate that TaTLP activation is triggered by components within the extract. However, we later found that the same effect was obtained when other non-ISPs were tested.

Those results suggested that TaTLP might enhance ISPs rather than actively exhibit IRI activity in itself; a similar case was reported for a TLP purified from hemolymph of overwintering insects. Surprisingly, we found that protein mediated enhancement of winter wheat ISPs was not limited to specific binding partners as in the case of insects. . It is believed that increased TH and IRI activity mediated by non-ISPs enhancers, could be attributed to the augmented size of the resulting ISPs -enhancer complex. In this way, a larger ice surface coverage could be obtained without increasing ISPs concentration.

We couldn't find any direct evidence of stable interaction between *T. aestivum* ISPs (TaISPs) and protein enhancers even after samples were frozen and thawed, a condition known to induce ISPs oligomerization in winter rye ISPs . Based on the experimental data obtained and considerations about the physiological relevance of the process, our hypothesis is that *T. aestivum* ISPs could recruit the enhancers on the ice crystals surface via protein-protein interaction; this phenomenon being triggered by the freezing event and reversed upon ice melting.

3.2. INTRODUCTION

3.2.1. Biomolecules enhancing antifreeze activity: the case of *Dendroides canadensis*

In the overwintering larvae of *D. canadensis*, AFPs role is to promote supercooling of body fluids by inhibiting endogenous nucleators in the hemolymph and gut (Olsen, Duman 1997a, Olsen, Duman 1997b)(Olsen, Duman 1997a, Olsen, Duman 1997b)(Olsen, Duman 1997a, Olsen, Duman 1997b)(Olsen, Duman 1997a, Olsen, Duman 1997b)(Olsen, Duman 1997a, Olsen, Duman 1997b) and to prevent inoculative freezing by external ice across the cuticle (Olsen, Sass et al. 1998). Several isoforms of *DAFP* have been found, consisting of 12-13 mer repeats with size ranging from 7.3 to 16.2 kDa and cysteines forming a network of disulfide bridges (Andorfer, Duman 2000) (see **Figure 3.2.1**).

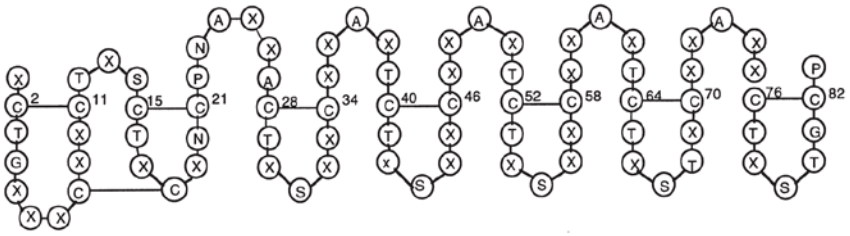

Figure 3.2.1.: Consensus sequence of DAFPs showing disulfide bridges between cysteines. Adapted from (Andorfer, Duman 2000)

Mid-winter average TH values of larval hemolymph were found to be typically around 3-6 °C, with some individuals showing peaks of 8-9°C. However, when DAFPs were purified from hemolymph, TH values decreased to 2.5 °C (Duman 1984). This finding was the first evidence that DAFPs alone couldn't account for total hemolymph TH activity, but rather relied on enhancers.

3.2.2. High molecular weight enhancers

First evidences of *DAFPs* enhancement came in 1991 (Wu, Duman et al. 1991), when it was found that antiserum raised against DAFPs significantly enhanced TH of hemolymph (see **Table 3.2.1.**). TH was increased to a greater extent when anti-IgG antiserum was added to the mix of Dc hemolymph and antiserum, while removal of antibodies by addition of Pansorbin (*i.e.* S. Aureus cells coupled with Protein A) abolished TH.

	Sample	TH (°C)
(1)	**33% Dc hemolymph**	1.20 ± 0.09
(2)	**33% Dc hemolymph + 33% DAFPs antiserum**	1.72 ± 0.08
(3)	**33% Dc hemolymph + 33% DAFPs antiserum + anti-IgG antiserum**	2.86 ± 0.1
(4)	**33% Dc hemolymph + 33% DAFPs antiserum + Pansorbin**	0

Table 3.2.1: Effects of DAFPs antisera on Dc hemolymph. % are expressed as v/v. Data from (Wu, Duman et al. 1991)

These observations led the authors to formulate the hypothesis that Antibodies could increase the overall hemolymph TH by binding to DAFPs, increasing their size and thus blocking a larger surface of the ice crystals. In the model proposed by Wu (**Figure 3.2.2**), antibodies are bound to two AFP, masking potential sites for ice growth from water molecules.

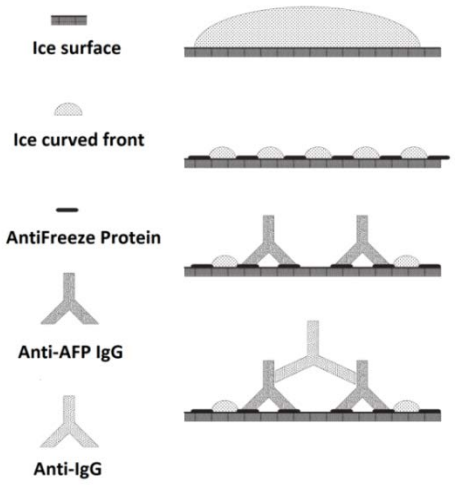

Figure 3.2.2: Proposed mechanisms of DAFPs TH enhacement by *DAFPs* antisera. Adapted from (Wu, Duman et al. 1991)

7 years later, DeLuca evaluated the effect of increasing AFP size on TH activity (DeLuca, Comley et al. 1998). In an attempt to test whether cooperativity was required in type III AFP binding to ice, AFP fusion proteins were generate to increase the overall diameter of the chimeric protein, with the aim of preventing side-by-side interactions that were postulated to be at the basis of the cooperative behavior. They found that the addition of a fusion partner to AFP did not impaired TH, but surprisingly enhanced it. Furthermore, TH increase seemed to correlate with increasing size of AFP fusion partner (**Figure 3.2.3 A**),
The authors suggested that by increasing the size of AFP trough the addition of a fusion partner, the resulting protein is able to cover a larger surface of the ice crystals, as it was previously suggested by the findings on DAFPs. They further speculated that the reason for TH increase by larger AFP is to be found in the nature of the mechanism by which AFP bind to the ice, described in the "absorption-inhibition" model (see **Section 2.1.3.1**) (Raymond, DeVries 1977). As this model postulates, the lowering of non-equilibrium freezing point by AFP is due to the increased energetic costs of adding water to a convex ice surface, thus AFP that increase ice curvature between adjacent binding sites at the same molar ratio (as in the case of larger AFP) would produce increased TH values (**Figure 3.2.3 B**).

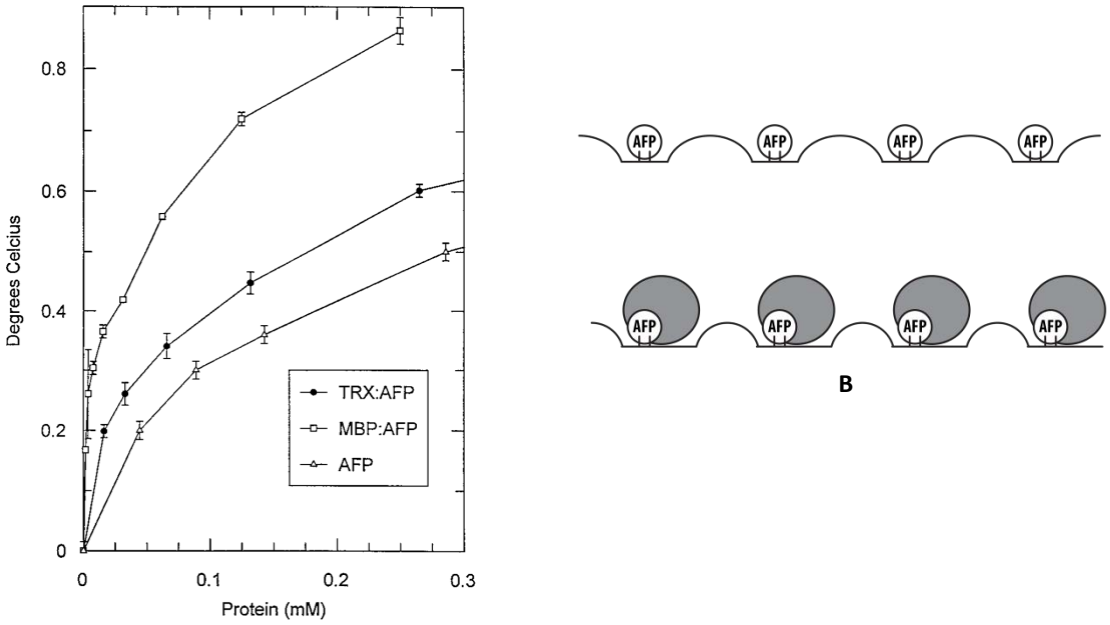

Figure 3.2.3: A: TRX:AFP (20 kDa); MBP:AFP (50 kDa); AFP (8 kDa, extimated). Values of TH (°C) are plotted against protein concentration. TRX: Thioredoxin; MBP: Maltose binding proteins; AFP: AFP type III; B: Proposed mechanisms for TH enhancement by larger AFP according to the absorbtion-inhibition molecules. Images adapted from (DeLuca, Comley et al. 1998)

Further studies on *D. canadensis* AFP enhancement disclosed new molecular enhancers (**Table 3.2.2**) (Wu, Duman 1991). For the first time, it was reported that addition of Ice Nucleating Proteins increased TH values of solutions containing DAFPs. Combinations of enhancers and AFP were found to produce synergistic increase of TH, suggesting that single AFP molecules could bind simultaneously to multiple partners. When a modified immunoblot was performed to ascertain whether this effect was due to interactions between enhancers and DAFPs, all validated enhancers were found to interact with DAFPs. The authors suggested that the increased TH values could be explained by the increased size of AFPs-enhancers complex (Wu, Duman et al. 1991).

The proposed model, however, doesn't offer a satisfactory explanation of why the high molecular weight enhancer *Tipula* LPIN (800 kDa) didn't outperformed lower molecular weight proteins such as PIN (70 kDa), Endogenous DC ice nucleator (70 kDa) and IgG of antisera (150 kDa), in TH assays (Table 3.2.2).

Enhancer	MW [kDa]	TH [°C]
None		1.6 ± 0.09
Gelatin [5 mg/ml] (80-375 kDa)	80-375	3.13 ± 0.15
Agar [0.1 mg/ml]		2.76 ± 0.16
DAFPs antiserum [0.5%]	150 (IgG)	3.18 ± 0.27
Ice nucleating proteins		
Tipula LPIN ice nucleator [1mg/ml] (800 kDa)	800	3.49 ± 0.15
Tipula PIN ice nucleator [1 mg/ml] (70 kDa)	70	3.98 ± 0.24
Endogenous *Dc* ice nucleator [1 mg/ml] (70 kDa)	70	5.24 ± 0.21
Combinations		
Tipula PIN + Gelatin		5.8 ± 0.28
DAFPs antiserum + Gelatin		4.21 ± 0.25
DAFPs [from other chromatographic fractions, with 1.6°C TH]		3.03 ± 0.37

Table 3.2.2: DAFPs Effect of addition of TH enhancers to a 4 mg/ml purified preparation of DAFPs. For each enhancer is reported its final concentration after addition to DAFPs, molecular weight and effect of total TH. Adapted from (Wu, Duman 1991)

3.2.3. Low molecular weight enhancers of TH

When endogenous low molecular solutes as poly-hydroxyy alcohols and organic acids were tested for their ability to increase DAFPs activity, Citrate was found to be the best enhancer, raising TH of recombinant DAFP-4 from 1.3 °C [without Citrate] to 6.8 °C [1M Citrate] (Li, Andorfer et al. 1998) (**Fig. 3.2.4**). Other solutes increased significantly TH activity of DAFP-4, however Glycerol is the only one that is known to be present at the tested concentrations in body fluids of *D. canadensis* .

In another study, J.G. Duman proposed that glycerol may also have a physiological role in promoting *D. canadiensis* supercooling, as it was found that glycerol (as well as Citrate) could enhance DAFPs mediated inhibition of ice nucleators within insect hemolymph (Duman 2002). The authors suggested that those solutes may act as a protein stabilizer by being preferentially excluded from the immediate region surrounding the proteins, forcing more water into this zone and thus stimulating protein-protein interactions (Wu, Duman 1991). AFP are believed to inhibit INPs by binding the active water organizing sites of the ice nucleator, even though this would cause a decrease in the number of active ice binding sites that can adhere to the ice surface and inhibit its growth. In this regard, interpretation

of TH enhancement by INPs addition to DAFPs (**Table 3.2.2)** appear still to be elusive. Before DAFPs enhancers were discovered, it was believed that only changes in DAFPs levels could account for seasonal variability of *D. canadanesis* TH. After it was found that TH values of winter *D. canadanesis* hemolymph was far from being maximized (addition of 0.5M citrate produced a 60% TH increase in the sample with higher TH, **Table 3.2.3**), the role of endogenous enhancers was the focus of a thorough analysis. The aim was to break down the components that contributed to the final hemolymph TH value (Duman, Serianni 2002). An extract of the data from *D. canadensis* hemolymph collected on the winters of 1998, 1999 and 2000 is shown in **Table 3.2.3**.

Briefly, larvae from 3 consecutives winters were collected and for each year the hemolymph were pooled and measured for AFPs concentrations, TH and Freezing Point depression activity. To establish whether hemolymph was maximized for TH, 1M citrate was added and its effect on the increase of TH was measured. Dialysis was performed to evaluate the contribution of DAFPs to the TH of hemolymph without the effect of small endogenous enhancers.

Hemolymph from 1999 winter scored the best TH value (5.3 °C), even though DAFPs concentration was close to that of the sample with lowest TH values (2.83 °C, year 2000). The lower freezing point value of 1999 hemolymph (-3.05) could be attributed to an increased content of glycerol, as a proof that small solutes can contribute significantly to TH enhancement once maximal TH activity at given concentration of AFPs is achieved (1999 vs 2000 samples).

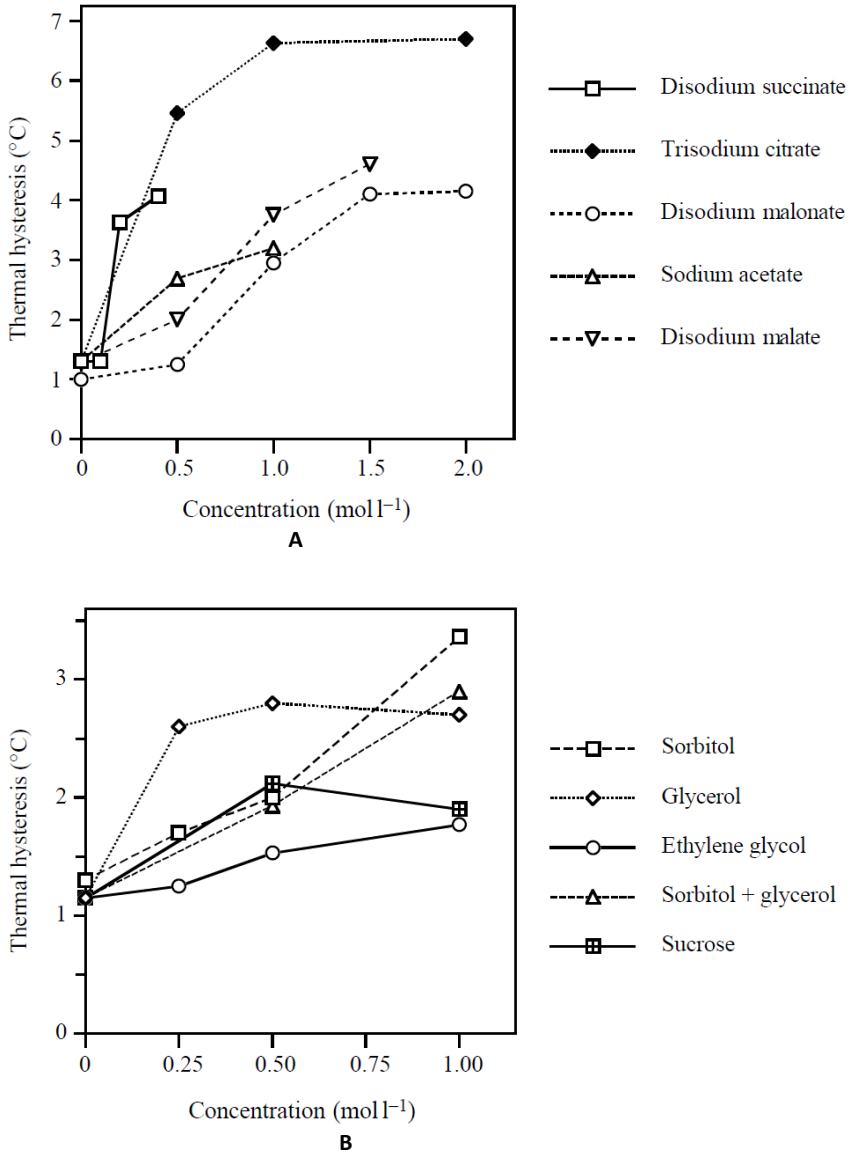

Figure 3.2.4: Effects of small solutes on DAFP-4 TH (4mg/ml). A: Organic acids, B: Polyhydryl alcochols. Adapted from (Li, Andorfer et al. 1998)

	TH [°C]		
Treatment	***1998***	***1999***	***2000***
Hemolymph **(pooled)**	3.07 (-1.10°C ; 1.6 mg/ml)	5.30 (-3.05 °C; 2.6 mg/ml)	2.83 (-2.04 °C, 2.4 mg/ml)
Hemolymph + 1M Citrate	5.47 (↑ 2.4; 78%)	8.5 (↑3.2; 60%)	6.9 (↑4.07; 144%)
Hemolymph dyalized	1.84 (↓ 1.23; 40%)	3.29 (↓2.01;38%)	1.83 (↓1.00; 35%)

Table 3.2.4.: TH values are reported within each cell; 3rd row: freezing point (°C) and DAFPs concentration (mg/ml) are reported in parentheses. 4th and 5th row: TH increase ↑ or decrease ↓ is expressed in °C and % in parentheses. Adapted from (Duman, Serianni 2002)

A few years later, it was reported that a solvent exposed Arginine in DAFPs-1 was critical for TH enhancement mediated by glycerol and citrate (Wang, Amornwittawat et al. 2009). This finding offered a hint of the molecular mechanism that could account for the binding of hydroxyl and carboxylate groups (Amornwittawat, Wang et al. 2008, Amornwittawat, Wang et al. 2009) to DAFPs. The possible complete molecular mechanisms by which this interaction could lead to the observed TH enhancement were not discussed in the papers.
Novel insights on Citrate enhancing effect over DAFPs came from recent papers (Ebbinghaus, Meister et al. 2010, Ebbinghaus, Meister et al. 2012) ((Meister, Ebbinghaus et al. 2013), where terahertz spectroscopy and Molecular Dynamics were used to prove that the ice binding site of some AFPs could influence water molecules dynamics over an extended range of hydration shells. Interfering on H-bonding dynamics of the surrounding water molecules was proposed to provide extensive specificity for ice binding by DAFPs, thus offering a possible explanation for their increased TH over other AFPs (Marshall, Tomczak et al. 2004). MD simulations on DAFPs-1 indicated a retardation of H-bond dynamics upon addition of sodium citrate that extended ca. 20-27 Å from the ice binding site; the effect of citrate on AFPs long range interaction with hydration layers was then proposed as a possible explanation for the TH enhancement (Meister, Ebbinghaus et al. 2013).

3.2.4. Self enhancing AFPs

After the first reports of protein mediated TH enhancement of DAFPs (Wu, Duman 1991), yeast two-hybrid assays was adopted as a mean to find new DAFPs interactors (Wang, Duman 2005), (Wang, Duman 2006). When recombinant DAFPs were added to one another, those identified by the yeast two-hybrid screen as interacting exhibited a synergistic enhancement of TH activity. In contrast, AFPs with no evidence of interactions failed to exhibit synergistic behaviour. **Figure 3.2.5** reports a schematic representation of synergistic interactions between DAFPs as revealed by two-hybrid assays and TH measurements. Note that DAFP-6 didn't show TH activity even if it only differs from

DAFPs-4 for 4 amino acids. Mutagenesis experiments demosntrated that the two amino acid that allow to discriminate between DAFPs-1 and DAFPs-2 are both important for the reciprocal enhancement of TH. The two-hybrid assay also identified a non-AFPs protein (no effect on TH activity) interacting with DAFPs-2 and DAFPs-1 end enhancing their activity (Wang, Duman 2006). The protein was called TLP-Dcan 1 as it was found to belong to the family of Thaumatin-Like Proteins, commonly found in plants.

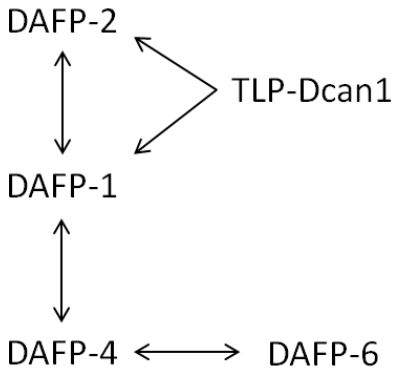

Figure 3.2.5: D.AFPsSelf-enhancing DAFPs. Proteins connected by arrows were shown to interact in yeast two hybrid assays. The direction of the arrow indicate the enhancing effect of a protein on the respective interactor. No arrows point in the direction of TLP-Dcan since this protein has no activity itself and therefore couldn't be enhanced. Adapted from (Wang, Duman 2006).

Besides the ability to enhance one another activity as proposed by the scheme in figure **3.2.5**, those proteins were found to exhibit the greatest TH when all of them were present with added Glycerol. (**Figure 3.2.6**).

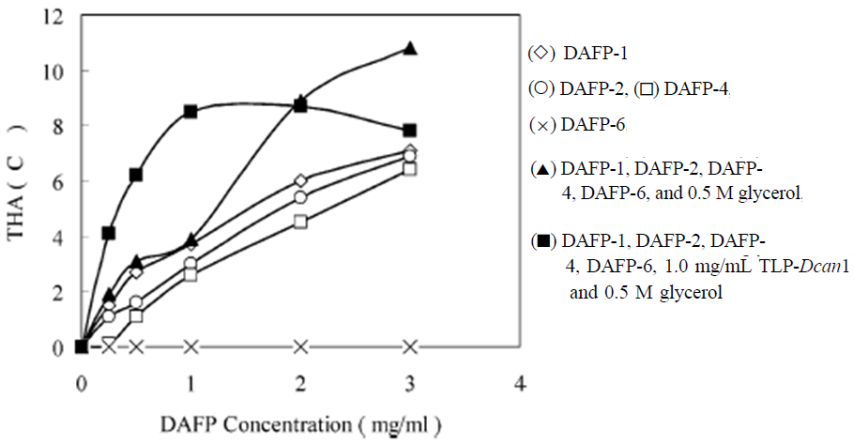

Figure 3.2.6: Synergistic effects of DAFPs. Adapted from (Wang, Duman 2006)

The mixture containing all DAFPs is maximally enhanced at higher concentrations (> 1mg/ml), while addition of Dcan1 and Glycerol enhanced TH of AFPs mixture at lower proteins concentrations (< 1 mg/ml). Besides the evidence of synergistic effect obtained by mixing DAFPs and TLP-Dcan1, it would be risky to draw conclusions on the physiological relevance of the curves depicted in **Figure 3.2.6**, as at present we don't know the ratios of the different protein species within the hemolymph. It appears clear at this point that overwintering insects can finely modulate the TH activity of their body fluids by controlling absolute concentrations of TH active species, as well as their combinations with other TH–inactive enhancers.

3.2.5. Oligomeric ISPs species in winter rye

Most of literature regarding ISPs from higher plants results from the work of Griffith and collaborators on winter rye (Griffith, Yaish 2004).Their extensive investigations on AF active species in apoplastic extracts of cold acclimated rye focused mainly on Pathogenesis-Related proteins that are expressed during cold acclimation of the seedlings. Winter rye ISPs characterized so far belong to the Thaumatin, Chitinase and Glucanase-like family (TLP, CLP and GLP) as shown by their reactivity against antisera in immunoblots

(**Figure 3.2.7**). Each of them was previously identified to have ice binding properties ((Hon, Griffith et al. 1994a)).

Isolation of ISPs in their native active form apoplastic extracts, was complicated by the fact the different protein species co-eluted in the same chromatographic fractions (Griffith, Ala et al. 1992), suggesting that they might associate in AF active oligomeric complexes. Total proteins from extracts were initially separated by native gel electrophoresis, eluted and tested for their AntiFreeze activity (**Figure 3.2.7 A and B**), then loaded on SDS-PAGE in denaturing conditions and immunoblotted against anti CLP, GLP and TLP antisera (**Figure 3.2.8 A, B, C**).

Nine protein species were separated by native PAGE electrophoresis of extracts from cold acclimated plants, while only 6 species appeared to present in NA samples (**Figure 3.2.5.1**). All of the native proteins (NP) from CA extracts contained multiple peptides except NP8 and 9, for a total of 13 polypeptides ranging from 122-16 kDa (**Figure 3.2.8 A**) some of them being identified as GLP, CLP or TLP (**Fig. 3.2.8 B-C**).

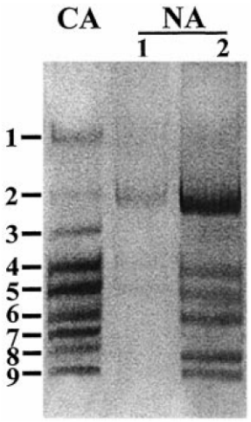

A

Sample	Protein Concentration	Antifreeze Activity Rating
	mg mL⁻¹	
Apoplastic extract		
Cold-acclimated	0.45 ± 0.12	5
Nonacclimated	0.56 ± 0.07	0
NP1	0.40 ± 0.09	0
NP2	0.50 ± 0.14	3
NP3	0.45 ± 0.10	3
NP4	0.52 ± 0.08	4
NP5	0.42 ± 0.08	3
NP6	0.48 ± 0.09	2
NP7	0.50 ± 0.10	2
NP8	0.45 ± 0.08	0
NP9	0.52 ± 0.15	0

B

Figure 3.2.7: A: Native gel electrophoresis: CA (Cold acclimated) and NA (Non Acclimated). Total proteins: CA:10 ug; NA 1: 2ug; NA 2 (concentrated): 10ug. B: Native bands were eluted from gel, concentrated and tested for AF activity. Rating was based on their ability to shape ice crystals, with 5 representing the highest activity and 0 no activity. AF activity of crude CA and NA extracts were also tested. Adapted from (Yu, Griffith 1999)

To test the hypothesis that ISPs oligomerization occurred *in vivo* and exclude that GLP, CLP and TLP co-eluting from some NPs was the result of similar electrophoretic mobility in native PAGE gels, separation techniques that exploited the selectivity of ISPs towards different ligands were adopted.

When CA extracts were immuno-precipitated using either anti-GLP, CLP or TLP antisera, each of them was found to co-precipitates GLP, CLP and TLP simultaneously.

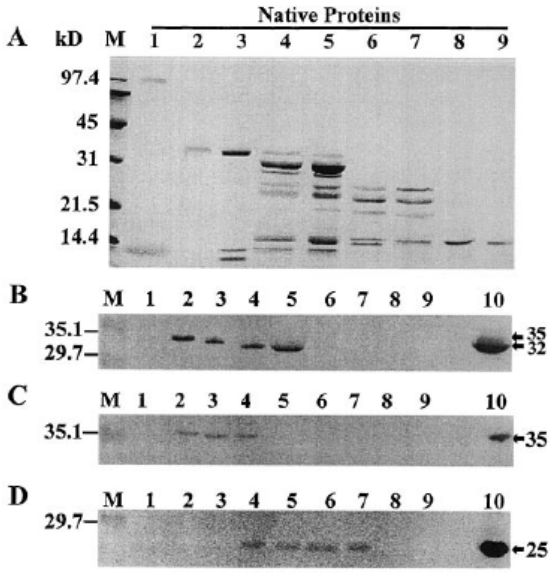

Figure 3.2.8: Native proteins eluted from native PAGE of CA extracts (1-9) were denatured and loaded on SDS-PAGE (A), blotted on nitrocellulose and probed with anti-GLP (B), anti-CLP (C) and anti-TLP antisera. Molecular weight of positives peptide is indicated on the right. Adapted from (Yu, Griffith 1999)

The authors could exclude possible cross reactivity of antisera as each of them specifically recognized different proteins within the extracts. In another test, when chitin affinity was applied to exploit the chitin binding ability of a 35 kDa CLP within the CA extract, NP3 was eluted. NP3 obtained with this procedure was denatured and loaded on SDS PAGE, producing the same protein pattern as that of NP3 isolated from native PAGE gel (Lane 3, **Figure 3.2.8 A**)

Finally, the possibility that GLP, CLP and TLP could form oligomeric complexes *in vivo*, was tested by assaying changes in enzymatic activity of CA extracts after incubation with antisera. The assumption behind this test, is that antisera could bind to different epitopes

of their protein targets masking critical residues or protein domains required for catalytic activity. Glucanase activity of CA extracts was found to be dramatically inhibited after incubation with each of the antisera (GLP, CLP and TLP) and the same was true for glucanase activity

To summarize, proofs that oligomeric ISPs complex form *in vivo* in the apoplast of cold acclimated winter rye were obtained by means of 1) native electrophoresis, 2) immunoprecipitation, 3) Chitin affinity chromatography. It is not clear why NA extracts contain some of the same native proteins that were isolated by native electrophoresis in CA samples and yet it didn't showed any AntiFreeze activity. The authors suggested that the arrangement of winter rye ISPs in oligomeric complexes could offer a mechanisms by which ISPs can increase their sizes, thus blocking a larger surface area on the ice crystals and produce increased Antifreeze activity, as it was proposed for *D. Canadensis* AFPs enhancement [(Wu, Duman et al. 1991, DeLuca, Comley et al. 1998)]. To determine whether further analogies can be drawn to DAFPs, it would be interesting to check whether purified native proteins isolated by native PAGE (Figure 3.2.5.1) showed decreased activity when compared to crude apoplastic extracts. Unfortunately, the method chosen by the authors to test ice structuring activity is rather qualitative, hindering precise comparisons among the samples.

3.2.5.1. Calcium ions and freezing and thawing influence ice structuring and chitinase activity of winter rye extracts

While there is no reports of known plant ISPs enhancers, studies on winter rye reported that Calcium ions can significantly impair residual AF activity of frozen apoplastic extracts once they were thawed [(Stressmann, Kitao et al. 2004)]. After noticing that freshly extracted ISPs in 20 mM Calcium chloride loose part of their Antifreeze activity upon freezing, the authors started a thorough investigation on the effect of calcium ions.

Figure **3.2.9** shows residual Antifreeze activity of winter rye extracts that were extensively dialyzed in buffers with increasing concentrations of ions before 3 freezing and thawing (FT) events.

Calcium chloride above 20mM significantly decreased antifreeze activity (A), while Magnesium Chloride produced partial activity loss only at 20mM (**B**). The influence of chloride was excluded by dialyzing the sample in sodium chloride (**B**) (no effect in the range from 20mM to 200mM was observef). Loss of activity was not likely to be due to salting out-mediated protein precipitation caused by freezing, as activity of dialyzed in NaCl and $MgCl_2$ wasn't affected even at high salt concentrations (**B**) (200mM). Furthermore, metal chelators had the ability to restore AF activity of frozen samples (C), without affecting initial AF activity of unfrozen samples (not shown).

As winter rye ISPs have been previously shown to form oligomeric complexes with PR proteins (some of them being chitinases) (Yu, Griffith 1999), potential influence of calcium ions and FT on structural reorganization of the protein complexes was assayed also by measuring chitinase activity and changes in tertiary and secondary protein structures by CD, Tryptophan fluorescence and native gel electrophoresis.

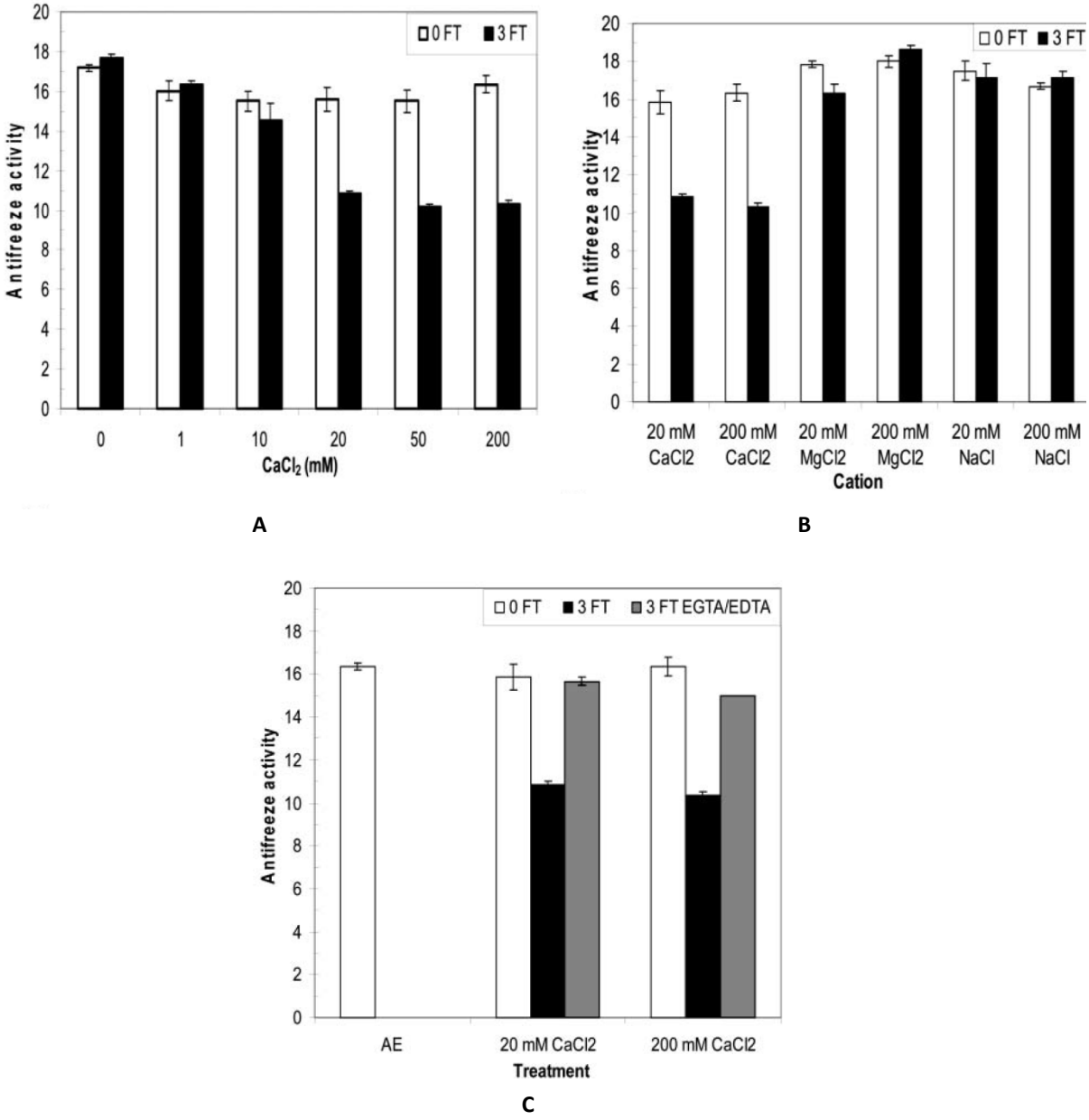

Figure 3.2.9: Effect of FT on winter rye extracts. Samples (5 µM total protein concentration) were frozen at -20°C for 2h and thawed rapidly thawed at room temperature. Antifreeze activity was assayed by examining ice crystals morphology in solution and expressed as the dilution rate at which AF could no longer be detected. A,B: Winter rye apoplastic extracts were dialyzed for 16h against CaCl2, MgCl2 and NaCl at pH 5.5 (0 FT) and assayed for activity before and after 3 FT cycles. 0 CaCl2 was obtained by dialysis with 5mM EDTA. C: To determine whether the effect of Ca2+ was reversible, samples in 20 and 200mM CaCl2 were frozen and thawed and then dialyzed against either 5mM EGTA or 50mM EDTA. Adapted from (Stressmann, Kitao et al. 2004)

Chitinase activity was found to be enhanced as Calcium concentration was increased, starting from 10 mM $CaCl_2$. At this concentration FT caused significant decrease of

enzymatic activity but couldn't be restored after addition of metal chelators EGDA and EDTA.

Freezing and thawing treatment and increasing the concentration of Calcium ions, affected the structure and re-organization of apoplastic proteins whitin CA extract. FT of 0 mM Ca^{2+} samples caused a large positive shift of the near-UV CD spectrum and disappearance of Trp fluorescence peak at 328 nm (C) as well as the loss of secondary structure elements coupled with increase in random coil.

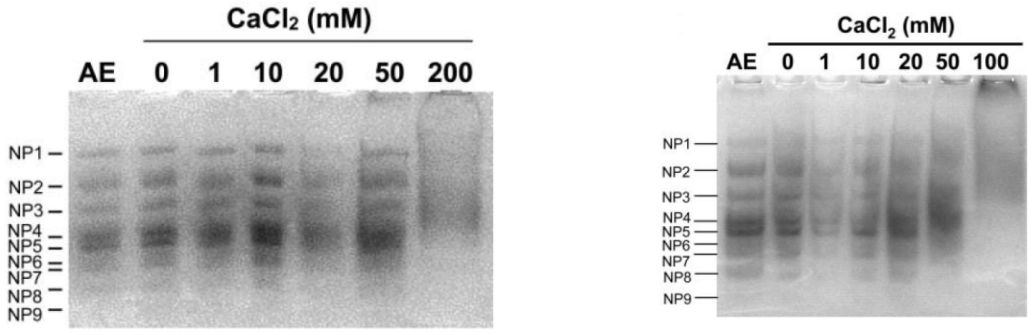

A B

Salt	*FT*	*λmax*
EDTA	+	327.7 ± 3, 360 ± 0.3
EDTA	-	355.2 ± 0.2
CaCl2	+	336.5 ± 0.2
CaCl2	-	335.2

C

Figure 3.2.9: Apoplastic proteins were dialyzed against (A) 0-200 mM CaCl2 and 5 µg loaded on native PAGE, (B) 0-100 mM CaCl2, FT 3 times and 10 µg loaded on native PAGE, (C) 5 mM EDTA EDTA or 20mM CaCl2, FT 3 times or kept at 4°C. Trp residues were excited at 280 nm and the wavelengths of maximum fluorescence emission recorded.

On this point the authors suggested that upon freezing, the ISPs complex could adopt a more "relaxed" conformation, still able to bind ice but with reduced chitinase activity (D.1 to D.2 transition, **Figure 3.2.10**). Addition of Ca^{2+} didn't affect AF activity, but did change the structure of winter rye ISPs , as shown by decreased migration in native PAGE (**Figure 3.2.9 A**), large positive change in near-UV CD, blue shift of Trp maximum fluorescence to 336.5 nm and sensible changes in secondary structures (loss of α-helical structure). It was suggested that upon binding of Ca^{2+} ions, winter rye ISPs could pack more tightly (**Figure 3.2.9 D.3**) and as a result, chitinase activity of the complex is increased. Only the

combination of freezing and thawing of apoplastic proteins in the presence of Ca^{2+} decreased both antifreeze and chitinase activity. The authors proposed that ISPs could undergo structural changes during freezing, exposing new Ca^{2+} binding sites that are different from those that enhance chitinase activity when calcium is present. Once Ca^{2+} is bound to these newly exposed binding sites, the structure or organization of the oligomers becomes more compact, and antifreeze and chitinase activity are inhibited (**Figure 3.2.10 D.4**).

To date, this is the only report on the modulation of plant ISPs activity, as opposite to the extensive literature produced on the ability of *D. canadensis* AFPs to be enhanced by endogenous and exogenous modulators.

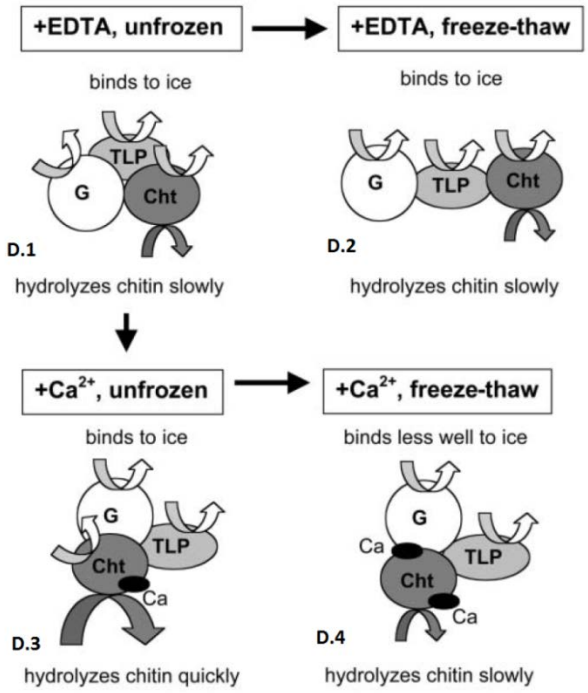

Figure 3.2.10: Hypothetical model summarizing changes observed in native apoplastic proteins exposed to Ca2+ and repeated freeze-thaw cycles. G: Glucanase, TLP: Thaumatin-Like, Cht: Chitinase.

3.3. MATERIALS AND METHODS

3.3.1. Cold acclimation of *T. aestivum*

Winter wheat seeds (*Triricum aestivum*, var. Cimabue) were kindly provided by Società Italiana Sementi. Seedlings were growth and cold acclimated with minor adaptation to routine protocols used to obtain ISPs from winter rye (Hon, Griffith et al. 1995)
Seeds were vernalized in vermiculite trays for 2 days at 4°C and germinated for 1 week at 21°C in a growth room at 21°C, 20% humidity, 16/8 h daylight/nighttime at 300 µmol $m^{-2}s^{-1}$. To induce ISPs production seedlings were moved to a cold room (4°C) at 12h daylight for 6 weeks. Control plants were kept in growth room at 21°C for another week. Plants were watered with modified Hoagland solution (Hoagland, Arnon 1950) as needed.

3.3.2. Apoplastic Protein Extraction

To recover apoplastic proteins, cut leaves were washed with abundant water and infiltrated with 20 mM $CaCl_2$ and Ascorbic acid at pH 3 under vacuum as described in litearature (Hassas-Roudsari 2011)(Hassas-Roudsari 2011, Hassas-Roudsari 2011, Hassas-Roudsari 2011)(Hassas-Roudsari 2011, Hassas-Roudsari 2011, Hassas-Roudsari 2011)(Hassas-Roudsari 2011, Hassas-Roudsari 2011, Hassas-Roudsari 2011)(Hassas-Roudsari 2011, Hassas-Roudsari 2011, Hassas-Roudsari 2011).
Leaves were blotted with adsorbent paper, pooled in syringes that were placed in 500 ml centrifuge bottles and centrifuged at 2000 g for 20 minutes at 4°C to recover apoplastic fluids. 200 µL aliquots were snap frozen in liquid nitrogen and kept at -80°C until used.

3.3.3. Protein quantification

Total proteins of CA_AE an NA_AE were quantified using the Bradford and BCA assay. To exclude possible interferences on absorbance values, proteins were precipitated in

acetone, the resulting supernatant dried in a SpeedVac and resuspended to the initial volume with milli-Q water. No significant background Absorbance was noticed when the Bradford reagent was used for protein quantification, on the contrary BCA measurements were highly biased even after extensive dialysis of the samples (possibly due to the high concentration of Ascorbic acid in the extraction buffer). Apoplastic extracts were concentrated 3 folds with 5 kDa concentrator (Vivaspin), added to 30 volumes of Bradford reagent and kept at room temperature for 5'. Samples were blanked against extraction buffer (20mM $CaCl_2$, 20mM Ascorbic acid) and absorbance recorded at 595 nm in a quartz cuvette with Agilent 8453 UV-Visible spectrophotometer. A calibration curve for protein concentration determination was obtained with BSA standards (0, 250, 500, 750, 1500 µg/ml).

3.3.4. Electrophoresis & Western blot

Protein electrophoresis was performed in denaturing conditions on Tris Tricine Precise 4-20 % pre-casted gel (Thermo) at 150 V. Acrylamide gels were blotted against Nitrocellulose membrane (Millipore) for 1.5 hours at 100V at 4°C, using a <biorad Mini Proten apparatus. After blotting, membrane was washed 6x5 minutes with TTBS (TBS + 1% Tween) and incubated for 45 minutes with 10% skim powered milk in TTBS. Chicken Anti-Thaumatin (Abcam AB3778) was added directly to the milk at a final dilution of 1:1000 and incubated for 1 hour. After 6x5' washing with TTBS, the membrane was incubated with Rabbit Anti Chicken IgY coupled with Peroxidase at a final dilution of 1:2500 in milk (Abcam AB6753) for 1h.

After 6x5' washing with TTBS, membrane was incubated with ECL (Amersham) for 1 minute and developed on Amersham Hyperfilm.

3.3.5. IRI assays

IRI assays were performed at the cold stage as described in Chapter 2 (material and methods). CA_AE samples were diluted 1:5 or 1:10 (CA_AE diluted) in milliQ water and added to one volume of enhancers in Sodium Acetate 50 mM pH 5. 46% w/V sucrose in Sodium acetate 50 mM was added 1:1 to the sample before analysis. CA_AE were incubated with enhancers for 1h in ice before being assayed for IRI activity.

3.3.6. Trypsin digestion

CA_AE was concentrated 2 fold with Vivaspin concentrator (5 kDa) and diluted 1:20 in Tris 20mM pH 7 (final dilution 1:10). 2.5% Trypsin (Sigma Aldrich) in PBS was added to CA_AE at a final concentration of 0.1%. In control samples, Trypsin was replaced with Tris buffer and the protease inhibitor cocktail PMSF (Sigma) added in two steps (after each hour) to a final concentration of 1mM. Digestion was performed for two hours or overnight at 37 °C

3.3.7. Pull Down Experiments

The procedure for immobilization of protein to NHS-Agarose and subsequent enrichment of target proteins (potential interaction) was adapted from the protocol supplied with NHS HP SpinTrap (GE Heathcare). 50 µg of TaTLP in 100 µL in coupling buffer were conjugated for 30' to 100 µL of 50% NHS-Sepharose 4 Fast Flow (Sigma Aldrich).
We chose to incubate TaTLP conjugated to NHS-Sepharose (TaTLP-NHS) with 100 µl of CA_AE (13 µg total protein) at the same conditions that were used in IRI assays (25mM Sodium Acetate) as opposite to use Binding Buffer (50mM Tris, 150mM NaCl, pH 7.5). The washing step before final elution was also performed in 25mM Sodium Acetate as opposite to Wash buffer (2M Urea, pH 7.5). In the final elution step, the resin was incubated with 2% SDS and boiled for 5 minutes.

Samples were collected at each step, resuspended 4:1 in denaturing sample buffer and 16 µL loaded on a Tris Tricine gradient (4-20%) gel.

Protein concentration prior to gel loading was performed by acetone precipitation of the sample and resuspension of the pellet in 1x denaturing sample buffer.

3.3.8. BLUE NATIVE gels

Blue Native kit purchased from Serva electrophoresis GmbH provided precast gradient 4-20% gel, native sample buffer and Anode and Cathode buffer for Blue native electrophoresis.

Samples were added to one volume of 2x sample buffer and loaded on acrylamide gel. After 5 minutes at 50V to allow proteins entering the gel as well as blue cathode buffer, voltage was increased to 300-350V for 45 minutes. After that, blue cathode buffer was replaced with buffer w/o Comassie, to allow visualization of dye front. The run was resumed until the dye exited the gel. Gels were fixed for 1h in 40% Ethanol, 10% Acetic acid and silver stained.

3.4. RESULTS

3.4.1. Extraction of ISPs from winter wheat seedlings

3.4.1.1. IRI activity: Cold acclimation vs. Non Acclimation

1 week old *Ta* seedlings grown at 21°C, were cold acclimated at 4°C for 6 weeks, as previous reports showed this timespan was sufficient to induce IRI activity in apoplastic extracts ((Hassas-Roudsari 2011). **Figure 3.4.1** shows the results of IRI assays on both Apoplastic Extracts from Cold Acclimated plants (CA_AE) and Non Acclimated (NA_AE). Protein concentration, estimated by Bradford Reagent, was 165 µg/ml for CA_AE and 25 µg/ml for NA_AE; protein extraction yield per gram of leaves was respectively 65 µg/g and 25 µg/g, in accordance with values reported in literature for winter wheat ((Antikainen, Griffith 1997). After being diluted with extraction buffer to obtain the same volume of extract/FW_{leaves} (1 ml/2.5 g), extracts were tested at 1:10 dilution in water (see final protein concentration before sucrose addition in figure description).

To confirm whether the IRI activity observed was ascribable to proteins, Trypsin was added at a final concentration of 0.1% w/V to CA_AE and residual activity was tested after 2 hours and over night incubation. **Figure 3.4.2** shows that after 2 hours of Trypsin treatment, all IRI activity of CA_AE sample is lost as the median ice crystal area is comparable to those produced by NA_CA. This data, together with the observation there is no significant difference between ice crystals sizes of Control (Tris Buffer) and NA_CA samples, indicates that proteins are the only IRI active compounds within the plant extracts.

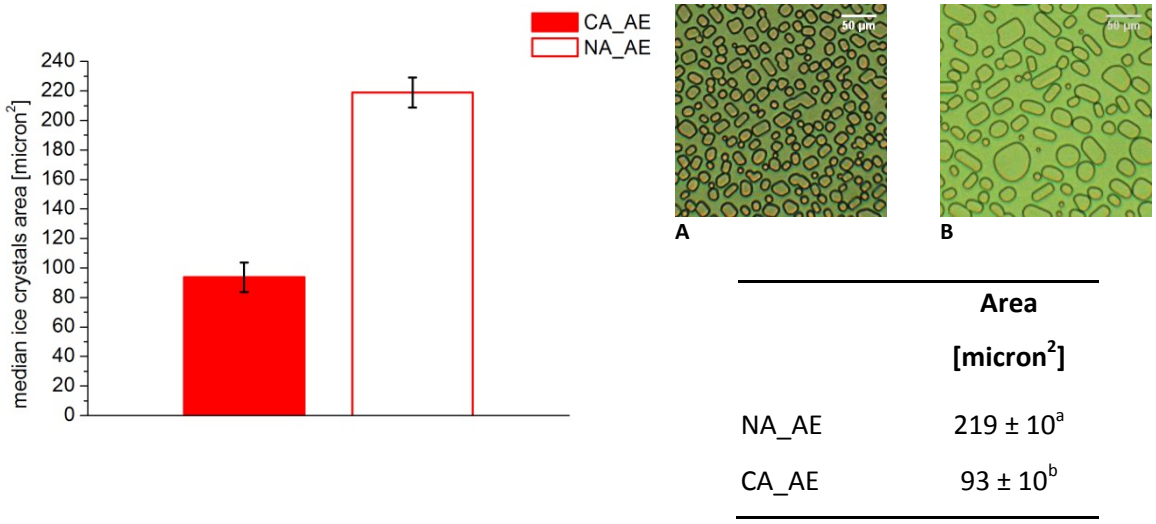

	Area [micron^2]
NA_AE	219 ± 10^a
CA_AE	93 ± 10^b

Figure 3.4.1: Results of IRI assay . A: CA_AE; B: NA_AE; Proteins concentration (before Sucrose addition): CA_AE: 16.5 µg/L, NA_AE: 6.3 µg/L. Means with different letters are significantly different at the 0.05 level (ANOVA), n=3

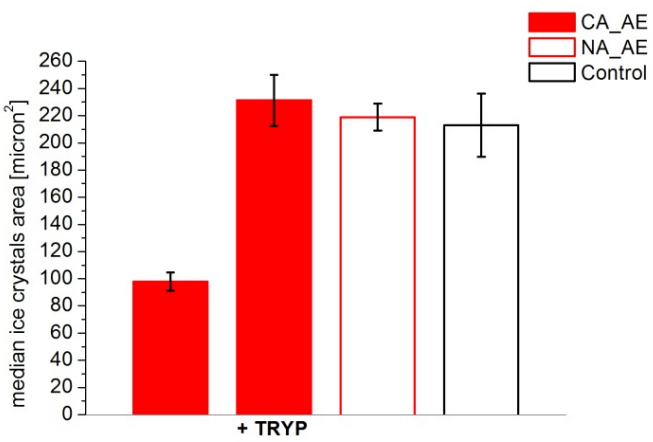

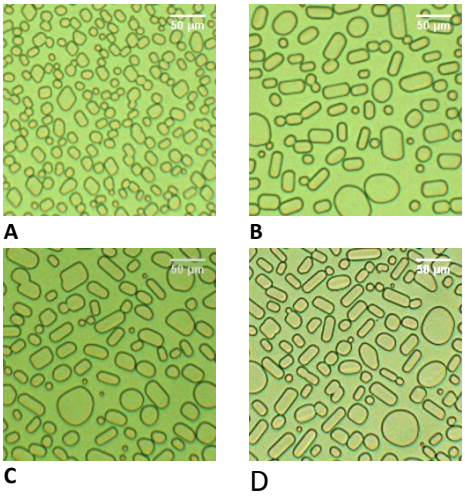

	Area [micron^2]
CA_AE	97 ± 7^a
CA_AE + Trypsin	231 ± 19^b
NA_AE	218 ± 10^b
Control	213 ± 23^b

Figure 3.4.2: Results of IRI assay. A: CA_AE; B: CA_NA + TRYP; C: NA_AE; D: Control (20mM Tris). Proteins concentration (before Sucrose addition): CA_AE: 16.5 µg/L, NA_AE: 6.3 µg/ml. Means with different letters are significantly different at the 0.05 level (ANOVA), n=3

3.4.1.2. Western blot

To check whether CA_WE contained TaTLP or other Thaumatin-Like proteins, CA_AE and recombinant TaTLP were loaded side by side on a SDS-PAGE, blotted on a Nitrocellulose membrane and probed against a commercial Anti-Thaumatin IgG. TaTLP migrated at 23 kDa (**Figure 3.4.3**), close to the molecular weight predicted from its sequence (21.3 kDa excluding the 22 aa signal sequence). Anti-Thaumatin IgG detected a total of three proteins in the CA_AE samples, migrating at approx. 100, 23 and 15 kDa (**Figure 3.4.3**). A search for Thaumatin-Like proteins against Uniprot reviewed database yielded 42 entries amongst plant proteins (Viridiplantae) spanning the range from 17 to 27 kDa. The 100 kDa proteins might then be an artifact due to cross reactivity of the Antibody, while the other two proteins fall in the appropriate size range for TLP. On the basis of its electrophoretic mobility, we concluded that the 23 kDa protein in CA_AE is TaTLP. Its concentration in CA_AE estimated by comparing the band intensity with that of recombinant TaTLP was calculated to be approximately 2 µM.

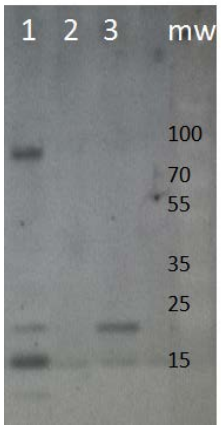

Figure 3.4.3: Lane 1: CA_WE (2.64 µg total protein); Lane 2: Sample buffer; Lane 3: recombinant TaTLP: 0.38 ug; Western blot: Anti.Thaumatin: 1:1000 , Anti IgG: 1:2500. Exposition: 10'

3.4.2. Enhancing IRI activity of apoplastic proteins extracts

3.4.2.1. Effect of exogenous proteins addition

The recombinant *Ta*TLP expressed by *P. pastoris* (see Chapter 2) didn't produced a significant IRI activity when compared to a control solution without ISPs . However, it is possible that TaTLP might require for its activity some co-factors or interactors that are only present in the plant.

A TLP lacking any AF activity was found to be an endogenous interactor of *D. canadensis* AFPs, enhancing their Thermal Hysteresis maximum values by several folds (Wang, Duman 2006). Given these premises, we decided to evaluate the effect of adding TaTLP to CA_AE on IRI activity.

3.4.2.1.1. IRI assays

Figure **3.4.4** shows that addition of TaTLP to IRI active CA_AE induced a significant decrease of average ice crystals size. To test whether this effect was due to specific interaction of TaISPs with TaTLP, we decided to use as a control the homologue

Thaumatin that had no previous report of TH or IRI activity. In the first place, the observation of IRI activity enhancement on CA_AE by Thaumatin let us think that this phenomenon may not be limited to specific TLPs, but rather related to common structural features shared by Thaumatin homologous proteins.

To further test this hypothesis, we decided to use Chymotrypsinogen as a control, being its molecular weight (25 kDa) comparable with that of *Ta*TLP (21 kDa) and that it has no reported IR activity nor homology with Thaumatin. Surprisingly, we found that even Chymotrypsinogen enhanced IRI activity of CA_AE, to the same extent as TaTLP and Thaumatin did. No significant difference ($P < 0.05$) in the ability of inhibit ice crystals growth were detected among the three treatment (+ TaTLP, Thaumatin and C. Trypsinogen).

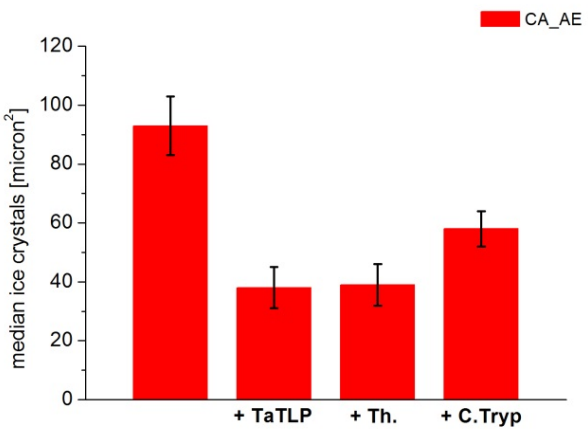

	Area [micron^2]
CA_AE	93 ± 10^a
+TaTLP	39 ± 6^b
+Thaumatin	38 ± 7^b
+C.rypsinogen	58 ± 6^b

Figure 3.4.4: Results of IRI assay; Proteins concentration (before Sucrose addition): CA_AE: 16.5 µg/L; TaTLP, Th., C.tryps: 20 µM (0.75 mg/ml). Means with different letters are significantly different at the 0.05 level (ANOVA), n=3

IRI enhancement by protein addition was noticed also when CA_AE was diluted 1:2 (**Figure 3.4.5).** We chose to use diluted CA_AE also to test the effect of concentration as well as size (**Fig.3.4.6**) of the protein enhancers, using a different batch of CA_AE (CA_AE II). Exogenous protein concentration was lowered by 6 folds, and Thyroglobulin was chosen to evaluate if increasing protein size could accentuate IRI, as suggested by reports on DAFPs and Fish AFPs type III (Wu, Duman et al. 1991), (DeLuca, Comley et al. 1998). Results are summarize in **Table 3.4.1** and will be discussed in **Paragraph 2.5**.

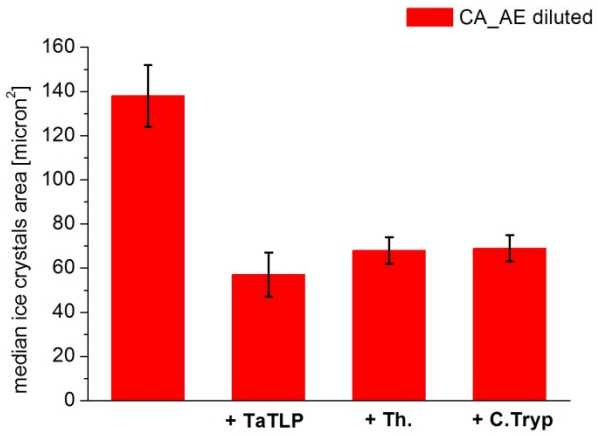

	Area [micron^2]
CA_AE diluted	138 ± 14^a
TaLP	57 ± 10^b
Thaumatin	68 ± 6^b
Chymotypsinogen	69 ± 6^b

Figure 3.4.5: Results of IRI assay on 3 replicates; Proteins concentration (before Sucrose addition): CA_AE diluted: 8 µg/L; TaTLP, Th., C.tryps: 30 µM. Means with different letters are significantly different at the 0.05 level (ANOVA), n=3

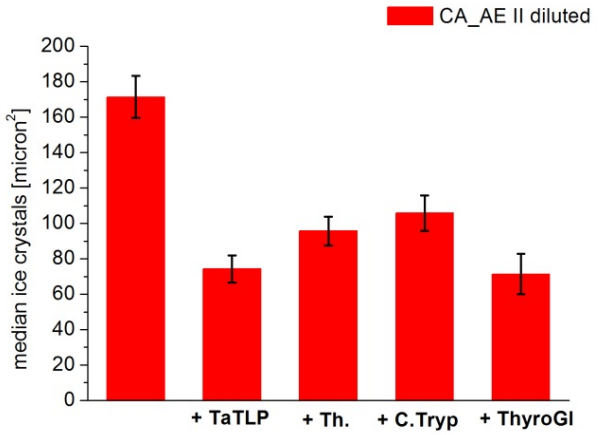

	Area [micron^2]
CA_AE II diluted	171 ± 12^a
+TaLP	74 ± 8^b
+Thaumatin	95 ± 8^c
+Chymotrypsinogen	105 ± 10^{c,d}
+Thyroglobulin	71 ± 11^b

Figure 3.4.6: Results of IRI assay on 3 replicates; Proteins concentration (before Sucrose addition): CA_AE II diluted: not measured; TaTLP, Th., C.tryps, ThyroGL: 5 µM. Means with different letters are significantly different at the 0.05 level (ANOVA), n=3 Means with different letters are significantly different at the 0.05 level (ANOVA), n=3

	CA_AE + 30µM prot. [micron^2]	% area reduction vs CA_AE	CA_AE dil. + 30 µM prot [micron^2]	% area reduction vs CA_AE	CA_AE II dil +5µM prot [micron^2]	% area reduction vs. CA_AE
No enhancer	93		138		171	
+ TaTLP	39	58%	57	59%	74	57%
+ Thaumatin	38	59%	68	51%	95	44%
+ Ch.Tryp	58	38%	69	50%	105	39%
+ ThyroGl					71	58%

Table 3.4.1: ice crystals median area values after addition of exogenous proteins to CA_AE extracts. The % reduction of ice crystals area after addition of the enhancer is also reported. For each set of experiments, the enhancer concentration is reported in µM before addition of Sucrose. Proteins concentrations of extracts before addition of Sucrose: CA_AE: 16.5 µg/ml, CA_AE dil: 8.25 µg/ml, CA_AE dil II: not calculated.

At this point, it wasn't clear whether the enhancing effect on TaISPs by enhancers was ascribable to IRI enhancement of endogenous TaISPs . *Ta*TLP was then added to NA_CA, which doesn't contain any ISPs and as a result, no significant effect on ice crystals dimensions was noticed (**Figure 3.4.6**).

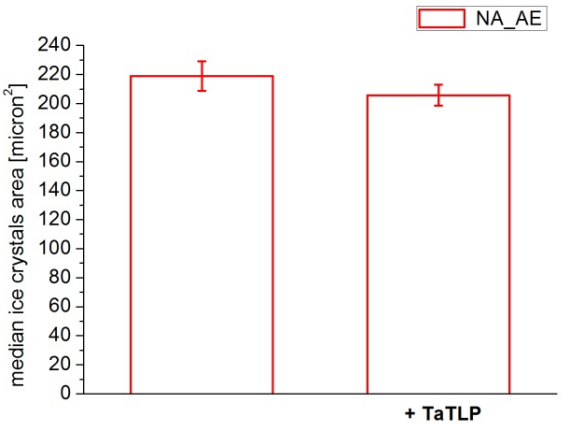

	Area [micron^2]
NA_AE	219 ± 10^a
+ *Ta*TLP	206 ± 7^a

Figure 3.4.6: Results of IRI assay on 3 replicates; Proteins concentration (before Sucrose addition): NA_AE: 6.3 µg/L; TaTLP: 30 µM. Means with different letters are significantly different at the 0.05 level (ANOVA), n=3

To evaluate if protein mediated IRI enhancement was common to ISPs from other sources, we replicated the test using a fish AFPs provided by Nichirei Foods company (Japan). Fish AFPs were dosed on the basis of previous experiments to obtain a population of ice crystals with sizes comparable to those obtained with CA_AE. When TaTLP was added to fish AFPs, no enhancement of IRI activity was obtained (**Fig 3.4.7**).

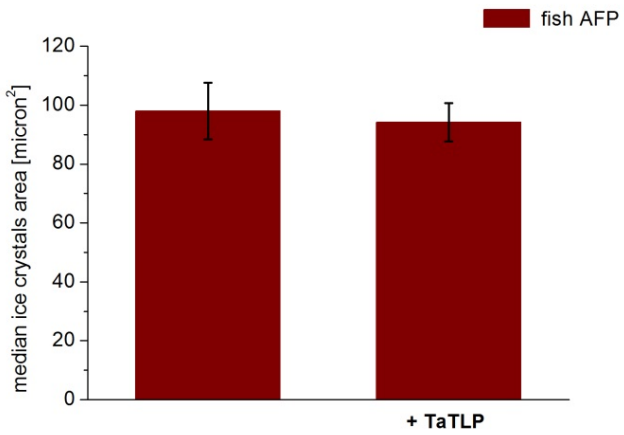

	Area [micron^2]
Fish AFPs	98 ± 9^a
+ *Ta*TLP	94 ± 6^a

Figure 3.4.7: Results of IRI assay on 3 replicates; Proteins concentration (before Sucrose addition): Fish AFPs: 0.035 mg/L; TaTLP: 30 µM. Means with different letters are significantly different at the 0.05 level (ANOVA), n=3

3.4.2.2.2. Pull down experiment

In 2003, Wang & Duman identified two species of TLPs enhancing *DAFPs* using the Yeast Two-Hybrid assay. (Wang, Duman 2006, Fields, Song 1989). Given that in our experience TaTLP was found amongst other proteins, to enhance AntiFreeze activity of TaISPs , we decided to apply an analogous strategy and use *Ta*TLP as a bait to fish possible ISPs interactor in CA_AE.

Since no commercial Antibody was available for *Ta*TLP and the Chicken IgY against Thaumatin didn't produced satisfactory results on IP tests, we decided to opt for the pull down technique, where the bait protein is directly conjugated to Agarose beads and this complex is then incubated with the source of potential protein interactors (see material and methods).

Figure 3.4.7 shows the results of the Pull Down experiment when Sepharose NHS beads conjugated with *Ta*TLP were incubated overnight with CA_AE and the samples loaded onto a gradient Tricine Gel 4-20%. *Lane 1* and *2* show compositions of TaTLP and CA_AE samples before incubation with the resins. TaTLP was successfully conjugated to NHS-Sepharose beads as the first wash of the resin resulted in poor amount of protein that was detectable after concentrating the sample 12 folds (*Lane 3*). *Lane 4* shows the unbound fraction obtained after incubating over night CA_AE with NHS -TaTLP. To discriminate between specific TaTLP interactors and proteins that could bind to the resin aspecifically, we incubated CA_AE with NHS-Agarose (*lane 5*, wash). After overnight incubation, the beads were washed with Sample Buffer 1x, boiled for 5 minutes and loaded on *lane* 7 (NHS-TaTLP + CA_AE) and 8 (NHS + CA_AE). Some CA_AE proteins were found to bind aspecifically to the resin, as shown in *Lane* 8. However, we couldn't find evidences to support the interaction between TaTLP and any protein within CA_AE, as indicated by the lack of significant differences in the electrophoretic profiles between samples 7 and 8.

Sample loaded in Lane 7 was also tested for IRI activity, but didn't produce any significant effect on ice crystals size compared to a control. However, it should be noted that IRI activity of CA_AE was completely abolished by addition of 2% SDS (Elution buffer) followed by boiling. Activity couldn't be recovered neither after acetone precipitation of proteins and resuspension in Sodium Acetate.

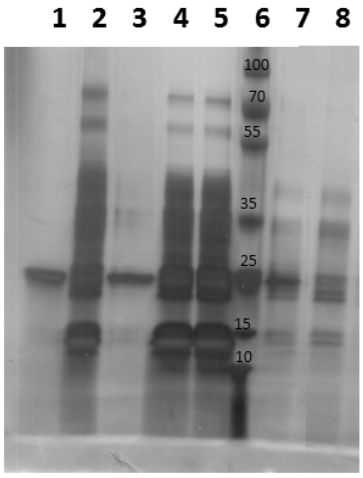

Lane	**Sample**
1	*Ta*TLP
2	CA_AE (0.13 µg/ml)
3	Uncojugated NHS-TaTLP (12x)
4	CA_AE + NHS-*Ta*TLP (Unbound)
5	CA_AE + NHS (Unbound)
6	MW
7	CA_AE + NHS-*Ta*TLP (Elution) (5x)
8	CA_AE + NHS (Elution) (5x)

Figure 3.4.7: Lane 1: TaTLP 0.5 mg/ml (1 uL); Lane 2: CA_AE 0.13 µg/ml (6 uL); Lane 3: Unconjugated TaTLP after incubation of Lane 1 sample with NHS Sepharose (6uL); Lane 4: Unbound CA_AE after incubation with NHS-TaTLP (6 uL); Lane 5: Unbound CA_AE after incubation with NHS (12 uL); Lane 7: Elution of NHS-TaTLP after incubation with CA_AE and washing, concentrated 2.5x with acetone (12 uL); Lane 8: Elution of NHS after incubation with CA_AE and washing, concentrated 2.5x with acetone (12 uL). Samples 3, 7 and 8 were concentrated to allow protein visualization after staining. Fold concentration (x) is reported for concentrated samples and expressed as the result of acetone precipitation and total volume loaded on gel.

3.4.2.3. Effect of Freezing & Thawing

Thus far, our data suggested that IRI activity of CA_AE could be enhanced simply by addition of non ISP proteins to the mixture. Granted that this effect was not related to modification of the colligative properties of the solution (no effect observed when TaTLP was added to NA_CA), the most straightforward hypothesis was that TaISPs were directly involved in this process. It is possible that enhancers are recruited by ISPs on ice crystals binding sites, thus hindering a larger surface on the ice crystals and limit ice growth with a more pronounced steric effect (Wang, Duman 2006), as postulated by the Kelvin Effect (see Section 1.1.3). If this is the case, we speculated that non-specific protein binding by ISPs would be quite detrimental for the plant to take place at physiological conditions, as this would deplete the cell from proteins that are required for its sustenance. One intriguing hypothesis is that TaISPs could recruit other non ISPs by non-specific interactions upon ice binding, just when the freezing event occur.

It was reported that ISPs from apoplastic extracts of cold acclimated winter rye undergo conformational changes upon freezing. If freezing occurs in the presence of Ca^{2+} above 20 mM, ISPs partially loose its ice structuring activity, as well as ordered secondary structures as evidenced by CD and Tryptophan fluorescence spectra (Yu, Griffith 1999). Furthermore, when apoplastic proteins were loaded in Native PAGE gels, freezing and thawing events reduced their electrophoretic mobility, resulting in fewer bands migrating at higher molecular weights in a dose depending manner as calcium ions concentration was increased.

We chose to test the hypothesis that freezing could induce stable oligomerization of TaISPs with enhancers, by means of measuring residual IRI activity after freezing as well as checking for proteins complex on native gel electrophoresis.

3.4.2.3.1. IRI assays

To test whether protein mediated TaISPs enhancement was somehow influenced by the freezing event, we measured IRI activity of CA_AE plus TaTLP before and after freezing. The rationale behind this the experiment relies on the assumption that TaTLP-TaISP complex could be large enough to cause significant decrease in ISPs molar concentration as well as reduced diffusion coefficient, that in turn will result in lower AF activity.

In order to obtain the maximum percentage of ISPs bound to ice we needed to act on two freezing process variables: annealing time (i.e. time allowed to ISPs to bind to ice) and ice surface available for ISPs binding. Several studies have indeed shown that some ISPs can stick to the ice with different kinetics, as TH values measured with nanoliter osmometer were found to be dependent, amongst other variables, on annealing time (Takamichi, Nishimiya et al. 2007, Kubota 2011, Drori, Celik et al. 2014). During the freezing cycle applied for standard IRI measurements with the Cold Stage (see section 3.2.4.2) , samples in 23% sucrose solutions are rapidly frozen down to -40°C and then brought to -5°C stepwise; at that stage a population of ice crystals is formed, yielding a greater ice surface than if the same frozen phase was formed as a continuous ice block. Temperature is then kept at -5°C for over 60 minutes, allowing sufficient time for ISPs to bind to ice crystals. Cold stage can offer a high degree of precision in controlling temperature gradient over the samples, so we chose to use it for this purpose. The effect of freezing on IRI activity was evaluated by applying a second consecutive freezing cycle to sample, and comparing ice crystals dimensions obtained after the first and second freezing cycle. Results are shown in **Figure 3.4.8** and discussed in **Paragraph 2.5**.

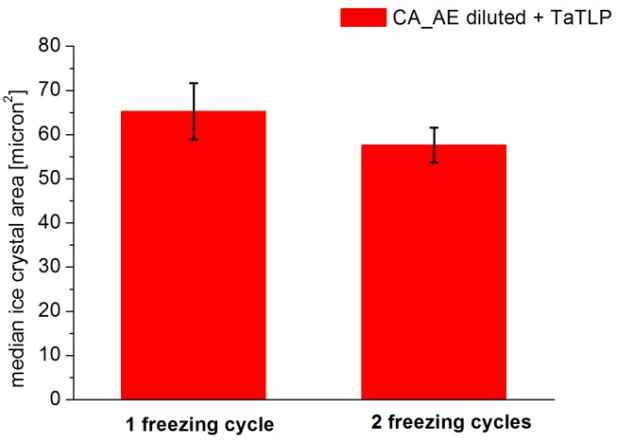

	Area [micron^2]
	CA_AE + *TaTLP*
Ater 1 freezing cycle	65 ± 6[a]
After 2 freezing cycles	57 ± 4[a]

Figure 3.4.8: Results of IRI assay on 3 replicates; Proteins concentration (before Sucrose addition): CA_AE diluted: 8 µg/L; TaTLP: 30 µM. Means with different letters are significantly different at the 0.05 level (ANOVA), n=3

3.4.2.3.2. BLUE NATIVE gel electrophoresis

To test whether the freezing events could lead to formation of stable oligomeric complexes between TaISPs and exogenous proteins (using *TaTLP* as a model) or other *Ta* proteins, we chose to evaluate changes in electrophoretic mobility of proteins before and after 5 freezing and thawing cycles, using Blue native PAGE. As opposite to common native gel electrophoresis, where no SDS is present and so protein mobility depends on protein size as well at its net charge, the use of Coomassie Brillant Blue dye confers negative charge without denaturing the proteins, allowing separation on the basis of their sizes (Schagger, von Jagow 1991)

Freezing and thawing cycles were applied to samples as shown in previous literature data on apoplastic ISPs from winter rye (Stressmann, Kitao et al. 2004), where FT was found to decrease electrophoretic mobility of ISPs .

We chose to decrease the ratio of micrograms of TaTLP added to CA_AE total proteins previously used in IRI assays (see Paragraph **3.4.2.1.1)**, from 1:0.2 to 0.1:0.2 (undiluted CA_AE); this precaution was necessary as the higher TaTLP molar ratio would have complicated to quali-quantitatively discriminate between TaTLP and TaTLP complexed to TaISPs . **Figure 3.4.9** shows the results of FT CA_AE, CA_AE + TaTLP and TaTLP on their electrophoretic mobility.

FT didn't produce any effect on electrophoretic mobility of TaTLP (Lane 5 and 6), but apparently neither did on any proteins species within CA_AE (Lane 1 and 2). If the hypothesis of TaISPs forming stable complexes with other proteins upon ice binding were true, we would have expected to see some difference in protein pattern already in FT CA_AE samples TaTLP. After addition to CA_AE, TaTLP didn't changed its electrophoretic mobility neither before freezing (Lane 3), indicating that interaction with wheat ISPs is not likely to occur neither at physiological conditions. It should be noted that Blue native PAGE didn't offered optimal resolution in the higher part of the gel corresponding to protein with higher molecular weight, but still we couldn't detect any significant increase in electrophoretic mobility of TaTLP after FT (Lane 3 and 4) and after incubation with CA_AE (Lane 5 vs Lane 3). These data demonstrate the lack of interaction between TaTLP and TaISPs and are coherent with the result of the Pull Down experiments.

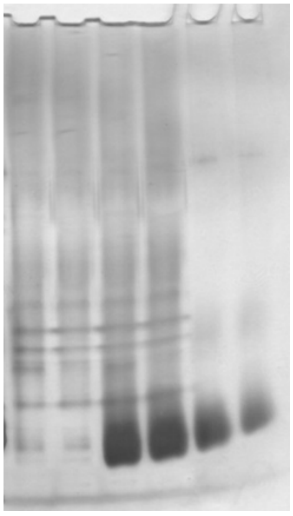

Lane	Sample
1	CA_AE
2	CA_AE 5 FT*
3	CA_AE + TaTLP
4	CA_AE + TaTLP 5FT
5	TaTLP
6	TaTLP 5 FT

Figure 3.4.9: Blue Native electrophoresis. Protein final concentration in samples: CA_AE: 8,2 µg/L; TaTLP: 0.75 mg/L. Loaded sample volume: 15uL
***5 FT: 5 Freeze & Thaw cycles (see materials and methods)**

3.5. DISCUSSION

After finding that TH of *D. canadiensis* AFPs was enhanced by DAFP interactors, it was proposed that this effect was due to the increased size of the AFss, hindering a larger ice surface from water molecules binding (Duman, Serianni 2002)

Proteins have generally a rather limited number of protein interactors, and in most cases, the specificity of the interaction is granted by domains where amino acids are orientated in arrays that constitute the signatures for binding. Non-specific interactions arise for example when proteins loose their fold and therefore expose hydrophobic residues, leading to aggregation of protein into insoluble aggregates. This in the case of protein denaturation due to physical (e.g. temperature) or chemical stress (e.g. salting out).

Non-specific interactions between biological molecules would constitute a tremendous problem in biology as 1) they would deprive the organisms from physiological mediators (e.g., Insulin in Diabetes) and 2) protein aggregates could induce toxicity (e.g. beta amyloid structures). It was therefore remarkably surprising to find out the apparent promiscuity by which TaISPs could be enhanced upon exogenous proteins addition. On the contrary, in the case of *D. canadensis* TH enhacement of AFPs was limited to specific protein partners and in some cases point mutations were sufficient to abolish this interaction and thus TH enhancement. It must be noted that while studies on *D. canadensis* AFPss measured Thermal Hysteresis, our investigations focused on another property of ISPs , which is Ice Recrystallization Inhibition. IRI assay is thought to be way more sensitive than TH measures, so it would be interesting to test whether TH enhancement would follow the same trend as it was found for IRI in our experiments, as well as measuring protein mediated IRI enhancement in DAFPss.

We question if our results have any physiological significance given the high concentrations (0.75 - 0.125 mg/mL) at which exogenous proteins were added to CA_AE (16 – 8 µg/ml).

Comparing the IRI activity values obtained after addition of TaTLPs on CA_AE (**Table 3.4.1**), it can be concluded that TaTLP was probably used in large excess being that it gave the same results, in terms of % Area reduction, when it was added at 0.75 and 0.125 g/L final concentration. One could then argue that TaTLP enhancing effect might be due excessive TaTLP protein dosage, but still, no IRI enhancement was observed in fish AFPss that were tested at the same conditions and with comparable IRI activity.

Protein mediated enhancement of ISPs would provide the plant cell with a mean to increase its AF activity without altering its osmotic equilibrium; the reason behind the enhanced ability to block ice is likely to be found in the increased dimensions of ISPs - enhancer complex, sheltering a larger area on ice crystals surface and increasing the curvature of the growing ice front lying between ISPs binding sites (DeLuca, Comley et al. 1998)

In our tests, protein enhancers size doesn't seem to have a significant impact on the extent of IRI enhancement, as shown by results obtained with Thyroglobulin and compared to those with TaTLP (**Table 3.4.1**). However, it is possible that TaISPs form oligomeric complexes carrying several copies of non-ISPs, thus masking the effect of increasing single non-ISPs size.

The results obtained with diluted CA_AE could be of great relevance for the food industry (**Figure 3.4.5 and 3.4.6**), as those findings would potentially allow manufacturers to formulate frozen foods products with reduced TaISPs . Thus far, high producing costs have been the most limiting factor in determining the commercial success of ISPs from natural sources.

We couldn't find any significant evidence of protein interaction when TaTLP was used as a bait in pull down experiments (**Figure 3.4.7)**, as we would have expected considering previous reports where 1) TLPs were found in ISPs complexes in winter rye apoplastic extracts (Yu, Griffith 1999) and 2) a *D. canadensis* TLP enhanced TH of hemolymph by interacting with some DAFPss.

Considering the detrimental effect that non-specific sequestering of apoplastic proteins by TaISPs would have on cell metabolism at normal physiological condition, it is reasonable to assume that this event could be triggered only by stress condition, as for example when freezing of plant tissues occur.

AFPssOur tests have failed at detecting stable oligomeric complexes between TaISPs and enhancers, even when freezing and thawing cycles were applied to samples. The fact that IRI didn't change significantly when a second freezing cycle was applied to samples could be due to the fact 1) the oligomerization didn't significantly altered the diffusion

coefficient of ISPs molecule or 2) the increased size around the Ice binding site could compensate for the slower binding kinetics.

Likewise, Coomassie Brilliant blue used in experiments with Blue Native PAGE could have biased electrophoretic mobility of samples by acting as a detergent and dissociating unstable complexes of TaISPs and their protein enhancers.

The most controversial argument in supporting our hypothesis of protein mediated ISPs enhancement, is the proposed mechanism by which ISPs can form interaction with protein partners, irrespective of any specificity. Speculating in this direction, one possibility is that arrays of ISPs bound to the ice surface result in the functionalization of the ice crystals, in the same way as charged/apolar functional groups are added to resins used for affinity chromatography As a result, functionalized ice crystals will be able to bind different proteins with low selectivity.

We believe that the best technique to test whether protein enhancers could bind to TaISPs once those are bound to ice, would be to apply fluorescence spectroscopy to ice crystals imaging. Microfluidic devices were recently developed to study the kinetics of ISPs binding to ice (Celik, Drori et al. 2013), allowing the researcher to rapidly change the solution surrounding a single ice crystals at constant subzero temperatures. Once TaISPs have been annealed to ice crystals surface, it would be then possible to introduce a solution of the protein enhancer conjugated to a fluorophore; if the enhancer could bind ISPs that are bound to the ice, after removing the second solution the ice crystals surface should fluoresce over the dark background.

4. WINTER WHEAT AS A SOURCE OF ICE STRUCTURING PROTEINS TO STABILIZE ICE CREAM PRODUCTS

4.1. ABSTRACT

As discussed in Chapter III, cold acclimation of winter wheat seedlings resulted in the accumulation of ISP that efficiently inhibited ice crystals growth in IRI assays. This chapter reports the optimization of the bioprocess to obtain ISPs from *T. aestivum* with ability to inhibit the Ice Recrystallization, which occurs in ice cream. Two extraction methods, involving direct boiling of the plant or the extracted plant juice, were tested for their ability to yield samples with IRI activity. High temperatures were effective in extracting thermostable ISPs from wheat seedlings, and the extracts produced thereof showed higher IRI activity when compared to standard apoplastic extracts. The most viable method to obtain thermostable ISPs from wheat, named Leaves Decoction Extraction, consisted in boiling the seedling for 10 minutes and recover the water of infusion afterwards. Industrial ice creams formulated with and without ISP from Leaves Decoction Extracts (LDE), were stored at fluctuating temperatures below 0 °C for 1 week to induce ice crystal growth by recrystallization processes. LDE did effectively reduced ice recrystallization rate at a final protein concentration of 1.8 ppm. At the end of the recrystallization cycle, LDE formulated ice cream showed ice crystals with half of the radius of control ice cream.

Five proteins species from LDE were eluted in IRI active fractions at the end of a purification process comprising ion exchange, gel filtration and reverse phase chromatography. These proteins migrated in two dimensional acrylamide gels in a narrow range of molecular weights and isoelectric points, suggesting that they might be isoforms of the same protein.

4.2. INTRODUCTION

4.2.1. Ice Recrystallization Inhibition enables freezing tolerance

One striking feature typical of plant ISPs is their extreme IRI activity at very low concentrations. IRI was detected at protein concentration of 25 µg/L in apoplastic extracts of winter rye [(Steponkus 1996)]. On the contrary, maximal TH expressed on average by plant ISP is generally modest (0.2-0.4 °C) and lower than other ISP species on a molar basis (Venketesh, Dayananda 2008a).

This dichotomy is the result of the survival strategy adopted by the plant to cope with cold, *i.e.* freezing tolerance. Being that plant can't avoid freezing, their ISPs may have evolved pronounced IRI activity to prevent tissues damages due to uncontrolled ice crystals growth [(Griffith, Lumb et al. 2005)].

Ice formation in planta is believed to start at the extracellular compartment, where the freezing temperatures of the liquid are higher due to the presence of lower concentration of solutes. Paradoxically, both Ice nucleating Proteins (INP) and ISP are required to mediate controlled freezing in planta. Rapid ice propagation occurs when a solution is supercooled several degrees below its freezing point and could be detrimental for cell survival (Karow Jr., Webb 1965)

INPs function is to initiate the freezing process in planta at higher subzero temperatures, mitigating the effect of excessive ice propagation rate. It was proposed that another result of controlled extracellular freezing, is the release of latent heat that further protect the intracellular compartment from freezing (Zachariassen, Kristiansen 2000).

Once ice is formed outside of the cells, recrystallization at constant subzero temperatures cause the progressive growth of ice crystals, that ultimately lead to mechanical stress and rupture of soft tissues [(Knight, Duman 1986)]. In this context, secretion of proteins with high IRI activity in the extracellular *milieu* would confer additional protection to the plant

4.2.2. ISP Types in plant

Although the first reports of Thermal Hysteresis proteins in the blood of artic fishes date back to 1971 (DeVries 1971), it was not until 1992 that two independent studies reported the first discovery of TH activity in plants juices: the xylem of bittersweet *S. dulcamara* (Urrutia, Duman et al. 1992) and apoplastic extracts of winter rye *S. cereale* (Griffith, Ala et al. 1992).

From 1992, TH and IRI activity were found in more than 60 different plant species, and ISPs were isolated from almost 15 of them (**Figure 4.2.1**) (Gupta, Deswal 2014a). Since the focus of the study presented here is Ice Recrystallization activity by plant ISP, only those for which IRI activity was documented will be discussed and referred to as Ice Recrystallization Inhibition Proteins (ISPs) hereafter.

The first ISPs to be isolated and characterized from a plant source was DcAFP, a 36 kDa protein from *Daucus carota* containing a Leucine Rich Repeat (LRR) region and showing similarity with antifungal Polygalacturonase Inhibitor Proteins (PGIP) (Smallwood, Worrall et al. 1999a). On the basis of its homology with PGIP, DcAFP was initially ascribed to family of Pathogenesis-Related proteins. Fungal PGIP play a critical role in the first step of plant infection by fungi, degrading components of the cell wall (Di Matteo, Bonivento et al. 2006). However, DcAFP wasn't found to interact with any PGIP in yeast two hybrid assays (Zhang, Wang et al. 2006). Structural predictions of DcAFP indicated that the Leucine Rich Repeat domain span across the entire protein, forming a regular right-handed β-helix consisting of 10 loops of 24-amino acid repeats with solvent exposed asparagine at the putative ice binding site (Zhang, Liu et al. 2004). The specific IRI activity of purified DcAFP is higher than that obtainable with fish AFPs. IRI could be detected at DcAFP < 1 μg/ml compared with > 5 μg/ml recombinant fish AFP type III (Smallwood, Worrall et al. 1999b).

S. No.	Plant	Material	MW (kDa)	Cellular localization	Homology	Properties	Reference
1	*Ammopiptanthus mongolicus*	Crude extract from leaves	40, 200 and 39	Cytoplasmic	Agglutinin	Glycosylated, heat stable, 0.9°C TH	Fei *et al.* 1994; Yong *et al.* 2000; Fei *et al.* 2008
2	*Bromus inermis*	Cell culture	33	Secreted/ Apoplastic	Class I chitinase	calcium independent antifreeze activity	Nakamura *et al.* 2008
3	*Chimonanthus praecox* L.	Corolla	33	Apoplastic	Class I chitinase	0.52°C TH	Zhang et al. 2011
4	*Daucus carrota*	Tap Root extract	36	Apoplastic	Polygalacturonase inhibitor protein	N-glycosylated, TH-0.36 at 150 µg/mL	Worrall *et al.* 1998; Smallwood *et al.* 1999
5	*Forsythia suspensa*	Crude extracts from bark and leaves	20	Cytoplasmic	Dehydrins	pH sensitive, optimum pH is 7 and it decreases on either side of the optimal pH	Simpson *et al.* 2005
6	*Hippophae rhamnoides*	Shoot	41	Apoplastic	Polygalacturonase inhibitor protein	Glycosylated, heat labile, 0.19°C TH and 9 fold IRI	Gupta and Deswal 2012
		Leaf	-	Apoplastic	-	-	
7	*Raphanus sativus*	Tuber and leaf	1.32	Apoplastic	No homology reported	TH in tuber and leaves 0.20±0.03 and 0.18±0.02°C respectively	Kawahara H *et al.* 2009
8	*Lolium perenne*	-	29	Apoplastic	No homology reported	TH and ice nucleation not detected (0.03), boiling stable, N-glycosylated	Sidebottom *et al.* 2000; Pudney *et al.* 2003
9	*Picea abies*	Leaf	70, 27	Apoplastic	Chitinase	TH 2.19 ± 0.83 at 400 µg/mL	Sabala*et al.* 1996; Jarzabeck *et al.* 2009
10	*Picea pungens*	Leaf	27	Apoplastic	Chitinase	TH 2.02 ± 0.40	Jarzabeck *et al.* 2009
11	*Prunus persica*	Bark	60	Cytoplasmic, nuclear and chloroplastic	Dehydrin	0.06°C TH	Wisniewski *et al.* 1999
12	*Rhodiola algida*	Cell culture	29–85		No homology reported	Glycosylated, heat labile	Lu *et al.* 2000
13	*Secale cerale*	Leaf	15–38	Apoplastic	Endochitinase, endoglucanase and thaumatin like proteins	Six AFPs	Hon *et al.* 1994; Hon *et al.* 1995
14	*Solonum dulcamara*	Stem	67	Cytoplasmic	WRKY transcription factor	High glycine content (23.7 mol %), TH-0.3°C at conc.10-35 mg/mL, glycosylated	Duman 1994
15	*Triticum aestivum*	Leaf	21.3	Apoplastic	Thaumatin like protein	Heat stable, rich in β-sheet and random coil	Chun *et al.* 1998; Kontogiorgos *et al.* 2007

Figure 4.2.1: A list of the ISP isolated and characterizes from plants so far. Boxed in red are ISP with documented IRI activity. Adapted from (Gupta, Deswal 2014a)

In 2000, a novel ISPs was isolated from the ryegrass *L. perenne* (Sidebottom, Buckley et al. 2000a), with no significant sequence similarity with other proteins. It was proposed that the 7 residue repeated motif of the consensus sequence X X N X V X G (**Figure 4.2.2 A**) could form two flat opposite-facing surfaces ('a' and 'b') of a left-handed beta roll (**Figure 4.2.2 B**, showing the crystal structure), that are complementary to the prism of plane of ice (Kuiper, Davies et al. 2001). Mutagenesis studies revealed that only the 'a' side has affinity for ice (Middleton, Brown et al. 2009); the Ice Binding Site was restricted to a 3 aa sequence with a conserved inward-pointing Valine that makes up the hydrophobic core and is coordinated by Asparagine ladders (**Figure 4.2.2 A**). The model was later validated by the crystallographic structure of recombinant *L. perenne* AFP (LpAFP) (Middleton, Marshall et al. 2012). To date, this is the only available crystallographic structure for a plant ISP. The IRI endpoint (i.e. the most diluted concentration at which IRI activity could still be detected) of a purified LpAFP fractions is 0.6 µg/ml.

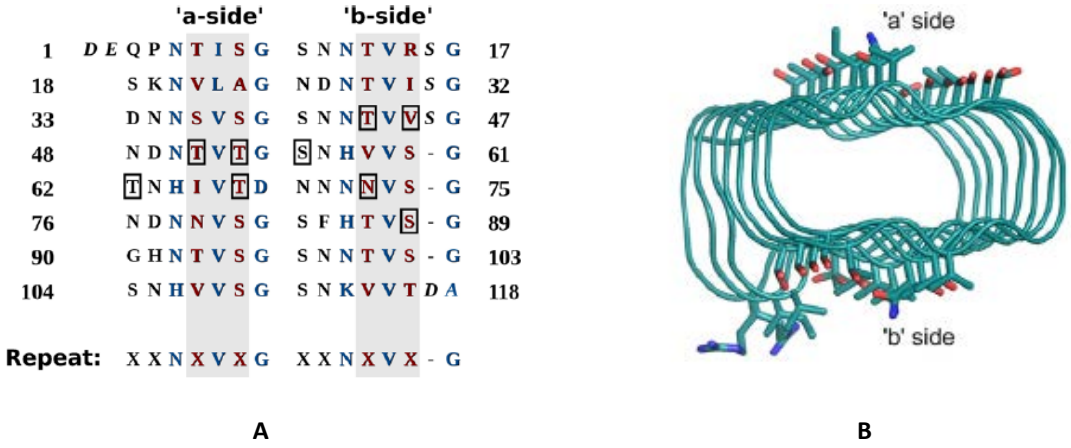

Figure 4.2.2: A: LpAFP sequence is represented so that each row represents one loop of the roll. Highlighted are the two ice binding sites, in blue inward pointing residues while in red residues that generate the ice binding faces. Boxes surround amino acids that were mutated to Tyrosine in mutagenesis studies (Middleton, Brown et al. 2009)**. B: 3D Structure of LpAFP. The main-chain atoms of the Ice are shown in cartoon representation. Side chains of amino acids within the ice binding site on a and b sides are shown as sticks. Cyan:carbon, Blue: Nitrogen, Red: Oxygen . Adapted from (**(Middleton, Marshall et al. 2012)**)**

A few years after the discovery of LpAFP, it was found that the translated C-terminal portion of two mRNA transcripts induced in cold acclimated in *T. aestivum* (taIRI-1 and taIRI-2), showed almost 50% sequence identity with LpAFP (Tremblay, Ouellet et al. 2005).

This domain was thus referred to as IRI domain. Furthermore, LRR motifs sharing homology with Receptor Kinase Domains (RKD) were identified the N-terminal domain of translated taIRI-1 and tIRI-2. Being that the recombinant products of the transcripts didn't show any kinase activity, it was proposed that also the LRR within the RKD domain could have evolved to bind ice, similarly to the LRR found in DcAFP. This hypothesis was validated by the recombinant expression of the RKD domain, which indeed showed IRI activity.

Another heat stable ISPs was found by Simpson in 2005 from the weeping *Forsythia suspense* (Simpson, Smallwood et al. 2005). The peptide mass fingerprinting analysis of the 20 kDa protein purified from barks revealed its homology with dehydrins. This is not the first report of a dehydrin bearing antifreeze activity, a 60 kDa protein with TH activity was previously isolated from *Prunus persica* (Wisniewski, Webb et al. 1999).

Lastly, IRI activity was also found in apoplastic extracts of cold acclimated winter rye (Griffith, Lumb et al. 2005). Apoplastic ISPs with ice shaping ability within these extracts belonged to the heterogeneous family of Pathogenesis-Related proteins 5 (Thompson, Fernandes et al. 2006), comprising proteins with homology to Thaumatin, Glucansase and Chitinases. Among those proteins, Chitinases were validated as ISPs both by recombinant expression in heterologous systems and by isolation from other plants (Gupta, Deswal 2014b).

4.2.3. ISPs are homologues to Pathogenesis-Related proteins

Most of plant ISPs identified so far share homologies with Pathogenesis-Related proteins (PR), i.e. proteins secreted by the plant in response to infection by pathogens. The question of whether ISPs possess also antifungal activity or ISPs and PR proteins are different species is still a matter of debate.

The case of ISPs from cold acclimated winter rye is rather emblematic: while apoplastic proteins in the extracts of cold acclimated plants have both ice binding and antifungal activity, the same proteins (or at least most of them) are secreted upon inoculation of the

plant with fungi. However, in this latter case, they don't possess any ice binding or ice shaping activity (Hon, Griffith et al. 1995).

Do winter rye ISPs and PR belong to two distinct families, and if this is the case why would a plant invest extra energy for the expression of antifungal activity upon cold acclimation?

The first question cannot be addressed by just considering the data presented in the literature on winter rye ISPs, being that most of the studies were performed on crude apoplastic extracts rather than on individual isolated protein species. A logical explanation for the second question is that without its defense mechanisms activated, a plant would be totally exposed to potentials attack by psychrophilic pathogens at subzero temperatures, with poor chances of survival . Being almost in a dormant state, it wouldn't be possible for the frozen plant to set up an *ad hoc* response to external attack; this is why it is more convenient for the plant to enter in the frozen stage with its immune system activated. **Figure 4.2.3** depicts a possible scenario for winter rye apoplastic proteins secreted upon cold stress and attacks by pathogens.

Winter rye proteins are not the only case of promiscuous ISPs, having other targets other than ice. Two chitinases from seabuckthorn exhibit simultaneously hydrolytic as well as antifreeze activity (TH and IRI) (Gupta, Deswal 2014b).

One possibility is that PR proteins could acquire novel functions after post-translational modifications that occur with cold acclimation. Being that several plant ISPs were reported to be highly glycosylated (**Figure 4.2.1**), it was proposed that PR proteins could acquire ice-binding activity by addition of glycan chains.

However, ice binding ability was found to be glycosylation dependent only for one ISPs, the AFP from of *S. dulcamara* (Duman 1994).

A more recent hypothesis suggests that ice-binding ability can be acquire by PR proteins after structural reorganization of the protein occurring throughout cold acclimation. In the case of two chitinases isolated from *A. mongolicus* with constitutive IRI activity, β secondary structures content as well as IRI activity were found to be increased in correspondence of cold acclimation (Gupta, Deswal 2014b).

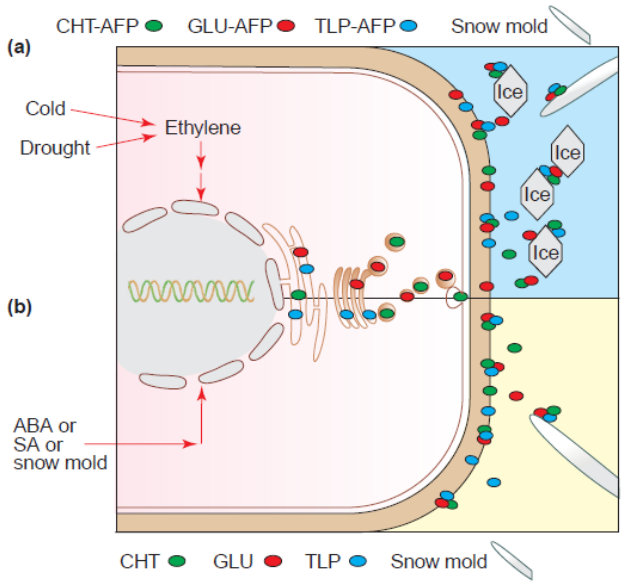

Figure 4.2.3: Regulation of AFPs and PR proteins in winter rye. Ethylene, Abscisic Acid (ABA) or Salicylic Acid (SA), mediates the response to biotic (cold, drought) or biotic (mold) through the expression of proteins with PR and/or AntiFreeze activity. Depending on their binding target, secreted proteins will either block ice growth or mold elongation. CHT: Chitinase; GLU: Glucanase; TLP: Thaumatin-Like. Adapted from {{190 Griffith,M. 2004}}

Most of the ISPs with homology to PR proteins show exclusively IRI activity or are expressed only upon cold acclimation. One example is the carrot DcAFP with homology to PGIP but no reports of Polygalacturonase Inhibition activity (Zhang, Wang et al. 2006).

The taIRI-1 mRNA transcript that codes for IRI-like proteins in wheat and show homology with Receptor Like Kinase proteins, is exclusively expressed as a result of cold acclimation and its recombinant product doesn't show any kinase activity (Tremblay, Ouellet et al. 2005).

For those proteins that are similar to PR but show exclusively IRI activity, it was proposed that ice binding activity could have arisen from gene duplication followed by 1) mutation of residues forming the ice binding site (Yeh, Moffatt et al. 2000) 2) integration of transposable elements that disrupted functional domains (Tremblay, Ouellet et al. 2005).

4.2.4. Accumulation, extraction and purification of winter wheat ISPs

The accumulation of proteins with IRI activity in the apoplast is a fundamental requisite to confer freezing tolerance to the plant (Thomashow 1998)()()()(). Depending on the plant type, longer cold acclimations time might be required to acquire maximum freezing tolerance. For winter wheat, 4-7 weeks at temperatures above freezing are generally required to complete cold acclimation (Appels, Eastwood et al.)

ISP transcripts were shown to accumulate within plant tissues 1-2 hours after exposition of the plant to cold temperatures (Tremblay, Ouellet et al. 2005, Meyer, Keil et al. 1999).

In the case of *T. aestivum* taIRI-1 and taIRI-2 expression levels reach plateau after 6 weeks of cold acclimation (Tremblay, Ouellet et al. 2005). This value is in good accordance with the finding that in winter wheat, maximal apoplastic protein concentration is obtained after 7 weeks of plant being exposed to low temperatures (Antikainen, Griffith 1997).

Wheat taIRI-1 transcript accumulated almost in every part of the plant upon cold acclimation, including leaves, roots and crown. DcAFP trascripts were also detected in every part of the carrot plant, including taproots, shoots and roots. Widespread tissues expression of ISPs with similarity to LpAFP was observed also in other plant species (Gupta, Deswal 2014a).

Almost all plant ISPs or putative ISPs were found in the apoplastic compartment of the cell (**Figure 4.2.1**). This finding is compatible with the physiological role of plant ISPs that is to mitigate the damage of ice crystals growth where the freezing event occur. Among ISP with cytoplasmic localization, a 20 kDa Dehydrin isolated from the bark and leaves of *F. suspentia* was found to have IRI activity. Previous reports on PCA60, a 60 kDa Dehydrin isolated from cold acclimated *P. persica* that was later found to possess moderate TH activity (Wisniewski, Webb et al. 1999), correlated the accumulation of this protein with the increased ability ox xylem fluids to supercool. It was proposed that Dehydrins could mediate their protective effect on the cells against freezing primarily by binding to and inhibiting Ice Nucleators that could penetrate the cytoplasm.

Most of the ISPs isolated and characterized so far from plant, were obtained by selective extraction of the apoplastic protein fraction. The procedure to recover AFPs from the apoplast of cold acclimated winter rye leaves was described for the first time in 1994 (Hon, Griffith et al. 1994b). Since then, this method became almost the standard to isolate ISPs from plant sources. It basically involves the infiltration of the plant tissue under vacuum with a buffer solution whose salts concentration and pH are designed to minimize extraction of cytoplasmatic proteins; the apoplastic exudate is then recovered by mild centrifugation of the infiltrated leaves. A great advantage offered by the selective extraction of apoplastic proteins over the extraction of total cell proteins, is the relative high purity of ISPs that it yields. Compared to the complexity of the cytoplasmatic and membrane fractions, only a few protein species are indeed secreted within the apoplast. On the contrary, this extraction procedure is quite far from being optimized for large production of plant ISPs. The discovery of the thermostable LpAFP from *L. perenne* (Sidebottom, Buckley et al. 2000b) allowed researchers and private companies to exploit its boiling resistance to ease the extraction process and the subsequent recovery of ISPs enriched protein fractions. Plus, thermo-tolerant proteins are of great interest for the industry when considering the high temperature treatments involved in the sanitization process required for most long-lasting food products.

In the case of LpAFP, the extraction process to recover the protein at high purity from the plant, consists of the steps of: 1) grinding of the frozen plant tissues, 2) resuspending the soluble proteins in extraction buffer and discarding insoluble particulate by centrifugation, 3) boiling the supernatant and recover the heat resistant proteins in solution (Lauersen, Brown et al. 2011). The use of high temperature treatment to facilitate the recovery of pure fractions of LpAFP from its natural source was also patented (Lillford, Mcarthur et al. 2005).

Depending on the grade of purity required for analysis, ISPs can be separated by conventional means of chromatography or protein electrophoresis. One powerful technique to isolate ISPs is to exploit their unique affinity for the ice phase. Using this principle, the Ice Affinity Purification technique was developed in the P.L. Davies lab

(Kuiper, Lankin et al. 2003b) and aided in the isolation and identification of several ISPs (Lauersen, Brown et al. 2011, Basu, Graham et al. 2015, Graham, Davies 2005)

In practice, a cold finger is immersed into a solution containing ISPs and ice nucleation is initiated on its surface after addition of ice seeds. By lowering the temperature of the cold finger at a very slow rate, the ice layer will grow selectively incorporating only ice binding compounds (i.e. ISPs). By applying several cycles of IAP of crude extracts containing ISPs, it was demonstrated that ISPs could be recovered to homogeneity. **Figure 4.2.4** depicts the steps of Ice Affinity Purification, while in **Figure 4.2.5** the protein fractions at various purifications stages of recombinant LpAFP are reported.

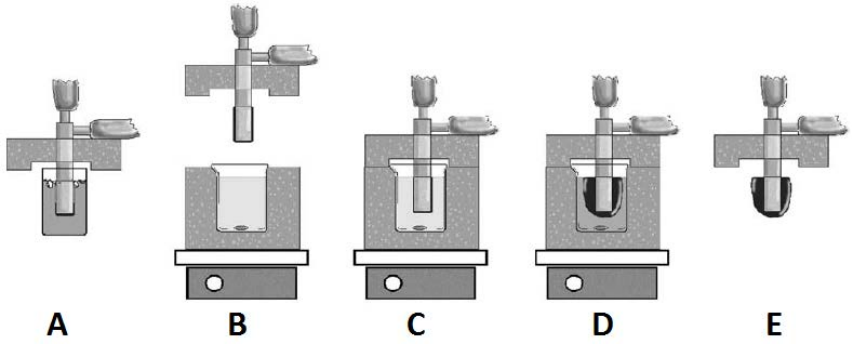

Figure 4.2.4: Ice Affinity Purification. A: formation of an ice layer around the cold finger, B-D: cold finger is immersed in the ISPs solution and cooled to stimulate ice front growth and incorporation of ISPs. E: ice bound fractions is recovered after melting. Adapted from (Kuiper, Lankin et al. 2003a)

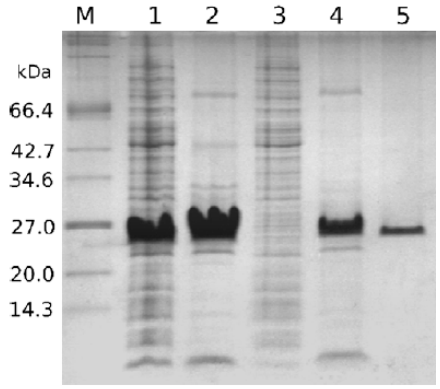

Figure 4.2.5: Purification of recombinant LpAFP from E.coli lysates. M: Molecular weight, 1: Crude E.coli lysate, 2: Supernatant of boiled lysate 3: Pellet of boiled lysate, 4: liquid fraction after IAP, 5: Ice fraction after IAP. LpAFP migrates at approx. 27 kDa. Adapted from {{218 Middleton,A.J. 2009}}

4.3. MATERIAL AND METHODS

4.3.1. Protein Extraction

Cold acclimated seedlings of *T. aestivum* were used as a source of ISPs and obtained as previously described in Chapter III.

- *Apoplastic Extraction* (Ae): The method was adapted from previous literature (Hon, Griffith et al. 1994a) and performed as described in Chapter III

- *Leaves Decoction Extraction* (LDe): hot boiling water was added at a ratio of 4:1 (w/w) in a beaker containing freshly collected wheat seedlings leaves and then boiled for 10 minutes. After cooling the beaker in an ice bath, the decoction water was recovered and centrifuged at 10000 g for 10 minutes. The supernatant was collected and 1 ml aliquots were snap frozen in liquid nitrogen and stored at -80°C until use. LDE used to formulate ice cream was obtained from a total of 160 g of wheat seedlings acclimated for 6 weeks. 590 ml of decoction water were recovered after boiling and concentrated on an Amicon Ultrafiltration device equipped with 3 kDa membranes to a final volume of 50ml. The concentrate was diafiltered by addition of 300 ml of water and concentrated again to a final volume of 50 ml. This volume was pooled into a 50ml falcon tube, snap frozen in liquid nitrogen and stored at -80°C until use.

- *Total protein extraction* (TPe): The method was adapted from previous literature reporting the purification of LpAFP from its native source (Lauersen, Brown et al. 2011). Freshly collected leaves of wheat seedlings were frozen in liquid nitrogen and grounded in a mortar to obtain a powder. Soluble proteins were extracted by mixing the powder with an equal volume of 10 mM Tris-HCl pH 7.5, 25 mM NaCl at 4°C for 20 minutes. Insoluble material was pellet at 8000g for 10 minutes at 4°C

and the resulting supernatants boiled for 5 minutes. Heat soluble proteins were recovered in the supernatant after centrifugation at 10000g for 30 minutes. 1 ml aliquots were snap frozen in liquid nitrogen and stored at -80°C until use.

4.3.2. Protein quantification

Protein quantification was performed using the Bradford quantification method as described in Chapter III. Before quantification samples were concentrated with 5 kDa Vivaspin 500 concentrators.

4.3.3. IRI assays

IRI assays as well as data analysis was performed as previously described in Chapter III. 5 µL of samples in Tris-HCl 20 mM pH 8 were added 1:1 (v/v) to a 46 % sucrose solution prepared in the same buffer.

4.3.4. Ice cream production and stabilization with winter wheat ISPs

4 liters of control ice cream mix were formulated using the following recipe: 8% vegetal oil, 10% defatted dry milk solids, 12 % sucrose, 5% glucose syrups, 0.5 % cremodan Cremodan SE 30 stabilizer (Danisco A/S, Denmark) containing 65% monodiglycerides and 35% hydrocolloid, water. Ice cream formulated with ISPs (4 lt.) was obtained by addition of 50 ml LDE concentrate to the mix.

The mix was pasteurized at 75°C for 30 seconds, homogenized at 65°C 200 bars and aged at 4°C for 16 hours. Ice cream was made with a MF-50 Laboratory Freezer (WCS) set to extrude ice cream at a temperature of -5.5 °C and 100 % overrun. All 4 liters of ice cream mix were used to make ice cream but only the last liter extruded from the freezer was collected. This precaution is required each time the freezer is started or a new ice cream setup is defined, being the first 3 lt required by the freezer to reach the desired operational parameters.

4.3.5. Ice crystals analysis in Ice Cream

The ice cream samples were analyzed by optical microscopy using a temperature-controlled stage (LTS 120, Linkam Scientific). The procedure was adapted to the ice cream industry standard method to analyze ice crystals in cream samples (Barfod, Da Lio et al. 2009). All instruments used for sample handling were pre-refrigerated at -18 °C.

A few grams of samples were drawn with a spatula from the inner portion of 80 g ice cream sticks and transferred to a beaker filled with 100 ml of tert-butanol. Here, the ice cream piece was pushed against the walls of the beaker to remove air. A few milligrams of de-gassed ice cream were quickly transferred on a microscope slide placed over the peltier device of the cold stage pre-cooled at -17°C. Nitrogen was insufflated into the stage to remove condensed vapors from the surface of the slide. Ice crystals were manually traced and with the aid of a graphic tablet. Area calculation was performed with the ImageJ plugin Object J.

For each sample, at least 4 images from 4 different samplings were acquired at a 10x magnification and a minimum of 1000 crystals was obtained for the statistical analysis of the data. Frequency count was performed on the logarithms of the area of ice crystals and the resulting population approximated to fit a normal distribution. Fitting and statistics were performed using software Origin Pro 8 Non Linear fitting Tool.

4.3.6. Purification of ISPs from LDE extracts

LDE extracts were concentrated 50 fold with 5 kDa Vivaspin 20 concentrators. 1 ml was loaded into a 6 ml Resource Q column pre-equilibrated with Tris-HCl 20 mM pH 8.

0.5 ml sample was loaded on a Superdex 200 10/300 column pre-equilibrated with Tris buffer at a flux of 0.5 ml/min.

For Reverse Phase chromatography, 380 µL sample was applied to a C4 analytical column (Phenomenex) pre-equlibrated with 95% Milli-Q water and 5% acetonitrile. Elution was performed with a linear gradient of 95% Acetonitrile.

Ion exchange and Gel Filtration chromatography were performed on an AKTA Purified FPLC system (GE Healthcare); RP chromatography was run on a 1100 Series HPLC system (Agilent Technologies) equipped with a diode array absorbance detector.

4.3.7. Isolectrofocusing & 2nd dimension SDS PAGE

Isoelectric focusing was performed using 13 cm Immobiline Dry Strip with linear pH interval 3-10 on Ettan IGPhor Isoelectric focusing system (GE Healthcare). Samples preparation and isoelectric focusing was performed according to the manufacturer instruction (Amersham Bioscienes).

LDE purified or crude extracts were precipitated with ice cold Acetone at -80 °C for 1 hour and pellet resuspended in 250 µl of denaturing Rehydration buffer for 30' at room temperature on a vortex. After centrifugation to remove insoluble matter, the supernatant was pipetted over ceramic strip holder (supplied with the IGPhor) and the strip gently applied over the sample. A layer of mineral oil was dispersed over the strip to avoid over-night drying.

The voltage protocol used for isoelectric focusing was adapted from previous trials performed in our lab and consisted in the following steps: 1) 1h: 0V, 2) 13h: 200V, 3) 10': 300V, 4) 30': 300-3500 V gradient, 5) 3h: 3500 V, 6) 30': 3500-8000 V, 7) 4h: 8000V. The temperature was set at 20°C and the maximum current value for each strip set at 5 µA.

Once the run was completed, the strip was briefly washed with Milli-Q water and incubated 15' in Denaturation buffer with 2% DTT to reduce disulfide bonds, plus other 15' in the same buffer with 2.5% iodoacetamide to alkylate reduced cysteine. In the last incubation step, bromophenol blue was added in traces to allow the monitoring of protein migration in SDS PAGE.

The strip was gently laid horizontally over a 13x13 cm 13% Acrylamide SDS PAGE, and hot 0.4% Agarose was poured to seal the IPG strip in place.

Electrophoresis was performed over-night by applying constant 9 mA to the gel; the next day the gel were briefly washed in water and stained with either Colloidal Coomassie or silver staining (Mortz, Krogh et al. 2001).

4.4. RESULTS

4.4.1. Optimization of ISPs extraction from *T. aestivum*

Three extractions protocols were tested on 6 weeks cold acclimated plants and each evaluated for their ability to yield active extracts that could prevent crystals growth in IRI assays. ISPs Each extraction process yielded a different amount of volume (ml) per gram of extracted leaves (column 2, **Table 4.4.1**). Since our scope is to evaluate the extraction yield of ISPs per gram of fresh vegetal material, the first step was to normalize the extracted volumes by concentration with Vivaspin devices. We chose to normalize the samples to a final concentrations of 1 ml of extract per 5 grams of extracted leaved (column 3). Concentrated extracts were then diluted 20 fold before IRI assay, to limit possible influences of small solutes on the colligative properties of the solution and eventually on ice recrystallization rates (column 4)

Extraction method	Extracted leaves/extract volume (g/ml)	Normalization (g/mL) [fold increase]	Dilution before IRI assay
Apoplastic protein Extract (AE)	0.875	5 [5.71x]	1:20
Leaves Decoction Extract (LDE)	0.25	5 [20x]	1:20
Total Protein Extract (TPE)	2.52	5 [2x]	1:20

Table 4.4.1: Values are reported in weight of fresh leaves extracted per volumes of extract obtained [g/ml]. *Column 2*: Concentration after extraction; Column 3: Concentration with 5 kDa Vivaspin; Column 4: Dilution rate before IRI assay.

The IRI activities of the three *T. aestivum* extracts are reported in **Figure 4.4.1**. As expected, all samples inhibited ice recrystallization compared to the buffer solution (Control) and among heat-treated extracts, Total Protein Extraction (TPe) yielded extracts that were significantly more active than those obtained with the Leaves Decoction

method (LDe). Surprisingly, LDE an TPE were more effective that Apoplastic Extracts (AE), thus indicating that boiling stable ISPs are present in leaves tissues and can successfully be recovered after boiling.

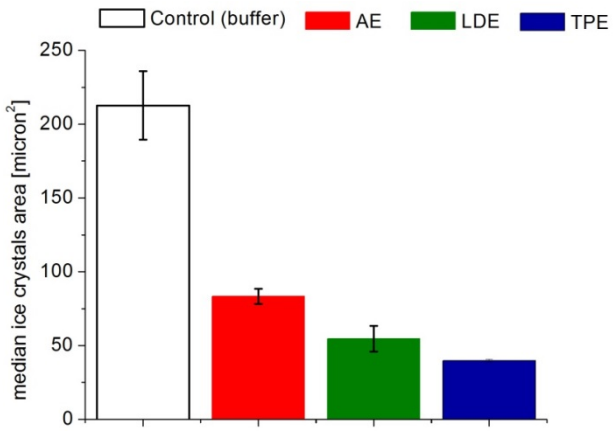

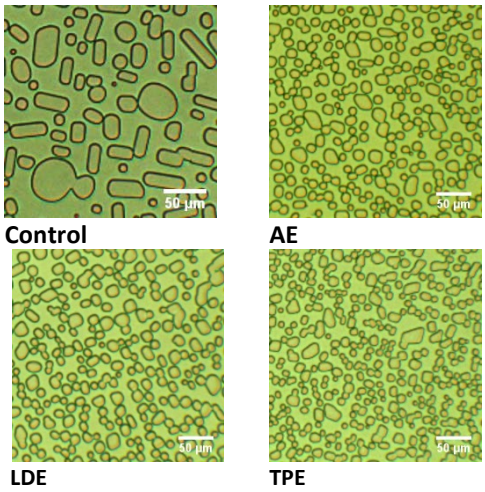

Figure 4.4.1: Results of IRI assay on extracts from cold acclimated plants. Protein concentration before sucrose addition: AE, 27.5 µg/ml; LDE, 12.5 µg/ml; TTE: 25.7 µg/ml. Upper-right panel: Photos of 23% sucrose formulated with extracts after 60' at -5 °C. Scale bar: 50 µm. Control: 20 mM Tris-HCl pH 8. Lower right panel: Means with different letters are significantly different at the 0.05 level (ANOVA), n=3.

	Area [micron^2]
Control	213 ± 23^a
AE	83 ± 5^b
LDE	55 ± 9^c
TPE	40 ± 1^d

The protein concentration of extracts was measured with Bradford assay, since BCA yielded strong background absorbance values even when proteins were removed from the samples by acetone precipitation. BCA assay is known to be influenced by reducing agents, such as Ascorbic Acid in AE or polyphenols that could have been co-extracted by heat treatment. Measurements were performed on extracts normalized for extraction volume (Column 3, **Table 4.4.1**) and corrected for final dilution rate before addition of Sucrose (Column 3, **Table 4.4.1**). The yield of extraction is calculated as total micrograms of proteins obtained per gram of extracted leaves. Results are reported in **Table 4.4.2**.

Among the three extraction methods, TPe yielded the highest amount of proteins per grams of fresh leaves (103 µg), followed by AE (65 µg) and LDE (48 µg).

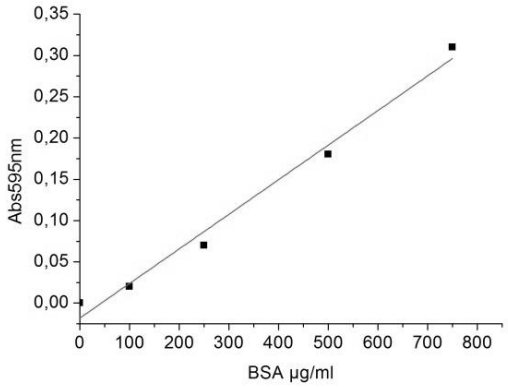

Sample	Abs_{595nm}	Normalized Extr. [µg/ml]	Corrected [µg/ml]	Yield [µg]
AE	0.19	545	27,5	65
LDE	0.09	241	12,05	48
TTE	0.18	514	25,7	103

Table 4.4.2: Protein concentration measured by Bradford assay. *Column 3*; protein concentration as measured on extracts normalized for extraction volumes. *Column 4*: Protein concentration before IRI assay; Column 5: total proteins per gram of extracted leaves.

Figure 4.4.2: BSA standard curve. 0, 100, 250, 500, 750 µg/ml. Linear correlation coefficient r^2= 0.98

In **Table 4.4.3**, the IRI activity of each extract is reported as percentage Inhibition of ice crystals growth compared to a control without ISPs. In the last column, percentage Inhibition of ice crystals growth is normalized for protein concentration. This descriptor allows us to compare the specific activity of extracted proteins on ice crystals growth inhibition. The higher this number, the higher fraction of total proteins are ISPs, assuming that 1) ISPs with comparable activity are present in the three extracts and 2) there is a direct correlation between ISPs concentrations and Ice Recrystallization Inhibition activity within the interval of concentrations tested.

By comparing the specific activities of extracts, LDE proteins appear thus to be respectively 4 and almost 3 times more efficient than AE and TTE on a weight basis, at inhibiting ice crystals growth in IRI assays (Column 4, **Table 4.4.3**). Those data suggest that Leaves Decoction Extraction yield protein extracts with either higher ISPs purity or ISPs species with higher activity. The second hypothesis implies that Leaves Decoction Extractions and Total Protein Extraction could yield ISPs species that are different from those extracted from the apoplast.

On the other hand, we can exclude that LDE will result in ISPs species that are different from those extracted with the TPE method, being that the latter is used for extraction of total proteins. In this case, the most likely scenario is that LDE contain a higher fraction of ISPs on a weight basis.

A great advantage offered by Leaves Decoction Extraction of wheat ISPs relies on the extreme simplicity of the method. Thermotolerant ISPs and a scalable extraction process are fundamental prerequisite for the commercial exploitation of plant ISPs. Thus, we decided to use LDE as a source of wheat ISPs with the ability to prevent ice recrystallization in ice cream.

Sample	% IR Inhibition	Protein conc. [µg/ml]	Specific activity (% Inhibition/Protein. Conc.)
AE	61%	27.5	1.52
LDE	74 %	12,05	6.16
TPE	81 %	25,7	2.15

Table 4.4.3. Ice Recrystallization Inhibition activity vs. protein concentration of extracts. Protein concentration is intended before the addition of sucrose for IRI assay. IR: Ice Recrystallization

To test whether IRI activity in LDE extracts was actually mediated by proteins, we treated the extract with Trypsin and compared the results with IRI assay performed on LDE from non-acclimated plants (NA_LDE) and Buffer solution (Control) (**Figure 4.4.3**). 2 hours Trypsin treatment of LDE caused complete loss of IRI activity of LDE, as indicated by the increase of median ice crystals area comparable to the values obtained from control (Buffer) and LDE extract from non-acclimated plants (NA_LDE).

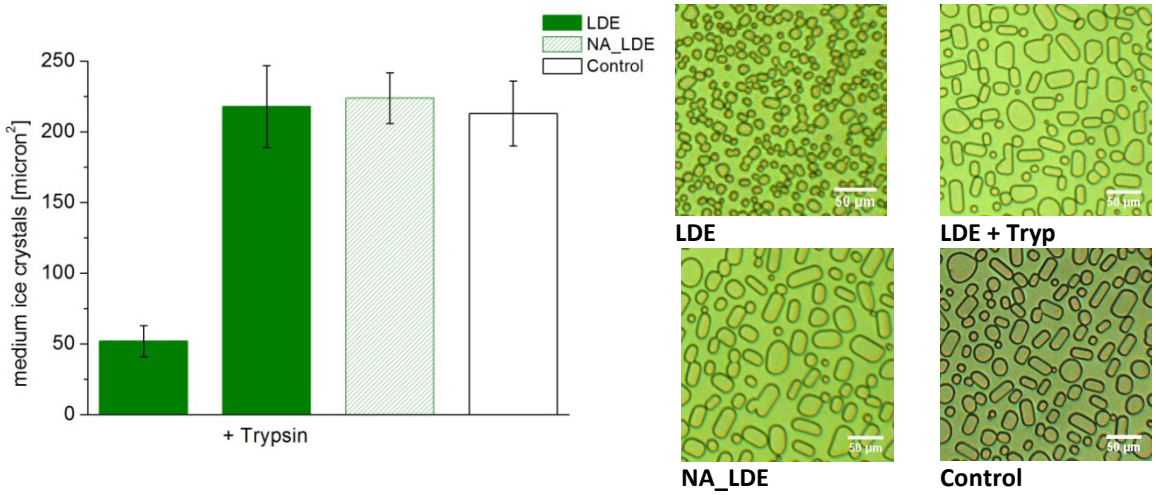

Figure 4.4.3: Results of IRI assay on LDE extracts. Protein concentration before sucrose addition: LDE, 12.5 µg/ml; NA_LDE: 11 µg/ml; Upper-right panel: Photos of 23% sucrose formulated with extracts after 60' at -5 °C. Scale bar: 50 µm. Control: 20 mM Tris-HCl pH 8. Lower right panel: Means with different letters are significantly different at the 0.05 level (ANOVA), n=3.

	Area [micron^2]
LDE	52 ± 11^a
LDE + Tryp	218 ± 29^b
NA_LDE	224 ± 18^b
Control	213 ± 23^b

Leaves Decoction Extracts obtained from plants at different cold acclimation time points were tested for their IRI activity and results are reported in **Figure 4.4.4**. The objective of this analysis was to determine for how long plants needed to be cold acclimated to maximize IRI activity of extracts.

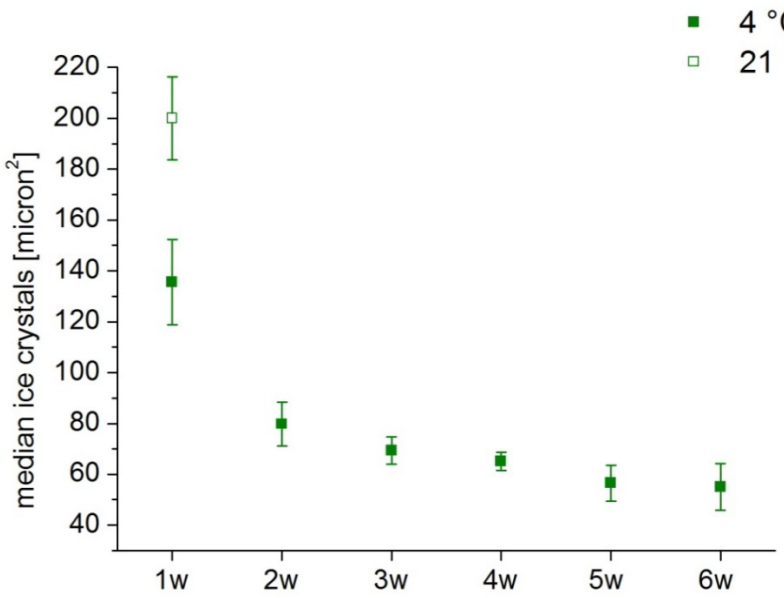

Sample	Area [micron^2]
1w 21°C	200 ± 16^{a}
1w 4°C	135 ± 17^{b}
2w 4°C	80 ± 9^{c}
3w 4°C	70 ± 5^{cd}
4w 4°C	65 ± 4^{cd}
5w 4°C	56 ± 7^{d}
6w 4°C	55 ± 9^{d}

Figure 4.4.4: Results on IRI assays on LDE extracts. 1 week old plant were kept at 21°C (□) for 1week or at 4°C (■) for 1-6 weeks. Right panel: Means with different letters are significantly different at the 0.05 level (ANOVA), n=3.

As expected from previous literature (Kawahara, Fujii et al. 2009) IRI activity of plant extracts reaches plateaux after prolonged times of cold acclimation. **Figure 4.4.4** shows that 1 week cold acclimation is sufficient for the plant to accumulate ISPs that can be extracted by LDE method. Moreover, extracts obtained from plants that were cold acclimated for 3 weeks showed IRI activity comparable to those exposed to cold for longer periods.

4.4.2. Leaves Decoction Extract contain ISPs that stabilize ice cream

Once the method to extract thermostable ISPs from wheat was chosen and the cultivation conditions required for maximum ISPs were identified, we were ready to test if this extract was able to inhibit ice recrystallization in ice cream.

LDE extract from 3 weeks cold acclimated wheat seedlings was chosen as the preferred source of ISPs for this experiment. The freezer used to produce ice cream, requires to process a minimum of 3-3.6 kg of ice cream mix before the operational parameters could be reached and thus the extruded ice cream considered of good quality. Given that our lab

scale capacity to produce cold acclimated seedlings was limited to approx. 160 g for each batch, we wanted to test whether this quantity could yield enough extract to still exhibit IRI activity once it was diluted in 4 kg of ice cream mix. 560 ml of LDE extracts were obtained from 140 g of cold acclimated seedlings, so a final 1:7 dilution was required to formulate 4 kg of ice cream. Extract was diluted 3.5 times and added 1:1 to the 23% sucrose solution for the IRI assay (1:7 final dilution). At this concentration the extract effectively inhibited ice crystals growth in IRI assay; a 44% decrease in median ice crystals area was observed upon addition of diluted LDE extract (**Figure 4.4.5**).

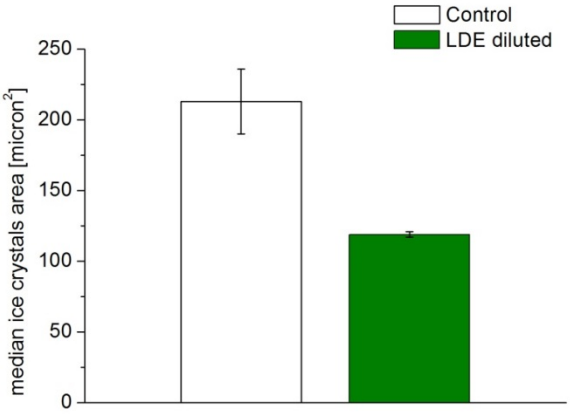

Sample	Area [micron^2]
Control	213 ± 23^a
LDE diluted	119 ± 2^b

Figure 4.4.5: IRI assay on diluted LDE. LDE was diluted 1:3.5 in assay buffer (Tris 20 mM, pH 8) to a final protein concentration of 3.7 µg/ml before addition of Sucrose. Right panel: Means with different letters are significantly different at the 0.05 level (ANOVA), n=3.

The next step was to add the extract to ice creams samples and see if it could perform as well as on sucrose model solution. 7.2 mg of total proteins from LDE were added to 4 kg of ice cream mix (1.8 ppm final concentration). Ice recrystallization was induced by thermal shock treatment (TS) that consisted of storing the ice cream samples at temperatures fluctuating between -18°C and -10°C for 1 week. Ice cream formulated without ISPs was used as a control (Untreated). **Figure 4.4.6** show photographs of ice cream samples kept at constant -20°C and after thermal shock.

For each ice cream sample, a minimum of 1000 ice crystals was collected and analyzed from different samplings; the resulting ice crystals population was fitted to normal

distribution and the median value used to make comparisons between average ice crystals size produced by each treatment (**Figure 4.4.7 and Table 4.4.5**). Median equivalent diameter was introduced in this analysis to allow comparison with literature data, and establish whether the ice crystals size of samples were above the threshold known to impart grainy and coarse texture to the product (50 µm diameter, vertical dashed line) (Cook, Hartel 2010a).

UNTREATED ICE CREAM

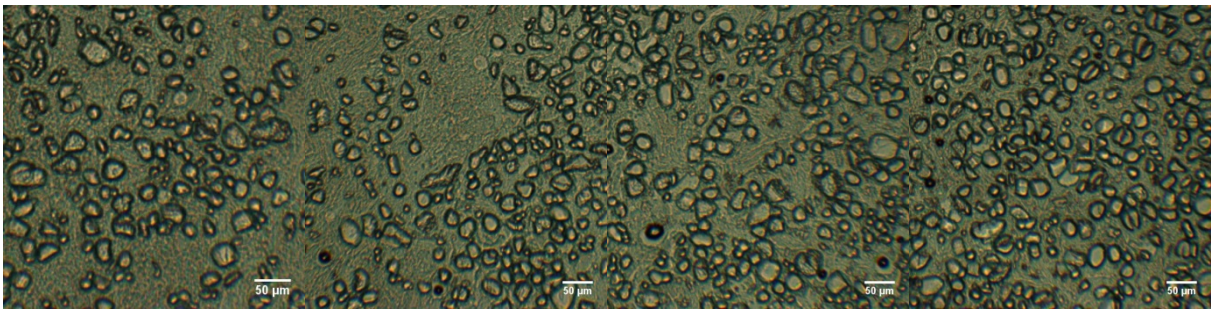

Constant Temperature

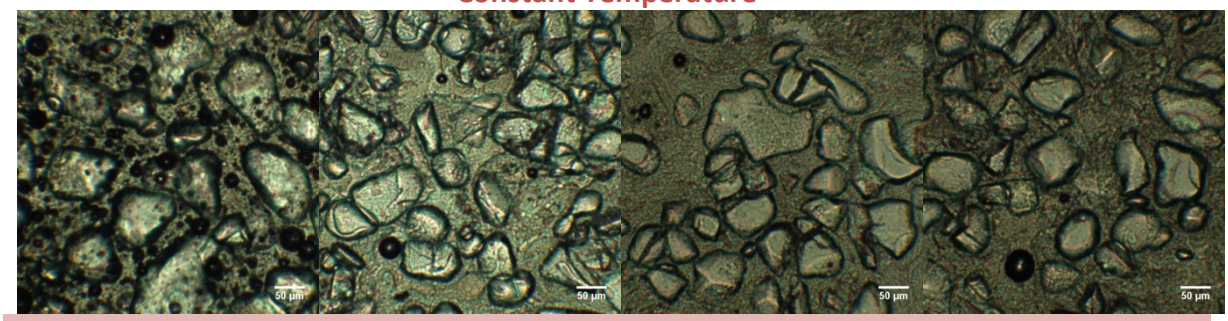

Thermal Shocked (TS)

ICE CREAM + LDE EXTRACT

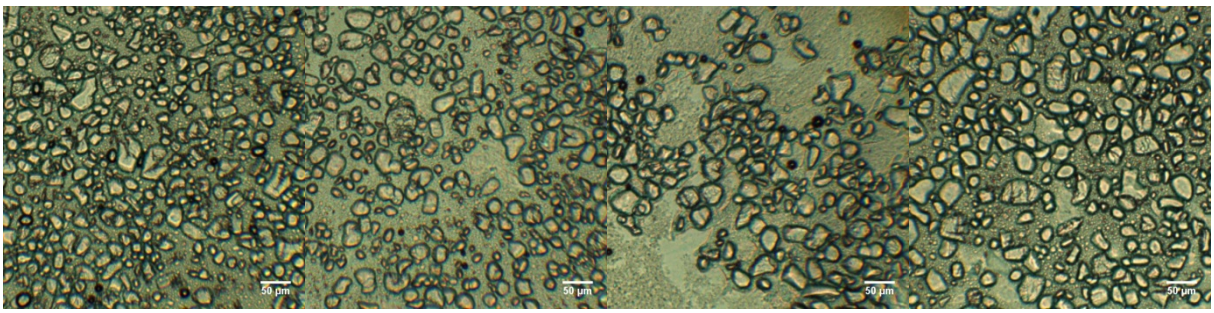

Constant temperature

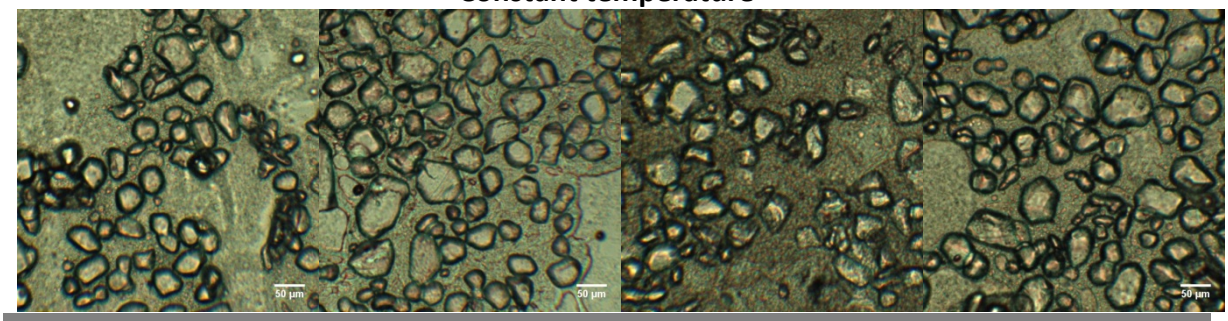

Thermal Shocked (TS)

Figure 4.4.6: Photos of ice cream samples at 10x magnification. Scale bar: 50 µm

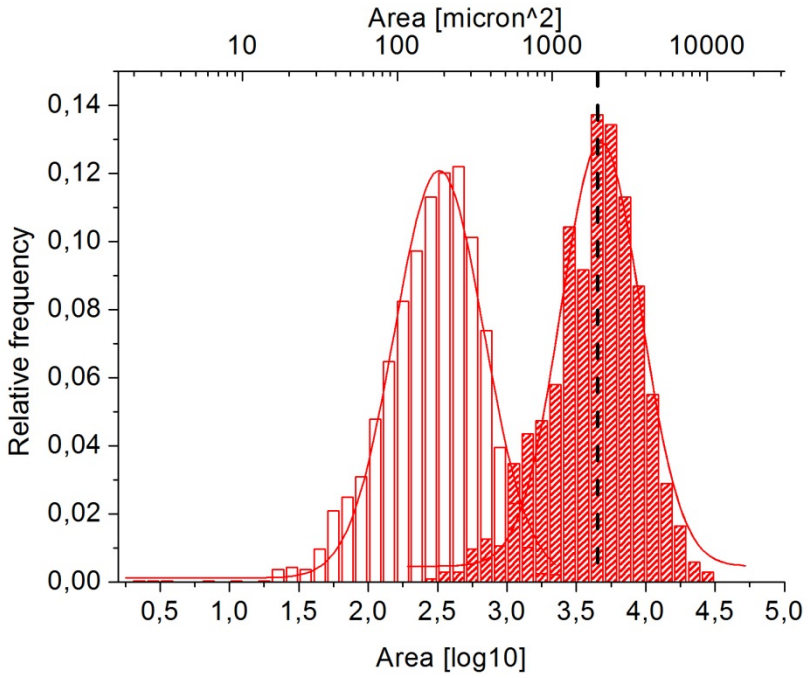

A

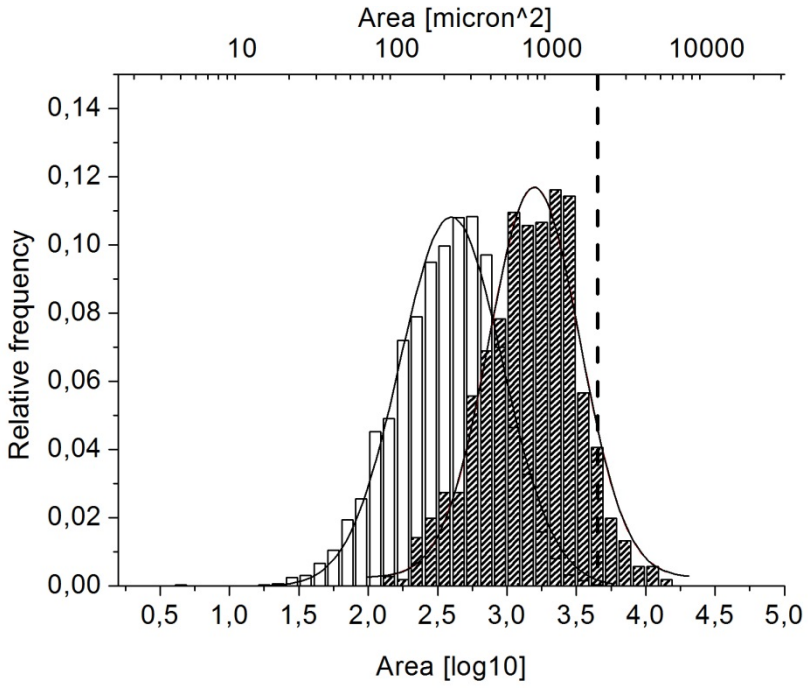

B

Figure 4.4.7: Ice crystals area populations of A: Untreated Ice cream pre (void bars) and after thermal shock (dense pattern). B: Ice cream formulated with LDE pre (void bars) and after (dense pattern) thermal shock. The dashed black lines represent the area of ice crystals having 50 µm equivalent diameter. Ice crystals subpopulations were normalized on total ice crystals. Bin size: 0.1 (log).

Sample	Images / N° crystals	Median area [micron^2]	Median eq. diameter [micron]	% crystals below treshold
Untreated Ice cream	3 / 2778	323.59	21.18	0
Untreated Ice cream (TS)	**5 / 1035**	**4786**	**78.8**	**84**
Ice cream + LDE	3 / 3359	398.11	22.52	0
Ice cream + LDE (TS)	**5 / 1059**	**1584.89**	**44.92**	**38**

Table 4.4.4: Statistical analysis of ice crystals populations of ice cream samples. Column 2 indicates the number of images analyzed to obtain the total number of crystals used for statistic calculations. Median equivalent diameter was calculated from median area approximating the crystals to circles. Shaded rows represent Thermal Shocked samples (TS).

Contrary to our expectations, the area of ice crystals population of ice cream formulated w. and w/o ISPs that were kept at -18°C were very close; the populations were almost indistinguishable if equivalent radius was used for comparison. We would have expected ice cream formulated with ISPs to have smaller ice crystals, as in the case of ice crystals at T=0 (-5°C) in IRI assays. A possible explanations for this finding, is that ice recrystallization contribution to ice crystals growth in the phase of ice cream making is negligible. Ice nucleation and dendritic growth are likely to be the most relevant phenomena, which occur within the refrigerated barrel where the ice cream mix start to freeze (see Chapter 1). Ice Recrystallization could be considered irrelevant also when ice cream is stored at constant temperature for short periods of time.

When Ice crystals growth was induced by Thermal Shock treatment, the population of ice crystals of Untreated Ice cream shifted towards larger sizes, showing a 4-fold increase of median equivalent radius. On the contrary, in ice cream formulated with addition of wheat ISPs to a final concentration of 1.8 ppm, ice crystals growth was drastically reduced and consequently the percentage of ice crystals above the threshold size for perception.

4.4.3. Isolation of ISPs from *T. aestivum*

We've seen that proteins from Leaves Decoction Extract were effective at preventing ice recrystallization in ice cream at a concentration of 1.8 ppm. However, it is reasonable to assume that not all the proteins within the extracts are necessarily ISPs. Object of further investigation was the isolation of active boiling-stable ISPs, to either validate at the protein level previously reported ISPs wheat genes and transcripts (Tremblay, Ouellet et al. 2005), or possibly identify new ISP species.

Since TLPs were previously identified as possible ISP candidates in apoplastic extracts of cold acclimated winter wheat (Kontogiorgos, Regand et al. 2007, Hon, Griffith et al. 1995), we tested whether these proteins were present in LDE extracts. Extracts obtained by Apoplastic Extraction (AE) or Leaves Decoction Extraction (LDE) were normalized for extraction volumes per gram of extracted leaves, loaded on Tris-Tricine gels and immunoblotted against Anti-Thaumatin antibody (**Figure 4.4.7**). Recombinant TaTLP was used as a positive control.

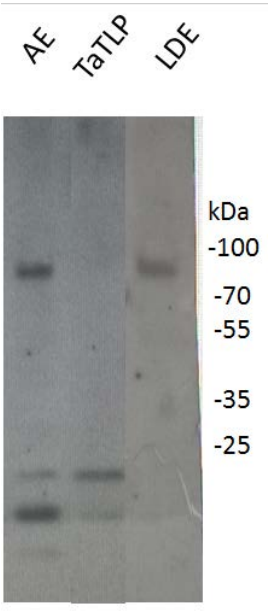

Figure 4.4.8: Immunoblot against Thaumatin antibody. Total proteins loaded, AE: 1.45 µg; TaTLP: 0.38 µg; LDE: 0.43 µg. Tris Tricine 4-20% gradient gel.

In AE extract, a band migrating at the same electrophoretic mobility of recombinant TaTLP is detected as previously shown. LDE performed significantly better than AE on IRI assay (**Figure 4.4.1**), however, no bands indicating the presence of TaTLP were detected in LDE extracts on immunoblots (**Figure 4.4.8**). These data suggests that TaTLP has limited effect, if any, on IRI activity of extracts from cold acclimated winter wheat. Positive bands at higher molecular weights detected in AE and LDE lanes are probably the result of anti-Thaumatin cross-reactivity with other plant proteins, since no such high molecular weight TLPs have been reported so far.

Previous attempts of purifying ISPs from natural sources using ice-affinity purification ((Kuiper, Lankin et al. 2003b)), proved unsuccessful in our lab (data not shown).

To isolate IRI active protein from Leaves Decoction Extracts, a purification process involving several chromatographic steps was adopted. The pure IRI active fraction obtained at the end of the multi-step purification was then analyzed by Isoelectric Focusing and 2^{nd} dimension gel electrophoresis.

LDE obtained from 14 g of cold acclimated seedlings was concentrated 50 fold using Centricon Vivaspin (5kDa) concentrators and loaded on a Resource Q column pre-equilibrated with Tris-HCl pH 8 20 mM (1 mg total protein). All IRI active proteins eluted in the unbound fraction (green box, **Figure 4.4.9**)

Fractions were pooled, concentrated to a final volume of 0.5 ml and loaded on a Superdex G200 column. Most of the IRI activity eluted in a total volume of 3.5 ml (green box, **Figure 4.4.10**), that was concentrated and loaded on a Reverse Phase C4 column.

IRI active fractions were eluted in a final volume of 1 ml by applying a linear gradient of to the C4column (green box, **Figure 4.4.11**) and dried on a SpeedVac to be further processed for Isoelectric Focusing (IEF). Pellet was resuspended in denaturing Rehydration Buffer and centrifuged to separate insoluble matter. To check whether ISPs were successfully resuspended at this stage, an aliquot of supernatant was dialyzed against water and tested for IRI activity. As shown in **Figure 4.4.12**, ice crystals growth was significantly inhibited when the soluble fraction (A) was compared to a control in IRI assay (B).

Interestingly, those ISPs could tolerate drying and denaturing conditions (8M urea, 1% DTT), regaining their functionality after dialysis.

After IEF and 2nd dimension SDS-PAGE, 5 proteins were detected in the gel, named *a,b,c,d,e* according to their increasing isoelectric point (**Figure 4.4.12 A**). Silver staining of the gel revealed no significant contamination by other proteins. Molecular weights and Isoelectric points of the purified proteins were estimated on the basis of electrophoretic mobility on the IEF strip and 2nd dimension acrylamide gel (**Table 4.4.5**). To confirm whether these proteins were expressed specifically as a result of cold acclimation, also whole LDE from cold acclimated and non-acclimated wheat seedlings were run on two-dimensional gels.

As expected, 5 proteins whose pI and MW matched those of proteins *a,b,c,d,e* were detected in Coomassie stained gels of whole LDE extracts from cold acclimated plants (**Figure 4.4.12 B**). On the contrary, Coomassie stained gels of whole LDE extract from non-acclimated plants revealed the absence of proteins in the corresponding gel area. To exclude that those proteins were expressed at lower levels in non-acclimated plants, silver staining (known for its higher sensitivity) was performed on gels (**Figure 4.4.12**). Even in this case, no species with an electrophoretic pattern comparable to a,b,c,d,e were detected.

To conclude, 5 IRI protein (a-d) that eluted in high IRI active fractions were recovered from extracts of cold-acclimated plants , confirming their specific involvement in the plant physiological adaptation to cold and response to freezing stress.

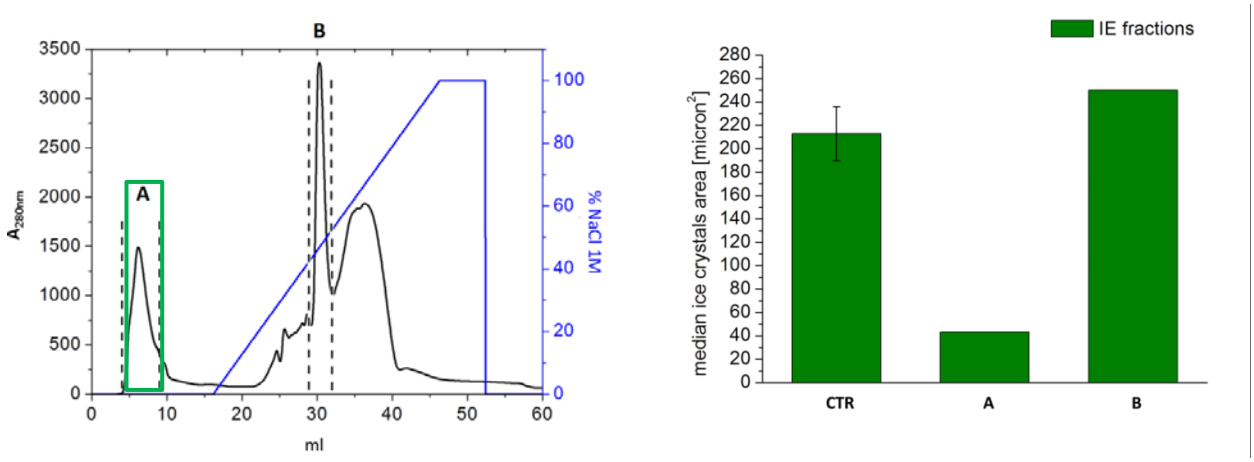

Figure 4.4.9: Ion exchange chromatoraphy (ResQ column). Fractions between dashed lines (left panel) were tested for IRI activity in IRI assay (right panel). Fractions in green boxes (left panel) were pooled and loaded on a Gel Filtration column (Figure 4.4.10)

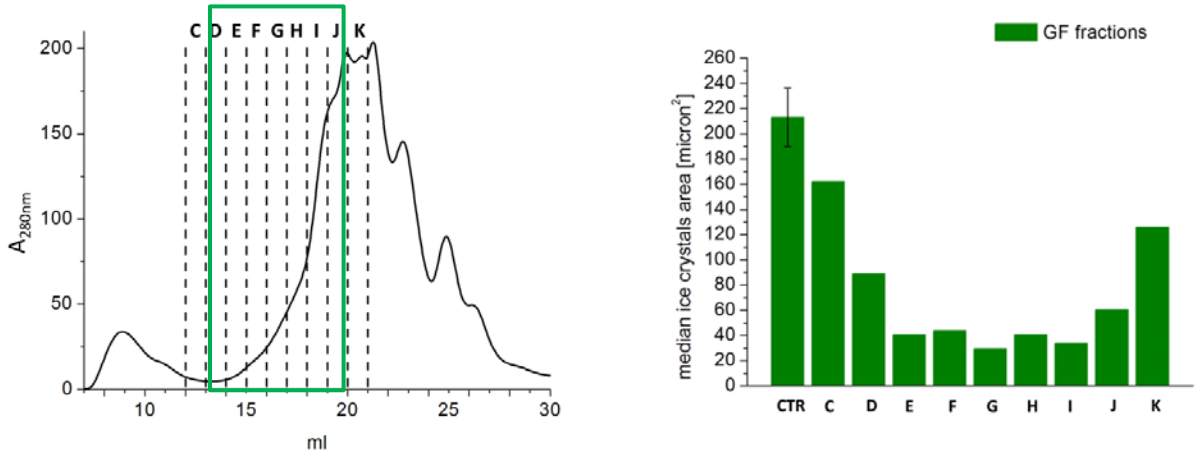

Figure 4.4.10: Gel Filtration chromatography (G200 column). Fractions between dashed lines (left panel) were tested for IRI activity in IRI assay (right panel). Fractions in green boxes (left panel) were pooled and loaded on a Reverse Phase column (Figure 4.4.11)

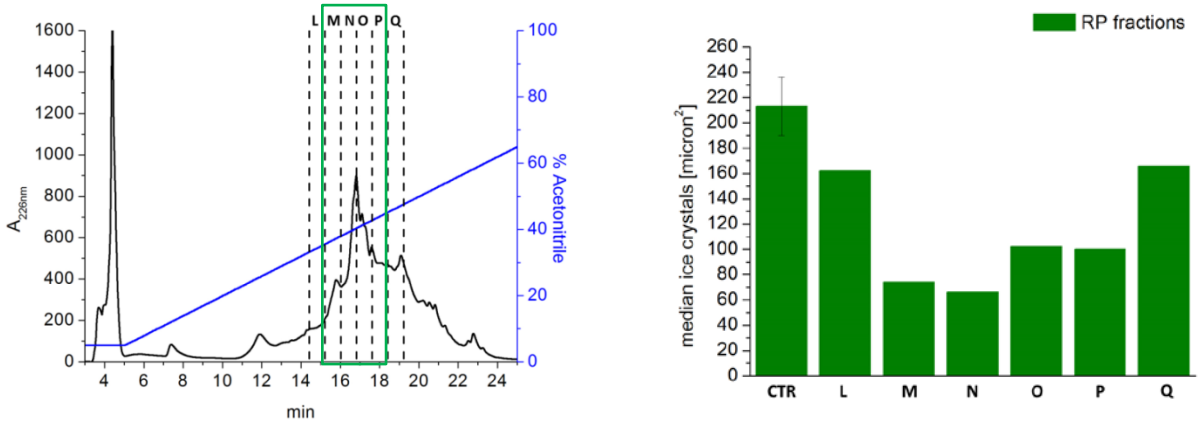

Figure 4.4.11: Reverse Phase Chromatography (C4 column, HPLC). Fractions between dashed lines (left panel) were tested for IRI activity in IRI assay (right panel). Fractions in green boxes (left panel) were pooled and loaded on Immobiline Strip for IEF.

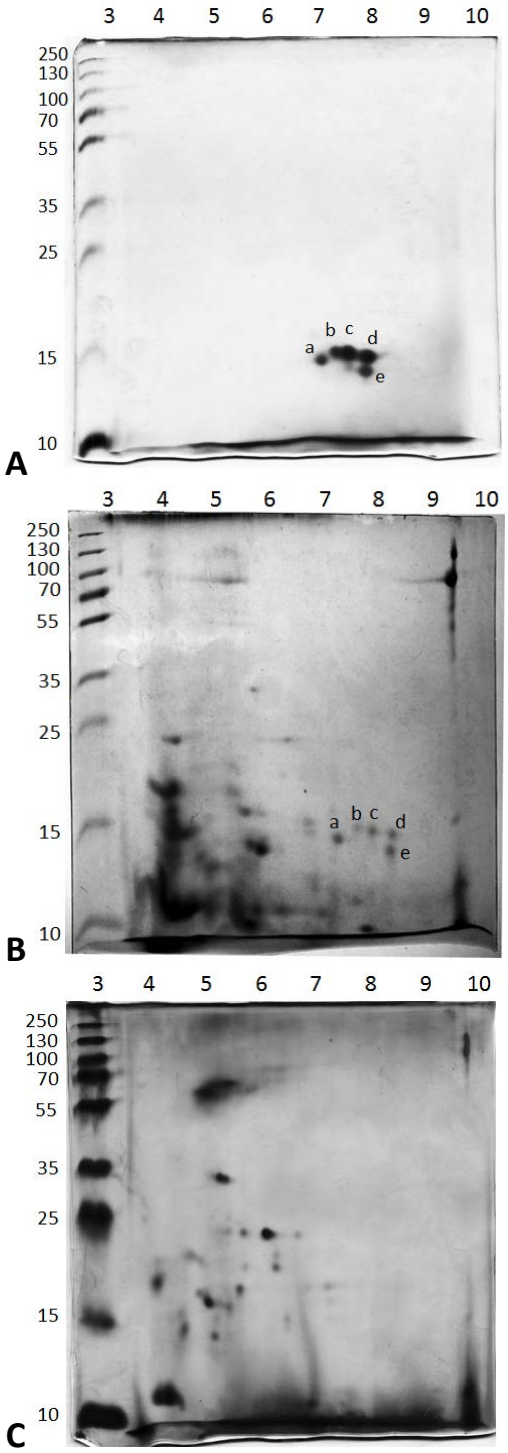

Figure 4.4.12: Two-Dimensional gel electrophoresis. 1st dimension: IEF, 2nd dimension: 12% SDS-PAGE. Horizontal scale: pI values. Vertical: Molecular weights (kDa). A: IRI active fraction isolated from 1ml of 50x LDE after IEF, GF and RP chromatography (Silver stain high sensitivity was adopted to estimate the purity of the protein fraction; B: 90 µl of 50x whole LDE extract from cold acclimated plants (Coomassie stain); C: 10 µL of 50 x whole LDE extract from non-acclimated plants (Silver stain).

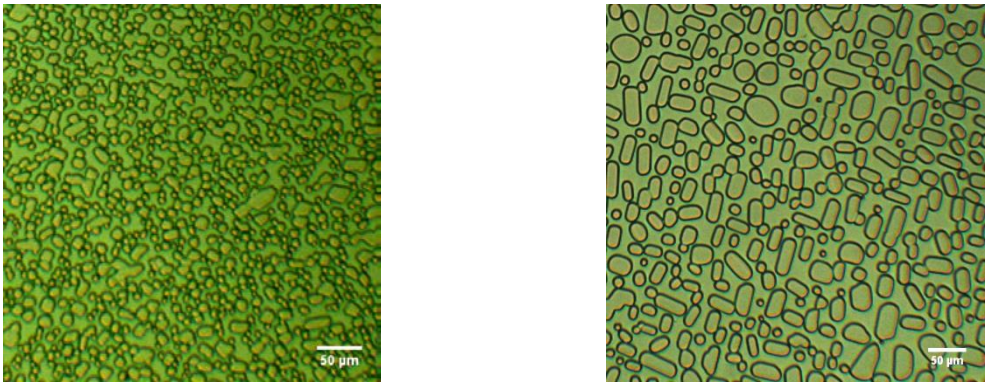

A B

Figure 4.4.13: IRI assay images showing ice crystals obtained after 60' at -5°C. A: IRI active fraction purified from LDE, resuspended in rehydration buffer and dialyzed against water, B: water.

Spot	MW (kDa)	pI
a	14.6	7.1
b	15.3	7.4
c	15.3	7.6
d	14.8	8
e	13.2	7.9

Table 4.4.5: Molecular weight and pI estimation of 5 proteins spot (a-e) eluted in IRI active fractions and loaded on a two dimensional gel (Figure 4.4.10 A).

4.5. DISCUSSION

The aim of this part of the project was to set up a feasible method to obtain wheat extracts with IRI activity, that could eventually be scaled up for bio-production of ISPs at industrial level. Resistance to heat is considered mandatory for most categories of food commodities, where high temperature treatment is required to prevent microbial spoilage. In addition to the standard leaves-infiltrating procedure to extract apoplastic ISPs (Chapter II), two other methods were adapted from patent ((Barfod, Da Lio et al. 2009)) and academic literature (Lauersen, Brown et al. 2011), involving high temperature treatment and total heat stable protein extraction.

The finding that wheat ISPs readily accumulated in the medium used to boil the leaves, represents a significant step forward toward the optimization of the extraction of relatively pure ISPs from plant. Steps of plant cells rupturing and separation of insoluble

material afterwards are no longer required and the purity of ISP obtained with this method is higher when compared to the extraction of total thermostable protein (see **Table 4.4.3**). Extracts derived from heat treatment (LDE and TPE) showed significantly higher IRI specific activity than AE (**Figure 4.4.1**). At present, it is not yet clear whether high temperatures improve ISPs extraction efficiency, or enable the recovery different ISP species (possibly more active) from those that are present in AE.

Other variables that could dramatically impact on the cost of ISPs sourcing from plants, are the time and energy required by the plant to grow and express sufficient levels of ISPs. The literature on ISPs accumulation in winter rye, postulates a cold acclimation period of 7-8 weeks, as this is the time required by the plants to become freezing tolerant. The purpose of our investigation was to obtain the IRI activity profile of extracts as a function of the time plant was exposed to cold. Once we chose LDE as our preferred method to extract thermostable ISPs, we found that maximal IRI activity was obtained from extracts of plants that were acclimated for 3 weeks (**Figure 4.4.4**). Given that those extracts do not necessarily represent the whole spectrum of ISPs expressed in all plant tissues, we can't conclude that 3 weeks is the time required by the plant to express maximal IRI activity. Nevertheless, this finding helps us to design a more cost efficient cultivation protocol to obtain ISPs from plants. To the best of our knowledge, this is the first report IRI activity being measured as a function of cold acclimation time.

Industrial ice cream was formulated with preparation of wheat ISPs obtained by LDE extraction at a final concentration of 1.8 ppm (0.00018%). Ice recrystallization was significantly reduced by addition of ISPs: ice crystals obtained after thermal shock treatment were almost half of the size of those obtained from control ice creams (**Figure 4.4.6**).

The total protein concentration used in our experiment is 14 times lower that that used by Reagand & Goff (0.0025%) (Regand, Goff 2006a) in previous reports of ice cream formulated with winter wheat ISPs. However, we don't know how the proteins used in that study were extracted from wheat, neither their grade of purity. Data about the dosage of the only ISP currently implemented in ice cream products (ISP type III) are not

available. Safety evaluation reports indicate a maximum proposed level of use in ice cream of 0.01% by weight (EFSA 2008). Being that the ice cream used in our study was formulated with the use of stabilizers, whose presence have been found to synergistically increase IRI activity of ISPs in ice cream, it would be interesting to understand how our extracts would behave in the absence of any ice phase stabilizers. Removal of additives in favor of plant extract with increased functionality is indeed the final goal of finding natural alternative to current ice cream formulations.

We managed to isolate IRI active proteins from LDE extracts by means of chromatography. The proteins that eluted with IRI active fraction obtained at the end of the three-step purification protocol migrated in two dimensional gels as 5 species having molecular weight around 15 kDa and isoelectric points from 7 to 8 (**Figure 4.4.12**).

Our hypothesis is that these proteins are likely isoforms, given their similarity in size and surface electrostatics that allowed for their co-elution in each chromatographic passage.

ISPs isoforms were previously reported in overwintering insects, where several cDNA encoded for proteins having different repeats number (Andorfer, Duman 2000). Insect ISPs isoforms have been shown to interact synergistically and increase Thermal Hysteresis of larval fluids to a greater extent than single ISPs did at the same concentration (see Chapter III).

The IRI activity of LDE purified fraction together with the finding that none of the five proteins is expressed in non-acclimated plants, suggest that proteins indicated in **Table 4.4.4** are specifically required by the plant to cope with freezing stress. This is not the case of all plant ISPs, being that some winter rye apoplastic ISPs were detected by immunoblots even in extracts from control plants (not acclimated) (Yu, Griffith 1999), plants treated with hormones (Yu, Griffith 2001) and infected with pathogens (Hiilovaara-Teijo, Hannukkala et al. 1999). In all of those cases, the proteins lacked the ice shaping ability typical of ISPs. The most accredited hypothesis is that in winter rye, ice binding domains evolved from pathogenesis related proteins after gene duplication and mutations events. It would be interesting to test whether IRI active proteins isolated by LDE, are also involved in physiological response to other abiotic and biotic *stimuli*.

Several attempts to perform in gel Trypsin digestion of the spots for subsequent MS/MS analysis have failed so far. One of the most critical step encountered in the process is the recovery of peptides from the gel. It was suggested that the poor extraction yield could be attributed to a high degree of protein glycosylation. To circumvent this possibility, we will deglycosilate the purified proteins obtained after RP chromatography with PNGase F and submit those samples (as well as untreated control) to MS/MS analysis without previous passage in two dimensional gels.

Until protein sequencing of the tryptic digested gel spots reveal some indications on the nature of the proteins, we can only make predictions based on homology with known IRI proteins.

Immunoblots against Anti Thaumatin antibody, excludes any contribution of TLP to the high IRI activity of LDE (**Figure 4.4.8**).

To date, the only evidence of proteins with putative IRI activity in winter wheat are at the transcriptional level. A few cDNA genes encoding polypeptides showing homology with ice binding sites of *L. perenne* ISP (Pudney, Buckley et al. 2003) were found to be upregulated upon cold acclimation in winter wheat (Tremblay, Ouellet et al. 2005, Sandve, Rudi et al. 2008). The IRI activity of two of those predicted proteins (IRI1 and IRI2) was validated on recombinant variants comprising full length and single domain versions (Tremblay, Ouellet et al. 2005).

MW and pI of all wheat predicted polypeptides bearing homology with *L. perenne* ISP were retrieved from Uniprot database and reported in **Table 4.4.6**, together with the experimental values obtained from two dimensional gels of LDE purified fractions (**Figure 4.4.12 A**). From the comparison of the two dataset, no perfect match could be made between predicted IRI proteins and those isolated with our methods. It should be noted however that calculated pI can sometimes differ from those obtained experimentally on IEF strips and molecular weight estimation based on electrophoretic mobility lacks appropriate accuracy to allow comparison with predicted data.

If the 5 ISPs isolated from wheat were to be heavily glycosylated, as suggested by their retention in the acrylamide matrix upon extraction, this would complicate even further

their identification of the basis of molecular weight and isoelectric point considerations. As new MS/MS experiments are currently undergoing, we expect soon to obtain a few amino acid sequence that will be used as templates for the amplification of ISPs related genes.

Predicted wheat IRI protein (Uniprot)			**IRI proteins isolated from LDE extracts**		
	MW (kDa)	**pI**		**MW (kDa)**	**pI**
IR1[a] *Q56B90_WHEAT*	29,104	8.2	a	14.6	7.15
IR2[a] *Q56B89_WHEAT*	42,886	8.6	b	15.3	7.42
IR3 *B9VR50_WHEAT*	19,046	9.6	c	15.3	7.62
IR4 *B9VR51_WHEAT*	18,245	9.23	d	14.8	8
			e	13.2	7.9

Table 4.4.6: Comparison between (A) wheat IRI proteins predicted from cDNA sequences of LpISPs homologues and (b) wheat IRI proteins purified from LDE (Figure 4.4.10 A). Uniprot entry name for predicted proteins is reported. [a] (Tremblay, Ouellet et al. 2005)

5. CONCLUSIONS AND FUTURE PERSPECTIVES

5.1. On the physiology of wheat ISP

We investigated the features of a TaTLP that was previously found in extracts of cold acclimated wheat seedlings and reported to be an Ice Structuring Protein {{109 Kontogiorgos,V. 2007}}. When the recombinant protein was tested for IRI activity, it didn't show any ability to control ice crystals growth. However, it did selectively bound to β-1,3 Glucan and exhibited glucanase activity towards Laminarin, two functional features typical of some TLP. Moreover, the investigation of its structural properties confirmed the data from the functional characterization, i.e. the protein was folded.

When different extraction protocols were evaluated for their ability to yield IRI active extracts, the LDE method over performed the standard AE protocol. However, while TaTLP and other TLP were detected in immunoblot of AE samples, no evidences of any TLP was detected in LDE samples.

Although these data are not conclusive proofs that TLP can't bind ice and prevent its growth, we found that their presence is not mandatory for the plant to express high levels of IRI activity.

In the search of ISP species that are found within LDE, we isolated 5 proteins, that on the basis of their similar pI and molecular weight are likely to be isoforms of the same protein species. The pI and MW of the 5 proteins extrapolated from two dimensional gels doesn't exactly match with those of putative wheat ISP (predicted from cDNA). However, drawing conclusions on mere comparison of those data would be risky at this stage. The identification of the proteins by means of MS/MS is currently undergoing. The idea of being in the presence of previously undiscovered IRIP is an exciting perspective. There are previous cases of novel protein being discovered years after the first reports of IRIP from the same organism. An emblematic example is offered by winter flounder: almost 30 years after the first report of the helical Type I AFP it was found that a larger hyperactive

isoforms was also expressed in its blood, enabling further extension of the blood Thermal Hysteresis gap beyond the limits of Type I AFP (Marshall, Fletcher et al. 2004).

This kind situation is not uncommon in the field of Ice Structuring Proteins, mainly because of the vast heterogeneity of structures and sequences that constitutes a distinguish feature of this family of proteins. For this reason, it is hardly impossible to conclude that no other IRIP are expressed by an organism only on the basis of the lack of homologous genes to previously characterized IRIP.

After finding that TaTLP did not exhibited any IRI activity, we went on with the characterization of the IRI activity of apoplastic ISP secreted of *T. aestivum*. We were very surprised to discover that upon addition of exogenous non-ISP proteins to apoplastic extracts, the overall IRI activity of the sample was significantly increased. To the best of our knowledge, this is the first report of plant ISP being enhanced. Unlike in the case of AFP from the insect *D. canadensis*, whose activity was also found to be enhanced by the addition of proteins, wheat apoplastic ISP don't seem to require specific partners for their enhancement.

AFP concentration within the body fluids of freeze avoiding animals are reported to be in the range of 1-2.5 mg/ml (*D. canadensis*, (Duman, Serianni 2002)) and 10-15 mg/ml (*P. americanus*,(Marshall, Fletcher et al. 2004)). At those concentration, most AFP show plateau of TH activity (Marshall, Fletcher et al. 2004). While freezing point depression provided by such high concentration of AFP allow fish avoid freezing in its natural habitat (-2°C), this may not be the case of insects and plants, that are potentially exposed to extreme temperatures. To this end, these organisms may have evolved a strategy to overcome the limit of ISP activity plateauing at the highest physiological concentration.

With the preliminary data available at this stage, it is premature to conclude whether or not protein mediated IRI enhancing has any physiological significance for the plant. However, the same effect was not observed when fish AFP were used in place of wheat extracts containing ISP, indicating that this phenomenon is not common to all the classes of AFP .

It is plausible to speculate that IRI enhancement is mediated by the formation of AFP-enhancer complex that result in AFP of increased size, thus capable of blocking a larger surface on the ice crystals and prevent its growth more efficiently. No evidences of such complexes were detected so far, even after freezing and thawing treatment, a condition known to stimulate the formation of ISP complex in winter rye {{55 Yu,X.M. 1999}}.

In an attempt to explain these finding at a molecular level, we propose that the ISP bound to the ice crystals, can coordinate the surface of the latter by exposing arrays of charged/apolar groupd towards the liquid phase of the solution. In this way, proteins in the unfrozen phase will stick to the coordinated ice crystals on the basis of their net surface charge/hydropathy. One method to validate this hypothesis would be to test the effect of enhancers on the basis of their surface charge properties. The data available on the enhancers so far are limited and those experiments weren't designer for this purpose. 3 of the validated enhancers (Thaumatin, TaTLP and Chymotrpsinogen) are basic proteins with an average pI of 8.2. On the contrary, Thyroglobulin is acidic with an extimated pI around 5.

In our opinion, the best way to validate our general model, would be to use fluorescence cold stage microscopy {{62 Celik,Y. 2013}}. By conjugating enhancers and ISP with fluorophores emitting at two different wavelength, it would be possible to monitor in real time their respective localization in the solution. If the two fluorescent signals occur to co-localize in correspondence of the ice crystals surface, that would offer a satisfactory proof that enhancers are recruited on the ice crystals surface by ISP.

From an applicative perspective, the enhancing potential of wheat ISP enable to achieve the same results in term of IRI activity, with lower quantities of ISP. This possibility would be regarded with great interest from the industry, since high producing cost is one of the factors the limited ISP commercial applications thus far.

5.2. On the application of wheat ISP for frozen food stabilization

One of the greatest advantage of working with seedlings is the low costs required to grown them. Wheat seedlings can be obtained in growth room without strict requirements of lighting and nutrients and recently, hydroponic cultivations systems were developed to reduce minimal operator handling and high yield of biomass. Wheat and barley seedlings are prevalently used as fodder for animal nutrition, and some manufacturers of hydroponic cultivations systems claim that a productivity of 1000 kg a day can be obtained at a cost of approximately 7 euro cents per kilogram. Considering that in our experiments 1 grams of fresh plant yielded almost 4 milliliters of extract that in turn was diluted 7 fold when added to ice cream, this mean that 28 kg of ice cream could be made of out of 1 kg of seedlings. In the best scenario, a cost of 0.25 euro cent per kilogram of ice cream formulated with LDE extract would give us enough margin to compensate for the costs associated with the additional step of cold storage (required for cold acclimation) and downstream processing.

The results obtained on ice cream formulated with LDE are preliminary but rather encouraging. The extract dosed at a final concentration of proteins of 1.8 ppm, confer extra stability against ice recrystallization in industrial ice cream. ISP from natural sources would potentially allow manufacturers to reformulate ice cream without the need of additives used as stabilizers of the ice phase. In this regard, it would be interesting to ascertain if, and how much ISP is required to prevent ice recrystallization on stabilizers-free or reduced stabilizers recipes.

Although theoretically possible, the task of using only ISP in place of ice crystals stabilizers (i.e. hydrocolloids) is a great challenge for food scientist. Hydrocolloids gel forming and water binding ability extends beyond the mere capacity of controlling ice crystals, and impact rheological properties that are required to produce a proper ice cream with the current technology. In addition to that, hydrocolloids are also used to promote a creamy, fatty texture and mouthfeel.

Beyond the application of ISP in ice cream, we plan to start some tests also on other frozen food commodities that could benefit from the protection against extensive crystals growth provided by ISP. One example of product that fall within this category is frozen dough for bread making, in which ice crystals growth control is necessary to prevent the disruption of dough structure and the resulting uneven leavening of the bread .

Besides the choice of a low cost source of ISP, other two factors should be taken into account when designing a bioprocess to source ISP from plant: what is the contribution of the extraction process to the final cost of the product and how the processing conditions will impact on its features.

The extraction method that was used to obtain ISP to stabilize ice cream, involve a single step boiling phase of the seedlings and the recovery of the ISP in the water used for extraction. This method doesn't foresee the use any kind of solvent or hazardous and potentially toxic chemical. The simplicity of the extraction process is a key feature to obtain the "natural status" for a novel ingredient. This is especially true in the case of European legislation that, as a rule of thumb, requires any product resulting from "non-conventional" extraction process has to be declared as an additive {{273 Melchor, S.B. 2012}}. Some examples of "non-conventional" processes are: smoking, carbon filtration, ion-exchange purification acid/alkali treatment, solvent-extraction, reverse osmosis etc. An emblematic case is that of Stevia, the natural sweetener derived from the plant *Stevia rebaudiana*. Being that with raw stevia extracts come significant off tastes, purified glycosides (e.g. the sweet tasting molecules) are generally preferred since they impart a more sucrose-like profile in the mouth. However, while the raw plant extract could be considered as a natural sweetener, the purified glycosides that are obtained from a solvent extraction process and must be declared as additive (E 960).

The adoption of high temperature treatment in the extraction process of ISP offer two principal advantages. It allows to obtain proteins that are thermostable, and as such, resistant to heat treatment required for to assure food sterility. Every ingredient that is added after the sterilization step introduce the risk of food contamination, so proteins that are stable after common sterilization treatment (75°C for less then a minute) have

considerable added value. The ISP recovered by our method have been shown to retain their functionality after boiling for 10 minutes.

In addition to that, the more obvious advantage of using high temperature, is that the product resulting from this process is itself sterile.

To conclude, the results obtained in the contest of this part of the PhD project, have provided a proof of concept that sourcing ISP from *T. aestivum* is compatible with the requirements of 1) reduced costs, 2) stabilization of frozen food (ice cream), 3) natural labeling.

From this point, the next step will be the scale up of the production process, to validate its feasibility at pre-industrial scales.

BIBLIOGRAPHY

AMERSHAM BIOSCIENES, 2-D Electrophoresis using immobilized pH gradients.

AMORNWITTAWAT, N., WANG, S., BANATLAO, J., CHUNG, M., VELASCO, E., DUMAN, J.G. and WEN, X., 2009. Effects of polyhydroxy compounds on beetle antifreeze protein activity. *Biochimica et biophysica acta,* **1794**(2), pp. 341-346.

AMORNWITTAWAT, N., WANG, S., DUMAN, J.G. and WEN, X., 2008. Polycarboxylates enhance beetle antifreeze protein activity. *Biochimica et biophysica acta,* **1784**(12), pp. 1942-1948.

ANDORFER, C.A. and DUMAN, J.G., 2000. Isolation and characterization of cDNA clones encoding antifreeze proteins of the pyrochroid beetle Dendroides canadensis. *Journal of insect physiology,* **46**(3), pp. 365-372.

ANTIKAINEN, M. and GRIFFITH, M., 1997. Antifreeze protein accumulation in freezing-tolerant cereals. *Physiologia Plantarum,* **99**(3), pp. 423-432.

APPELS, R., EASTWOOD, R., LAGUDAH, E., LANGRIDGE, P., MACKAY, M., MCINTYRE, L. and SHARP, P., 11th International Wheat Genetics Symposium 2008 Proceedings. **3**.

BAR-DOLEV, M., CELIK, Y., WETTLAUFER, J.S., DAVIES, P.L. and BRASLAVSKY, I., 2012. New insights into ice growth and melting modifications by antifreeze proteins. *Journal of the Royal Society, Interface / the Royal Society,* **9**(77), pp. 3249-3259.

BARFOD, N.M., DA LIO, M. and CHRISTENSEN, F.H., 2009. *Process for production of a frozen food product.* Google Patents.

BARRETT, J., 2001. Thermal hysteresis proteins. *The international journal of biochemistry & cell biology,* **33**(2), pp. 105-117.

BARTHAKUR, ,S., BABU, ,V. and BANSA, ,K.C., Over-expression of Osmotin Induces Proline Accumulation and Confers Tolerance to Osmotic Stress in Transgenic Tobacco.

BASU, K., GRAHAM, L.A., CAMPBELL, R.L. and DAVIES, P.L., 2015. Flies expand the repertoire of protein structures that bind ice. *Proceedings of the National Academy of Sciences of the United States of America,* .

BAYER-GIRALDI, M., JIN, E. and WILSON, P.W., 2014. Characterization of ice binding proteins from sea ice algae. *Methods in molecular biology (Clifton, N.J.),* **1166**, pp. 241-253.

BLIGH, J., 1990. Advances in Comparative and Environmental Physiology, 4. Animal Adaptation to Cold. Edited by Lawrence C. H. Wang. Pp. 441. (Springer-Verlag, Berlin, 1989.) DM 198.00 hardback. ISBN 3 540 50301 3. *Experimental physiology,* **75**(3), pp. 435-436.

BROWN, J.,R., SEYMOUR, J.,D., BROX, T.,I., SKIDMORE, M.,L., WANG, ,CHEN, CHRISTNER, B.,C., LUO, ,BING-HAO and CODD, S.,L., 2014. Recrystallization inhibition in ice due to ice binding protein activity detected by nuclear magnetic resonance. *Biotechnology Reports,* **3**, pp. 60-64.

BULHELLER, B.M. and HIRST, J.D., 2009. DichroCalc--circular and linear dichroism online. *Bioinformatics (Oxford, England),* **25**(4), pp. 539-540.

CELIK, Y., DRORI, R., PERTAYA-BRAUN, N., ALTAN, A., BARTON, T., BAR-DOLEV, M., GROISMAN, A., DAVIES, P.L. and BRASLAVSKY, I., 2013. Microfluidic experiments reveal that antifreeze proteins bound to ice crystals suffice to prevent their growth. *Proceedings of the National Academy of Sciences of the United States of America,* **110**(4), pp. 1309-1314.

CELIK, Y., GRAHAM, L.A., MOK, Y.F., BAR, M., DAVIES, P.L. and BRASLAVSKY, I., 2010. Superheating of ice crystals in antifreeze protein solutions. *Proceedings of the National Academy of Sciences of the United States of America,* **107**(12), pp. 5423-5428.

CEREGHINO, J.L. and CREGG, J.M., 2000a. Heterologous protein expression in the methylotrophic yeast Pichia pastoris. *FEMS microbiology reviews,* **24**(1), pp. 45-66.

CEREGHINO, J.L. and CREGG, J.M., 2000b. Heterologous protein expression in the methylotrophic yeast Pichia pastoris. *FEMS microbiology reviews,* **24**(1), pp. 45-66.

CHENG, C., 2003. Freezing avoidance in polar fishes. *Extremophiles,* **2**.

CHENG, C.H., 1998. Evolution of the diverse antifreeze proteins. *Current opinion in genetics & development,* **8**(6), pp. 715-720.

CLARKE, C.J., 2012. *The science of ice cream,* .

CLARKE, C.J., BUCKLEY, S.L. and LINDNER, N., 2002. Ice structuring proteins - a new name for antifreeze proteins. *Cryo letters,* **23**(2), pp. 89-92.

COOK, K.L.K. and HARTEL, R.W., 2010a. Mechanisms of Ice Crystallization in Ice Cream Production. *Comprehensive Reviews in Food Science and Food Safety,* **9**(2), pp. 213-222.

COOK, K.L.K. and HARTEL, R.W., 2010b. Mechanisms of Ice Crystallization in Ice Cream Production. *Comprehensive Reviews in Food Science and Food Safety,* **9**(2), pp. 213-222.

CREMATA, J.A., MONTESINO, R., QUINTERO, O. and GARCIA, R., 1998. Glycosylation profiling of heterologous proteins. *Methods in molecular biology (Clifton, N.J.),* **103**, pp. 95-105.

CRILLY, J.,F., RUSSELL, A.,B., COX, A.,R. and CEBULA, D.,J., 2008. Designing Multiscale Structures for Desired Properties of Ice Cream. *ndustrial & Engineering Chemistry Research,* **47**, pp. 6362-6367.

DAMASCENO, L.M., HUANG, C.J. and BATT, C.A., 2012. Protein secretion in Pichia pastoris and advances in protein production. *Applied Microbiology and Biotechnology,* **93**(1), pp. 31-39.

DARBY, R.A., CARTWRIGHT, S.P., DILWORTH, M.V. and BILL, R.M., 2012. Which yeast species shall I choose? Saccharomyces cerevisiae versus Pichia pastoris (review). *Methods in molecular biology (Clifton, N.J.),* **866**, pp. 11-23.

DAVIES, P.L., 2014. Ice-binding proteins: a remarkable diversity of structures for stopping and starting ice growth. *Trends in biochemical sciences,* **39**(11), pp. 548-555.

DAVIES, P.L., BAARDSNES, J., KUIPER, M.J. and WALKER, V.K., 2002. Structure and function of antifreeze proteins. *Philosophical Transactions of the Royal Society B: Biological Sciences,* **357**(1423), pp. 927-935.

DE VOS, A.M., HATADA, M., VAN DER WEL, H., KRABBENDAM, H., PEERDEMAN, A.F. and KIM, S.H., 1985. Three-dimensional structure of thaumatin I, an intensely sweet protein. *Proceedings of the National Academy of Sciences of the United States of America,* **82**(5), pp. 1406-1409.

DELUCA, C.I., COMLEY, R. and DAVIES, P.L., 1998. Antifreeze proteins bind independently to ice. *Biophysical journal,* **74**(3), pp. 1502-1508.

DEVRIES, A.L., 1971. Glycoproteins as biological antifreeze agents in antarctic fishes. *Science (New York, N.Y.),* **172**(3988), pp. 1152-1155.

DI MATTEO, A., BONIVENTO, D., TSERNOGLOU, D., FEDERICI, L. and CERVONE, F., 2006. Polygalacturonase-inhibiting protein (PGIP) in plant defence: a structural view. *Phytochemistry,* **67**(6), pp. 528-533.

DOLINSKY, T.J., NIELSEN, J.E., MCCAMMON, J.A. and BAKER, N.A., 2004. PDB2PQR: an automated pipeline for the setup of Poisson-Boltzmann electrostatics calculations. *Nucleic acids research,* **32**(Web Server issue), pp. W665-7.

DONHOWE, D.P., HARTEL, R.W. and BRADLEY JR., R.L., 1991. Determination of Ice Crystal Size Distributions in Frozen Desserts. *Journal of dairy science,* **74**(10), pp. 3334-3344.

DOXEY, A.,C., YAISH, M.,W., GRIFFITH, ,MARILYN and MCCONKEY, B.,J., Ordered surface carbons distinguish antifreeze proteins and their ice-binding regions.

DRORI, R., CELIK, Y., DAVIES, P.L. and BRASLAVSKY, I., 2014. Ice-binding proteins that accumulate on different ice crystal planes produce distinct thermal hysteresis dynamics. *Journal of the Royal Society, Interface / the Royal Society,* **11**(98), pp. 20140526.

DUMAN, J.G., 2002. The inhibition of ice nucleators by insect antifreeze proteins is enhanced by glycerol and citrate. *Journal of comparative physiology.B, Biochemical, systemic, and environmental physiology,* **172**(2), pp. 163-168.

DUMAN, J.G., 2001. Antifreeze and ice nucleator proteins in terrestrial arthropods. *Annual Review of Physiology,* **63**, pp. 327-357.

DUMAN, J.G., 1994. Purification and characterization of a thermal hysteresis protein from a plant, the bittersweet nightshade Solanum dulcamara. *Biochimica et biophysica acta,* **1206**(1), pp. 129-135.

DUMAN, J.G. and SERIANNI, A.S., 2002. The role of endogenous antifreeze protein enhancers in the hemolymph thermal hysteresis activity of the beetle Dendroides canadensis. *Journal of insect physiology,* **48**(1), pp. 103-111.

DUMAN, J.G., 1984. Thermal hysteresis antifreeze proteins in the midgut fluid of overwintering larvae of the beetle Dendroides canadensis. *Journal of Experimental Zoology,* **230**(3), pp. 355-361.

EBBINGHAUS, S., MEISTER, K., BORN, B., DEVRIES, A.L., GRUEBELE, M. and HAVENITH, M., 2010. Antifreeze glycoprotein activity correlates with long-range protein-water dynamics. *Journal of the American Chemical Society,* **132**(35), pp. 12210-12211.

EBBINGHAUS, S., MEISTER, K., PRIGOZHIN, M., DEVRIES, A., HAVENITH, M., DZUBIELLA, J. and GRUEBELE, M., 2012. Functional Importance of Short-Range Binding and Long-Range Solvent Interactions in Helical Antifreeze Peptides. *Biophysical journal,* **103**(2), pp. L20-2.

EFSA, 2008. Safety of Ice Structuring Protein (ISP). *The EFSA Journal,* **768**.

ELLMAN, G.L., 1959. Tissue sulfhydryl groups. *Archives of Biochemistry and Biophysics,* **82**(1), pp. 70-77.

ENGELEN, L. and VAN DER BILT, A., 2008. ORAL PHYSIOLOGY AND TEXTURE PERCEPTION OF SEMISOLIDS. *Journal of Texture Studies,* **39**(1), pp. 83-113.

FIELDS, S. and SONG, O., 1989. A novel genetic system to detect protein-protein interactions. *Nature,* **340**(6230), pp. 245-246.

FITZGERALD, I. and GLICK, B.S., 2014. Secretion of a foreign protein from budding yeasts is enhanced by cotranslational translocation and by suppression of vacuolar targeting. *Microbial cell factories,* **13**(1), pp. 125-014-0125-0.

FRACZKIEWICZ, R. and BRAUN, W., 1998. Exact and efficient analytical calculation of the accessible surface areas and their gradients for macromolecules. *Journal of Computational Chemistry,* **19**(3), pp. 319-333.

FRISHMAN, D. and ARGOS, P., 1995. Knowledge-based protein secondary structure assignment. *Proteins,* **23**(4), pp. 566-579.

FUCHS, H.C., BOHLE, B., DALL'ANTONIA, Y., RADAUER, C., HOFFMANN-SOMMERGRUBER, K., MARI, A., SCHEINER, O., KELLER, W. and BREITENEDER, H., 2006. Natural and recombinant molecules of the cherry allergen Pru av 2 show diverse structural and B cell characteristics but similar T cell reactivity. *Clinical & Experimental Allergy,* **36**(3), pp. 359-368.

GARNHAM, C.P., CAMPBELL, R.L. and DAVIES, P.L., 2011. Anchored clathrate waters bind antifreeze proteins to ice. *Proceedings of the National Academy of Sciences of the United States of America,* **108**(18), pp. 7363-7367.

GHOSH, R. and CHAKRABARTI, C., 2008. Crystal structure analysis of NP24-I: a thaumatin-like protein. *Planta,* **228**(5), pp. 883-890.

GOFF, H.D., 1997. Partial coalescence and structure formation in dairy emulsions. *Advances in Experimental Medicine and Biology,* **415**, pp. 137-148.

GRAETHER, S.P., DELUCA, C.I., BAARDSNES, J., HILL, G.A., DAVIES, P.L. and JIA, Z., 1999. Quantitative and qualitative analysis of type III antifreeze protein structure and function. *The Journal of biological chemistry,* **274**(17), pp. 11842-11847.

GRAHAM, L.A. and DAVIES, P.L., 2005. Glycine-Rich Antifreeze Proteins from Snow Fleas. *Science,* **310**(5747), pp. 461-461.

GRAHAM, L.A., LIOU, Y., WALKER, V.K. and DAVIES, P.L., 1997. Hyperactive antifreeze protein from beetles. *Nature,* **388**(6644), pp. 727-728.

GRENIER, J., POTVIN, C., TRUDEL, J. and ASSELIN, A., 1999a. Some thaumatin-like proteins hydrolyse polymeric beta-1,3-glucans. *The Plant Journal : for cell and molecular biology,* **19**(4), pp. 473-480.

GRENIER, J., POTVIN, C., TRUDEL, J. and ASSELIN, A., 1999b. Some thaumatin-like proteins hydrolyse polymeric beta-1,3-glucans. *The Plant Journal : for cell and molecular biology,* **19**(4), pp. 473-480.

GRIFFITH, M., ALA, P., YANG, D.S.C., HON, W.C. and MOFFATT, B.A., 1992. Antifreeze Protein Produced Endogenously in Winter Rye Leaves. *Plant Physiology,* **100**(2), pp. 593-596.

GRIFFITH, M., LUMB, C., WISEMAN, S.B., WISNIEWSKI, M., JOHNSON, R.W. and MARANGONI, A.G., 2005. Antifreeze proteins modify the freezing process in planta. *Plant Physiology,* **138**(1), pp. 330-340.

GRIFFITH, M. and YAISH, M.W., 2004. Antifreeze proteins in overwintering plants: a tale of two activities. *Trends in plant science,* **9**(8), pp. 399-405.

GRYCZYNSKI, I., WICZK, W., JOHNSON, M.L. and LAKOWICZ, J.R., 1988. Lifetime distributions and anisotropy decays of indole fluorescence in cyclohexane/ethanol mixtures by frequency-domain fluorometry. *Biophysical chemistry,* **32**(2-3), pp. 173-185.

GUO, S., GARNHAM, C.P., WHITNEY, J.C., GRAHAM, L.A. and DAVIES, P.L., 2012. Re-Evaluation of a Bacterial Antifreeze Protein as an Adhesin with Ice-Binding Activity. *PLoS ONE,* **7**(11), pp. e48805.

GUPTA, R. and DESWAL, R., 2014a. Antifreeze proteins enable plants to survive in freezing conditions. *Journal of Biosciences,* **39**(5), pp. 931-944.

GUPTA, R. and DESWAL, R., 2014b. Refolding of beta-Stranded Class I Chitinases of *Hippophae rhamnoides* Enhances the Antifreeze Activity during Cold Acclimation. *PLoS ONE,* **9**(3), pp. e91723.

HANSEN, T.N. and BAUST, J.G., 1988. Differential scanning calorimetric analysis of antifreeze protein activity in the common mealworm, Tenebrio molitor. *Biochimica et biophysica acta,* **957**(2), pp. 217-221.

HASSAS-ROUDSARI, M., 2011. Extraction, purification and study of mechanism of action of apoplastic Ice Structuring Proteins from cold acclimated winter wheat leaves. *PhD Thesis - University of Guelph,* .

HASSAS-ROUDSARI, M. and GOFF, H.D., 2012. Ice structuring proteins from plants: Mechanism of action and food application. *Food Research International,* **46**(1), pp. 425-436.

HAYWARD, S.A., MANSO, B. and COSSINS, A.R., 2014. Molecular basis of chill resistance adaptations in poikilothermic animals. *The Journal of experimental biology,* **217**(Pt 1), pp. 6-15.

HEGDE, R.S. and BERNSTEIN, H.D., 2006. The surprising complexity of signal sequences. *Trends in biochemical sciences,* **31**(10), pp. 563-571.

HIDEHISA, K., Characterizations of Functions of Biological Materials Having Controlling-Ability Against Ice Crystal Growth.

HIILOVAARA-TEIJO, M., HANNUKKALA, A., GRIFFITH, M., YU, X.M. and PIHAKASKI-MAUNSBACH, K., 1999. Snow-Mold-Induced Apoplastic Proteins in Winter Rye Leaves Lack Antifreeze Activity. *Plant Physiology,* **121**(2), pp. 665-674.

HOAGLAND and ARNON, 1950. The water-culture method for growing plants without soil.

HOBBS, P.V., 2010. *Oxford Classic Texts in the Physical Sciences,* **Ice Physics**.

HON, W.C., GRIFFITH, M., CHONG, P. and YANG, D., 1994a. Extraction and Isolation of Antifreeze Proteins from Winter Rye (Secale cereale L.) Leaves. *Plant Physiology,* **104**(3), pp. 971-980.

HON, W.C., GRIFFITH, M., CHONG, P. and YANG, D., 1994b. Extraction and Isolation of Antifreeze Proteins from Winter Rye (Secale cereale L.) Leaves. *Plant Physiology,* **104**(3), pp. 971-980.

HON, W.C., GRIFFITH, M., MLYNARZ, A., KWOK, Y.C. and YANG, D.S., 1995. Antifreeze proteins in winter rye are similar to pathogenesis-related proteins. *Plant Physiology,* **109**(3), pp. 879-889.

HUGHES, S.L., SCHART, V., MALCOLMSON, J., HOGARTH, K.A., MARTYNOWICZ, D.M., TRALMAN-BAKER, E., PATEL, S.N. and GRAETHER, S.P., 2013. The importance of size and disorder in the cryoprotective effects of dehydrins. *Plant Physiology,* **163**(3), pp. 1376-1386.

IDE, N., MASUDA, T. and KITABATAKE, N., 2007a. Effects of pre- and pro-sequence of thaumatin on the secretion by Pichia pastoris. *Biochemical and biophysical research communications,* **363**(3), pp. 708-714.

IDE, N., MASUDA, T. and KITABATAKE, N., 2007b. Effects of pre- and pro-sequence of thaumatin on the secretion by Pichia pastoris. *Biochemical and biophysical research communications,* **363**(3), pp. 708-714.

INVITROGEN CORP, 2010. EasySelect ^{TM} Pichia expression Expression Kit.

INVITROGEN CORP, Pichia Fermentation Process Guidelines.

JIA, Z. and DAVIES, P.L., 2002. Antifreeze proteins: an unusual receptor-ligand interaction. *Trends in biochemical sciences,* **27**(2), pp. 101-106.

JOHNSON, N., POWIS, K. and HIGH, S., 2013. Post-translational translocation into the endoplasmic reticulum. *Biochimica et Biophysica Acta (BBA) - Molecular Cell Research; Functional and structural diversity of the endoplasmic reticulum,* **1833**(11), pp. 2403-2409.

KANEKO, R. and KITABATAKE, N., 1999. Heat-induced formation of intermolecular disulfide linkages between thaumatin molecules that do not contain cysteine residues. *Journal of Agricultural and Food Chemistry,* **47**(12), pp. 4950-4955.

KAROW JR., A.M. and WEBB, W.R., 1965. Tissue freezing: A theory for injury and survival. *Cryobiology,* **2**(3), pp. 99-108.

KAWAHARA, H., FUJII, A., INOUE, M., KITAO, S., FUKUOKA, J. and OBATA, H., 2009. Antifreeze activity of cold acclimated Japanese radish and purification of antifreeze peptide. *Cryo letters,* **30**(2), pp. 119-131.

KNIGHT, C.A., HALLETT, J. and DEVRIES, A.L., 1988. Solute effects on ice recrystallization: an assessment technique. *Cryobiology,* **25**(1), pp. 55-60.

KNIGHT, C.A. and DUMAN, J.G., 1986. Inhibition of recrystallization of ice by insect thermal hysteresis proteins: A possible cryoprotective role. *Cryobiology,* **23**(3), pp. 256-262.

KONTOGIORGOS, V., REGAND, A., YADA, R.Y. and GOFF, H.D., 2007. Isolation and characterization of ice structuring proteins from cold-acclimated winter wheat grass extract for recrystallization inhibition in frozen foods. *Journal of Food Biochemistry,* **31**(2), pp. 139-160.

KRIMM, S., 1980. The hydrophobic effect: Formation of micelles and biological membranes, Charles Tanford, Wiley-Interscience, New York, 1980, 233 pp. price: $18.50. *Journal of Polymer Science: Polymer Letters Edition,* **18**(10), pp. 687-687.

KUBOTA, N., 2011. Effects of cooling rate, annealing time and biological antifreeze concentration on thermal hysteresis reading. *Cryobiology,* **63**(3), pp. 198-209.

KUIPER, M.J., DAVIES, P.L. and WALKER, V.K., 2001. A theoretical model of a plant antifreeze protein from Lolium perenne. *Biophysical journal,* **81**(6), pp. 3560-3565.

KUIPER, M.J., LANKIN, C., GAUTHIER, S.Y., WALKER, V.K. and DAVIES, P.L., 2003a. Purification of antifreeze proteins by adsorption to ice. *Biochemical and biophysical research communications,* **300**(3), pp. 645-648.

KUIPER, M.J., LANKIN, C., GAUTHIER, S.Y., WALKER, V.K. and DAVIES, P.L., 2003b. Purification of antifreeze proteins by adsorption to ice. *Biochemical and biophysical research communications,* **300**(3), pp. 645-648.

KUWABARA, C., ARAKAWA, K. and YOSHIDA, S., 1999. Abscisic acid-induced secretory proteins in suspension-cultured cells of winter wheat. *Plant & Cell Physiology,* **40**(2), pp. 184-191.

LAKOWICZ, J., 1999. *Principles of fluorescence spectrscopy.* 2nd edition edn. Springer US.

LAUERSEN, K.J., BROWN, A., MIDDLETON, A., DAVIES, P.L. and WALKER, V.K., 2011. Expression and characterization of an antifreeze protein from the perennial rye grass, Lolium perenne. *Cryobiology,* **62**(3), pp. 194-201.

LEONE, P., MENU-BOUAOUICHE, L., PEUMANS, W.J., PAYAN, F., BARRE, A., ROUSSEL, A., VAN DAMME, E.J. and ROUGE, P., 2006. Resolution of the structure of the allergenic and antifungal banana fruit thaumatin-like protein at 1.7-A. *Biochimie,* **88**(1), pp. 45-52.

LI, N., ANDORFER, C.A. and DUMAN, J.G., 1998. Enhancement of insect antifreeze protein activity by solutes of low molecular mass. *The Journal of experimental biology,* **201**(Pt 15), pp. 2243-2251.

LI, Z., XIONG, F., LIN, Q., D'ANJOU, M., DAUGULIS, A.J., YANG, D.S. and HEW, C.L., 2001. Low-temperature increases the yield of biologically active herring antifreeze protein in Pichia pastoris. *Protein expression and purification,* **21**(3), pp. 438-445.

LILLFORD, P.J., MCARTHUR, A.J., SIDEBOTTOM, C.M. and WILDING, P., 2005. *Frozen food product containing heat stable antifreeze protein.* Google Patents.

LIU, J.J., STURROCK, R. and EKRAMODDOULLAH, A.K., 2010. The superfamily of thaumatin-like proteins: its origin, evolution, and expression towards biological function. *Plant Cell Reports,* **29**(5), pp. 419-436.

LOUIS-JEUNE, C., ANDRADE-NAVARRO, M.A. and PEREZ-IRATXETA, C., 2012. Prediction of protein secondary structure from circular dichroism using theoretically derived spectra. *Proteins,* **80**(2), pp. 374-381.

LU, M., WANG, B., LI, Z., FEI, Y., WEI, L. and GAO, S., 2002a. Differential Scanning Calorimetric and Circular Dichroistic Studies on Plant Antifreeze Proteins. *Journal of Thermal Analysis and Calorimetry,* **67**(3), pp. 689-698.

LU, M., WANG, B., LI, Z., FEI, Y., WEI, L. and GAO, S., 2002b. Differential Scanning Calorimetric and Circular Dichroistic Studies on Plant Antifreeze Proteins. *Journal of Thermal Analysis and Calorimetry,* **67**(3), pp. 689-698.

MARSHALL, C.B., TOMCZAK, M.M., GAUTHIER, S.Y., KUIPER, M.J., LANKIN, C., WALKER, V.K. and DAVIES, P.L., 2004. Partitioning of fish and insect antifreeze proteins into ice suggests they bind with comparable affinity. *Biochemistry,* **43**(1), pp. 148-154.

MARSHALL, C.B., FLETCHER, G.L. and DAVIES, P.L., 2004. Hyperactive antifreeze protein in a fish. *Nature,* **429**(6988), pp. 153-153.

MAZUR, P., 1984. Freezing of living cells: mechanisms and implications. *The American Journal of Physiology,* **247**(3 Pt 1), pp. C125-42.

MEISTER, K., EBBINGHAUS, S., XU, Y., DUMAN, J.G., DEVRIES, A., GRUEBELE, M., LEITNER, D.M. and HAVENITH, M., 2013. Long-range protein-water dynamics in hyperactive insect antifreeze proteins. *Proceedings of the National Academy of Sciences of the United States of America,* **110**(5), pp. 1617-1622.

MENU-BOUAOUICHE, L., VRIET, C., PEUMANS, W.J., BARRE, A., VAN DAMME, E.J. and ROUGE, P., 2003. A molecular basis for the endo-beta 1,3-glucanase activity of the thaumatin-like proteins from edible fruits. *Biochimie,* **85**(1-2), pp. 123-131.

MEYER, K., KEIL, M. and NALDRETT, M.J., 1999. A leucine-rich repeat protein of carrot that exhibits antifreeze activity. *FEBS letters,* **447**(2-3), pp. 171-178.

MIDDLETON, A.J., BROWN, A.M., DAVIES, P.L. and WALKER, V.K., 2009. Identification of the ice-binding face of a plant antifreeze protein. *FEBS letters,* **583**(4), pp. 815-819.

MIDDLETON, A.J., MARSHALL, C.B., FAUCHER, F., BAR-DOLEV, M., BRASLAVSKY, I., CAMPBELL, R.L., WALKER, V.K. and DAVIES, P.L., 2012. Antifreeze protein from freeze-tolerant grass has a beta-roll fold with an irregularly structured ice-binding site. *Journal of Molecular Biology,* **416**(5), pp. 713-724.

MILLER, G.L., 1959. Use of Dinitrosalicylic Acid Reagent for Determination of Reducing Sugar. *Analytical Chemistry,* **31**(3), pp. 426-428.

MIN, K., HA, S.C., HASEGAWA, P.M., BRESSAN, R.A., YUN, D.J. and KIM, K.K., 2004. Crystal structure of osmotin, a plant antifungal protein. *Proteins,* **54**(1), pp. 170-173.

MORTZ, E., KROGH, T.N., VORUM, H. and GÖRG, A., 2001. Improved silver staining protocols for high sensitivity protein identification using matrix-assisted laser desorption/ionization-time of flight analysis. *Proteomics,* **1**(11), pp. 1359-1363.

NUTT, D.R. and SMITH, J.C., 2008. Dual function of the hydration layer around an antifreeze protein revealed by atomistic molecular dynamics simulations. *Journal of the American Chemical Society,* **130**(39), pp. 13066-13073.

OLSEN, T.,M. and DUMAN, J.,G., 1997b. Maintenance of the supercooled state in the gut fluid of overwintering pyrochroid beetle larvae, Dendroides canadensis: role of ice nucleators and antifreeze proteins. *Journal of Comparative Physiology B,* **167**(2), pp. 114-122.

OLSEN, T.,M. and DUMAN, J.,G., 1997a. Maintenance of the supercooled state in overwintering pyrochroid beetle larvae, Dendroides canadensis: role of hemolymph ice nucleators and antifreeze proteins. *Journal of Comparative Physiology B,* **167**(2), pp. 105-113.

OLSEN, T., SASS, S., LI , N. and DUMAN, J., 1998. Factors contributing to seasonal increases in inoculative freezing resistance in overwintering fire-colored beetle larvae dendroides canadensis. *J exp Biol,* **201**, pp. 1585-1594.

OSMOND, R.I., HRMOVA, M., FONTAINE, F., IMBERTY, A. and FINCHER, G.B., 2001. Binding interactions between barley thaumatin-like proteins and (1,3)-beta-D-glucans. Kinetics, specificity, structural analysis and biological implications. *European journal of biochemistry / FEBS,* **268**(15), pp. 4190-4199.

OTTE, S. and BARLOWE, C., 2004. Sorting signals can direct receptor-mediated export of soluble proteins into COPII vesicles. *Nature cell biology,* **6**(12), pp. 1189-1194.

PANADERO, J., RANDEZ-GIL, F. and PRIETO, J.A., 2005. Heterologous expression of type I antifreeze peptide GS-5 in baker's yeast increases freeze tolerance and provides enhanced gas production in frozen dough. *Journal of Agricultural and Food Chemistry,* **53**(26), pp. 9966-9970.

PARK, S.H., BOLENDER, N., EISELE, F., KOSTOVA, Z., TAKEUCHI, J., COFFINO, P. and WOLF, D.H., 2007. The Cytoplasmic Hsp70 Chaperone Machinery Subjects Misfolded and Endoplasmic Reticulum Import-incompetent Proteins to Degradation via the Ubiquitinâ€“Proteasome System. *Molecular biology of the cell,* **18**(1), pp. 153-165.

PERIN, G., 2012. Indagine sul potenziale utilizzo di una ice Structuring Protein di origine vegetale nel'industria alimentare. *M. Sc. thesis, University of Padua,* .

PERRI, F., ROMITELLI, F., RUFINI, F., SECUNDO, F., DI STASIO, E., GIARDINA, B. and VITALI, A., 2008. Different structural behaviors evidenced in thaumatin-like proteins: a spectroscopic study. *The protein journal,* **27**(1), pp. 13-20.

PUDNEY, P.D., BUCKLEY, S.L., SIDEBOTTOM, C.M., TWIGG, S.N., SEVILLA, M.P., HOLT, C.B., ROPER, D., TELFORD, J.H., MCARTHUR, A.J. and LILLFORD, P.J., 2003. The physico-chemical characterization of a boiling stable antifreeze protein from a perennial grass (Lolium perenne). *Archives of Biochemistry and Biophysics,* **410**(2), pp. 238-245.

RAOULT, F.M., 1884. The general law on the freezing of solvents. *Ann. Chem. Phys,* **2**, pp. 66.

RAYMOND, J.A., 2011. Algal ice-binding proteins change the structure of sea ice. *Proceedings of the National Academy of Sciences of the United States of America,* **108**(24), pp. E198.

RAYMOND, J.A. and DEVRIES, A.L., 1977. Adsorption inhibition as a mechanism of freezing resistance in polar fishes. *Proceedings of the National Academy of Sciences of the United States of America,* **74**(6), pp. 2589-2593.

REGAND, A. and GOFF, H.D., 2006a. Ice recrystallization inhibition in ice cream as affected by ice structuring proteins from winter wheat grass. *Journal of dairy science,* **89**(1), pp. 49-57.

REGAND, A. and GOFF, H.D., 2006b. Ice Recrystallization Inhibition in Ice Cream as Affected by Ice Structuring Proteins from Winter Wheat Grass. *Journal of dairy science,* **89**(1), pp. 49-57.

REGAND, A. and GOFF, H.D., 2005. Freezing and Ice Recrystallization Properties of Sucrose Solutions Containing Ice Structuring Proteins from Cold-Acclimated Winter Wheat Grass Extract. *Journal of Food Science,* **70**(9), pp. E552-E556.

REGHELIN, E., 2011. Plant derived sweet and Ice Structuring Proteins as new tools in food processing. *PhD thesis - university of Padua,* .

RIBOTTA, P.D., LEON, A.E. and ANON, M.C., 2001. Effect of freezing and frozen storage of doughs on bread quality. *Journal of Agricultural and Food Chemistry,* **49**(2), pp. 913-918.

RIENER, C.K., KADA, G. and GRUBER, H.J., 2002. Quick measurement of protein sulfhydryls with Ellman's reagent and with 4,4'-dithiodipyridine. *Analytical and bioanalytical chemistry,* **373**(4-5), pp. 266-276.

ROBERTS, W.K. and SELITRENNIKOFF, C.P., 1990. Zeamatin, an antifungal protein from maize with membrane-permeabilizing activity. *Journal of general microbiology,* **136**(9), pp. 1771-1778.

ROTHBLATT, J.A., WEBB, J.R., AMMERER, G. and MEYER, D.I., 1987. Secretion in yeast: structural features influencing the post-translational translocation of prepro-alpha-factor in vitro. *The EMBO journal,* **6**(11), pp. 3455-3463.

RUSSELL, A.B., CHENEY, P.E. and WANTLING, S.D., 1999. Influence of freezing conditions on ice crystallisation in ice cream. *Journal of Food Engineering,* **39**(2), pp. 179-191.

SALAMIN, K., SRIRANGANADANE, D., LÃ©CHENNE, B., JOUSSON, O. and MONOD, M., 2010. Secretion of an Endogenous Subtilisin by Pichia pastoris Strains GS115 and KM71. *Applied and Environmental Microbiology,* **76**(13), pp. 4269-4276.

SANDVE, S.R., RUDI, H., ASP, T. and ROGNLI, O.A., 2008. Tracking the evolution of a cold stress associated gene family in cold tolerant grasses. *BMC evolutionary biology,* **8**, pp. 245-2148-8-245.

SCHAGGER, H. and VON JAGOW, G., 1991. Blue native electrophoresis for isolation of membrane protein complexes in enzymatically active form. *Analytical Biochemistry,* **199**(2), pp. 223-231.

SCHATZ, G. and DOBBERSTEIN, B., 1996. Common principles of protein translocation across membranes. *Science (New York, N.Y.),* **271**(5255), pp. 1519-1526.

SCOTTER, A.J., MARSHALL, C.B., GRAHAM, L.A., GILBERT, J.A., GARNHAM, C.P. and DAVIES, P.L., 2006. The basis for hyperactivity of antifreeze proteins. *Cryobiology,* **53**(2), pp. 229-239.

SIDEBOTTOM, C., BUCKLEY, S., PUDNEY, P., TWIGG, S., JARMAN, C., HOLT, C., TELFORD, J., MCARTHUR, A., WORRALL, D., HUBBARD, R. and LILLFORD, P., 2000a. Heat-stable antifreeze protein from grass. *Nature,* **406**(6793), pp. 256.

SIDEBOTTOM, C., BUCKLEY, S., PUDNEY, P., TWIGG, S., JARMAN, C., HOLT, C., TELFORD, J., MCARTHUR, A., WORRALL, D., HUBBARD, R. and LILLFORD, P., 2000b. Heat-stable antifreeze protein from grass. *Nature,* **406**(6793), pp. 256.

SIMPSON, D.J., SMALLWOOD, M., TWIGG, S., DOUCET, C.J., ROSS, J. and BOWLES, D.J., 2005. Purification and characterisation of an antifreeze protein from Forsythia suspensa (L.). *Cryobiology,* **51**(2), pp. 230-234.

SINENSKY, M., 1974. Homeoviscous Adaptation: A Homeostatic Process that Regulates the Viscosity of Membrane Lipids in Escherichia coli. *Proceedings of the National Academy of Sciences of the United States of America,* **71**(2), pp. 522-525.

SINHA, J., PLANTZ, B.A., INAN, M. and MEAGHER, M.M., 2005. Causes of proteolytic degradation of secreted recombinant proteins produced in methylotrophic yeast Pichia pastoris: case study with recombinant ovine interferon-tau. *Biotechnology and bioengineering,* **89**(1), pp. 102-112.

SMALLWOOD, M., WORRALL, D., BYASS, L., ELIAS, L., ASHFORD, D., DOUCET, C.J., HOLT, C., TELFORD, J., LILLFORD, P. and BOWLES, D.J., 1999a. Isolation and characterization of a novel antifreeze protein from carrot (Daucus carota). *Biochemical Journal,* **340**(Pt 2), pp. 385-391.

SMALLWOOD, M., WORRALL, D., BYASS, L., ELIAS, L., ASHFORD, D., DOUCET, C.J., HOLT, C., TELFORD, J., LILLFORD, P. and BOWLES, D.J., 1999b. Isolation and characterization of a novel antifreeze protein from carrot (Daucus carota). *Biochemical Journal,* **340**(Pt 2), pp. 385-391.

SORHANNUS, U., 2011. Evolution of Antifreeze Protein Genes in the Diatom Genus Fragilariopsis: Evidence for Horizontal Gene Transfer, Gene Duplication and Episodic Diversifying Selection. *Evolutionary Bioinformatics Online,* **7**, pp. 279-289.

STEPONKUS, P., 1996. Advances in Low-Temperature Biology. **Volume 3,**.

STRESSMANN, M., KITAO, S., GRIFFITH, M., MORESOLI, C., BRAVO, L.A. and MARANGONI, A.G., 2004. Calcium interacts with antifreeze proteins and chitinase from cold-acclimated winter rye. *Plant Physiology,* **135**(1), pp. 364-376.

SZWACKA, M., BURZA, W., ZAWIRSKA-WOJTASIAK, R., GO?LI?SKI, M., TWARDOWSKA, A., GAJC-WOLSKA, J., KOSIERADZKA, I. and KIE?KIEWICZ, M., 2012. Genetically Modified Crops Expressing 35S-Thaumatin II Transgene: Sensory Properties and Food Safety Aspects. *Comprehensive Reviews in Food Science and Food Safety,* **11**(2), pp. 174-186.

TAKAMICHI, M., NISHIMIYA, Y., MIURA, A. and TSUDA, S., 2007. Effect of annealing time of an ice crystal on the activity of type III antifreeze protein. *The FEBS journal,* **274**(24), pp. 6469-6476.

THOMASHOW, M.F., 1998. Role of cold-responsive genes in plant freezing tolerance. *Plant Physiology,* **118**(1), pp. 1-8.

THOMPSON, C.E., FERNANDES, C.L., DE SOUZA, O.N., SALZANO, F.M., BONATTO, S.L. and FREITAS, L.B., 2006. Molecular modeling of pathogenesis-related proteins of family 5. *Cell biochemistry and biophysics,* **44**(3), pp. 385-394.

TREMBLAY, K., OUELLET, F., FOURNIER, J., DANYLUK, J. and SARHAN, F., 2005. Molecular Characterization and Origin of Novel Bipartite Cold-regulated Ice Recrystallization Inhibition Proteins from Cereals. *Plant and Cell Physiology,* **46**(6), pp. 884-891.

TRUDEL, J., GRENIER, J., POTVIN, C. and ASSELIN, A., 1998. Several Thaumatin-Like Proteins Bind to β-1,3-Glucans. *Plant Physiology,* **118**(4), pp. 1431-1438.

URRUTIA, M.E., DUMAN, J.G. and KNIGHT, C.A., 1992. Plant thermal hysteresis proteins. *Biochimica et biophysica acta,* **1121**(1-2), pp. 199-206.

VADHANA, A.K., SAMUEL, P., BERIN, R.M., KRISHNA, J., KAMATCHI, K. and MEENAKSHISUNDARAM, S., 2013. Improved secretion of Candida antarctica lipase B with its native signal peptide in Pichia pastoris. *Enzyme and microbial technology,* **52**(3), pp. 177-183.

VAN DAMME, E., CHARELS, D., MENU-BOUAOUICHE, L., PROOST, ,PAUL, BARRE, A., ROUGÈ, P. and PEUMANS, W., Biochemical, molecular and structural analysis of multiple thaumatin-like proteins from the elderberry tree (Sambucus nigra L.).

VENKETESH, S. and DAYANANDA, C., 2008a. Properties, potentials, and prospects of antifreeze proteins. *Critical reviews in biotechnology,* **28**(1), pp. 57-82.

VENKETESH, S. and DAYANANDA, C., 2008b. Properties, potentials, and prospects of antifreeze proteins. *Critical reviews in biotechnology,* **28**(1), pp. 57-82.

WANG, L. and DUMAN, J.G., 2006. A thaumatin-like protein from larvae of the beetle Dendroides canadensis enhances the activity of antifreeze proteins. *Biochemistry,* **45**(4), pp. 1278-1284.

WANG, L. and DUMAN, J.G., 2005. Antifreeze proteins of the beetle Dendroides canadensis enhance one another's activities. *Biochemistry,* **44**(30), pp. 10305-10312.

WANG, S., AMORNWITTAWAT, N., JUWITA, V., KAO, Y., DUMAN, J.G., PASCAL, T.A., GODDARD, W.A. and WEN, X., 2009. Arginine, a key residue for the enhancing ability of an antifreeze protein of the beetle Dendroides canadensis. *Biochemistry,* **48**(40), pp. 9696-9703.

WATERS, M.G., EVANS, E.A. and BLOBEL, G., 1988. Prepro-alpha-factor has a cleavable signal sequence. *The Journal of biological chemistry,* **263**(13), pp. 6209-6214.

WERTEN, M.W., VAN DEN BOSCH, T.J., WIND, R.D., MOOIBROEK, H. and DE WOLF, F.A., 1999. High-yield secretion of recombinant gelatins by Pichia pastoris. *Yeast (Chichester, England),* **15**(11), pp. 1087-1096.

WISNIEWSKI, M., WEBB, R., BALSAMO, R., CLOSE, T.J., YU, X. and GRIFFITH, M., 1999. Purification, immunolocalization, cryoprotective, and antifreeze activity of PCA60: A dehydrin from peach (Prunus persica). *Physiologia Plantarum,* **105**(4), pp. 600-608.

WU, D. and DUMAN, J.,G., 1991. Activation of antifreeze proteins from larvae of the beetle Dendroides canadensis. *Journal of Comparative Physiology B,* **161**(3), pp. 279-283.

WU, D.W., DUMAN, J.G. and XU, L., 1991. Enhancement of insect antifreeze protein activity by antibodies. *Biochimica et biophysica acta,* **1076**(3), pp. 416-420.

YEH, S., MOFFATT, B.A., GRIFFITH, M., XIONG, F., YANG, D.S., WISEMAN, S.B., SARHAN, F., DANYLUK, J., XUE, Y.Q., HEW, C.L., DOHERTY-KIRBY, A. and LAJOIE, G., 2000. Chitinase genes responsive to cold encode antifreeze proteins in winter cereals. *Plant Physiology,* **124**(3), pp. 1251-1264.

YU, X.M. and GRIFFITH, M., 2001. Winter rye antifreeze activity increases in response to cold and drought, but not abscisic acid. *Physiologia Plantarum,* **112**(1), pp. 78-86.

YU, X.M. and GRIFFITH, M., 1999. Antifreeze proteins in winter rye leaves form oligomeric complexes. *Plant Physiology,* **119**(4), pp. 1361-1370.

ZACHARIASSEN, K.E. and KRISTIANSEN, E., 2000. Ice Nucleation and Antinucleation in Nature. *Cryobiology,* **41**(4), pp. 257-279.

ZHANG, C., ZHANG, H., WANG, L., GAO, H., GUO, X.N. and YAO, H.Y., 2007. Improvement of texture properties and flavor of frozen dough by carrot (Daucus carota) antifreeze

protein supplementation. *Journal of Agricultural and Food Chemistry,* **55**(23), pp. 9620-9626.

ZHANG, D.Q., LIU, B., FENG, D.R., HE, Y.M., WANG, S.Q., WANG, H.B. and WANG, J.F., 2004. Significance of conservative asparagine residues in the thermal hysteresis activity of carrot antifreeze protein. *Biochemical Journal,* **377**(Pt 3), pp. 589-595.

ZHANG, D.Q., WANG, H.B., LIU, B., FENG, D.R., HE, Y.M. and WANG, J.F., 2006. Carrot antifreeze protein does not exhibit the polygalacturonase-inhibiting activity of PGIP family. *Yi chuan xue bao Acta genetica Sinica,* **33**(11), pp. 1027-1036.